UC Riverside
UC Riverside Electronic Theses and Dissertations

Title

A Multi-Omics Approach To Understand The Role of Leucine Aminopeptidase A in Defense Signaling

Permalink

https://escholarship.org/uc/item/3tn0n8j4

Author

Ortiz, Irma

Publication Date

2021

Copyright Information

Peer reviewed|Thesis/dissertation

UNIVERSITY OF CALIFORNIA
RIVERSIDE

A Multi-Omics Approach to Understand the Role of Leucine Aminopeptidase A in
Defense Signaling

A Dissertation submitted in partial satisfaction
of the requirements for the degree of

Doctor of Philosophy

in

Plant Biology

by

Irma Ortiz

March 2022

Dissertation Committee:
  Dr. Linda L. Walling, Chairperson
  Dr. Julia Bailey-Serres
  Dr. Meng Chen

The Dissertation of Irma Ortiz is approved:

_____

_____

_____

                                    Committee Chairperson

University of California, Riverside

Acknowledgements

Dedication

To my parents and brother. I love you. I could not have finished this without your

encouragement and support.

ABSTRACT OF THE DISSERTATION

A Multi-Omics Approach to Understand the Role of Leucine Aminopeptidase A in
Defense Signaling

by

Irma Ortiz

Doctor of Philosophy, Graduate Program in Plant Biology
University of California, Riverside, March 2022
Dr. Linda L. Walling, Chairperson

Plant leucine aminopeptidase A (LAP-A) modulates late wound responses and insect defense. LAP-A is an aminopeptidase and chaperone in the chloroplast stroma. Based on the ability of LAP-A to modulate transcripts in the wound-response pathway, we postulated that LAP-A sends a retrograde signal(s) to the nucleus to regulate nuclear gene expression in response to wounding and MeJA treatments. We use wild-type, LapA-silenced and LapA-overexpressing plants to explore the global impact of LAP-A deficiency or ectopic expression on the tomato metabolome. This dissertation has revealed that LAP-A has multiple impacts on tomato metabolites by altering the levels of amino acids and secondary metabolites involved in plant defense. Given the link to sulfur metabolism and LAP-A's ability to hydrolyze glutathione's catabolic product Cys-Gly, the role of LAP-A in GSH metabolism using targeted metabolomics and the three genotypes was assessed. These wound-time course experiments were designed to simultaneously measure H_2O_2 levels. LAP-A did not regulate the levels of glutathione (GSH), the redox status of GSH, nor the levels of Cys-Gly, Cys or γ-Glu-Cys. In the

absence of LAP-A, H_2O_2 levels are elevated indicating that LAP-A is important for the control of ROS. H_2O_2 is a known retrograde signal used in defense. To elucidate LAP-A's possible mechanism(s) of action, the proteins that bind to LAP-A, but not to the highly related LAP-N, were identified. The 86 LAP-A-interacting proteins that reside in the chloroplast suggests that LAP-A may exert its effects via the major chloroplast redox hub associated with 2-Cys-peroxiredoxin. LAP-A binds to NADPH thioredoxin reductase-C (NTRC1), which provides the reducing power to 2-Cys-peroxiredoxin for clearing H_2O_2 from the chloroplast; a model is presented. Additional LAP-A-interacting proteins suggest a role for LAP-A in modulating the activity of the stromal Clp protease. Finally, this dissertation reports the first tomato stromal proteome. The 1254 stromal proteins identified were manually annotated. This is the first evidence for the chloroplast location of 550 tomato proteins. This study is foundational for current initiatives to understand the LAP-A- and MeJA-dependent changes in the tomato stromal proteome, which should provide additional insights into the global impacts of LAP-A during plant stress responses.

Table of Contents

List of Figures

Tables

Supplemental tables cited in the dissertation, A Multi-Omics Approach to Understand the

Role of Leucine Aminopeptidase A in Defense Signaling are included in a link in

Dropbox:

https://www.dropbox.com/sh/zhbo74wz8qyi9b1/AAA0O_N6IndYM6P75bRsrZq2a?dl=0

Introduction

Plant- Pathogen/ Pest Interactions: PTI, EST and ETI

Plants are sessile organisms that are unable flee when challenged by pathogens and pests or other environmental stresses. Plant pathogens are organisms that complete their life cycles inside plant hosts with a negative effect to plant health. Plant pests are insects, nematodes and mammals that consume plants. Pathogens and pests have coevolved with plants. The zigzag plant defense response model describes the highly conserved plant-defense response to pathogens (Jones and Dangl 2006). Pattern-recognition receptors (PRRs) can recognize conserved external microbe-associated molecular patterns (MAMPs) or pathogen-associated molecular patterns (PAMPs), such as lipopolysaccharides, flagellin and chitin (Zhou and Zhang 2020). This recognition activates pattern-triggered immunity (PTI) in the plant host. PTI responses include plant cell wall fortification, induction of genes that encode antimicrobial proteins, and reactive oxygen species (ROS) production. PTI is the first line of defense. It helps control non-host responses and controls infection by non-adapted pathogens.

There is selective pressure on pathogens to produce proteins or effector molecules to interfere with PTI responses and, in turn, result in effector-triggered susceptibility (ETS). However, the pathogen-derived effectors also place selective pressure on plants to recognize effectors to limit pathogen success. Plants have resistance (R) genes that directly or indirectly recognize effector molecules or modifications caused by effectors. Many pathogen effectors are recognized by the plant host intracellular nucleotide-binding (NB)-leucine rich repeat (LRR) receptors to induce effector-triggered immunity (ETI) (Erb and Reymond 2019). Pathogen effector-encoding genes that induce ETI are called avirulence (avr) genes. The plant defense mechanisms activated during ETI

overlap extensively with PTI, although distinctions exist (Hatsugai et al. 2017; Tsuda et al. 2009); for example, during ETI hypersensitive cell death response (HR) can also occur (Erb and Reymond 2019). For example, the Pseudomonas syringae's AvrPto effector causes an avirulent reaction (lack of disease) in Solanum lycopersicum (tomato) that carry the Pto resistance gene (Pedley and Martin 2003); when pathogens lack an avirulence gene that corresponds to a R gene a PTI response is deployed.

Plant perception of damage

In addition to perceiving pathogen-derived effectors/elicitors, plants can perceive plant-derived molecules that are produced by pathogen attack, mechanical wounding or herbivore-induced damage (Erb and Reymond 2019). Foundational studies beginning in the 1970's in Solanum lycopersicum (tomato) established many of the principles of wound/herbivore-provoked signals and signal transduction (Green and Ryan 1972; McFarland and Ryan 1974). More recently, the model Arabidopsis thaliana has further elucidated the pathways that perceive cellular damage (Li et al. 2020a; Toyota et al. 2018).

Damage responses are induced when plant-derived damage-associated molecular patterns (DAMPs) are released after plant tissue damage and perceived by PRRs. These responses are local, as damaged plant cells signal to adjacent plant cells using a mixture of DAMPs. Primary DAMPs include ATP, cell wall fragments and fragmented DNA (Quintana-Rodriguez et al. 2018). Secondary DAMPs include plant host molecules produced or modified after wounding or microbial infection. These DAMPs serve exclusively as defense signals; the systemin peptides are one such example (Li et al. 2020b).

eATP: After wounding, extracellular ATP (eATP) is released immediately from the cytoplasm to the extracellular environment. Initially identified and intensively studied in Arabidopsis, eATP is sensed by the L-type lectin receptor kinase P2K1/DORN1 (DOES NOT RESPOND TO NUCLEOTIDES 1) and P2K2 (Choi et al. 2014; Pham et al. 2020). This induces membrane depolarization, Ca^{2+} influx, ROS formation, expression of defense-related genes, and enhanced plant defense (Chen et al. 2017; Chen et al. 2021; Tripathi et al. 2018). Although, eATP receptors have not yet been identified in tomato, eATP is an important part of damage signaling in this species. Wu et al. (2012) showed that herbivores attempt to suppress eATP levels in tomato foliage. ATP-hydrolyzing enzymes present in caterpillar saliva reduced foliar ATP levels and suppressed the induction of JA- and ET-responsive genes; by reducing ATP levels, herbivore success was enhanced (Wu et al. 2012a).

Oligogalacturonides (OGs): Plant cell wall fragments, OGs are also released after wounding (Ferrari et al. 2013). OGs are derived from homogalacturonan, the main component of pectin. Wall-Associated Kinase (WAK) proteins are receptors of OGs (Kohorn and Kohorn 2012). The perception of OGs induces the Arabidopsis plant defense responses including: reactive oxygen species (ROS) production (Bellincampi et al. 2000), mitogen-activated protein kinase (MAPK) activation (Denoux et al. 2008), and nitric oxide (NO) (Rasul et al. 2012). In tomato, OGs induce protease inhibitor proteins (PINs), which directly antagonize insect gut metabolism (Moloshok et al. 1992; Ryan and Jagendorf 1995; Doares et al. 1995b).

Plant host fragmented DNA: Upon cellular damage, host-plant DNA is released into the apoplast to induce early plant defense responses (Quintana-Rodriguez et al. 2018). No DNA plant receptors that perceive these DNA fragments have been identified

to date. However, a recent study showed that adding plant host fragmented DNA to tomato leaves induces Ca^{2+} influx from the apoplastic space to the cytoplasm and ROS production along with inducing expression of genes involved in plant immunity including wound-induced proteinase inhibitor 1 (Pin1) (Barbero et al. 2021). Several heat shock proteins and chaperones were downregulated (Barbero et al. 2021).

Systemin as a DAMP: Secondary DAMPs include the peptides involved in defense signaling. The peptide systemin is the first reported bioactive peptide that induced plant defense responses (Pearce et al. 1991) and systemin-like proteins are limited to members of the Solanoideae (Constabel et al. 1998). Prosystemin (systemin's 200 amino acid precursor) accumulates in the cytosol after wounding and herbivory (Narváez-Vásquez and Ryan 2004). Upon cellular damage, subtilisin-like proteases (phytaspases) that are stored in the vacuole are released and prosystemin is processed to release the bioactive 18-aa systemin peptide (Beloshistov et al. 2018).

Two receptor-like kinases (RLKs) bind systemin. SYSTEMIN RECEPTOR 1 (SYR1) has high-binding affinity for systemin, while SYR2 has a lower affinity (Wang et al. 2018). SYR1-dependent systemin perception results in plant defense responses including a ROS burst, ethylene (ET) production and the expression of wound-induced proteinase inhibitor genes (PINs) (Narvaez-Vasquez et al. 1999; O'Donnell et al. 1996; Wang et al. 2018). Wang et al. (2018) also demonstrated that local and systemic signaling after mechanical damage can be SYR1 independent, which suggests that jasmonic acid (JA), H_2O_2, hydraulic changes, or electrical waves may be important for these responses (Farmer et al. 2014; Rhodes et al. 1996). Also, systemin-treated plants showed enhanced resistance to the moth Spodoptera littoralis and pathogen Botrytis cinerea by

increased production of volatile organic compounds (VOCs) and induction of defense genes such as PINs (Coppola et al. 2019).

Hydroxyproline-rich systemins (HypSys): A second class of defense-signaling peptides first identified in the Solanaceae are the HypSys related peptides (Pearce 2011). HypSys are glycoproteins that are structurally unrelated to systemin, but they also are important for defense signaling after wounding and herbivory (Pearce et al. 2001) (Pearce and Ryan 2003). HypSys originates from pre-protein precursor (proHypSys) with signal peptides for protein secretion. HypSys are now known to have roles in defense such as induction of PINs (Pearce 2011).

Pep1 in Arabidopsis: The discovery of plant elicitor peptide, Pep1, in Arabidopsis and its orthologs in other plants revolutionized our understanding of DAMP signaling (Huffaker et al. 2006; Li et al. 2020b). AtPep1 is a 23-amino acid peptide that is derived from the C-terminus of a 92-amino acid precursor protein encoded from PROPEP1 gene (Huffaker et al. 2006). The Arabidopsis genome has eight PROPEP genes expressed in roots and slightly in leaves (Bartels et al. 2013; Huffaker et al. 2006). PROPEP1 is induced by wounding and MeJA (Huffaker and Ryan 2007). Exogenous treatments of Peps induce ethylene production and suppress plant seedling growth (Bartels et al. 2013). Pep1 are perceived by two related LRR-RKs, Pep1 RECEPTOR 1 (PEPR1) and PEPR2 (ref 186, erf 2019) In addition, exogenous Peps affect plant defense by inducing defense genes such as PDFs and WRKYs and inducing resistance to pathogens such as Pseudomonas syringae (Huffaker and Ryan 2007; Yamaguchi et al. 2010).

Maize PEP3: Maize PEPs (ZmPEP), orthologues to Arabidopsis PEPs, also regulate responses against herbivores. Spodoptera exigua (beet armyworm) oral secretions induce ZmPROPEP3 precursor gene followed by production of JA, ethylene,

expression of defense genes, and VOCs to deter herbivory (Huffaker et al. 2013). Benzoxazinoid, 2-hydroxy-4,7-dimethoxy- 1,4-benzoxazin-3-one glucoside (HDMBOA-Glc), a well-known maize defense metabolite (Niemeyer 2009; Tzin et al. 2015), also accumulated by treatment of ZmPEP3.

HAMPS: Insect-derived metabolites or proteins acting as elicitors, identified by a plant receptor and inducing defense responses are designated as herbivore-associated molecular patterns (HAMPs) and were recently reviewed (Erb and Reymond 2019). The first HAMP was discovered in oral secretions of beet armyworm. This HAMP is a fatty acid-amino acid (aa) conjugate, N-(17-hydroxylinolenoyl)-L-glutamine (volicitin), found to induce VOCs in maize (Alborn et al. 2000). N-linolenoyl-L-glutamine (Gln-18:3) elicited defense responses against beet armyworm and overlap with the defense responses elicited by ZmPep3, such as JA accumulation 2 h after treatments (Huffaker et al. 2013; Poretsky et al. 2021).

The HAMP inceptin is a disulfide-bridged peptide (ICDINGVCVDA) derived from a plant ATPase γ subunit and was first identified in Spodoptera frugipera oral secretions (Schmelz et al. 2006). Recently the inceptin receptor was identified. This leucine-rich repeat inceptin receptor (INR) triggers inceptin-induced responses and enhanced defense against beet armyworms in tobacco (Steinbrenner et al. 2020).

Responses to different HAMPs can be species specific. For example, Schmelz et al. (2009) showed tomato and Arabidopsis plants do not elicit a plant defense response to the following HAMPs: volicitin, Gln-18:3, inceptin, and caeliferin A16:0. However, tomatoes do respond to the HAMP glucose oxidase by inducing defense responses (Louis et al. 2013). In contrast, in tobacco glucose oxidase suppresses defense

responses suggesting that plants within the same family can have distinct responses to HAMPs (Diezel et al. 2009).

JA Biosynthesis, Perception, and Mediator Interactions with MYCs

JA production via the octadecanoid pathway and perception of bioactive form JA-Isoleucine (JA-Ile) is critical for the induction of damage- and herbivore feeding-induced responses in plants (Wasternack and Feussner 2018). The octadecanoid pathway is activated after tissue damage (e.g., mechanical wounding or herbivory) and after perception of DAMPS and HAMPs. As a result, oxygenated lipids such as 12-oxo-cis-10,15-phytodienoic acid (OPDA) and JA are generated (Howe 2018). JA biosynthesis initiates in the chloroplast membrane when phospholipases (PLD, PLA_2) release α-linolenic acid, which is converted to 13-hydroperoxylinolenic acid by 13-lipoxygenases (LOX) (Hause et al. 2003). The allene oxide synthase (AOS) enzyme uses 13-hydroperoxylinolenic acid to produce 12,13(S)-epoxylinolenic acid and allene oxide cyclase (AOC) converts 12,13(S)-epoxylinolenic acid into cis-(+) OPDA. JASSY exports OPDA to the outer chloroplast membrane (Guan et al. 2019).

JA biosynthesis in the peroxisome: Subsequent metabolic reactions to generate the bioactive form of JA occur in the peroxisome. OPDA is transported into the peroxisome by an ATP-transporter Comatose (COMATOSE) (Theodoulou et al. 2005). OPDA is reduced by OPDA reductases 2 and 3 (OPR2 and OPR3) to yield 3-oxo-2-(cis-2'-pentenyl) cyclopentane-1-octanoic acid (OPC-8:0) (Schaller and Stintzi 2009). OPC-8:0 is converted to (+)-7-isojasmonic acid by three rounds of oxidation. The JA-resistant 1 (JAR1) enzyme conjugates Ile to JA resulting in the bioactive jasmonoyl-isoleucine (JA-Ile) (Suza and Staswick 2008; Suza et al. 2010). An alternative pathway for JA biosynthesis has also been suggested in which OPDA directly enters oxidation to yield

4,5-didehydro-JA (ddh-JA) (Howe 2018; Chini et al. 2018). Subsequently OPR2 reduces ddh-JA to JA and conjugated to Ile by JAR1. More recently, 12-hydroxy-jasmonoyl-isoleucine (12OH-JA-Ile) was identified as a bioactive derivative of JA-Ile (Poudel et al. 2019). Other identified bioactive conjugates of JA include: JA-Leu, JA-Val, JA-Met, and JA-Ala; these conjugates are less active and not as well studied as JA-Ile (Yan et al. 2016; Thines et al. 2007; Katsir et al. 2008).

Bioactive conjugates of JA transported to the nucleus: To activate JA-dependent genes, JA-Ile must be transported to the nucleus. AtJAT1 (AtABCG16) is a nuclear- and plasma-membrane ABC transporter that translocates JA-Ile to the nucleus and mediates cellular export of JA (Li et al. 2017; Nguyen et al. 2017). By controlling cellular JA levels and levels of JA-Ile in the nucleus, JAT1 can regulate the critical JA concentration required for JA-mediated signaling in defense and development.

JA-regulated transcriptional reprogramming: In the nucleus, the JA ZIM domain (JAZ) proteins act as transcriptional repressors of JA-regulated genes (Howe et al. 2018). JAZ proteins and their co-receptors, NINJA and TOPLESS (TPL), bind to the master regulator MYC2 when JA-Ile levels are low (Howe et al. 2018). This repressive complex sequesters the transcription factors in tomato (MYC2) and Arabidopsis (MYC2, MYC3, MYC4), which are needed for activating many JA-responsive genes (Chini et al. 2007; Wang et al. 2021; Du et al. 2017; Major et al. 2017). When the levels of JA-Ile rise in the nucleus, JA-Ile is bound by the JA receptor CORONATINE-INSENSITIVE 1 (COI1), an F-box protein that associates with other proteins to make up the SCF-COI1 ubiquitin ligase-complex (Thines et al. 2007). This SCF-COI1 complex recruits and ubiquitinates JAZs, thereby facilitating their degradation by the 26S proteasome (Wasternack and Song 2017). In the absence of JAZ repressors, MYC2 binds to

promoters to activate JA-dependent signaling. Recently, JA perception by COI1 was found to be important at the interface of defense and high temperature stress (Havko et al. 2020). Tomato plants exposed to moderate heat stress resulted in heat shock proteins (HSP90) stabilizing COI1 proteins and in enhanced JA responses. In addition, plants exposed to moderate heat temperatures resulted in negative ramifications for plant defense and plant fitness such as enhanced susceptibility to herbivores, reduced plant photosynthesis, and inhibited plant growth (Havko et al. 2020).

The JA-regulated transcriptional reprogramming up-regulates JA-response genes such as MYC2 and genes that encode enzymes in the biosynthesis of secondary metabolites involved in plant immunity, such as terpenes, glucosinolates, alkaloids, and phenolics (Hickman et al. 2017; Zander et al. 2020). JA is also converted to volatile methyl jasmonate (MeJA) by SAM-dependent carboxyl methyltransferase (Wasternack and Song 2017). MeJA is an airborne signal in interplant communication to activate plant defense responses (Farmer and Ryan 1990).

JA-regulated wound signaling in tomato: In tomato, JA-regulated wound signaling is biphasic (Orozco-Cardenas et al. 2001). During the early phase of wound responses (0.5 to 2 h after wounding), gene products (LOX, AOS, AOC, prosystemin) that amplify wound signaling are activated. During the late phase of wound responses (4-24 hr post wounding), a volatile blend and anti-nutritive proteins, such as polyphenol oxidases (PPOs) and proteinase inhibitors (Pin1 and Pin2) accumulate (Fowler et al. 2009; Howe 2004; Degenhardt et al. 2010; Dicke and Baldwin 2010). While MeJA controls both early and late wound responses in tomato, hydrogen peroxide (H_2O_2), nitric oxide (NO) and Leucine aminopeptidase (LAP) modulate the late branch of the wound response (Orozco-Cardenas et al. 2001; Orozco-Cardenas and Ryan 2002; Fowler et al. 2009;

9

Chao et al. 1999). These modulators act downstream from JA biosynthesis and perception, with H_2O_2 and LAP activating and NO repressing the late wound response (Orozco-Cardenas and Ryan 2002; Fowler et al. 2009; Chao et al. 1999). In tomato, NO represses H_2O_2 accumulation and H_2O_2-dependent resistance to the necrotrophic fungal pathogen Botrytis cinerea negatively affecting JA-induced gene expression (Małolepsza and Rózalska 2005). The mechanism of LAP action is unknown and is the focus of this dissertation. In contrast, NO works synergistically with H_2O_2 to promote disease resistance in Arabidopsis (Torres et al. 2006).

Hormone Crosstalk During the Plant Wound Response

To finely tune plant responses to damage, pathogen and pest attack, hormone signaling pathways communicate (crosstalk). The JA-signaling pathway crosstalks with pathways regulated by salicylic acid (SA), abscisic acid (ABA), ET, gibberellic acid (GA), brassinosteroid (BR), cytokinin (CK), and auxin (indole acetic acid, IAA) (Meldau et al. 2012). The current dogma is that JA and ET regulate defenses against necrotrophic pathogens and herbivores, while SA is primarily involved in defense against biotrophic pathogens (Glazebrook 2005). The interactions between SA and ET and JA signaling are best studied (Li et al. 2019).

SA and JA crosstalk: SA and JA response pathways act antagonistically or in collaboration to trigger plant defenses and it is plant-species specific. JA blocks the accumulation of SA by modulating the interaction between MYC2 and three NAC transcription factor (TF) family genes (ANAC019, ANAC055, and ANAC072). NAC TFs regulate the expression of SA biosynthesis genes (Zheng et al. 2012). Phloem-feeding insects may induce both SA- and JA-dependent pathways (Walling 2000). During aphid

feeding, SA and JA pathways are simultaneously expressed in the Mi-gene mediated resistance in tomato (Martinez de Ilarduya et al. 2003). During whitefly nymph feeding, SA-regulated RNAs increase, while JA- and ET-regulated RNAs are unresponsive or decline due to JA-SA crosstalk (Zarate et al. 2007; Kempema et al. 2007); however, the JA-regulated defenses are critical for curtailing whitefly success on Arabidopsis plants (Zarate et al. 2007).

SA acts on multiple sites in the wound-signaling pathway. It inhibits AOS activity to down regulate the octadecanoid pathway (Pena-Cortés et al. 1993). Surprisingly, SA treatment does not affect 12-OPDA levels, but JA levels decrease. This suggests that SA may also negatively affect the release or transport of 12-OPDA in the peroxisome (Felton et al. 1989; Green and Ryan 1972; Doherty et al. 1988). SA also suppresses JA responses downstream of the SCF-COI1-JAZ complex (Van der Does et al. 2013). Several players that mediate crosstalk between the SA and the JA-dependent defense-signaling pathways include: the signaling protein MAP KINASE 4 (MPK4) and the transcription factors WRKY70 and NONEXPRESSOR OF PATHOGENESIS-RELATED PROTEIN 1 (NPR1). NPR1 is SA receptor and master regulator mediating the antagonistic crosstalk between SA and JA. NRP1 is required for SA-induction of WRKY70, which represses the ET/JA-signaling pathway (Ding et al. 2018; Li et al. 2004; Wu et al. 2012b). In npr1 mutants, the repressive effect of SA on JA-induced defense gene (e.g., PDF1.2) expression is eliminated (Spoel et al. 2003). The reciprocity of SA and JA crosstalk is not seen in regulation of all SA- and JA-responsive genes and may be species specific (Irigoyen et al. 2020). In addition, whether SA and JA are antagonistic, synergistic or additive is dependent on relative SA and JA levels (Mur et al. 2006).

ET and JA crosstalk: ET is known for its role in abiotic and biotic stresses, as well as in plant development including fruit ripening (Pattyn et al. 2021). The JA-signaling pathway in Arabidopsis has two branches. One which is solely JA dependent and a second that is dependent on both ET and JA (Lorenzo and Solano 2005) that cross-communicate with other hormonal pathways, such as the ET and ABA pathways via transcription factors. The transcription factor ORA59 is a main hub of the JA- and ET-signaling pathways that interacts with ERF1 and RAP2.3 (Lorenzo et al. 2003; Pré et al. 2008; Kim et al. 2018). The ethylene response factor 1 (ERF1) acts as a positive regulator of JA and ET signaling and in Arabidopsis ERF1 activates defense responses (Lorenzo et al. 2003). JA accumulation leads to de-repression of ET transcription factors (EIN3/EIL1) and induction of ET-JA responsive genes such as PDFs (Lorenzo et al. 2003; Pré et al. 2008; Zhu et al. 2011; Penninckx et al. 1998). ORA59 and RAP2.3 interaction positively regulate plant defense responses (Kim et al. 2018).

In tomato, following leaf injury or application of oligogalacturonides, systemin, or JA, PINs accumulate, and ET becomes detectable within 30 min (O'Donnell et al. 1996). This increase in ET accumulation is attributed to transcriptional upregulation of genes encoding the rate-limiting biosynthetic enzyme 1-aminocyclopropane-1-carboxylate synthase (ACS) and 1-aminocylopropane-1-carboxylate oxidase (ACO) (Vanderstraeten and Van Der Straeten 2017).

The use of loss-of-function or gain-of-function mutants was used to explore the roles of ET and JA in plant and herbivore interactions. Tian et al. (2014) studied the never-ripe (Nr) tomato mutant, which exhibits a partial block in ET perception and the defenseless (def1) tomato mutant that is deficient in JA biosynthesis. Partial blocking of ET perception did not show enhanced plant susceptibility as they had expected. In contrast,

blocking ET perception and synthesis in maize resulted in enhanced plant susceptibility to caterpillar feeding (Harfouche et al. 2006). In addition, ET and JA can negatively interact. For example, in tobacco, ET negatively regulated JA-induced nicotine biosynthesis (Kahl et al. 2000). Finally, the use of ET-signaling mutants in Arabidopsis showed differences in plant resistance. ET-signaling mutants elevated Arabidopsis resistance to a generalist herbivore, Egyptian cotton worm and had undetectable effects to herbivore, diamondback (Stotz et al. 2000).

ABA and JA interactions: ABA is "the drought-stress" plant hormone (Takahashi and Shinozaki 2019). In tomato, ABA accumulates 24 h after wounding or systemin treatment and analysis of ABA mutants demonstrated ABA is required for increases in PIN2 RNAs (Dammann et al. 1997; PenaCortes et al. 1996). The MYC2 transcription factor is the main integrator of JA- and ABA-signaling suggesting that wound and dehydration responses regulate some of the same genes (Boter et al. 2004; Dombrecht et al. 2007; Reymond et al. 2000). The tomato orthologs JAMYC2 and JAMYC10 of A. thaliana's MYC2 regulate wound-responsive genes (e.g., LAP and Pins) in tomato (Boter et al. 2004). These studies show ABA plays a synergistic role in amplifying a wound response in desiccated tomatoes. However, in some pathogen-plant interactions, ABA enhances plant susceptibility. This has been attributed to ABA interactions with the two JA-dependent branches of defense signaling, which has been best studied in Arabidopsis (Anderson et al. 2004). ABA negatively regulates the JA/ET-dependent defense pathway via MYC2. In response to herbivores, an upregulation of ABA signaling facilitated pea aphid feeding in Arabidopsis (Guo et al. 2016). In addition, induction of ABA signals decreased the accumulation of Arabidopsis defense compounds and was beneficial for green peach aphids (Hillwig et al. 2016).

The interactions of JA and ABA are also emphasized in mechanisms that regulate stomatal closure. For example, recently the GUARD CELL OUTWARD-RECTIFYING K$^+$ (GORK) channel was identified as a K$^+$-efflux channel that is essential for JA- and ABA-mediated stomatal closure (Förster et al. 2019). Stomatal closure is important in plant defense because stomata are an important portal for pathogen entry into the leaf interior (Xin and He 2013).

GA and JA crosstalk: GA is known to stimulate plant growth and delay tomato fruit ripening (Gupta and Chakrabarty 2013; Dostal and Leopold 1967). Crosstalk between JA and GA regulates the growth inhibition of whole plants that typically occurs during defense responses. This has been best characterized in Arabidopsis. The GA and JA pathways interact via DELLA proteins to fine tune the JA signaling controlled by MYC2. The GA-signaling repressor, DELLA, binds to JAZ proteins. The DELLA-JAZ protein interaction liberates JA-signaling transcription factors, such as MYC2, to up-regulate JA-response genes (Gao et al. 2011; Hou et al. 2010). In the presence of GA, DELLAs are degraded and can no longer sequester JAZ proteins, resulting in the predominance of the repressive MYC2-JAZ-corepressor complex. This leads to repression of JA-response genes and GA-mediated plant growth. GA and JA signaling antagonistic crosstalk during defense against necrotrophs reinforces the premise that plant defense occurs at the expense of growth (Meldau et al. 2012); this growth/defense reciprocity is also clearly demonstrated in SA and JA interactions and is linked to the circadian rhythm (Zhou et al. 2015).

BRs, CK and JA crosstalk: BRs promote developmental processes in plants, including cell division and growth (Peres et al. 2019). BRs also influence plant defense to several pathogens (Nakashita et al. 2003) and recruit systemin to plasma membranes

(Malinowski et al. 2009). BR receptors such as BRI1-associated receptor kinase 1 (BAK) are important for basal resistance against pathogens (Yamada et al. 2016). Furthermore, BRs interact with the JA pathway. The first evidence for this was provided by the isolation of a suppressor mutant (psc1) that partially restored the JA-insensitivity of root growth and failed to restore anthocyanin production in the coi1 mutant of Arabidopsis (Ren et al. 2009). psc1 is a leaky mutation in the BR biosynthetic gene DWF4. Subsequent studies using additional BR mutants, as well as brassinolide and BR biosynthesis inhibitor treatments, confirmed the influence of BRs in the regulation of anthocyanin biosynthesis genes, which are JA-dependent (Peng et al. 2011). There are also links between CK levels and the accumulation of secondary metabolites associated with plant immunity). In poplar, CK treatments induced genes that encode enzymes in JA-biosynthesis genes, increased JA levels and antagonized insect performance (Dervinis et al. 2010). Links between BRs and CKs are less well studied.

Auxin and JA crosstalk: Positive crosstalk exists between JA and auxin. The master regulator of JA responses, MYC2, cross-regulates auxin by activation of Auxin Response Factor (ARF18) (Zander et al. 2020). The co-chaperone SGT1b (Suppressor of G2 allele of skp1) is required for JA and IAA responses in both tomatoes and Arabidopsis after pathogen infection (Uppalapati et al. 2011). In Arabidopsis, SGT1b maintains steady state levels of COI1 for JA signaling and TIR1 F-box proteins important in auxin signaling (Zhang et al. 2015). Finally, auxin accumulation after wounding serves to repair or protect the wound sites and regenerate lost tissue. In Arabidopsis, auxin accumulates at the wound site within a day and the gene encoding WUSHCHEL-related homeobox 11 (WOX11) transcription factor is induced for tissue repair (Hu and Xu 2016; Liu et al. 2014).

15

Chloroplast Retrograde Signaling

The chloroplast is the plant cell's metabolic hub. There is a bidirectional communication between the nucleus-to-plastid (anterograde) and plastid-to-nucleus (retrograde) signaling important for plastid functionality (de Souza et al. 2017; Jiang and Dehesh 2021). The first retrograde signaling discovery was discovered on two barley (Hordeum vulgare) chloroplast ribosome-deficient mutants, whose defects in plastid functions led to downregulation of nuclear-encoded plastid proteins, phosphoribulokinase and glyceraldehyde-phosphate dehydrogenase (Bradbeer et al. 1979). This study began the robust, yet still emerging, field of retrograde signaling. Initially, the focus was on plastid biogenesis and its coordination with chlorophyll biosynthesis that is controlled by nuclear genes in young seedlings of barley, mustard, pea, or Arabidopsis (Oelmüller et al. 1986; Sullivan and Gray 1999; Susek et al. 1993).

Today, it is clear that there are two forms of retrograde signaling: biogenic and operational signaling. Biogenic signals act during the initial stages of plastid development and regulate photosynthesis-associated nuclear gene expression during light-regulated development and after disruption of plastid protein synthesis. Operational signals are generated in response to biotic and abiotic stresses (Pogson et al. 2008). Below I highlight key regulators of plant retrograde signaling. The vast majority of these studies have been conducted in Arabidopsis with the exception of the foundational studies noted above.

Genomes uncoupled 1 (GUN1): The genomes uncoupled (gun) mutants provided deep insights into the biogenic retrograde signals used in Arabidopsis (Koussevitzky et al. 2007). Initial genetic screens in Arabidopsis using an inhibitor of chloroplast-specific

protein translation, lincomycin, and photooxidative stress treatment, norflurazon (NF), resulted in repressed expression of photosynthesis-associated nuclear genes (PhANGs) and led to the discovery of six GUNs (Cottage et al. 2008; Zhao et al. 2018). All six GUNs, except for GUN1, encode enzymes in the tetrapyrrole biosynthesis or metabolism (Shimizu and Masuda 2021). GUN1 encodes a pentatricopeptide repeat protein that functions in both biogenic and operational retrograde signaling (Zhao et al. 2018); isolation of GUN1 interacting proteins is providing insights into its many modes of regulating retrograde signaling (Huang et al. 2021; Jia et al. 2019).

The Clp proteolytic complex of the chloroplast stroma keeps GUN1 levels low under non-stress conditions (Tadini et al. 2020). By binding the ClpC1 chaperone, GUN1 is kept at low levels in plants. However, GUN1 accumulates during early steps of chloroplast biogenesis and under stress including high light, heat, drought, and ROS (Wu et al. 2018). GUN1 binds to porphyrins reducing protochlorophyllide synthesis and, thereby, lessens the tetrapyrrole biosynthetic pathway flux in chloroplasts (Shimizu and Masuda 2021; Susek et al. 1993). Porphyrin rings possess photodynamic properties that can generate ROS during light stress, primarily singlet oxygen leading to photooxidative damage and cell death (op den Camp et al. 2003). Therefore, it is important for plants to regulate tetrapyrrole biosynthesis, as lower levels of protochlorophyllide curtail the production of ROS that damage cellular macromolecules.

GUN1 has a big impact on the transcription and editing of plastid-genome encoded genes in Arabidopsis (Tadini et al. 2020). In chloroplasts, two different RNA polymerases transcribe different sets of chloroplast genes: Nuclear-encoded RNA polymerase (NEP) and plastid-encoded polymerase (PEP) (Börner et al. 2015). NEP transcribes housekeeping genes and PEP transcribes over 80% of the plastid genes, predominately

17

those associated with photosynthesis (Hajdukiewicz et al. 1997). Lincomycin treatments result in suppression of PEP-dependent transcription. To compensate for the loss of PEP-dependent transcription, GUN1 interacts with NEP to deploy the Δ-rpo adaptive response, which encompasses an accumulation of NEP-dependent transcripts (Tadini et al. 2020). The impaired PEP dependent proteins are classified in several categories: plastid transcription regulation, plastid transcripts maturation, plastid translation, and plastid proteostasis maintenance.

In addition, GUN1 accumulation during stress conditions and early stages of chloroplast biogenesis leads to GUN1 interactions with Multiple Organellar RNA-editing factor 2 (MORF2), a member of plastid RNA editosome, which is a collection of three RNA-editing factors in the plastid (Zhao et al. 2019). The MORF2 targets are NEP-dependent transcripts. The MORF2-GUN1 interactions negatively regulates RNA-editing efficiencies (Zhao et al. 2019; Zhao et al. 2020).

The GUN1-dependent suppression of PhANGs may contribute to protection from oxidative stress (Zhang et al. 2011). In addition, GUN1-dependent upregulation of NEP-dependent transcripts upon suppression of PEP activity may maintain the housekeeping functions of plastids and reducing oxidative damage to photosynthesis.

Methylerythritol cyclodiphosphate (MEcPP): MEcPP is synthesized via the plastidial methylerythritol phosphate (MEP) pathway (Zhou and Pichersky 2020). This pathway produces the precursors of a wide variety of isoprenoids and MEcPP regulates chloroplast-nuclear communication functioning as an operational signal (Xiao et al. 2012). As MEcPP influences JA-SA crosstalk and my project focuses on the role of JA-induced LAP-A in regulated defenses, this section in expanded relative to other retrograde signal sections (see below).

MEcPP's role in retrograde signaling was revealed in Arabidopsis through a forward-genetic screen to identify regulators of HYDROGENPEROXIDE LYASE (HPL). The ceh1 (CONSTITUTIVELY EXPRESSING HPL, hsd-4) expresses HPL transcripts constitutively. CEH1 encodes hydroxymethylbutenyl diphosphate synthase (HDS) a key enzyme of the MEP pathway. The ceh1 mutant caused the metabolite MEcPP to accumulate resulting in a stunted growth phenotype (Xiao et al. 2012). MEcPP accumulates in response to numerous stresses including high light, oxidative stress, high temperatures, heavy metals, and aphid feeding (Li and Sharkey 2013; Ostrovsky et al. 1998; Wang et al. 2017; Xiao et al. 2012; Kimura et al. 2003).

Accumulation of MEcPP in the plastid induces selected nuclear-encoded, stress-response genes classifying MEcPP as a retrograde signal (Lemos et al. 2016; Walley et al. 2015; Wang et al. 2017; Xiao et al. 2012). These MEcPP- response genes are activated in a Ca^{2+}-dependent manner via the calmodulin-binding transcription activator 3 (CAMTA3) (Benn et al. 2016). CAMTA3 regulates general stress-response genes in the nucleus by binding to the rapid stress-response element (RSRE). MEcPP coordinates light and hormonal signaling, specifically through PHYB protein abundance and by suppressing the expression of nuclear transcription factors phytochrome-interacting factor 4/5 (PIF4/5), which are responsible for the induction of auxin and ethylene biosynthetic genes (Jiang et al. 2020). In this manner, MEcPP leads to reduction of auxin and ET levels to regulate plant growth in response to high light environments (Jiang et al. 2020). In addition, MEcPP decreases the abundance of the auxin transporter protein PIN1 and thereby affects auxin distribution; this further increases PHYB abundance and modulates ET-auxin levels to regulate plant growth (Jiang et al. 2018).

MEcPP also impacts plant defense. High levels of MEcPP induce the expression of the SA biosynthetic enzyme gene ISOCHORISMATE SYNTHASE 1 (ICS1) and, not surprisingly, the ceh1 mutant accumulates high levels of SA and confers enhanced resistance to the biotrophic pathogen Pseudomonas syringae (Xiao et al. 2012). Transcriptome profiling of the ceh1 mutant revealed that MEcPP regulates SA-JA crosstalk (Lemos et al. 2016). When MEcPP levels are elevated JA-response genes are activated despite the presence of high SA levels (Lemos et al. 2016). In addition, different alleles of the HDS gene (cbl4-2, cbs3, hds3) also accumulated high levels of MEcPP, ME-glycosides, and SA constitutively and conferred resistance to biotrophs (Hyalperonospera arabidopsis and P. syringae) but did not influence resistance to necrotrophs (Plectosphaerella cucumerina or Botryis cinerea) (Gil et al. 2005). In all studies the accumulation of SA and resistance was dependent on known regulators of the SA-signaling pathway. In addition, the response to MEcPP may be dependent on a plant's developmental stage (González-Cabanelas et al. 2015).

MEcPP also modulates defenses to herbivory. Arabidopsis hds-3 and ceh1 mutants are more resistant to the cabbage aphid (Onkokesung et al. 2019; González-Cabanelas et al. 2015). However, plant resistance to cabbage white caterpillars were not enhanced (Onkokesung et al. 2019). The analysis of primary and secondary metabolites in non-infested and infested hds3 mutants showed lower levels of glucosinolates and isoprenoid metabolites compared to non-infested and infested wild-type plants. As a result, it affected the metabolic flux whereby the plants are more resistant to aphid attack. There is evidence that glucosinolate levels are regulated in response to biotic stress including wounding, herbivory, and SA treatments (Bidart-Bouzat and

Kliebenstein 2008; Kim and Jander 2007; Mewis et al. 2006; Brown et al. 2003; Kliebenstein et al. 2002).

Nucleotide phosphatase (SAL1) and 3'-phosphoadenosine 5'-phosphate (PAP): The SAL1-PAP chloroplast retrograde signal functions in response to drought and high light in Arabidopsis classifying it as an operational signal (Estavillo et al. 2011; Chan et al. 2016a; Chan et al. 2016b). In non-stress conditions, the nucleotide phosphatase SAL1 dephosphorylates PAP to produce adenosine monophosphate in the chloroplast. High light and drought repress SAL1, which leads to overaccumulation of PAP. High light stress generates ROS such as singlet oxygen ($^1O_2$) at photosystem II (PSII) and superoxide (O_2^-) at photosystem I, which is catabolized to H_2O_2 in photosystem I (PSI) (Asada 2000). ROS accumulation results in the inactivation of SAL1 in the chloroplast and allowing accumulation of the substrate, PAP (Chan et al. 2016a).

PAP moves from the chloroplast to the nucleus via a bidirectional transporter ADP/ATP carrier of the thylakoid membrane, TAAC/ PAPST1 (Zhao et al. 2019; Estavillo et al. 2011; Chan et al. 2016a; Gigolashvili et al. 2012). PAP inhibits RNA-degrading activity of the 5' to 3' exoribonuclease (XRN) altering posttranscriptional gene silencing, mRNA turnover, and transcription. Nuclear XRN2 and XRN3 act on uncapped RNAs (e.g., excised hairpin loops form part of precursor microRNA transcripts) (Liu and Chen 2016). Gy et al. (2007) showed uncapped RNAs accumulate in sal1 mutants.

PAP indirectly regulates stomatal closure as an avoidance response to drought stress (Pornsiriwong et al. 2017). The PAP-XRN interaction in the nucleus activates the anion channel SLOW ANION CHANNEL-ASSOCIATED 1 (SLAC1) leading to stomatal closure as a response to abiotic stress (Pornsiriwong et al. 2017). PAP also influences JA and IAA signaling to impair plant growth as a response to perceived high light and

drought. PAP induction of LOX2 enhances JA levels and regulation of leaf development (Rodríguez et al. 2010). PAP induction of auxin and phyB degradation downregulates hypocotyl growth (Ishiga et al. 2017; Jiang et al. 2020).

SAL1-PAP retrograde signaling also affects defense by regulating the glucosinolate biosynthetic pathway and hormone signaling (Ishiga et al. 2017). Arabidopsis sal1 mutants (fry1-2 and alx8) are hypersusceptible to the pathogens Pseudomonas syringae pv. tomato DC3000 (a hemibiotroph) and Pectobacterium carotovorum subsp. carotovorum EC1 (a nectrotroph) compared to wild-type Col-0 and SAL1-overexpression plants (Ishiga et al. 2017). Mutations in sal1 also compromise ETI. This correlates with down regulation of the SA- and JA-signaling pathways, as evidenced by expression of sentinel genes, as well as decreased levels of glucosinolates.

Apocarotenoids and β-cyclocitral: Carotenoids are MEP pathway-derived isoprenoid compounds synthesized in plastids (Cazzonelli and Pogson 2010). Apocarotenoids and β-cyclocitra are important for the light-harvesting apparatus; acting as ROS scavengers, they protect the photosynthetic machinery from ROS that is generated during photosynthesis and stress (Cazzonelli and Pogson 2010). Apocarotenoids include the phytohormones ABA and strigolactones (SLs). In addition, cis-carotene-derived apocarotenoids and β-cyclocitral are retrograde signals. Apocarotenoids are formed enzymatically or spontaneously and they stimulate expression of nuclear-genome-encoded genes including: ELONGATED HYPOCOTYL5 (HY5), PHYTOCHROME-INTERACTING FACTOR3 (PIF3) and many photosynthesis-associated nuclear genes (PhANGs) (Cazzonelli et al. 2020).

β-cyclocitral, a β-carotene oxidation by-product, is generated in chloroplasts under high light and activates β-cyclocitral transcription of ICS1, which is responsible for the

production of SA (D'Alessandro et al. 2018). The rise in SA and changes in redox state promotes the translocation of SA receptor, NPR1, from the cytosol to the nucleus acting as a transcriptional activator of SA and SA-response genes. Plants with high levels of β-cyclocitral display resistance to high light and have enhanced resistance to bacterial pathogens (D'Alessandro et al. 2018; Lv et al. 2015; Liu et al. 2020). β-cyclocitral also induces SCARECROW-LIKE14 (SCL14) and ABA-responsive NAC (ANAC) transcription factor transcripts, which enhances plant growth and results in a phenotype of acclimation to high light (D'Alessandro et al. 2018). Application of β-cyclocitral enhances root growth and branching in Arabidopsis, rice, and tomato (Dickinson et al. 2019). Whereas the role of β-cyclocitral in plant defense is understudied, its role in increasing SA levels and promoting NPR1 translocation suggests a possible role in defense. In accordance, β-cyclocitral treatments protects African spider plants from two-spotted spider mites and grapevines from the oomycete Plasmopara viticola causing downy mildew (Nyalala et al. 2013; Lazazzara et al. 2018).

Transcription factor mobility between plastid and nucleus: Chloroplast development requires communication with the nucleus; dual-localized proteins and transcription factors may also facilitate chloroplast-to-nucleus communication. Transcription factors such as the PHD TYPE TRANSCRIPTION FACTOR WITH TRANSMEMBRANE DOMAINS (PTM) and WHIRLY1 are putative retrograde signals; they are able to translocate from the chloroplast to the nucleus (Foyer et al. 2014; Isemer et al. 2012; Sun et al. 2011). PTM is a chloroplast envelope-bound plant homeodomain (PHD) transcription factor that is cleaved in response to photooxidative stress and its truncated product moves to the nucleus to regulate photosynthetic gene expression (Sun et al. 2011). However, the role of PTM in retrograde signaling was

recently challenged (Page et al. 2017) and it has been suggested that PTM be removed from the retrograde signal list (Mielecki et al. 2020).

WHIRLY1 moves from the chloroplast to the nucleus after perception of redox changes in the photosynthetic apparatus that convert the WHIRLY1 oligomer to a monomer (Ren et al. 2017; Foyer et al. 2014). The monomeric WHIRLY1 is folded to reveal a nuclear localization signal motif that allows its relocation to the nucleus similarly to the SA receptor, NRP1 where it interacts with TGACG-sequence-specific protein-binding (TGA) transcription factors (Rochon et al. 2006). Once in the nucleus, WHIRLY1 induces PR and WRKY53 gene expression.

The transcription factor ABSCISIC ACID INSENSITIVE4 (ABI4) is not mobile but may be involved in retrograde signaling. ABI4 appears to have a role in mitochondria-to-nucleus signaling as evidenced by its role in regulating the mitochondrial ALTERNATIVE OXIDASE gene (Giraud et al. 2009). The role of ABI4 in chloroplast-to-nucleus retrograde signaling has remained more controversial; with some groups implicating ABI4 and GUN1 in the same signaling pathway, others concluding ABI4 and GUN1 may regulate independent pathways, and others that could not generate a gun1 phenotype from four different abi4 alleles (Mielecki et al. 2020).

ROS and Redox Hubs in the Chloroplast: Aside from their potential toxicity to plants, low levels of ROS and their associated redox networks serve as cellular signals. ROS is created in several cellular locations including the apoplast (via the plasma membrane bound NADPH oxidases), chloroplast, mitochondrion, and peroxisome (Foyer and Noctor 2016). In the chloroplast, ROS is generated in as byproducts of photosynthetic light reactions: $^{1}O_2$ at PSII and O_2^- at PSI (Asada 2000). Superoxide anion (O_2^-) s the short-lived precursor of H_2O_2, as O_2^- is rapidly dismutated by

superoxide dismutases (SODs) to form H_2O_2. Most research regarding ROS as retrograde signals is done in Arabidopsis (Cejudo et al. 2020).

H_2O_2 is longer lived than the other ROS and can move from the chloroplast to alter cytosolic and nuclear redox states and regulate nuclear gene expression (Exposito-Rodriguez et al. 2017; Vogel et al. 2014). H_2O_2 movement may be facilitated by aquaporins (Bienert and Chaumont 2014). In addition, stromules (stroma-filled tubules) that physical connect chloroplasts with the nucleus may also facilitate for H_2O_2 translocation (Dietz et al. 2016). To demonstrate that H_2O_2 is a retrograde signal, cells expressing a genetically encoded H_2O_2 sensor were exposed to high light, which elevates ROS levels. These studies showed that H_2O_2 originating from the chloroplast is transferred to the nucleus (Exposito-Rodriguez et al. 2017). These data suggested a close association between the chloroplast and nuclei avoiding the need to translocate through the cytoplasm (Exposito-Rodriguez et al. 2017).

$^1O_2$ is another retrograde signal, despite its short half-life (200 ns) that was revealed by studies on the Arabidopsis Fluorescent In Blue Light (FLU) gene, which is a negative regulator of tetrapyrrole biosynthesis (Kauss et al. 2012; Meskauskiene et al. 2001). When dark-adapted flu plants are transferred to light, the photosensitizing protochlorophyllide molecules generate $^1O_2$, which cause bleaching of young seedlings and growth inhibition in mature plants (Wagner et al. 2004) due to oxidation of β-carotene (see section above) or damage to D1 protein necessitating turnover and replacement (Krieger-Liszkay et al. 2008; Ramel et al. 2012). The light induced flu phenotype is suppressed by inactivation of EXECUTER1 (EX1) and EX2 (Lee et al. 2007). executer mutants block the transmission of the $^1O_2$-generated signal to the nucleus that reprograms expression of ~5% of the genome. Recent data indicate, $^1O_2$

generated in thylakoids oxidizes a Trp residue of EX1. FtsH2-dependent cleavage of the oxidized EX1 protein is necessary for induction of this signaling pathway (Dogra et al. 2017; Dogra et al. 2019; Wang et al. 2016). More stable second messengers derived from $^1O_2$ in the plastid activate a signaling pathway to regulate nuclear gene expression. The $^1O_2$ induces expression of nuclear-encoded SA- and JA-response genes, including PR1 and several WRKYs (Danon et al. 2005).

Recently, a new $^1O_2$-induced retrograde signaling pathway has been discovered: the $^1O_2$-SAFEGUARD1 (SAFE1) pathway independent of EX1 (Wang et al. 2020). SAFE1 is localized in the chloroplast stroma and is degraded after induction of $^1O_2$. In the absence of SAFE1, grana margins of chloroplast thylakoids are targets of $^1O_2$ and damaged grana margins results in stress signaling independent of EX1. Plant phenotypes are cell death of young seedlings and growth inhibition of mature plants. Therefore, SAFE1 protects grana margins from damage caused by $^1O_2$.

Treatments in Arabidopsis seedlings with methyl viologen (MV), a $O_2^{\cdot-}$ propagator, show an upregulation of nuclear genes in microarray data. These data suggest that changes in $O_2^{\cdot-}$ levels can be perceived (directly or indirectly) and, therefore, $O_2^{\cdot-}$ can be considered a retrograde signal (Scarpeci et al. 2008; Laloi et al. 2007). As a short-lived ROS, $O_2^{\cdot-}$ is not likely to move to the nucleus to execute its control, therefore a mobile secondary signal is needed. ROS signaling depends on the post-translational modification of ROS targets (Mock and Dietz 2016; Liebthal and Dietz 2017). The targets are often enzymes of metabolic pathways or stress-associated metabolites. In addition, $O_2^{\cdot-}$ can act on redox-mediated regulation of enzymes in metabolite biosynthetic pathways. For example, $O_2^{\cdot-}$ acts on carotenoids to oxidize and generate a retrograde signals such as β-cyclocitral as previously discussed (Ramel et al. 2012).

To limit damage to cellular components and to assure ROS-generated retrograde signals are transient, ROS levels are controlled by the action of ROS scavenging systems/antioxidants (Hasanuzzaman et al. 2020). Non-enzymatic ROS scavenging systems include carotenoids, ascorbate, and glutathione (Pinnola and Bassi 2018). Enzymatic ROS scavenging systems include: Cu/Zn-and Fe-superoxide dismutases (SODs), ascorbate peroxidase (APX), and 2-Cys Peroxiredoxin (2-Cys Prx) (Pilon et al. 2011; Serrato et al. 2004) (Puerto-Galán et al. 2015). SODs act on O_2^- to produce H_2O_2, which can then generate hydroxyl radicals ($^\bullet OH^-$) by the Fenton reaction (Asada 2000; Khorobrykh et al. 2020)

The NADP-dependent Thioredoxin Reductase C (NTRC) and 2-Cys-peroxiredoxin (2-Cys-Prx) is a key redox regulatory system in chloroplasts. NTRC acts as the primary reductant of 2-Cys Prxs, the most abundant chloroplast thiol-dependent peroxidases that scavenge H_2O_2 (Nikkanen and Rintamäki 2019). 2-CysPrx interactors have been identified (Muthuramalingam et al. 2009). Together NTRC and 2-CysPrx regulate metabolic enzymes, such as FBPase (Konig et al. 2002; Collin et al. 2003; Broin and Rey 2003; Laxa et al. 2007; Rey et al. 2005; Muthuramalingam et al. 2009), and molecules that are associated with retrograde signaling. For example, this redox system regulates the stability of tetrapyrrole biosynthetic enzymes [eg., GluTR, Mg-protoporphyrin IX methyltransferase (CHLM), the CHLI subunit of Mg-chelatase, and the Mg-protoporphyrin IX methylester cyclase (CYC)] that produce the photosensitizing tetrapyrroles critical of signaling by EX1 and EX2 and ultimately produce chlorophyll as the end-product (Stenbaek et al. 2008; Richter et al. 2013; Richter et al. 2018; Pérez-Ruiz et al. 2014). The NTRC/2-Cys-Prx redox system may also modulate the redox state of phosphatase SAL1, which activates the retrograde signal PAP (Chan et al. 2016a). It

has also recently been proposed that 2-Cys-Prxs and its substrate H_2O_2 may regulate transcription of HSP70-4, HSP90-1, and other stress-response genes (Ojeda et al. 2021; Pérez-Ruiz et al. 2017).

GSH is an essential non-enzymatic antioxidant and metabolite that regulates redox status in plant cells among other cellular roles (Noctor et al. 2012). GSH is a tripeptide composed of Glu, Cys, and Gly in which the Glu attaches to the Cys at the γ–carboxyl group of Glu (Noctor et al. 2012). GSH is synthesized by two enzymatic reactions. First, the γ-EC synthase (γ-ECS; GSH1) forms the γ-Glu-Cys bond. Second, the GSH synthase (GSH-S; GSH2) joins Gly to the γ-Glu-Cys dipeptide (Meister 1988; Mullineaux and Rausch 2005; Rennenberg 1980). GSH1 and GSH2 transcripts accumulate in response to JA and H_2O_2 treatments (Queval et al. 2009; Xiang and Oliver 1998). Glutathione degradation is not as well characterized as its biosynthesis (Bachhawat and Kaur 2017). This dissertation will explore further glutathione catabolism in tomato wild-type and mutant plants by our protein of interest, Leucine aminopeptidase A.

Leucyl aminopeptidases – A potential defense regulatory hub

As noted in the JA signaling section of this Introduction, the tomato leucyl aminopeptidase (LAP-A) is a regulator of the tomato defense response. The over-arching goal of Walling lab is to understand the full spectrum of LAP-A-dependent changes at the transcriptome, proteome and metabolome levels. To provide context for the goals of my dissertation, an overview of LAPs in plants, animals and microbes is provided. I also review our current understanding of the tomato LAPs and their role in defense.

Overview of aminopeptidases in plants, animals, and microbes: Peptidases hydrolyze internal peptide bonds (endoprotease) or bonds the amino (N) or carboxyl (C) terminus (aminopeptidase or carboxypeptidase) or proteins and peptides (Rawlings and Barrett 2013). In addition, postranslational modifications of target proteins (such as phosphorylation, oxidation of residues, and ubiquitination) can tag a protein for degradation (Ling et al. 2019). Proteolysis is essential for protein turnover and nitrogen recycling during seed germination, plant growth, development, and leaf senescence (Kelley and Estelle 2012; Van der Hoorn 2008). Proteolysis occurs in all stages of plant development from embryogenesis, inflorescence development, programmed cell death, circadian rhythms to phytohormone signaling and stress responses (Sharma and Gayen 2021).

Aminopeptidases cleave N-terminal residues from peptides and proteins (Walling 2013). Aminopeptidases are important for protein turnover, maturation, and peptide catabolism (van Endert 2011; Meinnel et al. 2006). In addition, aminopeptidases may expose the penultimate residue that affects a protein's half-life as predicted by the N-degron pathway (Walling 2006; Graciet and Wellmer 2010; Varshavsky 2011). Plant aminopeptidases regulate diverse processes such as meiotic recombination (Sanchez-Moran et al. 2004), cell cycle progression (Peer et al. 2009), seedling development (Peer et al. 2009), and defense (Fowler et al. 2009).

LAPs are conserved in plants, animals, and microbes (Straeter and Lipscomb 2013; Colloms 2013; Matsui et al. 2006; Nandan and Nampoothiri 2017; Panpetch and Sirikantaramas 2021; Mathew et al. 2021; Wanat et al. 2019). The ~55-kDa LAP subunits assemble into homo-hexamers. Animal LAPs are important for turnover of oxidatively damaged proteins in the eye lens and Cys-Gly catabolism (a product of

glutathione catabolism) and for antigen presentation (Taylor 1985; Cappiello et al. 2004; Jösch et al. 2003). The microbial LAPs (PepA) are aminopeptidases, as well as DNA-binding proteins; they are responsible for site-specific recombination and function as a transcription factors that modulate several operons (Stirling et al. 1989; Charlier et al. 1995). In tomato, LAP modulates wound signaling (Fowler et al. 2009).

Plant LAPs and LAP-A History: In tomato, there are two classes of LAPs that are distinguished by their isoelectric point; LAP-A is acidic and LAP-N is neutral. Plastid import and immunolocalization studies indicate that LAP-A and LAP-N are localized in the chloroplast stroma (Narvaez-Vasquez et al. 2008; Tu et al. 2003). In tomato, LAP-N is encoded by a single gene. LAP-N and LAP-N-like proteins are conserved in all plants and accumulate in all organs (Chao et al. 2000; Gu et al. 1999; Tu et al. 2003; Chao et al. 1999; Milligan and Gasser 1995). LAP-N proteins are constitutively expressed within the plant and unresponsive to stress (Tu et al. 2003; Chao et al. 2000). The tomato LAP-A protein is encoded by two highly related genes LapA1 and LapA2. These genes are regulated during plant development and in response to abiotic and biotic stress. LAP-A is discussed in greater detail below.

Arabidopsis LAP: Arabidopsis has three LAP genes (LAP1-3) that are most similar to tomato's LAP-N (Walling 2013). None of the Arabidopsis LAP genes are induced by wounding (Bartling and Nosek 1994; Bartling and Weiler 1992; Waditee-Sirisattha et al. 2011a). LAP2 and LAP3 are chloroplast localized, and LAP1 resides within the cytosol (Bartling and Weiler 1992). Like the tomato LAPs, the Arabidopsis LAPs possess both aminopeptidases (Bartling and Nosek 1994; Waditee-Sirisattha et al. 2011b) and chaperone activities (Scranton et al. 2012; Waditee-Sirisattha et al. 2011b). The Arabidopsis LAP2 preferentially hydrolyzing N-terminal Leu, Met and Phe residues and

is a regulator of cell growth, photosynthesis and nitrogen metabolism (Waditee-Sirisattha et al. 2011a; Waditee-Sirisattha et al. 2011b). In contrast, The Arabidopsis LAP1 catabolizes cytosolic Cys-Gly (Kumar et al. 2015).

LAP-A subcellular localization and biochemical functions: In contrast to the ubiquitous LAPs of Arabidopsis and tomato LAP-N proteins, LAP-A is present only in a subset of Solanaceae (Chao et al. 2000; Hartl et al. 2008; Herbers et al. 1994; Dammann et al. 1997). In tomato, there are two highly related genes that encode LAP-A (LapA1 and LapA2) (Gu et al. 1996b). LapA RNAs accumulate during floral and fruit development and at high levels in mature flowers (Tu et al. 2003; Pautot et al. 1993; Chao et al. 1999). LapA RNAs do not accumulate or are at low levels in foliage from healthy plants (Chao et al. 1999).

LapA has also been studied in potato. LapA RNAs accumulate in potato (Solanum tuberosum) tubers after wounding and in response exogenous ABA and JA (Hildmann et al. 1992). Similar to potato, tomato LAP-A mRNA, proteins, and activity are induced after mechanical wounding (Pautot et al. 1993; Gu et al. 1996a; Gu et al. 1996b; Pautot et al. 1991).

The tomato LAP-A is well characterized biochemically (Gu et al. 1999; Gu and Walling 2000; Walling 2013; Gu and Walling 2002; Duprez et al. 2014). In vitro studies on synthetic peptides showed LAP-A preferably hydrolyzes substrates with basic (Arg) and nonpolar (Leu, Val, Ile and Ala) residues at the N-terminal and penultimate residues (Gu and Walling 2000; Gu et al. 1999). The N-terminus (+1) and penultimate residue (+2) residues of peptides influence both the substrate affinity (K_m) and the catalytic ability (V_{max} and k_{cat}) of LAP-A (Gu and Walling 2000; Gu et al. 1999; Gu and Walling 2002). One of the goals of discovering the X-ray crystal structure of LAP-A was to define LAP-

A's central cavity to identify the rest of the preferential residues for a putative substrate. However, the hexamer LAP-A central cavity formed by the substrate-binding channels is wider than expected (Duprez et al. 2014). LAP-A can bind and hydrolyze peptide substrates larger than six residues indicating the LAP-A may have a role in the turnover of small peptides and the hydrolysis of the termini of full length proteins (Duprez et al. 2014).

In addition, LAP-A is a molecular chaperone that prevents protein unfolding and aggregation and promotes protein refolding (Scranton et al. 2012; Walling 2013). Three assays (thermal restriction enzyme protection, thermal citrate synthase aggregation, and luciferase refolding assays) were used to monitor protein protection from heat-induced damage (Scranton et al. 2012). LAP-A's chaperone activity may be important for plant immune responses against insects. LAP-A may maintain the protein conformation and activity of defense proteins such as threonine deaminase and arginase, which function as anti-nutritive proteins in insects by depleting amino acids in herbivore's midgut (Chen et al. 2005).

Cell fractionation studies and immunoblot analyses of chloroplasts and total proteins showed wound-induced LAP-A is localized in plastids (Gu et al. 1996b). An in vitro-transport study with pea chloroplasts showed transit peptides from LAP-A and LAP-N precursor proteins functioned as targeting signals into leaf chloroplasts (Narvaez-Vasquez et al. 2008). Finally, an immunocytochemical assay using LAP-polyclonal and a LAP-A-specific antiserum showed low levels of LAPs in healthy leaves, and levels accumulated within chloroplasts of leaf mesophyll cells after wounding or MeJA treatment of tomato plants (Narvaez-Vasquez et al. 2008).

The chloroplast-localized LAP-A is critical for a robust wound response (Fowler et al. 2009). LapA RNA levels increase 4 to 24 h after mechanical wounding (Chao et al. 1999). LapA RNAs and proteins increase in response to biotic (Manduca sexta, Spodoptera littoralis, Phytophtora parasitica, and Pseudomonas syringae) and abiotic stresses (water deficit and salinity), systemin, MeJA, ET, and ABA (Chao et al. 1999; Pautot et al. 2001; Pautot et al. 1993; Bottin et al. 1994; Jwa and Walling 2001; Dammann et al. 1997).

Transgenic tomato plants to study LAP-A: The genetic analysis of plants with altered LAP-A levels in tomato was performed by Pautot et al. (2001) using a LapA-antisense construct 35S:asLapA1 (LapA-AS). While these plants had lower levels of LapA RNAs in healthy and wounded leaves, the levels of LAP-A proteins from healthy and wounded leaves from control and LapA-AS were not significantly different. In addition, no negative effects on caterpillar (Manduca sexta) and P. syringae pv. tomato growth were observed.

In Fowler et al. (2009), transgenic tomato lines that ectopically express LAP-A using a 35S promoter, P35S:LapA1 (LapA-OX) were constructed and tested for resistance to herbivory. LapA-OX plants display no fitness costs. LapA-OX are more resistant to M. sexta feeding as measure by reduced foliage consumption and reduced larval masses relative to wild-type (wild-type) plants. Some of the P35S:LapA1 lines silenced the transgene (LapA-SI). LapA-SI are more susceptible to insect feeding than wild-type plants. More LapA-SI foliage was consumed and masses of larvae fed on LapA-SI were x-fold larger than those that fed on wild-type plants. These mutant plants provide a route to study LAP-A's role in plant immunity (Fowler et al. 2009).

LAP-A exerts its control by upregulating late wound-response nuclear genes (e.g., PPO, Pin1, Pin2) and by downregulating pathogenesis-related 1 (PR-1c and PR-1a2) and two dehydrin (TAS14 and Dhn3) genes (Fowler et al. 2009; Scranton et al. 2013). The late-wound response transcripts accumulate to lower levels in LapA-SI in comparison to wild-type plants. Reciprocally, the late-wound response transcripts accumulate to higher levels in LapA-OX plants. LAP-A does not influence early wound-response genes (LOX-D, AOS, Prosystemin). LAP-A acts downstream of JA biosynthesis as shown by the inability of JA to restore the late wound response transcript accumulation in LapA-SI and LapA-AS plants (Fowler et al. 2009). The late branch of tomato wound signaling is positively modulated by H_2O_2 and negatively modulated by nitric oxide (Orozco-Cardenas et al. 2001; Orozco-Cardenas and Ryan 2002).

What is the LAP-dependent retrograde signal?

Since LAP-A resides in the stroma and controls nuclear gene expression, it must produce or modulate a retrograde signal (Fowler et al. 2009; Jung and Chory 2010; Jiang and Dehesh 2021; de Souza et al. 2017). Several defense regulators begin their synthesis within the plastid including: H_2O_2, NO, JA, SA, GA, BR, and ABA (Fowler et al. 2009; Orozco-Cardenas et al. 2001; Orozco-Cardenas and Ryan 2002; Doares et al. 1995a; Chao et al. 1999; Pena-Cortes et al. 1996). LAP-A does not alter JA, JA-Ile, SA, SA-glucoside, ABA, or ABA-glucoside levels after wounding (Scranton and Walling, unpublished) and therefore it is likely to regulate a novel retrograde signal. As retrograde signals can be mobile proteins, peptides, chemicals, or metabolites that perceive and dissipate ROS, the LAP-dependent retrograde signal(s) is hard to guess. The use of tomato wild-type (cultivar), LapA-SI, and LapA-OX plants should help us identify the

34

targets and the mechanism of LAP-A action and the identity of the LAP-A dependent signal(s).

The Walling lab applies a multi-omics approach to understand the mechanisms of LAP-A-dependent signaling to identify LAP-A substrates. Using MeJA time courses and wild-type, LapA-SI and LapA-OX plants, we are defining the magnitude of transcriptome reprogramming in response to MeJA and will identify genes whose expression are LAP-A dependent (Roche and Walling, unpublished results). Using MeJA treatments of wild-type, LapA-SI and LapA-OX plants, we have explored the MeJA and LAP-A dependent proteome and N-terminal proteome (Bhattacharya, Ortiz and Walling, unpublished results). I have contributed to both proteomics and metabolomics studies of wild-type and LAP mutant plants.

My Dissertation has four goals:

Goal 1. Leverage a tomato Chloroplast Proteome (Atlas) to predict putative LAP-A substrates.

Goal 2. Chapter 1: The tomato chloroplast Atlas and defining the tomato stromal proteome.

Goal 3. Chapter 2: LAP-A and MeJA regulate primary and secondary metabolites in an array of biochemical pathways.

Goal 4. Chapter 3: LAP-A's role in redox homeostasis and sulfur assimilation.

Goal 1. Leveraging a tomato Chloroplast Stromal Proteome Atlas to predict putative LAP-A substrates.

My initial goal was to identify putative LAP-A biological substrates based on two sets of data. First, I was to use our biochemical studies that identified the residues at the N-terminus (+1) and penultimate residue (+2) that promoted or inhibited peptide hydrolysis

35

by LAP-A (Gu and Walling 2000, 2002), (see Section "Plant LAPs and LAP-A History"). Second, I was to use an X-ray crystal structure of LAP-A to predict the residues of putative LAP-A substrates. Based on the size of the LAP-A substrate-binding pocket, I was to predict the residues at the +1 to +4 positions of putative substrates.

In anticipation of the X-ray crystal structures, I used five different subcellular localization algorithms to identify the tomato proteins that were in silico predicted to reside within the tomato chloroplast. This collection of proteins (the Chloroplast Proteome Atlas) is described in Chapter 1. The Atlas provided a subset of tomato proteins be interrogated for their likelihood of being hydrolyzed by LAP-A. While I was developing the Atlas, our first tomato LAP-A crystal structure was completed (Duprez et al. 2014). We showed that the substrate-binding pocket of each LAP-A protomer was relatively large and predicting the residues at the +2, +3 and +4 positions was not feasible. While my plans to identify putative substrates in silico were dashed, the Atlas has been a useful tool for our proteomics studies.

Goal 2: Defining the tomato stromal proteome subset of the chloroplast proteome Atlas.

To identify putative LAP-A substrates, it was critical to define the tomato stromal proteome. In Chapter 1, I describe an collaborative project with Oindrila Bhattacharya (UC Riverside PhD candidate in the CMDB program) to delineate the tomato stromal proteome; we have contributed equally to the work in this chapter and when published, we will be co-first authors. To date, only the stromal proteomes of Arabidopsis (Olinares et al. 2010; Peltier et al. 2006; Lundquist et al. 2017) and maize (Huang et al. 2013) are described. With recent advances in the accuracy and depth of proteome coverage, this work is a significant contribution to the chloroplast proteome field and bioinformatics field

for proteins' subcellular predictions. I describe the methods used to construct a theoretical tomato chloroplast proteome (the Atlas). Along with resources from Arabidopsis, the Atlas was used to enable our identification of the tomato stromal proteome and to identify a set of proteins that co-purified with tomato chloroplasts (Bhattacharya, Ortiz and Walling 2020). Our extensive manual curation of the tomato stromal proteome allowed functions to be assigned to all but 88 of the 1254 stromal proteome.

Goal 3. Leucine aminopeptidase A and MeJA regulate primary and secondary metabolites in an array of biochemical pathways.

In Chapter 2, I used targeted and untargeted metabolomics to discover the metabolites regulated by LAP-A and MeJA. Wild-type, LapA-SI, and LapA-OX plants were treated with MeJA. These time-course experiments defined the temporal response of metabolites regulated by MeJA and the metabolites that accumulated in a LAP-A dependent manner. I identified both primary and secondary metabolites that were regulated by LAP-A and/ or MeJA. A more in-depth analysis of selected metabolites was performed on four amino acid pathways (Ile, Leu, Met and Thr) and three secondary metabolite pathways with roles in defense including flavonoids, pipecolic acid and steroidal glycoalkaloids. For pipecolic acid and steroidal glycoalkaloids, I correlated metabolites with the levels of the respective biosynthetic enzymes from proteomics data sets. In addition, I performed qRT-PCR to correlate temporal changes in these metabolites with transcript levels of key biosynthetic enzymes. For these studies, I focused on Met, Thr, and Lys biosynthesis pathways and two groups of secondary metabolites (pseudoalkaloids and flavonoids).

Goal 4: Leucine aminopeptidase A in redox homeostasis and sulfur assimilation

In Chapter 3, I sought to identify putative LAP-A substrates. I performed wounding time-course experiments with wild-type, LapA-SI and LapA-OX plants. My hypothesis was that LAP-A controlled glutathione levels or glutathione redox status. This was based on the observation that bovine lens, Arabidopsis and tomato LAPs hydrolyze Cys-Gly (a catabolic product of glutathione) (Cappiello et al. 2004; Kumar et al. 2015; Scranton et al. 2012; Bachhawat and Kaur 2017). I used targeted metabolomics to monitor glutathione and its catabolites over time. Using biochemical assays, I also measured GSH:GSSG ratios. Second, based on knowledge that H_2O_2 is a modulator of the late branch of wound signaling in tomato (Orozco-Cardenas et al. 2001; Orozco-Cardenas and Ryan 1999), LAP-A regulates late wound response genes (Fowler et al. 2009), and H_2O_2 is a retrograde signal (Exposito-Rodriguez et al. 2017), I tested the hypothesis that LAP-A controls the levels of H_2O_2 after wounding. I used the wounding time-course of wild-type, LapA-SI, and LapA-OX to measure H_2O_2 levels using biochemical assays. I discovered that LAP-A regulates H_2O_2 and the ratio of GSH:GSSG in tomato leaf tissue.

To further understand LAP-A's role in redox signaling, I tested the response of nine ROS-responsive genes to H_2O_2 in wild-type, LapA-SI and LapA-OX plants; these genes were previously identified based on Arabidopsis orthologs or evidence of ROS-regulated genes in tomato fruit exposed to oxidative stress (Scranton 2013; Destro et al. 2011; Guo et al. 2010; Ioannidi et al. 2009; Queval et al. 2009; Sagi et al. 2004). I also measured transcript levels of a subset of genes that encode proteins for the biosynthesis of sulfur assimilation and biosynthesis of Cys, which is used for GSH biosynthesis.

Finally, to identify putative LAP-A substrates, affinity purification proteomics studies were performed. His-tagged LAP-A-wild-type, LAP-A-R431A, LAP-N-wild-type, and LAP-

N-K354E proteins were immobilized separately on columns and leaf protein extracts were used to identify putative LAP-A interacting proteins. The use of catalytically inactive LAP-A (LAP-A-R431A) and LAP-N (K354E) mutants assured us that we retain LAP substrates bound to each LAP. It was possible that enzymatically active wild-type LAP would cleave the N-terminal residue of a substrate and release the cleavage product; these substrates would evade detection. I identified specific LAP-A interactors that reproducibly interacted with either LAP-A and/or LAP-A-R431A but not with LAP-N and/or LAP-N-K354E. In addition, given the role of LAP-A in modulating H_2O_2 levels and protein homeostasis and its role in controlling defenses to herbivory, we discuss putative interactors that are linked to these functions.

References

Alborn HT, Jones TH, Stenhagen GS, Tumlinson JH (2000) Identification and Synthesis of Volicitin and Related Components from Beet Armyworm Oral Secretions. Journal of Chemical Ecology 26 (1):203-220. doi:10.1023/A:1005401814122

Anderson JP, Badruzsaufari E, Schenk PM, Manners JM, Desmond OJ, Ehlert C, Maclean DJ, Ebert PR, Kazan K (2004) Antagonistic interaction between abscisic acid and jasmonate-ethylene signaling pathways modulates defense gene expression and disease resistance in Arabidopsis. Plant Cell 16 (12):3460-3479. doi:10.1105/tpc.104.025833

Asada K (2000) The water-water cycle as alternative photon and electron sinks. Philos Trans R Soc Lond B Biol Sci 355 (1402):1419-1431. doi:10.1098/rstb.2000.0703

Bachhawat AK, Kaur A (2017) Glutathione Degradation. Antioxidants & Redox Signaling 27 (15):1200-1216. doi:10.1089/ars.2017.7136

Barbero F, Guglielmotto M, Islam M, Maffei ME (2021) Extracellular Fragmented Self-DNA Is Involved in Plant Responses to Biotic Stress. Frontiers in Plant Science 12 (1558). doi:10.3389/fpls.2021.686121

Bartels S, Lori M, Mbengue M, van Verk M, Klauser D, Hander T, Böni R, Robatzek S, Boller T (2013) The family of Peps and their precursors in Arabidopsis: differential expression and localization but similar induction of pattern-triggered immune responses. Journal of experimental botany 64 (17):5309-5321

Bartling D, Nosek J (1994) Molecular and immunological characterization of leucine aminopeptidase in Arabidopsis thaliana: a new antibody suggests a semi-constitutive regulation of a phylogenetically old enzyme. Plant Science 99 (2):199-209. doi:https://doi.org/10.1016/0168-9452(94)90177-5

Bartling D, Weiler EW (1992) Leucine aminopeptidase from Arabidopsis thaliana. Molecular evidence for a phylogenetically conserved enzyme of protein turnover in higher plants. Eur J Biochem 205 (1):425-431. doi:10.1111/j.1432-1033.1992.tb16796.x

Bellincampi D, Dipierro N, Salvi G, Cervone F, De Lorenzo G (2000) Extracellular H(2)O(2) induced by oligogalacturonides is not involved in the inhibition of the auxin-regulated rolB gene expression in tobacco leaf explants. Plant Physiol 122 (4):1379-1385. doi:10.1104/pp.122.4.1379

Beloshistov RE, Dreizler K, Galiullina RA, Tuzhikov AI, Serebryakova MV, Reichardt S, Shaw J, Taliansky ME, Pfannstiel J, Chichkova NV, Stintzi A, Schaller A, Vartapetian AB (2018) Phytaspase-mediated precursor processing and maturation of the wound hormone systemin. New Phytologist 218 (3):1167-1178. doi:https://doi.org/10.1111/nph.14568

Benn G, Bjornson M, Ke H, De Souza A, Balmond EI, Shaw JT, Dehesh K (2016) Plastidial metabolite MEcPP induces a transcriptionally centered stress-response hub via the transcription factor CAMTA3. Proceedings of the National Academy of Sciences 113 (31):8855-8860. doi:10.1073/pnas.1602582113

Bidart-Bouzat MG, Kliebenstein DJ (2008) Differential levels of insect herbivory in the field associated with genotypic variation in glucosinolates in Arabidopsis thaliana. J Chem Ecol 34 (8):1026-1037. doi:10.1007/s10886-008-9498-z

Bienert GP, Chaumont F (2014) Aquaporin-facilitated transmembrane diffusion of hydrogen peroxide. Biochim Biophys Acta 1840 (5):1596-1604. doi:10.1016/j.bbagen.2013.09.017

Börner T, Aleynikova AY, Zubo YO, Kusnetsov VV (2015) Chloroplast RNA
polymerases: Role in chloroplast biogenesis. Biochimica et Biophysica Acta
(BBA) - Bioenergetics 1847 (9):761-769.
doi:https://doi.org/10.1016/j.bbabio.2015.02.004

Boter M, Ruíz-Rivero O, Abdeen A, Prat S (2004) Conserved MYC transcription factors
play a key role in jasmonate signaling both in tomato and Arabidopsis. Genes
Dev 18 (13):1577-1591. doi:10.1101/gad.297704

Bottin A, Veronesi C, Pontier D, Esquerretugaye MT, Blein JP, Rusterucci C, Ricci P
(1994) Differential Responses of Tobacco Cells to Elicitors From Two
Phytophtora Species. Plant Physiology and Biochemistry 32 (3):373-378

Bradbeer JW, Atkinson YE, BÖRner T, Hagemann R (1979) Cytoplasmic synthesis of
plastid polypeptides may be controlled by plastid-synthesised RNA. Nature 279
(5716):816-817. doi:10.1038/279816a0

Broin M, Rey P (2003) Potato plants lacking the CDSP32 plastidic thioredoxin exhibit
overoxidation of the BAS1 2-cysteine peroxiredoxin and increased lipid
peroxidation in thylakoids under photooxidative stress. Plant Physiology 132
(3):1335-1343. doi:10.1104/pp.103.021626

Brown PD, Tokuhisa JG, Reichelt M, Gershenzon J (2003) Variation of glucosinolate
accumulation among different organs and developmental stages of Arabidopsis
thaliana. Phytochemistry 62 (3):471-481. doi:https://doi.org/10.1016/S0031-
9422(02)00549-6

Cappiello M, Lazzarotti A, Buono F, Scaloni A, D'Ambrosio C, Amodeo P, Mendez BL,
Pelosi P, Del Corso A, Mura U (2004) New role for leucyl aminopeptidase in
glutathione turnover. Biochemical Journal 378:35-44. doi:10.1042/bj20031336

Cazzonelli CI, Hou X, Alagoz Y, Rivers J, Dhami N, Lee J, Marri S, Pogson BJ (2020) A
cis-carotene derived apocarotenoid regulates etioplast and chloroplast
development. Elife 9. doi:10.7554/eLife.45310

Cazzonelli CI, Pogson BJ (2010) Source to sink: regulation of carotenoid biosynthesis in plants. Trends Plant Sci 15 (5):266-274. doi:10.1016/j.tplants.2010.02.003

Cejudo FJ, González M-C, Pérez-Ruiz JM (2020) Redox regulation of chloroplast metabolism. Plant Physiol 186 (1):9-21. doi:10.1093/plphys/kiaa062

Chan KX, Mabbitt PD, Phua SY, Mueller JW, Nisar N, Gigolashvili T, Stroeher E, Grassl J, Arlt W, Estavillo GM, Jackson CJ, Pogson BJ (2016a) Sensing and signaling of oxidative stress in chloroplasts by inactivation of the SAL1 phosphoadenosine phosphatase. Proc Natl Acad Sci U S A 113 (31):E4567-4576. doi:10.1073/pnas.1604936113

Chan KX, Phua SY, Crisp P, McQuinn R, Pogson BJ (2016b) Learning the Languages of the Chloroplast: Retrograde Signaling and Beyond. In: Merchant SS (ed) Annual Review of Plant Biology, Vol 67, vol 67. Annual Review of Plant Biology. pp 25-+. doi:10.1146/annurev-arplant-043015-111854

Chao WS, Gu YQ, Pautot V, Bray EA, Walling LL (1999) Leucine aminopeptidase RNAs, proteins, and activities increase in response to water deficit, salinity, and the wound signals systemin, methyl jasmonate, and abscisic acid. Plant Physiology 120 (4):979-992. doi:10.1104/pp.120.4.979

Chao WS, Pautot V, Holzer FM, Walling LL (2000) Leucine aminopeptidases: the ubiquity of LAP-N and the specificity of LAP-A. Planta 210 (4):563-573. doi:10.1007/s004250050045

Charlier D, Hassanzadeh G, Kholti A, Gigot D, Pierard A, Glansdorff N (1995) carP, involved in pyrimidine regulation of the Escherichia coli carbamoylphosphate synthetase operon encodes a sequence-specific DNA-binding protein identical to XerB and PepA, also required for resolution of ColEI multimers. Journal of Molecular Biology 250 (4):392-406. doi:10.1006/jmbi.1995.0385

Chen D, Cao Y, Li H, Kim D, Ahsan N, Thelen J, Stacey G (2017) Extracellular ATP elicits DORN1-mediated RBOHD phosphorylation to regulate stomatal aperture. Nature Communications 8 (1):2265. doi:10.1038/s41467-017-02340-3

Chen D, Hao F, Mu H, Ahsan N, Thelen JJ, Stacey G (2021) S-acylation of P2K1 mediates extracellular ATP-induced immune signaling in Arabidopsis. Nature Communications 12 (1):2750. doi:10.1038/s41467-021-22854-1

Chen H, Wilkerson CG, Kuchar JA, Phinney BS, Howe GA (2005) Jasmonate-inducible plant enzymes degrade essential amino acids in the herbivore midgut. Proc Natl Acad Sci U S A 102 (52):19237-19242. doi:10.1073/pnas.0509026102

Chini A, Fonseca S, Fernández G, Adie B, Chico JM, Lorenzo O, García-Casado G, López-Vidriero I, Lozano FM, Ponce MR, Micol JL, Solano R (2007) The JAZ family of repressors is the missing link in jasmonate signalling. Nature 448 (7154):666-671. doi:10.1038/nature06006

Chini A, Monte I, Zamarreño AM, Hamberg M, Lassueur S, Reymond P, Weiss S, Stintzi A, Schaller A, Porzel A, García-Mina JM, Solano R (2018) An OPR3-independent pathway uses 4,5-didehydrojasmonate for jasmonate synthesis. Nat Chem Biol 14 (2):171-178. doi:10.1038/nchembio.2540

Choi J, Tanaka K, Cao Y, Qi Y, Qiu J, Liang Y, Lee SY, Stacey G (2014) Identification of a plant receptor for extracellular ATP. Science 343 (6168):290-294. doi:10.1126/science.343.6168.290

Collin V, Issakidis-Bourguet E, Marchand C, Hirasawa M, Lancelin JM, Knaff DB, Miginiac-Maslow M (2003) The Arabidopsis plastidial thioredoxins - New functions and new insights into specificity. Journal of Biological Chemistry 278 (26):23747-23752. doi:10.1074/jbc.M302077200

Colloms SD (2013) Leucyl Aminopeptidase PepA. Handbook of Proteolytic Enzymes, Vols 1 and 2, 3rd Edition. doi:10.1016/b978-0-12-382219-2.00334-3

Constabel CP, Yip L, Ryan CA (1998) Prosystemin from potato, black nightshade, and bell pepper: primary structure and biological activity of predicted systemin polypeptides. Plant Molecular Biology 36 (1):55-62. doi:10.1023/A:1005986004615

Coppola M, Lelio ID, Romanelli A, Gualtieri L, Molisso D, Ruocco M, Avitabile C, Natale R, Cascone P, Guerrieri E, Pennacchio F, Rao R (2019) Tomato Plants Treated with Systemin Peptide Show Enhanced Levels of Direct and Indirect Defense Associated with Increased Expression of Defense-Related Genes. Plants (Basel) 8 (10). doi:10.3390/plants8100395

Cottage AJ, Mott EK, Wang J-H, Sullivan JA, MacLean D, Tran L, Choy M-K, Newell C, Kavanagh TA, Aspinall S, Gray JC GUN1 (GENOMES UNCOUPLED1) Encodes a Pentatricopeptide Repeat (PPR) Protein Involved in Plastid Protein Synthesis-Responsive Retrograde Signaling to the Nucleus. In, Dordrecht, 2008. Photosynthesis. Energy from the Sun. Springer Netherlands, pp 1201-1205

D'Alessandro S, Ksas B, Havaux M (2018) Decoding β-Cyclocitral-Mediated Retrograde Signaling Reveals the Role of a Detoxification Response in Plant Tolerance to Photooxidative Stress. Plant Cell 30 (10):2495-2511. doi:10.1105/tpc.18.00578

Dammann C, Rojo E, Sánchez-Serrano JJ (1997) Abscisic acid and jasmonic acid
activate wound-inducible genes in potato through separate, organ-specific signal
transduction pathways. The Plant Journal 11 (4):773-782.
doi:https://doi.org/10.1046/j.1365-313X.1997.11040773.x

Danon A, Miersch O, Felix G, Camp RG, Apel K (2005) Concurrent activation of cell
death-regulating signaling pathways by singlet oxygen in Arabidopsis thaliana.
Plant J 41 (1):68-80. doi:10.1111/j.1365-313X.2004.02276.x

de Souza A, Wang JZ, Dehesh K (2017) Retrograde Signals: Integrators of
Interorganellar Communication and Orchestrators of Plant Development. Annu
Rev Plant Biol 68:85-108. doi:10.1146/annurev-arplant-042916-041007

Degenhardt DC, Refi-Hind S, Stratmann JW, Lincoln DE (2010) Systemin and jasmonic
acid regulate constitutive and herbivore-induced systemic volatile emissions in
tomato, Solanum lycopersicum. Phytochemistry 71 (17-18):2024-2037.
doi:10.1016/j.phytochem.2010.09.010

Denoux C, Galletti R, Mammarella N, Gopalan S, Werck D, De Lorenzo G, Ferrari S,
Ausubel FM, Dewdney J (2008) Activation of defense response pathways by
OGs and Flg22 elicitors in Arabidopsis seedlings. Mol Plant 1 (3):423-445.
doi:10.1093/mp/ssn019

Dervinis C, Frost CJ, Lawrence SD, Novak NG, Davis JM (2010) Cytokinin Primes Plant
Responses to Wounding and Reduces Insect Performance. Journal of Plant
Growth Regulation 29 (3):289-296. doi:10.1007/s00344-009-9135-2

Destro T, Prasad D, Martignago D, Lliso Bernet I, Trentin AR, Renu IK, Ferretti M, Masi
A (2011) Compensatory expression and substrate inducibility of γ-glutamyl
transferase GGT2 isoform in Arabidopsis thaliana. Journal of experimental
botany 62 (2):805-814

Dicke M, Baldwin IT (2010) The evolutionary context for herbivore-induced plant volatiles: beyond the 'cry for help'. Trends Plant Sci 15 (3):167-175. doi:10.1016/j.tplants.2009.12.002

Dickinson AJ, Lehner K, Mi J, Jia KP, Mijar M, Dinneny J, Al-Babili S, Benfey PN (2019) β-Cyclocitral is a conserved root growth regulator. Proc Natl Acad Sci U S A 116 (21):10563-10567. doi:10.1073/pnas.1821445116

Dietz KJ, Turkan I, Krieger-Liszkay A (2016) Redox- and Reactive Oxygen Species-Dependent Signaling into and out of the Photosynthesizing Chloroplast. Plant Physiology 171 (3):1541-1550. doi:10.1104/pp.16.00375

Diezel C, von Dahl CC, Gaquerel E, Baldwin IT (2009) Different Lepidopteran Elicitors Account for Cross-Talk in Herbivory-Induced Phytohormone Signaling   Plant Physiology 150 (3):1576-1586. doi:10.1104/pp.109.139550

Ding Y, Sun T, Ao K, Peng Y, Zhang Y, Li X, Zhang Y (2018) Opposite Roles of Salicylic Acid Receptors NPR1 and NPR3/NPR4 in Transcriptional Regulation of Plant Immunity. Cell 173 (6):1454-1467.e1415. doi:10.1016/j.cell.2018.03.044

Doares SH, Narvaezvasquez J, Conconi A, Ryan CA (1995a) Salicylic Acid Inhibits Synthesis of Proteinase Inhibitors in Tomato Leaves Induced by Systemin and Jasmonic Acid. Plant Physiology 108 (4):1741-1746

Doares SH, Syrovets T, Weiler EW, Ryan CA (1995b) Oligogalacturonides and chitosan activate plant defensive genes through the octadecanoid pathway. Proc Natl Acad Sci U S A 92 (10):4095-4098. doi:10.1073/pnas.92.10.4095

Dogra V, Duan J, Lee KP, Lv S, Liu R, Kim C (2017) FtsH2-Dependent Proteolysis of EXECUTER1 Is Essential in Mediating Singlet Oxygen-Triggered Retrograde Signaling in Arabidopsis thaliana. Frontiers in Plant Science 8 (1145). doi:10.3389/fpls.2017.01145

Dogra V, Li M, Singh S, Li M, Kim C (2019) Oxidative post-translational modification of EXECUTER1 is required for singlet oxygen sensing in plastids. Nat Commun 10 (1):2834. doi:10.1038/s41467-019-10760-6

Doherty HM, Selvendran RR, Bowles DJ (1988) The wound response of tomato plants can be inhibited by aspirin and related hydroxy-benzoic acids. Physiological and Molecular Plant Pathology 33 (3):377-384. doi:https://doi.org/10.1016/0885-5765(88)90004-5

Dombrecht B, Xue GP, Sprague SJ, Kirkegaard JA, Ross JJ, Reid JB, Fitt GP, Sewelam N, Schenk PM, Manners JM, Kazan K (2007) MYC2 differentially modulates diverse jasmonate-dependent functions in Arabidopsis. Plant Cell 19 (7):2225-2245. doi:10.1105/tpc.106.048017

Dostal HC, Leopold AC (1967) Gibberellin delays ripening of tomatoes. Science 158 (3808):1579-1580. doi:10.1126/science.158.3808.1579

Du MM, Zhao JH, Tzeng DTW, Liu YY, Deng L, Yang TX, Zhai QZ, Wu FM, Huang Z, Zhou M, Wang QM, Chen Q, Zhong SL, Li CB, Li CY (2017) MYC2 Orchestrates a Hierarchical Transcriptional Cascade That Regulates Jasmonate-Mediated Plant Immunity in Tomato. Plant Cell 29 (8):1883-1906. doi:10.1105/tpc.16.00953

Duprez K, Scranton MA, Walling LL, Fan L (2014) Structure of tomato wound-induced leucine aminopeptidase sheds light on substrate specificity. Acta Crystallographica Section D-Biological Crystallography 70:1649-1658. doi:10.1107/s1399004714006245

Erb M, Reymond P (2019) Molecular Interactions Between Plants and Insect Herbivores. Annual Review of Plant Biology 70 (1):527-557. doi:10.1146/annurev-arplant-050718-095910

Estavillo GM, Crisp PA, Pornsiriwong W, Wirtz M, Collinge D, Carrie C, Giraud E, Whelan J, David P, Javot H, Brearley C, Hell R, Marin E, Pogson BJ (2011) Evidence for a SAL1-PAP Chloroplast Retrograde Pathway That Functions in Drought and High Light Signaling in Arabidopsis   The Plant Cell 23 (11):3992-4012. doi:10.1105/tpc.111.091033

Exposito-Rodriguez M, Laissue PP, Yvon-Durocher G, Smirnoff N, Mullineaux PM (2017) Photosynthesis-dependent H2O2 transfer from chloroplasts to nuclei provides a high-light signalling mechanism. Nature Communications 8 (1):49. doi:10.1038/s41467-017-00074-w

Farmer EE, Gasperini D, Acosta IF (2014) The squeeze cell hypothesis for the activation of jasmonate synthesis in response to wounding. New Phytol 204 (2):282-288. doi:10.1111/nph.12897

Farmer EE, Ryan CA (1990) Interplant communication: airborne methyl jasmonate induces synthesis of proteinase inhibitors in plant leaves. Proc Natl Acad Sci U S A 87 (19):7713-7716. doi:10.1073/pnas.87.19.7713

Felton GW, Donato K, Del Vecchio RJ, Duffey SS (1989) Activation of plant foliar oxidases by insect feeding reduces nutritive quality of foliage for noctuid herbivores. J Chem Ecol 15 (12):2667-2694. doi:10.1007/bf01014725

Ferrari S, Savatin D, Sicilia F, Gramegna G, Cervone F, De Lorenzo G (2013) Oligogalacturonides: plant damage-associated molecular patterns and regulators of growth and development. Frontiers in Plant Science 4 (49). doi:10.3389/fpls.2013.00049

Förster S, Schmidt LK, Kopic E, Anschütz U, Huang S, Schlücking K, Köster P, Waadt
R, Larrieu A, Batistič O, Rodriguez PL, Grill E, Kudla J, Becker D (2019)
Wounding-Induced Stomatal Closure Requires Jasmonate-Mediated Activation of
GORK K+ Channels by a Ca2+ Sensor-Kinase CBL1-CIPK5 Complex.
Developmental Cell 48 (1):87-99.e86.
doi:https://doi.org/10.1016/j.devcel.2018.11.014

Fowler JH, Narvaez-Vasquez J, Aromdee DN, Pautot V, Holzer FM, Walling LL (2009)
Leucine Aminopeptidase Regulates Defense and Wound Signaling in Tomato
Downstream of Jasmonic Acid. Plant Cell 21 (4):1239-1251.
doi:10.1105/tpc.108.065029

Foyer CH, Karpinska B, Krupinska K (2014) The functions of WHIRLY1 and REDOX-
RESPONSIVE TRANSCRIPTION FACTOR 1 in cross tolerance responses in
plants: a hypothesis. Philos Trans R Soc Lond B Biol Sci 369 (1640):20130226.
doi:10.1098/rstb.2013.0226

Foyer CH, Noctor G (2016) Stress-triggered redox signalling: what's in pROSpect?
Plant, Cell & Environment 39 (5):951-964. doi:https://doi.org/10.1111/pce.12621

Gao XH, Xiao SL, Yao QF, Wang YJ, Fu XD (2011) An updated GA signaling 'relief of
repression' regulatory model. Mol Plant 4 (4):601-606. doi:10.1093/mp/ssr046

Gigolashvili T, Geier M, Ashykhmina N, Frerigmann H, Wulfert S, Krueger S, Mugford
SG, Kopriva S, Haferkamp I, Flügge U-I (2012) The Arabidopsis Thylakoid
ADP/ATP Carrier TAAC Has an Additional Role in Supplying Plastidic
Phosphoadenosine 5′-Phosphosulfate to the Cytosol. The Plant Cell 24
(10):4187-4204. doi:10.1105/tpc.112.101964

Gil MJ, Coego A, Mauch-Mani B, Jordá L, Vera P (2005) The Arabidopsis csb3 mutant reveals a regulatory link between salicylic acid-mediated disease resistance and the methyl-erythritol 4-phosphate pathway. Plant J 44 (1):155-166. doi:10.1111/j.1365-313X.2005.02517.x

Giraud E, Van Aken O, Ho LH, Whelan J (2009) The transcription factor ABI4 is a regulator of mitochondrial retrograde expression of ALTERNATIVE OXIDASE1a. Plant Physiol 150 (3):1286-1296. doi:10.1104/pp.109.139782

Glazebrook J (2005) Contrasting mechanisms of defense against biotrophic and necrotrophic pathogens. Annu Rev Phytopathol 43:205-227. doi:10.1146/annurev.phyto.43.040204.135923

González-Cabanelas D, Wright LP, Paetz C, Onkokesung N, Gershenzon J, Rodríguez-Concepción M, Phillips MA (2015) The diversion of 2-C-methyl-d-erythritol-2,4-cyclodiphosphate from the 2-C-methyl-d-erythritol 4-phosphate pathway to hemiterpene glycosides mediates stress responses in Arabidopsis thaliana. The Plant Journal 82 (1):122-137. doi:https://doi.org/10.1111/tpj.12798

Graciet E, Wellmer F (2010) The plant N-end rule pathway: structure and functions. Trends Plant Sci 15 (8):447-453. doi:10.1016/j.tplants.2010.04.011

Green TR, Ryan CA (1972) Wound-Induced Proteinase Inhibitor in Plant Leaves: A Possible Defense Mechanism against Insects. Science 175 (4023):776-777. doi:10.1126/science.175.4023.776

Gu YQ, Chao WS, Tu CJ, Walling LL (1996a) Processing and localization of the wound-induced leucine aminopeptidase of Lycopersicon esculentum. Plant Physiology 111 (2):96-96

Gu YQ, Chao WS, Walling LL (1996b) Localization and post-translational processing of the wound-induced leucine aminopeptidase proteins of tomato. Journal of Biological Chemistry 271 (42):25880-25887

Gu YQ, Holzer FM, Walling LL (1999) Overexpression, purification and biochemical characterization of the wound-induced leucine aminopeptidase of tomato. European Journal of Biochemistry 263 (3):726-735. doi:10.1046/j.1432-1327.1999.00548.x

Gu YQ, Walling LL (2000) Specificity of the wound-induced leucine aminopeptidase (LAP-A) of tomato - Activity on dipeptide and tripeptide substrates. European Journal of Biochemistry 267 (4):1178-1187. doi:10.1046/j.1432-1327.2000.01116.x

Gu YQ, Walling LL (2002) Identification of residues critical for activity of the wound-induced leucine aminopeptidase (LAP-A) of tomato. European Journal of Biochemistry 269 (6):1630-1640. doi:10.1046/j.1432-1327.2002.02795.x

Guan L, Denkert N, Eisa A, Lehmann M, Sjuts I, Weiberg A, Soll J, Meinecke M, Schwenkert S (2019) JASSY, a chloroplast outer membrane protein required for jasmonate biosynthesis. Proceedings of the National Academy of Sciences 116 (21):10568-10575. doi:10.1073/pnas.1900482116

Guo H, Sun Y, Peng X, Wang Q, Harris M, Ge F (2016) Up-regulation of abscisic acid signaling pathway facilitates aphid xylem absorption and osmoregulation under drought stress. J Exp Bot 67 (3):681-693. doi:10.1093/jxb/erv481

Guo YS, Huang CJ, Xie Y, Song FM, Zhou XP (2010) A tomato glutaredoxin gene SlGRX1 regulates plant responses to oxidative, drought and salt stresses. Planta 232 (6):1499-1509. doi:10.1007/s00425-010-1271-1

Gupta R, Chakrabarty SK (2013) Gibberellic acid in plant. Plant Signaling & Behavior 8 (9):e25504. doi:10.4161/psb.25504

Gy I, Gasciolli V, Lauressergues D, Morel JB, Gombert J, Proux F, Proux C, Vaucheret H, Mallory AC (2007) Arabidopsis FIERY1, XRN2, and XRN3 are endogenous RNA silencing suppressors. Plant Cell 19 (11):3451-3461. doi:10.1105/tpc.107.055319

Hajdukiewicz PT, Allison LA, Maliga P (1997) The two RNA polymerases encoded by the nuclear and the plastid compartments transcribe distinct groups of genes in tobacco plastids. EMBO J 16 (13):4041-4048. doi:10.1093/emboj/16.13.4041

Harfouche AL, Shivaji R, Stocker R, Williams PW, Luthe DS (2006) Ethylene signaling mediates a maize defense response to insect herbivory. Mol Plant Microbe Interact 19 (2):189-199. doi:10.1094/mpmi-19-0189

Hartl M, Merker H, Schmidt DD, Baldwin IT (2008) Optimized virus-induced gene silencing in Solanum nigrum reveals the defensive function of leucine aminopeptidase against herbivores and the shortcomings of empty vector controls. New Phytologist 179 (2):356-365. doi:10.1111/j.1469-8137.2008.02479.x

Hasanuzzaman M, Bhuyan M, Zulfiqar F, Raza A, Mohsin SM, Al Mahmud J, Fujita M, Fotopoulos V (2020) Reactive Oxygen Species and Antioxidant Defense in Plants under Abiotic Stress: Revisiting the Crucial Role of a Universal Defense Regulator. Antioxidants 9 (8). doi:10.3390/antiox9080681

Hatsugai N, Igarashi D, Mase K, Lu Y, Tsuda Y, Chakravarthy S, Wei H-L, Foley JW, Collmer A, Glazebrook J, Katagiri F (2017) A plant effector-triggered immunity signaling sector is inhibited by pattern-triggered immunity. The EMBO Journal 36 (18):2758-2769. doi:https://doi.org/10.15252/embj.201796529

Hause B, Hause G, Kutter C, Miersch O, Wasternack C (2003) Enzymes of jasmonate biosynthesis occur in tomato sieve elements. Plant Cell Physiol 44 (6):643-648. doi:10.1093/pcp/pcg072

Havko NE, Das MR, McClain AM, Kapali G, Sharkey TD, Howe GA (2020) Insect herbivory antagonizes leaf cooling responses to elevated temperature in tomato. Proceedings of the National Academy of Sciences 117 (4):2211-2217. doi:10.1073/pnas.1913885117

Herbers K, Prat S, Willmitzer L (1994) Functional analysis of a leucine aminopeptidase from Solanum tuberosum L. Planta 194 (2):230-240. doi:10.1007/bf01101682

Hickman R, Van Verk MC, Van Dijken AJH, Mendes MP, Vroegop-Vos IA, Caarls L, Steenbergen M, Van der Nagel I, Wesselink GJ, Jironkin A, Talbot A, Rhodes J, De Vries M, Schuurink RC, Denby K, Pieterse CMJ, Van Wees SCM (2017) Architecture and Dynamics of the Jasmonic Acid Gene Regulatory Network. Plant Cell 29 (9):2086-2105. doi:10.1105/tpc.16.00958

Hildmann T, Ebneth M, Penacortes H, Sanchezserrano JJ, Willmitzer L, Prat S (1992) General roles of abscisic and jasmonic acids in gene activation as a result of mechanical wounding. Plant Cell 4 (9):1157-1170. doi:10.1105/tpc.4.9.1157

Hillwig MS, Chiozza M, Casteel CL, Lau ST, Hohenstein J, Hernández E, Jander G, MacIntosh GC (2016) Abscisic acid deficiency increases defence responses against Myzus persicae in Arabidopsis. Mol Plant Pathol 17 (2):225-235. doi:10.1111/mpp.12274

Hou X, Lee LY, Xia K, Yan Y, Yu H (2010) DELLAs modulate jasmonate signaling via competitive binding to JAZs. Dev Cell 19 (6):884-894. doi:10.1016/j.devcel.2010.10.024

54

Howe GA (2004) Jasmonates as signals in the wound response. Journal of Plant Growth
Regulation 23 (3):223-237. doi:10.1007/s00344-004-0030-6

Howe GA (2018) Metabolic end run to jasmonate. Nature Chemical Biology 14 (2):109-
110. doi:10.1038/nchembio.2553

Howe GA, Major IT, Koo AJ (2018) Modularity in Jasmonate Signaling for Multistress
Resilience. Annual Review of Plant Biology 69 (1):387-415. doi:10.1146/annurev-
arplant-042817-040047

Hu X, Xu L (2016) Transcription Factors WOX11/12 Directly Activate WOX5/7 to
Promote Root Primordia Initiation and Organogenesis. Plant Physiology 172
(4):2363-2373. doi:10.1104/pp.16.01067

Huang M, Friso G, Nishimura K, Qu X, Olinares PD, Majeran W, Sun Q, van Wijk KJ
(2013) Construction of plastid reference proteomes for maize and Arabidopsis
and evaluation of their orthologous relationships; the concept of orthoproteomics.
J Proteome Res 12 (1):491-504. doi:10.1021/pr300952g

Huang X-Q, Wang L-J, Kong M-J, Huang N, Liu X-Y, Liang H-Y, Zhang J-X, Lu S (2021)
At3g53630 encodes a GUN1-interacting protein under norflurazon treatment.
Protoplasma 258 (2):371-378. doi:10.1007/s00709-020-01578-x

Huffaker A, Pearce G, Ryan CA (2006) An endogenous peptide signal in Arabidopsis
activates components of the innate immune response. Proceedings of the
National Academy of Sciences 103 (26):10098-10103

Huffaker A, Pearce G, Veyrat N, Erb M, Turlings TC, Sartor R, Shen Z, Briggs SP,
Vaughan MM, Alborn HT, Teal PE, Schmelz EA (2013) Plant elicitor peptides are
conserved signals regulating direct and indirect antiherbivore defense. Proc Natl
Acad Sci U S A 110 (14):5707-5712. doi:10.1073/pnas.1214668110

Huffaker A, Ryan CA (2007) Endogenous peptide defense signals in Arabidopsis differentially amplify signaling for the innate immune response. Proceedings of the National Academy of Sciences 104 (25):10732-10736

Ioannidi E, Kalamaki MS, Engineer C, Pateraki I, Alexandrou D, Mellidou I, Giovannonni J, Kanellis AK (2009) Expression profiling of ascorbic acid-related genes during tomato fruit development and ripening and in response to stress conditions. Journal of Experimental Botany 60 (2):663-678. doi:10.1093/jxb/ern322

Irigoyen ML, Garceau DC, Bohorquez-Chaux A, Lopez-Lavalle LAB, Perez-Fons L, Fraser PD, Walling LL (2020) Genome-wide analyses of cassava Pathogenesis-related (PR) gene families reveal core transcriptome responses to whitefly infestation, salicylic acid and jasmonic acid. BMC Genomics 21 (1):93. doi:10.1186/s12864-019-6443-1

Isemer R, Mulisch M, Schäfer A, Kirchner S, Koop HU, Krupinska K (2012) Recombinant Whirly1 translocates from transplastomic chloroplasts to the nucleus. FEBS Lett 586 (1):85-88. doi:10.1016/j.febslet.2011.11.029

Ishiga Y, Watanabe M, Ishiga T, Tohge T, Matsuura T, Ikeda Y, Hoefgen R, Fernie AR, Mysore KS (2017) The SAL-PAP Chloroplast Retrograde Pathway Contributes to Plant Immunity by Regulating Glucosinolate Pathway and Phytohormone Signaling. Mol Plant Microbe Interact 30 (10):829-841. doi:10.1094/mpmi-03-17-0055-r

Jia Y, Tian H, Zhang S, Ding Z, Ma C (2019) GUN1-Interacting Proteins Open the Door for Retrograde Signaling. Trends Plant Sci 24 (10):884-887. doi:10.1016/j.tplants.2019.07.005

Jiang J, Dehesh K (2021) Plastidial retrograde modulation of light and hormonal signaling: an odyssey. New Phytol 230 (3):931-937. doi:10.1111/nph.17192

Jiang J, Rodriguez-Furlan C, Wang J-Z, de Souza A, Ke H, Pasternak T, Lasok H, Ditengou FA, Palme K, Dehesh K (2018) Interplay of the two ancient metabolites auxin and MEcPP regulates adaptive growth. Nature Communications 9 (1):2262. doi:10.1038/s41467-018-04708-5

Jiang J, Xiao Y, Chen H, Hu W, Zeng L, Ke H, Ditengou FA, Devisetty U, Palme K, Maloof J, Dehesh K (2020) Retrograde Induction of phyB Orchestrates Ethylene-Auxin Hierarchy to Regulate Growth. Plant Physiol 183 (3):1268-1280. doi:10.1104/pp.20.00090

Jones JDG, Dangl JL (2006) The plant immune system. Nature 444 (7117):323-329. doi:10.1038/nature05286

Jösch C, Klotz LO, Sies H (2003) Identification of cytosolic leucyl aminopeptidase (EC 3.4.11.1) as the major cysteinylglycine-hydrolysing activity in rat liver. Biol Chem 384 (2):213-218. doi:10.1515/bc.2003.023

Jung HS, Chory J (2010) Signaling between Chloroplasts and the Nucleus: Can a Systems Biology Approach Bring Clarity to a Complex and Highly Regulated Pathway? Plant Physiology 152 (2):453-459. doi:10.1104/pp.109.149070

Jwa NS, Walling LL (2001) Influence of elevated CO2 concentration on disease development in tomato. New Phytologist 149 (3):509-518. doi:10.1046/j.1469-8137.2001.00063.x

Kahl J, Siemens DH, Aerts RJ, Gäbler R, Kühnemann F, Preston CA, Baldwin IT (2000) Herbivore-induced ethylene suppresses a direct defense but not a putative indirect defense against an adapted herbivore. Planta 210 (2):336-342. doi:10.1007/pl00008142

Katsir L, Schilmiller AL, Staswick PE, He SY, Howe GA (2008) COI1 is a critical component of a receptor for jasmonate and the bacterial virulence factor coronatine. Proceedings of the National Academy of Sciences 105 (19):7100-7105. doi:10.1073/pnas.0802332105

Kauss D, Bischof S, Steiner S, Apel K, Meskauskiene R (2012) FLU, a negative feedback regulator of tetrapyrrole biosynthesis, is physically linked to the final steps of the Mg(++)-branch of this pathway. FEBS Lett 586 (3):211-216. doi:10.1016/j.febslet.2011.12.029

Kelley DR, Estelle M (2012) Ubiquitin-mediated control of plant hormone signaling. Plant physiology 160 (1):47-55

Kempema LA, Cui X, Holzer FM, Walling LL (2007) Arabidopsis transcriptome changes in response to phloem-feeding silverleaf whitefly nymphs. Similarities and distinctions in responses to aphids. Plant Physiol 143 (2):849-865. doi:10.1104/pp.106.090662

Khorobrykh S, Havurinne V, Mattila H, Tyystjärvi E (2020) Oxygen and ROS in Photosynthesis. Plants (Basel) 9 (1). doi:10.3390/plants9010091

Kim JH, Jander G (2007) Myzus persicae (green peach aphid) feeding on Arabidopsis induces the formation of a deterrent indole glucosinolate. The Plant journal : for cell and molecular biology 49 (6):1008-1019

Kim NY, Jang YJ, Park OK (2018) AP2/ERF Family Transcription Factors ORA59 and RAP2.3 Interact in the Nucleus and Function Together in Ethylene Responses. Front Plant Sci 9:1675. doi:10.3389/fpls.2018.01675

Kimura M, Yamamoto YY, Seki M, Sakurai T, Sato M, Abe T, Yoshida S, Manabe K, Shinozaki K, Matsui M (2003) Identification of Arabidopsis Genes Regulated by High Light–Stress Using cDNA Microarray. Photochemistry and Photobiology 77 (2):226-233. doi:https://doi.org/10.1562/0031-8655(2003)0770226IOAGRB2.0.CO2

Kliebenstein DJ, Figuth A, Mitchell-Olds T (2002) Genetic architecture of plastic methyl jasmonate responses in Arabidopsis thaliana. Genetics 161 (4):1685-1696. doi:10.1093/genetics/161.4.1685

Kohorn B, Kohorn S (2012) The cell wall-associated kinases, WAKs, as pectin receptors. Frontiers in Plant Science 3 (88). doi:10.3389/fpls.2012.00088

Konig J, Baier M, Horling F, Kahmann U, Harris G, Schurmann P, Dietz KJ (2002) The plant-specific function of 2-Cys peroxiredoxin-mediated detoxification of peroxides in the redox-hierarchy of photosynthetic electron flux. Proceedings of the National Academy of Sciences of the United States of America 99 (8):5738-5743. doi:10.1073/pnas.072644999

Koussevitzky S, Nott A, Mockler TC, Hong F, Sachetto-Martins G, Surpin M, Lim J, Mittler R, Chory J (2007) Signals from chloroplasts converge to regulate nuclear gene expression. Science 316 (5825):715-719

Krieger-Liszkay A, Fufezan C, Trebst A (2008) Singlet oxygen production in photosystem II and related protection mechanism. Photosynth Res 98 (1-3):551-564. doi:10.1007/s11120-008-9349-3

Kumar S, Kaur A, Chattopadhyay B, Bachhawat AK (2015) Defining the cytosolic pathway of glutathione degradation in Arabidopsis thaliana: role of the ChaC/GCG family of gamma-glutamyl cyclotransferases as glutathione-degrading enzymes and AtLAP1 as the Cys-Gly peptidase. Biochem J 468:73-85. doi:10.1042/bj20141154

Laloi C, Stachowiak M, Pers-Kamczyc E, Warzych E, Murgia I, Apel K (2007) Cross-talk between singlet oxygen- and hydrogen peroxide-dependent signaling of stress responses in Arabidopsis thaliana. Proc Natl Acad Sci U S A 104 (2):672-677. doi:10.1073/pnas.0609063103

Laxa M, Koenig J, Dietz K-J, Kandlbinder A (2007) Role of the cysteine residues in Arabidopsis thaliana cyclophilin CYP20-3 in peptidyl-prolyl cis-trans isomerase and redox-related functions. Biochemical Journal 401:287-297. doi:10.1042/bj20061092

Lazazzara V, Bueschl C, Parich A, Pertot I, Schuhmacher R, Perazzolli M (2018) Downy mildew symptoms on grapevines can be reduced by volatile organic compounds of resistant genotypes. Scientific Reports 8 (1):1618. doi:10.1038/s41598-018-19776-2

Lee KP, Kim C, Landgraf F, Apel K (2007) EXECUTER1- and EXECUTER2-dependent transfer of stress-related signals from the plastid to the nucleus of Arabidopsis thaliana. Proceedings of the National Academy of Sciences 104 (24):10270-10275. doi:10.1073/pnas.0702061104

Lemos M, Xiao Y, Bjornson M, Wang JZ, Hicks D, Souza A, Wang CQ, Yang P, Ma S, Dinesh-Kumar S, Dehesh K (2016) The plastidial retrograde signal methyl erythritol cyclopyrophosphate is a regulator of salicylic acid and jasmonic acid crosstalk. J Exp Bot 67 (5):1557-1566. doi:10.1093/jxb/erv550

Li J, Brader G, Palva ET (2004) The WRKY70 transcription factor: a node of convergence for jasmonate-mediated and salicylate-mediated signals in plant defense. Plant Cell 16 (2):319-331. doi:10.1105/tpc.016980

Li M, Wang F, Li S, Yu G, Wang L, Li Q, Zhu X, Li Z, Yuan L, Liu P (2020a) Importers Drive Leaf-to-Leaf Jasmonic Acid Transmission in Wound-Induced Systemic Immunity. Molecular Plant 13 (10):1485-1498. doi:10.1016/j.molp.2020.08.017

60

Li N, Han X, Feng D, Yuan D, Huang L-J (2019) Signaling Crosstalk between Salicylic Acid and Ethylene/Jasmonate in Plant Defense: Do We Understand What They Are Whispering? International Journal of Molecular Sciences 20 (3):671

Li Q, Wang C, Mou Z (2020b) Perception of Damaged Self in Plants1 [OPEN]. Plant Physiology 182 (4):1545-1565. doi:10.1104/pp.19.01242

Li Q, Zheng J, Li S, Huang G, Skilling SJ, Wang L, Li L, Li M, Yuan L, Liu P (2017) Transporter-Mediated Nuclear Entry of Jasmonoyl-Isoleucine Is Essential for Jasmonate Signaling. Molecular Plant 10 (5):695-708. doi:https://doi.org/10.1016/j.molp.2017.01.010

LI Z, SHARKEY TD (2013) Metabolic profiling of the methylerythritol phosphate pathway reveals the source of post-illumination isoprene burst from leaves. Plant, Cell & Environment 36 (2):429-437. doi:https://doi.org/10.1111/j.1365-3040.2012.02584.x

Liebthal M, Dietz K-J (2017) The Fundamental Role of Reactive Oxygen Species in Plant Stress Response. In: Sunkar R (ed) Plant Stress Tolerance: Methods and Protocols. Springer New York, New York, NY, pp 23-39. doi:10.1007/978-1-4939-7136-7_2

Ling Q, Broad W, Trösch R, Töpel M, Demiral Sert T, Lymperopoulos P, Baldwin A, Jarvis RP (2019) Ubiquitin-dependent chloroplast-associated protein degradation in plants. Science 363 (6429):eaav4467. doi:10.1126/science.aav4467

Liu J, Sheng L, Xu Y, Li J, Yang Z, Huang H, Xu L (2014) WOX11 and 12 Are Involved in the First-Step Cell Fate Transition during de Novo Root Organogenesis in Arabidopsis Plant Cell 26 (3):1081-1093. doi:10.1105/tpc.114.122887

Liu L, Chen X (2016) RNA Quality Control as a Key to Suppressing RNA Silencing of Endogenous Genes in Plants. Molecular Plant 9 (6):826-836. doi:https://doi.org/10.1016/j.molp.2016.03.011

Liu Y, Sun T, Sun Y, Zhang Y, Radojičić A, Ding Y, Tian H, Huang X, Lan J, Chen S, Orduna AR, Zhang K, Jetter R, Li X, Zhang Y (2020) Diverse Roles of the Salicylic Acid Receptors NPR1 and NPR3/NPR4 in Plant Immunity. Plant Cell 32 (12):4002-4016. doi:10.1105/tpc.20.00499

Lorenzo O, Piqueras R, Sánchez-Serrano JJ, Solano R (2003) ETHYLENE RESPONSE FACTOR1 integrates signals from ethylene and jasmonate pathways in plant defense. Plant Cell 15 (1):165-178. doi:10.1105/tpc.007468

Lorenzo O, Solano R (2005) Molecular players regulating the jasmonate signalling network. Curr Opin Plant Biol 8 (5):532-540. doi:10.1016/j.pbi.2005.07.003

Louis J, Peiffer M, Ray S, Luthe DS, Felton GW (2013) Host-specific salivary elicitor(s) of European corn borer induce defenses in tomato and maize. New Phytol 199 (1):66-73. doi:10.1111/nph.12308

Lundquist PK, Mantegazza O, Stefanski A, Stühler K, Weber APM (2017) Surveying the Oligomeric State of Arabidopsis thaliana Chloroplasts. Molecular Plant 10 (1):197-211. doi:https://doi.org/10.1016/j.molp.2016.10.011

Lv F, Zhou J, Zeng L, Xing D (2015) β-cyclocitral upregulates salicylic acid signalling to enhance excess light acclimation in Arabidopsis. J Exp Bot 66 (15):4719-4732. doi:10.1093/jxb/erv231

Major IT, Yoshida Y, Campos ML, Kapali G, Xin XF, Sugimoto K, de Oliveira Ferreira D, He SY, Howe GA (2017) Regulation of growth-defense balance by the JASMONATE ZIM-DOMAIN (JAZ)-MYC transcriptional module. New Phytol 215 (4):1533-1547. doi:10.1111/nph.14638

Malinowski R, Higgins R, Luo Y, Piper L, Nazir A, Bajwa VS, Clouse SD, Thompson PR, Stratmann JW (2009) The tomato brassinosteroid receptor BRI1 increases binding of systemin to tobacco plasma membranes, but is not involved in systemin signaling. Plant Mol Biol 70 (5):603-616. doi:10.1007/s11103-009-9494-x

Małolepsza U, Rózalska S (2005) Nitric oxide and hydrogen peroxide in tomato resistance. Nitric oxide modulates hydrogen peroxide level in o-hydroxyethylorutin-induced resistance to Botrytis cinerea in tomato. Plant Physiol Biochem 43 (6):623-635. doi:10.1016/j.plaphy.2005.04.002

Martinez de Ilarduya O, Xie Q, Kaloshian I (2003) Aphid-induced defense responses in Mi-1-mediated compatible and incompatible tomato interactions. Mol Plant Microbe Interact 16 (8):699-708. doi:10.1094/mpmi.2003.16.8.699

Mathew R, Wunderlich J, Thivierge K, Cwiklinski K, Dumont C, Tilley L, Rohrbach P, Dalton JP (2021) Biochemical and cellular characterisation of the Plasmodium falciparum M1 alanyl aminopeptidase (PfM1AAP) and M17 leucyl aminopeptidase (PfM17LAP). Scientific Reports 11 (1):2854. doi:10.1038/s41598-021-82499-4

Matsui M, Fowler JH, Walling LL (2006) Leucine aminopeptidases: diversity in structure and function. Biological Chemistry 387 (12):1535-1544. doi:10.1515/bc.2006.191

McFarland D, Ryan CA (1974) Proteinase Inhibitor-inducing Factor in Plant Leaves: A Phylogenetic Survey 1 2. Plant Physiology 54 (5):706-708. doi:10.1104/pp.54.5.706

Meinnel T, Serero A, Giglione C (2006) Impact of the N-terminal amino acid on targeted protein degradation. Biological Chemistry 387 (7):839-851. doi:10.1515/bc.2006.107

Meister A (1988) Glutathione metabolism and its selective modification. J Biol Chem 263 (33):17205-17208

Meldau S, Erb M, Baldwin IT (2012) Defence on demand: mechanisms behind optimal defence patterns. Annals of Botany 110 (8):1503-1514. doi:10.1093/aob/mcs212

Meskauskiene R, Nater M, Goslings D, Kessler F, op den Camp R, Apel K (2001) FLU: A negative regulator of chlorophyll biosynthesis in Arabidopsis thaliana. Proceedings of the National Academy of Sciences 98 (22):12826-12831. doi:10.1073/pnas.221252798

Mewis I, Tokuhisa JG, Schultz JC, Appel HM, Ulrichs C, Gershenzon J (2006) Gene expression and glucosinolate accumulation in Arabidopsis thaliana in response to generalist and specialist herbivores of different feeding guilds and the role of defense signaling pathways. Phytochemistry 67 (22):2450-2462. doi:10.1016/j.phytochem.2006.09.004

Mielecki J, Gawroński P, Karpiński S (2020) Retrograde Signaling: Understanding the Communication between Organelles. International Journal of Molecular Sciences 21 (17):6173

Milligan SB, Gasser CS (1995) Nature and regulation of pistil-expressed genes in tomato. Plant Molecular Biology 28 (4):691-711. doi:10.1007/bf00021194

Mock H-P, Dietz K-J (2016) Redox proteomics for the assessment of redox-related posttranslational regulation in plants. Biochimica et Biophysica Acta (BBA) - Proteins and Proteomics 1864 (8):967-973. doi:https://doi.org/10.1016/j.bbapap.2016.01.005

Moloshok T, Pearce G, Ryan CA (1992) Oligouronide signaling of proteinase inhibitor genes in plants: Structure-activity relationships of di- and trigalacturonic acids and their derivatives. Archives of Biochemistry and Biophysics 294 (2):731-734. doi:https://doi.org/10.1016/0003-9861(92)90748-L

Mullineaux PM, Rausch T (2005) Glutathione, photosynthesis and the redox regulation of stress-responsive gene expression. Photosynth Res 86 (3):459-474. doi:10.1007/s11120-005-8811-8

Mur LA, Kenton P, Atzorn R, Miersch O, Wasternack C (2006) The outcomes of concentration-specific interactions between salicylate and jasmonate signaling include synergy, antagonism, and oxidative stress leading to cell death. Plant Physiol 140 (1):249-262. doi:10.1104/pp.105.072348

Muthuramalingam M, Seidel T, Laxa M, de Miranda SMN, Gaertner F, Stroeher E, Kandlbinder A, Dietz K-J (2009) Multiple redox and non-redox interactions define 2-Cys Peroxiredoxin as a regulatory hub in the chloroplast. Molecular Plant 2 (6):1273-1288. doi:10.1093/mp/ssp089

Nakashita H, Yasuda M, Nitta T, Asami T, Fujioka S, Arai Y, Sekimata K, Takatsuto S, Yamaguchi I, Yoshida S (2003) Brassinosteroid functions in a broad range of disease resistance in tobacco and rice. The Plant Journal 33 (5):887-898. doi:https://doi.org/10.1046/j.1365-313X.2003.01675.x

Nandan A, Nampoothiri KM (2017) Molecular advances in microbial aminopeptidases. Bioresource Technology 245:1757-1765. doi:https://doi.org/10.1016/j.biortech.2017.05.103

Narvaez-Vasquez J, Florin-Christensen J, Ryan CA (1999) Positional specificity of a phospholipase A activity induced by wounding, systemin, and oligosaccharide elicitors in tomato leaves. Plant Cell 11 (11):2249-2260. doi:10.1105/tpc.11.11.2249

Narváez-Vásquez J, Ryan CA (2004) The cellular localization of prosystemin: a
    functional role for phloem parenchyma in systemic wound signaling. Planta 218
    (3):360-369. doi:10.1007/s00425-003-1115-3

Narvaez-Vasquez J, Tu C-J, Park S-Y, Walling LL (2008) Targeting and localization of
    wound-inducible leucine aminopeptidase A in tomato leaves. Planta 227 (2):341-
    351. doi:10.1007/s00425-007-0621-0

Nguyen CT, Martinoia E, Farmer EE (2017) Emerging Jasmonate Transporters.
    Molecular Plant 10 (5):659-661. doi:https://doi.org/10.1016/j.molp.2017.03.007

Niemeyer HM (2009) Hydroxamic Acids Derived from 2-Hydroxy-2H-1,4-Benzoxazin-
    3(4H)-one: Key Defense Chemicals of Cereals. Journal of Agricultural and Food
    Chemistry 57 (5):1677-1696. doi:10.1021/jf8034034

Nikkanen L, Rintamäki E (2019) Chloroplast thioredoxin systems dynamically regulate
    photosynthesis in plants. Biochem J 476 (7):1159-1172.
    doi:10.1042/bcj20180707

Noctor G, Mhamdi A, Chaouch S, Han Y, Neukermans J, Marquez-Garcia B, Queval G,
    Foyer CH (2012) Glutathione in plants: an integrated overview. Plant Cell and
    Environment 35 (2):454-484. doi:10.1111/j.1365-3040.2011.02400.x

Nyalala SO, Petersen MA, Grout BWW (2013) Volatile compounds from leaves of the
    African spider plant (Gynandropsis gynandra) with bioactivity against spider mite
    (Tetranychus urticae). Annals of Applied Biology 162 (3):290-298.
    doi:https://doi.org/10.1111/aab.12021

O'Donnell PJ, Calvert C, Atzorn R, Wasternack C, Leyser HMO, Bowles DJ (1996)
    Ethylene as a Signal Mediating the Wound Response of Tomato Plants. Science
    274 (5294):1914-1917. doi:10.1126/science.274.5294.1914

Oelmüller R, Levitan I, Bergfeld R, Rajasekhar VK, Mohr H (1986) Expression of nuclear genes as affected by treatments acting on the plastids. Planta 168 (4):482-492. doi:10.1007/bf00392267

Ojeda V, Jiménez-López J, Romero-Campero FJ, Cejudo FJ, Pérez-Ruiz JM (2021) A chloroplast redox relay adapts plastid metabolism to light and affects cytosolic protein quality control. Plant Physiol 187 (1):88-102. doi:10.1093/plphys/kiab246

Olinares PD, Ponnala L, van Wijk KJ (2010) Megadalton complexes in the chloroplast stroma of Arabidopsis thaliana characterized by size exclusion chromatography, mass spectrometry, and hierarchical clustering. Mol Cell Proteomics 9 (7):1594-1615. doi:10.1074/mcp.M000038-MCP201

Onkokesung N, Reichelt M, Wright LP, Phillips MA, Gershenzon J, Dicke M (2019) The plastidial metabolite 2-C-methyl-D-erythritol-2,4-cyclodiphosphate modulates defence responses against aphids. Plant Cell Environ 42 (7):2309-2323. doi:10.1111/pce.13538

op den Camp RGL, Przybyla D, Ochsenbein C, Laloi C, Kim C, Danon A, Wagner D, Hideg Ev, Göbel C, Feussner I, Nater M, Apel K (2003) Rapid Induction of Distinct Stress Responses after the Release of Singlet Oxygen in Arabidopsis. The Plant Cell 15 (10):2320-2332. doi:10.1105/tpc.014662

Orozco-Cardenas M, Ryan CA (1999) Hydrogen peroxide is generated systemically in plant leaves by wounding and systemin via the octadecanoid pathway. Proc Natl Acad Sci U S A 96 (11):6553-6557. doi:10.1073/pnas.96.11.6553

Orozco-Cardenas ML, Narvaez-Vasquez J, Ryan CA (2001) Hydrogen peroxide acts as a second messenger for the induction of defense genes in tomato plants in response to wounding, systemin, and methyl jasmonate. Plant Cell 13 (1):179-191. doi:10.2307/3871162

Orozco-Cardenas ML, Ryan CA (2002) Nitric oxide negatively modulates wound
signaling in tomato plants. Plant Physiology 130 (1):487-493.
doi:10.1104/pp.008375

Ostrovsky D, Diomina G, Lysak E, Matveeva E, Ogrel O, Trutko S (1998) Effect of
oxidative stress on the biosynthesis of 2-C-methyl-D-erythritol-2,4-
cyclopyrophosphate and isoprenoids by several bacterial strains. Arch Microbiol
171 (1):69-72. doi:10.1007/s002030050680

Page MT, Kacprzak SM, Mochizuki N, Okamoto H, Smith AG, Terry MJ (2017)
Seedlings Lacking the PTM Protein Do Not Show a genomes uncoupled (gun)
Mutant Phenotype. Plant Physiol 174 (1):21-26. doi:10.1104/pp.16.01930

Panpetch P, Sirikantaramas S (2021) Fruit ripening-associated leucylaminopeptidase
with cysteinylglycine dipeptidase activity from durian suggests its involvement in
glutathione recycling. BMC Plant Biology 21 (1):69. doi:10.1186/s12870-021-
02845-6

Pattyn J, Vaughan-Hirsch J, Van de Poel B (2021) The regulation of ethylene
biosynthesis: a complex multilevel control circuitry. New Phytol 229 (2):770-782.
doi:10.1111/nph.16873

Pautot V, Holzer FM, Chaufaux J, Walling LL (2001) The induction of tomato leucine
aminopeptidase genes (LapA) after Pseudomonas syringae pv. tomato infection
is primarily a wound response triggered by coronatine. Molecular Plant-Microbe
Interactions 14 (2):214-224. doi:10.1094/mpmi.2001.14.2.214

Pautot V, Holzer FM, Reisch B, Walling LL (1993) Leucine aminopeptidase: an inducible
component of the defense response in Lycopersicon esculentum (tomato).
Proceedings of the National Academy of Sciences of the United States of
America 90 (21):9906-9910. doi:10.1073/pnas.90.21.9906

Pautot V, Holzer FM, Walling LL (1991) Differential expression of tomato proteinase inhibitor I and II genes during bacterial pathogen invasion and wounding. Molecular Plant-Microbe Interactions 4 (3):284-292. doi:10.1094/mpmi-4-284

Pearce G (2011) Systemin, hydroxyproline-rich systemin and the induction of protease inhibitors. Curr Protein Pept Sci 12 (5):399-408. doi:10.2174/138920311796391106

Pearce G, Moura DS, Stratmann J, Ryan CA (2001) Production of multiple plant hormones from a single polyprotein precursor. Nature 411 (6839):817-820. doi:10.1038/35081107

Pearce G, Ryan CA (2003) Systemic Signaling in Tomato Plants for Defense against Herbivores: ISOLATION AND CHARACTERIZATION OF THREE NOVEL DEFENSE-SIGNALING GLYCOPEPTIDE HORMONES CODED IN A SINGLE PRECURSOR GENE *. Journal of Biological Chemistry 278 (32):30044-30050. doi:10.1074/jbc.M304159200

Pearce G, Strydom D, Johnson S, Ryan CA (1991) A polypeptide from tomato leaves induces wound-inducible proteinase inhibitor proteins. Science 253 (5022):895-897. doi:10.1126/science.253.5022.895

Pedley KF, Martin GB (2003) MOLECULAR BASIS OF PTO-MEDIATED RESISTANCE TO BACTERIAL SPECK DISEASE IN TOMATO. Annual Review of Phytopathology 41 (1):215-243. doi:10.1146/annurev.phyto.41.121602.143032

Peer WA, Hosein FN, Bandyopadhyay A, Makam SN, Otegui MS, Lee G-J, Blakeslee JJ, Cheng Y, Titapiwatanakun B, Yakubov B, Bangari B, Murphy AS (2009) Mutation of the Membrane-Associated M1 Protease APM1 Results in Distinct Embryonic and Seedling Developmental Defects in Arabidopsis. Plant Cell 21 (6):1693-1721. doi:10.1105/tpc.108.059634

Peltier JB, Cai Y, Sun Q, Zabrouskov V, Giacomelli L, Rudella A, Ytterberg AJ, Rutschow H, van Wijk KJ (2006) The oligomeric stromal proteome of Arabidopsis thaliana chloroplasts. Mol Cell Proteomics 5 (1):114-133. doi:10.1074/mcp.M500180-MCP200

Pena-Cortés H, Albrecht T, Prat S, Weiler EW, Willmitzer L (1993) Aspirin prevents wound-induced gene expression in tomato leaves by blocking jasmonic acid biosynthesis. Planta 191 (1):123-128

PenaCortes H, Prat S, Atzorn R, Wasternack C, Willmitzer L (1996) Abscisic acid-deficient plants do not accumulate proteinase inhibitor II following systemin treatment. Planta 198 (3):447-451. doi:10.1007/bf00620062

Peng Z, Han C, Yuan L, Zhang K, Huang H, Ren C (2011) Brassinosteroid enhances jasmonate-induced anthocyanin accumulation in Arabidopsis seedlings. J Integr Plant Biol 53 (8):632-640. doi:10.1111/j.1744-7909.2011.01042.x

Penninckx IAMA, Thomma BPHJ, Buchala A, Métraux J-P, Broekaert WF (1998) Concomitant Activation of Jasmonate and Ethylene Response Pathways Is Required for Induction of a Plant Defensin Gene in Arabidopsis. Plant Cell 10 (12):2103-2113. doi:10.1105/tpc.10.12.2103

Peres A, Soares JS, Tavares RG, Righetto G, Zullo MAT, Mandava NB, Menossi M (2019) Brassinosteroids, the Sixth Class of Phytohormones: A Molecular View from the Discovery to Hormonal Interactions in Plant Development and Stress Adaptation. Int J Mol Sci 20 (2). doi:10.3390/ijms20020331

Pérez-Ruiz JM, Guinea M, Puerto-Galán L, Cejudo FJ (2014) NADPH thioredoxin reductase C is involved in redox regulation of the Mg-chelatase I subunit in Arabidopsis thaliana chloroplasts. Mol Plant 7 (7):1252-1255. doi:10.1093/mp/ssu032

Pérez-Ruiz JM, Naranjo B, Ojeda V, Guinea M, Cejudo FJ (2017) NTRC-dependent redox balance of 2-Cys peroxiredoxins is needed for optimal function of the photosynthetic apparatus. Proc Natl Acad Sci U S A 114 (45):12069-12074. doi:10.1073/pnas.1706003114

Pham AQ, Cho SH, Nguyen CT, Stacey G (2020) Arabidopsis Lectin Receptor Kinase P2K2 Is a Second Plant Receptor for Extracellular ATP and Contributes to Innate Immunity. Plant Physiol 183 (3):1364-1375. doi:10.1104/pp.19.01265

Pilon M, Ravet K, Tapken W (2011) The biogenesis and physiological function of chloroplast superoxide dismutases. Biochim Biophys Acta 1807 (8):989-998. doi:10.1016/j.bbabio.2010.11.002

Pinnola A, Bassi R (2018) Molecular mechanisms involved in plant photoprotection. Biochem Soc Trans 46 (2):467-482. doi:10.1042/bst20170307

Pogson BJ, Woo NS, Förster B, Small ID (2008) Plastid signalling to the nucleus and beyond. Trends Plant Sci 13 (11):602-609. doi:10.1016/j.tplants.2008.08.008

Poretsky E, Ruiz M, Ahmadian N, Steinbrenner AD, Dressano K, Schmelz EA, Huffaker A (2021) Comparative analyses of responses to exogenous and endogenous antiherbivore elicitors enable a forward genetics approach to identify maize gene candidates mediating sensitivity to herbivore-associated molecular patterns. The Plant Journal 108 (5):1295-1316. doi:https://doi.org/10.1111/tpj.15510

Pornsiriwong W, Estavillo GM, Chan KX, Tee EE, Ganguly D, Crisp PA, Phua SY, Zhao C, Qiu J, Park J, Yong MT, Nisar N, Yadav AK, Schwessinger B, Rathjen J, Cazzonelli CI, Wilson PB, Gilliham M, Chen ZH, Pogson BJ (2017) A chloroplast retrograde signal, 3'-phosphoadenosine 5'-phosphate, acts as a secondary messenger in abscisic acid signaling in stomatal closure and germination. Elife 6. doi:10.7554/eLife.23361

Poudel AN, Holtsclaw RE, Kimberlin A, Sen S, Zeng S, Joshi T, Lei Z, Sumner LW, Singh K, Matsuura H, Koo AJ (2019) 12-Hydroxy-Jasmonoyl-l-Isoleucine Is an Active Jasmonate That Signals through CORONATINE INSENSITIVE 1 and Contributes to the Wound Response in Arabidopsis. Plant and Cell Physiology 60 (10):2152-2166. doi:10.1093/pcp/pcz109

Pré M, Atallah M, Champion A, De Vos M, Pieterse CM, Memelink J (2008) The AP2/ERF domain transcription factor ORA59 integrates jasmonic acid and ethylene signals in plant defense. Plant Physiol 147 (3):1347-1357. doi:10.1104/pp.108.117523

Puerto-Galán L, Pérez-Ruiz JM, Guinea M, Cejudo FJ (2015) The contribution of NADPH thioredoxin reductase C (NTRC) and sulfiredoxin to 2-Cys peroxiredoxin overoxidation in Arabidopsis thaliana chloroplasts. Journal of Experimental Botany 66 (10):2957-2966. doi:10.1093/jxb/eru512

Queval G, Thominet D, Vanacker H, Miginiac-Maslow M, Gakière B, Noctor G (2009) H2O2-Activated Up-Regulation of Glutathione in Arabidopsis Involves Induction of Genes Encoding Enzymes Involved in Cysteine Synthesis in the Chloroplast. Molecular Plant 2 (2):344-356. doi:https://doi.org/10.1093/mp/ssp002

Quintana-Rodriguez E, Duran-Flores D, Heil M, Camacho-Coronel X (2018) Damage-associated molecular patterns (DAMPs) as future plant vaccines that protect crops from pests. Scientia Horticulturae 237:207-220. doi:https://doi.org/10.1016/j.scienta.2018.03.026

Ramel F, Birtic S, Ginies C, Soubigou-Taconnat L, Triantaphylidès C, Havaux M (2012) Carotenoid oxidation products are stress signals that mediate gene responses to singlet oxygen in plants. Proceedings of the National Academy of Sciences 109 (14):5535-5540. doi:10.1073/pnas.1115982109

Rasul S, Dubreuil-Maurizi C, Lamotte O, Koen E, Poinssot B, Alcaraz G, Wendehenne
D, Jeandroz S (2012) Nitric oxide production mediates oligogalacturonide-
triggered immunity and resistance to Botrytis cinerea in Arabidopsis thaliana.
Plant Cell Environ 35 (8):1483-1499. doi:10.1111/j.1365-3040.2012.02505.x

Rawlings ND, Barrett AJ (2013) Handbook of Proteolytic Enzymes Introduction:
Metallopeptidases and Their Clans. Handbook of Proteolytic Enzymes, Vols 1
and 2, 3rd Edition. Elsevier Science Bv, Amsterdam. doi:10.1016/b978-0-12-
382219-2.00077-6

Ren C, Han C, Peng W, Huang Y, Peng Z, Xiong X, Zhu Q, Gao B, Xie D (2009) A leaky
mutation in DWARF4 reveals an antagonistic role of brassinosteroid in the
inhibition of root growth by jasmonate in Arabidopsis. Plant physiology 151
(3):1412-1420

Ren Y, Li Y, Jiang Y, Wu B, Miao Y (2017) Phosphorylation of WHIRLY1 by CIPK14
Shifts Its Localization and Dual Functions in Arabidopsis. Mol Plant 10 (5):749-
763. doi:10.1016/j.molp.2017.03.011

Rennenberg H (1980) Glutathione metabolism and possible biological roles in higher
plants. Phytochemistry 21 (12):2771-2781. doi:https://doi.org/10.1016/0031-
9422(80)85045-X

Rey P, Cuine S, Eymery F, Garin J, Court M, Jacquot JP, Rouhier N, Broin M (2005)
Analysis of the proteins targeted by CDSP32, a plastidic thioredoxin participating
in oxidative stress responses. Plant Journal 41 (1):31-42. doi:10.1111/j.1365-
313X.2004.02271.x

Reymond P, Weber H, Damond M, Farmer EE (2000) Differential gene expression in
response to mechanical wounding and insect feeding in Arabidopsis. Plant Cell
12 (5):707-720. doi:10.1105/tpc.12.5.707

Rhodes JD, Thain JF, Wildon DC (1996) The pathway for systemic electrical signal
conduction in the wounded tomato plant. Planta 200 (1):50-57

Richter AS, Pérez-Ruiz JM, Cejudo FJ, Grimm B (2018) Redox-control of chlorophyll
biosynthesis mainly depends on thioredoxins. FEBS Lett 592 (18):3111-3115.
doi:10.1002/1873-3468.13216

Richter AS, Peter E, Rothbart M, Schlicke H, Toivola J, Rintamäki E, Grimm B (2013)
Posttranslational influence of NADPH-dependent thioredoxin reductase C on
enzymes in tetrapyrrole synthesis. Plant Physiol 162 (1):63-73.
doi:10.1104/pp.113.217141

Rochon A, Boyle P, Wignes T, Fobert PR, Després C (2006) The Coactivator Function
of Arabidopsis NPR1 Requires the Core of Its BTB/POZ Domain and the
Oxidation of C-Terminal Cysteines. The Plant Cell 18 (12):3670-3685.
doi:10.1105/tpc.106.046953

Rodríguez VM, Chételat A, Majcherczyk P, Farmer EE (2010) Chloroplastic
Phosphoadenosine Phosphosulfate Metabolism Regulates Basal Levels of the
Prohormone Jasmonic Acid in Arabidopsis Leaves. Plant Physiology 152
(3):1335-1345. doi:10.1104/pp.109.150474

Ryan CA, Jagendorf A (1995) Self defense by plants. Proceedings of the National
Academy of Sciences 92 (10):4075. doi:10.1073/pnas.92.10.4075

Sagi M, Davydov O, Orazova S, Yesbergenova Z, Ophir R, Stratmann JW, Fluhr R
(2004) Plant respiratory burst oxidase homologs impinge on wound
responsiveness and development in Lycopersicon esculentum. The Plant cell 16
(3):616-628. doi:10.1105/tpc.019398

Sanchez-Moran E, Jones GH, Franklin FCH, Santos JL (2004) A puromycin-sensitive aminopeptidase is essential for meiosis in Arabidopsis thaliana. Plant Cell 16 (11):2895-2909. doi:10.1105/tpc.104.024992

Scarpeci TE, Zanor MI, Carrillo N, Mueller-Roeber B, Valle EM (2008) Generation of superoxide anion in chloroplasts of Arabidopsis thaliana during active photosynthesis: a focus on rapidly induced genes. Plant Mol Biol 66 (4):361-378. doi:10.1007/s11103-007-9274-4

Schaller A, Stintzi A (2009) Enzymes in jasmonate biosynthesis – Structure, function, regulation. Phytochemistry 70 (13):1532-1538. doi:https://doi.org/10.1016/j.phytochem.2009.07.032

Schmelz EA, Carroll MJ, LeClere S, Phipps SM, Meredith J, Chourey PS, Alborn HT, Teal PEA (2006) Fragments of ATP synthase mediate plant perception of insect attack. Proceedings of the National Academy of Sciences 103 (23):8894-8899. doi:10.1073/pnas.0602328103

Schmelz EA, Engelberth J, Alborn HT, Tumlinson JH, Teal PEA (2009) Phytohormone-based activity mapping of insect herbivore-produced elicitors. Proceedings of the National Academy of Sciences 106 (2):653-657. doi:10.1073/pnas.0811861106

Scranton MA (2013) Elucidation of the Role of Leucine Aminopeptidase A in the Wound Response Pathway in Tomato. UC Riverside.

Scranton MA, Fowler JH, Girke T, Walling LL (2013) Microarray Analysis of Tomato's Early and Late Wound Response Reveals New Regulatory Targets for Leucine Aminopeptidase A. Plos One 8 (10). doi:10.1371/journal.pone.0077889

Scranton MA, Yee A, Park S-Y, Walling LL (2012) Plant Leucine Aminopeptidases
Moonlight as Molecular Chaperones to Alleviate Stress-induced Damage.
Journal of Biological Chemistry 287 (22):18408-18417.
doi:10.1074/jbc.M111.309500

Serrato AJ, Pérez-Ruiz JM, Spínola MC, Cejudo FJ (2004) A novel NADPH thioredoxin
reductase, localized in the chloroplast, which deficiency causes hypersensitivity
to abiotic stress in Arabidopsis thaliana. J Biol Chem 279 (42):43821-43827.
doi:10.1074/jbc.M404696200

Sharma P, Gayen D (2021) Plant protease as regulator and signaling molecule for
enhancing environmental stress-tolerance. Plant Cell Reports.
doi:10.1007/s00299-021-02739-9

Shimizu T, Masuda T (2021) The Role of Tetrapyrrole- and GUN1-Dependent Signaling
on Chloroplast Biogenesis. Plants (Basel) 10 (2). doi:10.3390/plants10020196

Spoel SH, Koornneef A, Claessens SM, Korzelius JP, Van Pelt JA, Mueller MJ, Buchala
AJ, Métraux JP, Brown R, Kazan K, Van Loon LC, Dong X, Pieterse CM (2003)
NPR1 modulates cross-talk between salicylate- and jasmonate-dependent
defense pathways through a novel function in the cytosol. Plant Cell 15 (3):760-
770. doi:10.1105/tpc.009159

Steinbrenner AD, Munoz-Amatriain M, Chaparro AF, Aguilar-Venegas JM, Lo S, Okuda
S, Glauser G, Dongiovanni J, Shi D, Hall M, Crubaugh D, Holton N, Zipfel C,
Abagyan R, Turlings TCJ, Close TJ, Huffaker A, Schmelz EA (2020) A receptor-
like protein mediates plant immune responses to herbivore-associated molecular
patterns. Proceedings of the National Academy of Sciences of the United States
of America 117 (49):31510-31518. doi:10.1073/pnas.2018415117

Stenbaek A, Hansson A, Wulff RP, Hansson M, Dietz KJ, Jensen PE (2008) NADPH-dependent thioredoxin reductase and 2-Cys peroxiredoxins are needed for the protection of Mg-protoporphyrin monomethyl ester cyclase. FEBS Lett 582 (18):2773-2778. doi:10.1016/j.febslet.2008.07.006

Stirling CJ, Colloms SD, Collins JF, Szatmari G, Sherratt DJ (1989) xerB, an Escherichia coli gene required for plasmid ColE1 site-specific recombination, is identical to pepA, encoding aminopeptidase A, a protein with substantial similarity to bovine lens leucine aminopeptidase. Embo Journal 8 (5):1623-1627

Stotz HU, Pittendrigh BR, Kroymann Jr, Weniger K, Fritsche J, Bauke A, Mitchell-Olds T (2000) Induced Plant Defense Responses against Chewing Insects. Ethylene Signaling Reduces Resistance of Arabidopsis against Egyptian Cotton Worm But Not Diamondback Moth1. Plant Physiology 124 (3):1007-1018. doi:10.1104/pp.124.3.1007

Straeter N, Lipscomb WN (2013) Leucyl Aminopeptidase (Animal). Handbook of Proteolytic Enzymes, Vols 1 and 2, 3rd Edition. doi:10.1016/b978-0-12-382219-2.00330-6

Sullivan JA, Gray JC (1999) Plastid translation is required for the expression of nuclear photosynthesis genes in the dark and in roots of the pea lip1 mutant. Plant Cell 11 (5):901-910. doi:10.1105/tpc.11.5.901

Sun X, Feng P, Xu X, Guo H, Ma J, Chi W, Lin R, Lu C, Zhang L (2011) A chloroplast envelope-bound PHD transcription factor mediates chloroplast signals to the nucleus. Nat Commun 2:477. doi:10.1038/ncomms1486

Susek RE, Ausubel FM, Chory J (1993) Signal transduction mutants of arabidopsis uncouple nuclear CAB and RBCS gene expression from chloroplast development. Cell 74 (5):787-799. doi:https://doi.org/10.1016/0092-8674(93)90459-4

Suza WP, Rowe ML, Hamberg M, Staswick PE (2010) A tomato enzyme synthesizes (+)-7-iso-jasmonoyl-L-isoleucine in wounded leaves. Planta 231 (3):717-728. doi:10.1007/s00425-009-1080-6

Suza WP, Staswick PE (2008) The role of JAR1 in Jasmonoyl-l-isoleucine production during Arabidopsis wound response. Planta 227 (6):1221-1232. doi:10.1007/s00425-008-0694-4

Tadini L, Jeran N, Peracchio C, Masiero S, Colombo M, Pesaresi P (2020) The plastid transcription machinery and its coordination with the expression of nuclear genome: Plastid-Encoded Polymerase, Nuclear-Encoded Polymerase and the Genomes Uncoupled 1-mediated retrograde communication. Philosophical Transactions of the Royal Society B: Biological Sciences 375 (1801):20190399. doi:doi:10.1098/rstb.2019.0399

Takahashi F, Shinozaki K (2019) Long-distance signaling in plant stress response. Curr Opin Plant Biol 47:106-111. doi:10.1016/j.pbi.2018.10.006

Taylor A (1985) Leucine aminopeptidase activity is diminished in aged hog, beef, and human lens. Progress in clinical and biological research 180:299-302

Theodoulou FL, Job K, Slocombe SP, Footitt S, Holdsworth M, Baker A, Larson TR, Graham IA (2005) Jasmonic Acid Levels Are Reduced in COMATOSE ATP-Binding Cassette Transporter Mutants. Implications for Transport of Jasmonate Precursors into Peroxisomes. Plant Physiology 137 (3):835-840. doi:10.1104/pp.105.059352

Thines B, Katsir L, Melotto M, Niu Y, Mandaokar A, Liu G, Nomura K, He SY, Howe GA, Browse J (2007) JAZ repressor proteins are targets of the SCFCOI1 complex during jasmonate signalling. Nature 448 (7154):661-665. doi:10.1038/nature05960

Tian DL, Peiffer M, De Moraes CM, Felton GW (2014) Roles of ethylene and jasmonic acid in systemic induced defense in tomato (Solanum lycopersicum) against Helicoverpa zea. Planta 239 (3):577-589. doi:10.1007/s00425-013-1997-7

Torres MA, Jones JDG, Dangl JL (2006) Reactive oxygen species signaling in response to pathogens. Plant physiology 141 (2):373-378

Toyota M, Spencer D, Sawai-Toyota S, Jiaqi W, Zhang T, Koo AJ, Howe GA, Gilroy S (2018) Glutamate triggers long-distance, calcium-based plant defense signaling. Science 361 (6407):1112-1115. doi:doi:10.1126/science.aat7744

Tripathi D, Zhang T, Koo AJ, Stacey G, Tanaka K (2018) Extracellular ATP Acts on Jasmonate Signaling to Reinforce Plant Defense. Plant Physiol 176 (1):511-523. doi:10.1104/pp.17.01477

Tsuda K, Sato M, Stoddard T, Glazebrook J, Katagiri F (2009) Network Properties of Robust Immunity in Plants. PLOS Genetics 5 (12):e1000772. doi:10.1371/journal.pgen.1000772

Tu CJ, Park SY, Walling LL (2003) Isolation and characterization of the neutral leucine aminopeptidase (LapN) of tomato. Plant Physiology 132 (1):243-255. doi:10.1104/pp.102.013854

Tzin V, Fernandez-Pozo N, Richter A, Schmelz EA, Schoettner M, Schäfer M, Ahern KR, Meihls LN, Kaur H, Huffaker A, Mori N, Degenhardt J, Mueller LA, Jander G (2015) Dynamic Maize Responses to Aphid Feeding Are Revealed by a Time Series of Transcriptomic and Metabolomic Assays Plant Physiology 169 (3):1727-1743. doi:10.1104/pp.15.01039

Uppalapati SR, Ishiga Y, Ryu CM, Ishiga T, Wang K, Noël LD, Parker JE, Mysore KS (2011) SGT1 contributes to coronatine signaling and Pseudomonas syringae pv. tomato disease symptom development in tomato and Arabidopsis. New Phytologist 189 (1):83-93

Van der Does D, Leon-Reyes A, Koornneef A, Van Verk MC, Rodenburg N, Pauwels L, Goossens A, Körbes AP, Memelink J, Ritsema T, Van Wees SC, Pieterse CM (2013) Salicylic acid suppresses jasmonic acid signaling downstream of SCFCOI1-JAZ by targeting GCC promoter motifs via transcription factor ORA59. Plant Cell 25 (2):744-761. doi:10.1105/tpc.112.108548

Van der Hoorn RA (2008) Plant proteases: from phenotypes to molecular mechanisms. Annu Rev Plant Biol 59:191-223

van Endert P (2011) Post-proteasomal and proteasome-independent generation of MHC class I ligands. Cellular and Molecular Life Sciences 68 (9):1553-1567. doi:10.1007/s00018-011-0662-1

Vanderstraeten L, Van Der Straeten D (2017) Accumulation and Transport of 1-Aminocyclopropane-1-Carboxylic Acid (ACC) in Plants: Current Status, Considerations for Future Research and Agronomic Applications. Front Plant Sci 8:38. doi:10.3389/fpls.2017.00038

Varshavsky A (2011) The N-end rule pathway and regulation by proteolysis. Protein Science 20 (8):1298-1345. doi:10.1002/pro.666

Vogel MO, Moore M, König K, Pecher P, Alsharafa K, Lee J, Dietz KJ (2014) Fast retrograde signaling in response to high light involves metabolite export, MITOGEN-ACTIVATED PROTEIN KINASE6, and AP2/ERF transcription factors in Arabidopsis. Plant Cell 26 (3):1151-1165. doi:10.1105/tpc.113.121061

Waditee-Sirisattha R, Hattori A, Shibato J, Rakwal R, Sirisattha S, Takabe T, Tsujimoto M (2011a) Role of the Arabidopsis leucine aminopeptidase 2. Plant Signaling & Behavior 6 (10):1581-1583. doi:10.4161/psb.6.10.17105

Waditee-Sirisattha R, Shibato J, Rakwal R, Sirisattha S, Hattori A, Nakano T, Takabe T, Tsujimoto M (2011b) The Arabidopsis aminopeptidase LAP2 regulates plant growth, leaf longevity and stress response. New Phytologist 191 (4):958-969. doi:10.1111/j.1469-8137.2011.03758.x

Wagner D, Przybyla D, Op den Camp R, Kim C, Landgraf F, Lee KP, Würsch M, Laloi C, Nater M, Hideg E, Apel K (2004) The genetic basis of singlet oxygen-induced stress responses of Arabidopsis thaliana. Science 306 (5699):1183-1185. doi:10.1126/science.1103178

Walley J, Xiao Y, Wang JZ, Baidoo EE, Keasling JD, Shen Z, Briggs SP, Dehesh K (2015) Plastid-produced interorgannellar stress signal MEcPP potentiates induction of the unfolded protein response in endoplasmic reticulum. Proc Natl Acad Sci U S A 112 (19):6212-6217. doi:10.1073/pnas.1504828112

Walling LL (2000) The Myriad Plant Responses to Herbivores. Journal of Plant Growth Regulation 19 (2):195-216. doi:10.1007/s003440000026

Walling LL (2006) Recycling or regulation? The role of amino-terminal modifying
enzymes. Current Opinion in Plant Biology 9 (3):227-233.
doi:10.1016/j.pbi.2006.03.009

Walling LL (2013) Leucyl Aminopeptidase (Plant). Handbook of Proteolytic Enzymes,
Vols 1 and 2, 3rd Edition. doi:10.1016/b978-0-12-382219-2.00331-8

Wanat W, Talma M, Pawełczak M, Kafarski P (2019) Phosphonic Acid Analogues of
Phenylglycine as Inhibitors of Aminopeptidases: Comparison of Porcine
Aminopeptidase N, Bovine Leucine Aminopeptidase, Tomato Acidic Leucine
Aminopeptidase and Aminopeptidase from Barley Seeds. Pharmaceuticals 12
(3):139

Wang DD, Li P, Chen QY, Chen XY, Yan ZW, Wang MY, Mao YB (2021) Differential
Contributions of MYCs to Insect Defense Reveals Flavonoids Alleviating Growth
Inhibition Caused by Wounding in Arabidopsis. Frontiers in Plant Science 12.
doi:10.3389/fpls.2021.700555

Wang J-Z, Li B, Xiao Y, Ni Y, Ke H, Yang P, de Souza A, Bjornson M, He X, Shen Z,
Balcke GU, Briggs SP, Tissier A, Kliebenstein DJ, Dehesh K (2017) Initiation of
ER Body Formation and Indole Glucosinolate Metabolism by the Plastidial
Retrograde Signaling Metabolite, MEcPP. Molecular Plant 10 (11):1400-1416.
doi:10.1016/j.molp.2017.09.012

Wang L, Einig E, Almeida-Trapp M, Albert M, Fliegmann J, Mithöfer A, Kalbacher H,
Felix G (2018) The systemin receptor SYR1 enhances resistance of tomato
against herbivorous insects. Nature Plants 4 (3):152-156. doi:10.1038/s41477-
018-0106-0

Wang L, Kim C, Xu X, Piskurewicz U, Dogra V, Singh S, Mahler H, Apel K (2016) Singlet oxygen- and EXECUTER1-mediated signaling is initiated in grana margins and depends on the protease FtsH2. Proceedings of the National Academy of Sciences 113 (26):E3792-E3800. doi:10.1073/pnas.1603562113

Wang L, Leister D, Guan L, Zheng Y, Schneider K, Lehmann M, Apel K, Kleine T (2020) The Arabidopsis SAFEGUARD1 suppresses singlet oxygen-induced stress responses by protecting grana margins. Proceedings of the National Academy of Sciences 117 (12):6918-6927. doi:10.1073/pnas.1918640117

Wasternack C, Feussner I (2018) The Oxylipin Pathways: Biochemistry and Function. Annu Rev Plant Biol 69:363-386. doi:10.1146/annurev-arplant-042817-040440

Wasternack C, Song S (2017) Jasmonates: biosynthesis, metabolism, and signaling by proteins activating and repressing transcription. J Exp Bot 68 (6):1303-1321. doi:10.1093/jxb/erw443

Wu G-Z, Chalvin C, Hoelscher M, Meyer EH, Wu XN, Bock R (2018) Control of Retrograde Signaling by Rapid Turnover of GENOMES UNCOUPLED1 Plant Physiology 176 (3):2472-2495. doi:10.1104/pp.18.00009

Wu S, Peiffer M, Luthe DS, Felton GW (2012a) ATP hydrolyzing salivary enzymes of caterpillars suppress plant defenses. PLoS One 7 (7):e41947. doi:10.1371/journal.pone.0041947

Wu Y, Zhang D, Chu Jee Y, Boyle P, Wang Y, Brindle Ian D, De Luca V, Després C (2012b) The Arabidopsis NPR1 Protein Is a Receptor for the Plant Defense Hormone Salicylic Acid. Cell Reports 1 (6):639-647. doi:10.1016/j.celrep.2012.05.008

Xiang C, Oliver DJ (1998) Glutathione metabolic genes coordinately respond to heavy metals and jasmonic acid in Arabidopsis. Plant Cell 10 (9):1539-1550. doi:10.1105/tpc.10.9.1539

Xiao Y, Savchenko T, Baidoo Edward EK, Chehab Wassim E, Hayden Daniel M, Tolstikov V, Corwin Jason A, Kliebenstein Daniel J, Keasling Jay D, Dehesh K (2012) Retrograde Signaling by the Plastidial Metabolite MEcPP Regulates Expression of Nuclear Stress-Response Genes. Cell 149 (7):1525-1535. doi:10.1016/j.cell.2012.04.038

Xin XF, He SY (2013) Pseudomonas syringae pv. tomato DC3000: A Model Pathogen for Probing Disease Susceptibility and Hormone Signaling in Plants. In: VanAlfen NK (ed) Annual Review of Phytopathology, Vol 51, vol 51. Annual Review of Phytopathology. Annual Reviews, Palo Alto, pp 473-498. doi:10.1146/annurev-phyto-082712-102321

Yamada K, Yamashita-Yamada M, Hirase T, Fujiwara T, Tsuda K, Hiruma K, Saijo Y (2016) Danger peptide receptor signaling in plants ensures basal immunity upon pathogen-induced depletion of BAK1. EMBO J 35 (1):46-61. doi:10.15252/embj.201591807

Yamaguchi Y, Huffaker A, Bryan AC, Tax FE, Ryan CA (2010) PEPR2 is a second receptor for the Pep1 and Pep2 peptides and contributes to defense responses in Arabidopsis. The Plant Cell 22 (2):508-522

Yan J, Li S, Gu M, Yao R, Li Y, Chen J, Yang M, Tong J, Xiao L, Nan F, Xie D (2016) Endogenous Bioactive Jasmonate Is Composed of a Set of (+)-7-iso-JA-Amino Acid Conjugates. Plant Physiol 172 (4):2154-2164. doi:10.1104/pp.16.00906

Zander M, Lewsey MG, Clark NM, Yin L, Bartlett A, Saldierna Guzmán JP, Hann E, Langford AE, Jow B, Wise A, Nery JR, Chen H, Bar-Joseph Z, Walley JW, Solano R, Ecker JR (2020) Integrated multi-omics framework of the plant response to jasmonic acid. Nature Plants 6 (3):290-302. doi:10.1038/s41477-020-0605-7

Zarate SI, Kempema LA, Walling LL (2007) Silverleaf whitefly induces salicylic acid defenses and suppresses effectual jasmonic acid defenses. Plant Physiol 143 (2):866-875. doi:10.1104/pp.106.090035

Zhang X-C, Millet YA, Cheng Z, Bush J, Ausubel FM (2015) Jasmonate signalling in Arabidopsis involves SGT1b–HSP70–HSP90 chaperone complexes. Nature Plants 1 (5):15049. doi:10.1038/nplants.2015.49

ZHANG Z-W, YUAN S, XU F, YANG H, CHEN Y-E, YUAN M, XU M-Y, XUE L-W, XU X-C, LIN H-H (2011) Mg-protoporphyrin, haem and sugar signals double cellular total RNA against herbicide and high-light-derived oxidative stress. Plant, Cell & Environment 34 (6):1031-1042. doi:https://doi.org/10.1111/j.1365-3040.2011.02302.x

Zhao X, Huang J, Chory J (2018) genome uncoupled1 Mutants Are Hypersensitive to Norflurazon and Lincomycin. Plant Physiology 178 (3):960-964. doi:10.1104/pp.18.00772

Zhao X, Huang J, Chory J (2019) GUN1 interacts with MORF2 to regulate plastid RNA editing during retrograde signaling. Proc Natl Acad Sci U S A 116 (20):10162-10167. doi:10.1073/pnas.1820426116

Zhao X, Huang J, Chory J (2020) Unraveling the Linkage between Retrograde Signaling and RNA Metabolism in Plants. Trends in Plant Science 25 (2):141-147. doi:10.1016/j.tplants.2019.10.009

Zheng X-y, Spivey Natalie W, Zeng W, Liu P-P, Fu Zheng Q, Klessig Daniel F, He
Sheng Y, Dong X (2012) Coronatine Promotes Pseudomonas syringae Virulence
in Plants by Activating a Signaling Cascade that Inhibits Salicylic Acid
Accumulation. Cell Host & Microbe 11 (6):587-596.
doi:10.1016/j.chom.2012.04.014

Zhou F, Pichersky E (2020) The complete functional characterisation of the terpene
synthase family in tomato. New Phytologist 226 (5):1341-1360.
doi:https://doi.org/10.1111/nph.16431

Zhou J-M, Zhang Y (2020) Plant Immunity: Danger Perception and Signaling. Cell 181
(5):978-989. doi:10.1016/j.cell.2020.04.028

Zhou M, Wang W, Karapetyan S, Mwimba M, Marqués J, Buchler NE, Dong X (2015)
Redox rhythm reinforces the circadian clock to gate immune response. Nature
523 (7561):472-476. doi:10.1038/nature14449

Zhu Z, An F, Feng Y, Li P, Xue L, A M, Jiang Z, Kim JM, To TK, Li W, Zhang X, Yu Q,
Dong Z, Chen WQ, Seki M, Zhou JM, Guo H (2011) Derepression of ethylene-
stabilized transcription factors (EIN3/EIL1) mediates jasmonate and ethylene
signaling synergy in Arabidopsis. Proc Natl Acad Sci U S A 108 (30):12539-
12544. doi:10.1073/pnas.1103959108

Chapter 1: The tomato chloroplast soluble proteome leveraging a plastid-protein localization prediction Atlas

Abstract

Chloroplasts are sites of metabolic hubs with wide-ranging functionality. The functions are primarily photosynthesis to a myriad biosynthetic functionality such as retrograde signaling relaying the organelle status to the nucleus. The chloroplast stromal proteome of tomato (Solanum lycopersicum) showcased 1,254 proteins from MudPIT nano LC-MS/MS studies. We leveraged reproducibility, robust in-house protein localization-predictions (the Atlas) and subcellular localization databases to assign credibility to proteins. We identified significantly more proteins than the Arabidopsis stromal proteome (241 proteins), including ~550 novel proteins in the tomato plastid proteome. We assigned molar abundance, sub-organellar localization and primary functions to proteins. The focus is on retrograde signaling given the chloroplast localization of wound-inducible leucine aminopeptidase A (LAP-A) and its ability to modulate nuclear gene expression. Other protein functionalities of our focus were redox hubs, protein homeostasis, photosynthetic complexes, and the chloroplast's non-photosynthetic biosynthetic features, as this lays the cornerstone to our future work.

Introduction

Chloroplasts are essential organelles of green algae, land plants and some protists. Differentiating from proplastids, chloroplasts are tissue-specific and formed in response to endogenous signals (Jarvis and López-Juez 2013). Well known for their role in photosynthesis, chloroplasts serve as metabolic hubs. They are engaged in the biosynthesis of amino acids, starch, fatty acids, lipids, terpenoids, purine and pyrimidine bases, various pigments, vitamins, co-factors, as well as major biochemical pathways, such as nitrogen and sulfur metabolism (Buchanan et al. 2015; Rolland et al. 2012).

Approximately 2500 proteins reside within chloroplasts (Abdallah et al. 2000). The vast majority are nuclear genome encoded, synthesized in the cytosol, imported into the chloroplast, and sorted into one of six sub-compartments (Cline and Dabney-Smith 2008; Nakai 2018; Thomson et al. 2020). N-terminal transit peptides facilitate the import of the majority of nuclear genome-encoded proteins into the chloroplast, while other proteins use non-canonical pathways for protein import into the chloroplast, including transit through the endoplasmic reticulum (Armbruster et al. 2009).

Due to the emergence of its well annotated genome in 2000 (Initiative 2000), proteomes of Arabidopsis thaliana organelles including chloroplasts, mitochondria, peroxisomes, and vacuoles have been intensively studied (Carter et al. 2004; Kleffmann et al. 2004; Millar et al. 2006; Reumann et al. 2007; Zybailov et al. 2008). This includes the protein cohorts in Arabidopsis chloroplast sub-compartments: the envelope, stroma, thylakoid membrane, and lumen (Ferro et al. 2003; Friso et al. 2004; Olinares et al. 2010; Peltier et al. 2006; Peltier et al. 2002; Schubert et al. 2002). Several studies have

88

combined gel or column fractionation in conjunction to MS/MS to elucidate the oligomeric complexes of the chloroplast (Lundquist et al. 2017; Olinares et al. 2010; Peltier et al. 2006). Finally, the proteomes of different plastid forms have also been established for maize developing plastids and chloroplasts (Majeran et al. 2012), wheat amyloplasts (Andon et al. 2002), rice and barley etioplasts (Ploscher et al. 2011; Von Zychlinski et al. 2005), tobacco proplastids (Baginsky et al. 2004), and chromoplasts from seven species (Barsan et al. 2010; Barsan et al. 2012; Siddique et al. 2006; Wang et al. 2013).

Of particular interest is the chloroplast's role in sensing and transmitting signals to report organellar and cellular homeostasis (de Souza et al. 2017; Krupinska et al. 2020; Unal et al. 2020; Wang et al. 2020b). Chloroplasts have intimate and dynamic relationships with other organelles such as the nucleus, peroxisomes, mitochondria and endomembrane system to enable signaling of cellular stress (Mehrshahi et al. 2013; Mullineaux et al. 2020; Oikawa et al. 2019). The diversity of signal pathways has primarily been elucidated genetically and biochemically in Arabidopsis allowing the discovery of a diverse set of metabolites (e.g., reactive oxygen species, isoprenoid intermediates, phosphonucleotides, chlorophyll precursors, carotenoid metabolites) and transcription factors to orchestrate these crucial communications (de Souza et al. 2017b; Wang et al. 2020b). In addition, recent studies in Arabidopsis and other plants have shown that the chloroplast serves a critical signaling hub in plant-pathogen interactions (Yang et al. 2021; Fernandez and Burch-Smith 2019).

Defining the constituents of chloroplast proteomes and their dynamics in response to biotic stress in crop plants is an emerging research area. In tomato, the stromal protein leucine aminopeptidase (LAP-A) controls expression of nuclear genes after herbivory,

wounding and treatments with methyl jasmonate (Fowler et al. 2009; Scranton et al. 2013). The bifunctional LAP-A has both aminopeptidase and chaperone (Gu et al. 1996a; Gu et al. 1999; Scranton et al. 2012), therefore we have proposed that LAP-A-dependent signal(s) may be generated post-translationally to orchestrate chloroplast-to-nucleus signaling. With our long-term objective of understanding the LAP-A-dependent stromal proteome dynamics during biotic stress, we have determined a foundational component – the tomato stromal proteome.

Recent advances in sensitivity and accuracy in mass spectrometry (MS) joined with the availability of the annotated tomato nuclear and chloroplast genomes (Sato et al. 1999; Kahlau et al. 2006) and a high-yielding chloroplast and stromal protein isolation protocols optimized for tomato (Bhattacharya et al. 2020) has allowed for an unprecedented in-depth understanding of the tomato chloroplast stromal proteome. Using nanoLC-MS/MS and two strategies to detect stromal proteins, we provide strong empirical evidence for 1,254 proteins in the tomato stromal proteome. With minimal contamination from other subcellular fractions of the chloroplast, this represents the largest stromal proteome to date and provides an important insight into the complexity of the tomato stromal proteome. Our proteome adds 550 additional proteins to the previous characterization of tomato chromoplasts (Barsan et al. 2010; Barsan et al. 2012) and 104 proteins not previously identified in Arabidopsis thaliana proteomics studies. The stromal proteins were manually curated and classified into 11 protein functional categories allowing accessibility of our dataset.

This chapter is a collaboration between Linda Walling, Oindrila Bhattacharya, (graduate student) and myself. I did the Atlas construction and collaborated with the data analysis.

Experimental Procedures

Chloroplast and stroma isolation

Tomato plants (Solanum lycopersicum UC82b) were grown to the three to four true-leaf stage (five-weeks-old) as described in Bhattacharya et al. (2020). Briefly, surface-sterilized tomato seeds were grown in UC Soil Mix 3 in flats with 18-section inserts in a growth chamber at 28°C for 16 hr with 400 µmol m^{-2} s^{-1} light and 22°C for 8 hr (dark). Plants were watered daily and fertilized weekly with a 0.35% (w/v) MiracleGro Tomato Plant Food solution. Twenty-seven h prior to the chloroplast isolation, tomato plants were transferred to the dark to reduce starch. Five independent chloroplast preparations were made using leaves from 18 dark-adapted plants per preparation. Chloroplasts were isolated using a high-yielding chloroplast and stromal protein isolation methods optimized for tomato leaves as described in Bhattacharya et al. (2020).

Stromal protein isolation

Chloroplast stromal proteins were isolated as described by Bhattacharya et al. (2020). For each biological replicate, chloroplast soluble proteins (110 µg) were precipitated with four volumes of acetone, precipitated overnight (16 hr) at -20°C and pelleted at 15,000 g for 30 min at 4°C. The supernatant was discarded. The pellet was manually dislodged and washed with 1 mL methanol to remove residual water. The sample was centrifuged at 15,000 g for 15 min at 4°C. Supernatant was removed. The protein pellet was air-dried and stored at -20°C until use.

To enhance identification of chloroplast stromal proteins, which may be obscured by abundant proteins in the 55- to 75-kDa range, stromal proteins (100 µg/lane) were fractionated by 12% SDS-PAGE and gels were stained with Coomassie Blue R-250 (Gu

et al. 1996b; Rosenberg et al. 1997). The region of the gel with the abundant 50- to 75-kDa proteins was excised. The proteins in remaining gel fragments were separated into three fractions based on mass. Gel pieces were minced and destained in 50 mM ammonium bicarbonate in 50% acetonitrile with vigorous shaking at room temperature for 30 min. Destaining was repeated until gel pieces were devoid of Coomassie Blue R-250. After the final wash, gel pieces were dehydrated in 100% acetonitrile for 50 min at room temperature with vigorous shaking. Gel pieces were dried using a SpeedVac for 15 min at 30°C and stored at -20°C until use.

Acetone protein pellets were resuspended in 100 µL trypsin solution (10 µg/mL trypsin, 50 mM ammonium bicarbonate (pH 8), 10% acetonitrile) and incubated at 37°C overnight. The gel protein samples were soaked with sufficient volume of trypsin solution (10 µg/ml trypsin, 50 mM ammonium bicarbonate) and incubated overnight at 37°C. After trypsin digestion, five acetone-precipitated and three gel-extracted stromal protein samples were analyzed by nanoLC-MS/MS.

NanoLC-MS/MS

A MudPIT approach was employed to analyze the trypsin-treated samples. A nanoAcquity UPLC (Waters, Milford, MA) and an Orbitrap Fusion MS (Thermo Scientific, San Jose, CA) were configured to perform online 2D-nanoLC/MS/MS analysis. 2D-nanoLC was performed online using the nanoAcquity UPLC in an At-Column Dilution configuration. The first-dimension LC mobile phases were 20 mM ammonium formate (pH 10) (mobile phase A) and acetonitrile (mobile phase B) and was achieved with five-min elutions off a NanoEase trap column (Waters) using five stepwise increases in acetonitrile (13%, 18%, 21.5%, 27%, and 50% acetonitrile). A final flushing step with

80% acetonitrile was used to clean the column. Each fraction was then analyzed online using a second dimension LC gradient. The second dimension nano-UPLC method was described previously (Drakakaki et al. 2012).

Orbitrap Fusion MS method was based on a data-dependent acquisition (DDA) survey. The MS-acquired data from 1 to 69 min over a 70-min gradient. The nanoESI source was used with spray voltage at 2000 V, sweep gas at 0, and ion transfer tube temperature at 275°C. Orbitrap mass analyzer was used for MS1 scan with resolution set at 60,000. MS mass range was 300-1800 m/z. AGC target for each scan was set at 500,000 with maximal ion injection time set at 100 ms.

Precursor ions with intensity 10,000 or higher were selected for MS^2 scans, which were performed with the Ion-Trap mass analyzer in the rapid scan mode. The sequence of individual MS^2 scans was from the most- to least-intense precursor ions using the top-speed mode and a cycle time of 4 sec. Precursor ions apex peak detection was enabled, using an expected peak width of 10 sec and Desired Apex Window set to 30%. The minimum peak intensity threshold was set to 1e4. Higher-energy collisional dissociation (HCD) with 25-35% normalized activation energy was used for fragmentation. The quadrupole was used for precursor isolation with 2 m/z isolation window. MS^2 mass range was set to auto/normal with the first mass set at 120 m/z. Maximal injection time was 100 msec with the AGC target set at 10,000. Ions were injected for all available parallelizable time. A 120-sec exclusion window was applied to all abundant ions to avoid repetitive MS^2 scanning on the same precursor ions using 10 ppm error tolerance. Charge states from 2 to 8 were selected for MS2 scan and undetermined charge states were excluded. All MS2 spectra were recorded in the centroid mode.

The raw MS files were processed and analyzed using Proteome Discoverer version 2.1 (Thermo Scientific, San Jose, CA). Sequest HT search engine was used to match all MS data to a tomato protein database (ITAG 2.4 annotation release) or the tomato Atlas and concatenated target/decoy databases were used for determining false discovery rates (Elias et al. 2005). The search parameters were the following: trypsin with 2 missed cleavages, minimal peptide length for six amino acids, MS1 mass tolerance 20 ppm, MS2 mass tolerance 0.6 Da, and Gln→pyro-Glu (N-term Q), oxidation (M), and N-terminal acetylation as variable modifications. Only proteins with 1% FDR cut-off were considered in the final result. Primary data is summarized in Table 1.S1 and these data were uploaded to the ProteomeXchange Consortium via PRIDE (http://www.proteomexchange.org/).

Annotation of the proteins of the stromal proteome

All identified proteins (1% FDR) were manually annotated. Peptide spectral matches (PSMs) and frequency of detection in tomato eight stromal samples were the first criteria for inclusion/exclusion of the tomato chloroplast soluble proteome. Proteins that were detected once with 1 PSM, identified with a single peptide or sporadically identified (in less than 40% of the samples analyzed) were removed from consideration (Bhattacharya et al. 2020). the exceptions were proteins that had empirical evidence for residence within the chloroplast based on the tomato literature or Arabidopsis orthologs identified in the Plant Proteome Database (PPDB; http://ppdb.tc.cornell.edu/) (Sun et al. 2009), the Plastid Protein Database (plprot; http://www.plprot.ethz.ch/) (Kleffmann et al. 2006), and Subcellular Localization Database for Arabidopsis (SUBA4; http://suba.live/) (Hooper et al. 2017). The PPDB database was filtered for chloroplast-localized proteins with empirical evidence for localization within the chloroplast. The plprot database

describes proteins localized in all plastid forms and was filtered for Arabidopsis homologs. SUBA4 was filtered for proteins with experimentally validated localizations within Arabidopsis plastids. Proteins that were predicted to chloroplast localized by more than three localization algorithms were also retained (see below). For all remaining proteins, gene names were based on the tomato literature, Sol Genomics database, updated with recent NCBI annotations, and, when appropriate, gene names were aligned with Arabidopsis thaliana orthologs, which were identified by the program Eggnog (Huerta-Cepas et al. 2019) (Table 1.S2). Data from the primary literature and/or The Arabidopsis Information Resource site (TAIR; https://www.arabidopsis.org/) and Mercator and MapMan BIN ontologies (http://www.plabipd.de/portal/mercator-sequence-annotation/) were used for protein curation (Berardini et al. 2015; Lohse et al. 2014; Thimm et al. 2004). The full set of manually annotated proteins of the tomato stromal proteome are found in Table 1.S2A. During manual annotation, we found that 50 proteins were misannotated in ITAG2.4 and were subsequently corrected in ITAG4.0 and XXX had their Sol Genomics ID changed to reflect improved annotation. The identity of the proteins excluded from analysis and those with new IDs are provide in Table 1.S2B.

The tomato chloroplast protein Atlas

The 34,727 proteins of the deduced proteome of tomato (ITAG 2.4 annotation release) were downloaded from the Sol Genomics Network (http://www.solgenomics.net/) and imported into an R file, which included the amino acid sequences and gene annotations. Protein subcellular predictions for all of the sequences were performed using four stand-alone software programs on the UCR Linux Biocluster, which included: TargetP version 1.1b   (http://www.cbs.dtu.dk/services/TargetP/),   ChloroP   version   1.1

(http://www.cbs.dtu.dk/services/ChloroP/), WoLF PSORT version 0.2 (http://www.wolfpsort.org/), and YLoc (http://abi.inf.uni-tuebingen.de/Services/YLoc/webloc.cgi/) (Briesemeister et al. 2010; Emanuelsson et al. 2000; Emanuelsson et al. 1999; Horton et al. 2007). The subcellular predictions using the online version Predotar (http://urgi.versailles.inra.fr/predotar/predotar.html) were also made (Small et al. 2004). Proteins predicted to have a plastid location by one or more organellar prediction algorithms were included in the tomato chloroplast protein Atlas. Of the 87 conserved open-reading frames in the tomato chloroplast genome, six are in the inverted repeat and encode identical proteins. Therefore, 81 chloroplast-genome encoded proteins were added to the Atlas (Daniell et al. 2006). The Atlas cataloged 7,466 proteins, which was maintained in an MS Excel file, with Sol Genomics Network (SGN) loci identifiers. At times, in the absence of functional or experimental evidence from Arabidopsis databases or the literature, the reproducible detection and strong Atlas predictions were the criteria for retention of a protein in the chloroplast stromal proteome. TMpred was used to confirm the presence of transmembrane domains of tomato chloroplast integral membrane proteins (Hofmann and Stoffel 1993). Lumenal transit peptides were predicted using PredSL and TargetP-2.0 (Almagro Armenteros et al. 2019; Petsalaki et al. 2006). Venn diagrams were drawn using the VennDiagram package in RStudio Version 1.4.1717 open-source software (Chen and Boutros 2011).

Features of the algorithms for the construction of the Atlas

The subcellular localization of plant cell proteins can be predicted by machine learning methods. The standard in proteomics to predict protein's subcellular localization is to use more than one subcellular prediction tool for more robust predictions. Five subcellular-localization programs (TargetP, ChloroP, Yloc, Predator, and WolfPSort)

were used to construct a theoretical tomato chloroplast proteome (the Atlas). The five prediction tools were trained on different sets of proteins with known subcellular localizations. Hydrophobicity, charge and volume of amino acids were residue features that these algorithms identified and utilized. Most of the algorithms used to construct the Atlas trained on a small number of proteins from tomato or other members of the Solanaeceae. Hence each algorithm provides a general predictor of a protein's subcellular localization. Below are the training dataset features for the five algorithms.

TargetP 1.1 was trained on plant and non-plant protein data sets obtained from Swiss-Prot release 36. A plant proteins used to train this algorithm included 141 proteins with chloroplast transit peptides. There were 29 tomato proteins included in the training dataset and one was LAP-A. ChloroP was trained on only five tomato proteins from a total of 75 plant proteins containing a chloroplast transit peptide. YLoc was trained on a data set from Uniprot knowledgebase (KB). There were 22 tomato proteins in the plant training dataset of which LAPA (Q10712 and Q42876) was included. PROSITE motifs and GO terms from close homologous sequences were implemented in the design of YLoc algorithm predictions. The training dataset for Predotar included proteins of known or presumed location obtained from SWISS-PROT release 39.13. A total of 588 proteins with known chloroplast transit peptides were in this training dataset and 34 tomato proteins were included. WoLF PSORT had a training dataset of 744 plant proteins from Uniprot version 45. However, WoLF PSORT did not clearly iterate if tomato proteins were utilized for their training dataset.

Relative protein abundance

Relative protein abundance was calculated based on emPAI (exponentially modified protein abundance index) (Ishihama et al. 2005). PAI is the ratio of the number detected

peptides to the number of observable peptides per protein (Rappsilber et al. 2002) and was obtained for each protein from ThermoScientific Proteome Discoverer (PD) 2.1 output. emPAI is calculated as 10^{PAI} -1. The relative protein abundance (mol fraction) was calculated by dividing the emPAI of a protein by the sum of emPAIs of all the proteins in the entire dataset. The molar fraction was multiplied by 100 to obtain the mol percent of each protein.

Results

Isolation and nanoLC-MS/MS analysis of the tomato chloroplast stromal proteome

We developed a high-yielding chloroplast and stromal protein isolation protocol to identify with confidence and accuracy the protein complement of the tomato chloroplast stromal proteome (Bhattacharya et al. 2020). Given the enhanced accuracy and sensitivity of the LTQ-Orbitrap, we directly analyzed soluble chloroplast extracts that had chloroplast membranes removed by ultracentrifugation. A robust set of 2,135 proteins with a 1% FDR were obtained from the five biological replicates precipitated in 80% acetone and the three samples analyzed after 12% PAGE. The different methods of protein isolation yielded 880 and 67 new unique proteins from the acetone-precipitated and PAGE gel samples, respectively (Table 1.S2). Proteins were curated using a tomato chloroplast protein Atlas, databases with experimental evidence for a protein's plastidial localization (plprot, SUBA4 and PPDB), functional relatedness to Arabidopsis orthologs, and evidence present in the literature (Table 1.S2).

To increase the confidence and significance of our dataset, we used rigorous criteria to define the tomato stromal proteome. Of the 2,135 proteins detected, 628 were removed from further analysis based on the fact that they were identified once by 1

peptide spectral match (PSM), with a single unique peptide, or sporadically (in less than 40% of the samples analyzed) (Bhattacharya et al. 2020) (Figure 1). However, we retained any protein with a known chloroplast location to gain insights into low-abundance proteins in our stromal preparations.

The remaining 1,507 proteins were identified unambiguously with 9,843 new unique peptides and 92,183 peptide spectral matches (PSMs) from which 1,254 proteins were designated as the stromal proteome and 253 were classified as co-isolating proteins (CIPs), which were excluded from the stromal proteome (Tables 1.S1-1.S2). CIPs were reproducibly isolated but their Arabidopsis homologs had empirical evidence for or protein localization algorithms strongly predicted residence in other subcellular compartments (Bhattacharya et al. 2020). The detection of some of the CIPs may reflect their dual localization within tomato cells. However, if these CIPs are chloroplast localized, they do not using canonical transit peptides (Jarvis and López-Juez 2013; Nakai 2018; Thomson et al. 2020). It is also possible that the CIPs reflect the close proximity of and connections between other organelles such as the nucleus, peroxisome, mitochondria, and endomembrane system (Andersson et al. 2007; Barton et al. 2018; Exposito-Rodriguez et al. 2017; Gao et al. 2016; Higa et al. 2014; Islam and Takagi 2010; Mehrshahi et al. 2013; Mullineaux et al. 2020; Oikawa et al. 2019; Hooper et al. 2017).

Curation of the tomato stromal proteome: Leveraging the tomato chloroplast protein Atlas and Arabidopsis protein localization databases

The use of multiple machine-learning algorithms is best practice for predicting the residence of plant proteins in subcellular compartments such as the chloroplast (Hooper

et al. 2017; Richly and Leister 2004). Here, five subcellular-localization programs (TargetP, ChloroP, Predotar, WoLF PSORT, and YLoc) were used to construct a theoretical tomato chloroplast proteome (the Atlas) (Briesemeister et al. 2010; Emanuelsson et al. 2007; Emanuelsson et al. 1999; Hooper et al. 2017; Horton et al. 2007) (Table 1.S3A). The Atlas included 87 chloroplast genome-encoded proteins (Daniell et al. 2006; Kahlau et al. 2006) and 7,466 nuclear genome-encoded proteins predicted to be localized in the plastid by one or more programs (Figure 2, Table 1.S3A). The Atlas constitutes ~22% of the tomato genome making it a liberal predictor of chloroplast localization. This approach was reasonable since each algorithm brought different computational approaches to predict protein locations and were trained on different sets of proteins.

At the core of the Atlas are 930 proteins that were predicted to be chloroplast localized by all five programs (Figure 2; Table 1.S3A). While no single algorithm accurately identified all of the 1,254 proteins in the tomato stromal proteome, each algorithm identified a set of unique proteins ranging from 61 (WolfPSort) to 390 (ChloroP), stressing the unique contributions of each program to the Atlas. (Table 1.S2). Only 3,276 proteins in the tomato Atlas had an Arabidopsis ortholog with a chloroplast location detected one or more Arabidopsis protein databases (Figure 3, Table 1.S3B), with PPDB had the most overlap with the Atlas (76%).

Of the 1,254 proteins in the tomato stromal proteome, 83%, 87% and 44% of these proteins had one or more Arabidopsis homologs in PPDB, SUBA4 and plprot databases, respectively (Table 1.S2, Table 1.S4). A core of 518 proteins (41.4%) was detected in all three databases (Table 1.S2, Figure 4). These proteins were enriched for proteins involved in protein folding and targeting, tetrapyrrole synthesis, redox, and TCA

metabolism. While proteins associated with DNA synthesis, amino acid metabolism, photosynthesis, and glycolysis were under represented.

Sub-organellar localization of proteins and molar abundance

Immunoblots that tested the purity of the stromal protein preparations suggested that the tomato stromal proteome may harbor thylakoid lumenal proteins and was depleted of thylakoid integral membrane proteins (Bhattacharya et al. 2020). Accordingly, we identified 155 integral membrane proteins (Table 1.S5A). All of these tomato proteins had one or more transmembrane domains as predicted by TMpred (Hofmann and Stoffel 1993) (Table 1.S5A). Ninety-five of these proteins were thylakoid membrane proteins, 28 proteins are in the inner or outer membranes of the envelope, three are membrane proteins of plastoglobules, and three are associated with both chloroplast membrane systems; the remaining 26 were designated as membrane proteins based on the literature, PPDB, or TMpred. Based on the number of proteins detected, integral membrane proteins constitute 12% of the stromal proteome. However, it should be noted that 45 of the integral membrane proteins were sporadically detected (>40% of acetone or gel samples) (Table 1.S5A).

Fifty-nine proteins that reside within the tomato chloroplast lumen were identified (Table 1.1). Relative to the membrane proteins, there were 2.7-fold fewer lumenal proteins detected in the stromal proteome. Over 81% of the lumenal proteins were detected frequently (in six to eight of the eight samples) and they represented a total of 4.7 % of the stromal proteome. The lumenal proteins had a diverse array of functions and included: 12 immunophilins (cyclophilins and FKPBs), three C-terminal processing proteases, three DEG protease subunits, 11 lumenal proteins associated with PSI, PSII

101

and the NAD(P)H complex, as well as 23 proteins involved photosystem maintenance or assembly (Table 1.1). Nine of the ten tomato FKBP proteins predicted to be chloroplast localized by Waseem et al. (2018) were detected in the stromal proteome; only FKBP12, which was predicted to be localized to both the cytosol and chloroplast, was not detected. We also detected ten lumenal proteins with orthologs in Arabidopsis that were previously not detected in other studies, as well as tomato's PPO-F and PPO-A.

The number of chloroplast membrane and lumenal proteins overestimates their contribution to the stromal proteome. A better assessment was provided by the exponentially modified protein abundance index (emPAI) (Table 1.S2). The emPAI was used to normalize the abundance of the stromal proteins based on the number of detected peptides versus the number of observable peptides per protein to provide an estimate of a protein's molar abundance (Ishihama et al. 2005). The mol % tomato's stromal proteins varied over a 7.4×10^5-fold range, with the majority of proteins in the

10^{-3} to 10^{-2} mol % categories (Figure 5, Table 1.S2). The 155 integral membrane proteins varied over a 1633-fold range and represented a total of 0.59 mol % of the stromal proteome (Table 1.S5A). In contrast, the 59 lumenal proteins accounted for 3.9 mol % of the stromal proteome and varied over a 6004-fold range (Table 1.1). The most abundant lumenal protein was OEE3, constituting 40% of the lumen protein mass. Collectively, tomato chloroplast membrane and lumenal proteins constituted 4.5% of the mass of proteins in the stromal proteome, representing a minor proportion of the tomato stromal proteome.

Relative abundance of proteins and novel proteins in the tomato chloroplast stromal proteome

A small number of studies have provided insights into dicot stromal proteomes. To elucidate chloroplast complexes and soluble proteomes in Arabidopsis, these studies used SDS-PAGE (Ferro et al. 2003; Peltier et al. 2006), size exclusion chromatography (Peltier et al. 2006), affinity chromatography (Bayer et al. 2011), or blue native-PAGE (Lundquist et al. 2017) to pre-fractionate proteins prior to mass spectroscopy analyses. To benchmark the tomato stromal proteome relative to the Arabidopsis stromal proteome, we compared the relative abundance of the tomato stromal proteins to the relative normalized abundance of the 241 Arabidopsis stromal proteins identified by Peltier et al. (2006).

The top two abundance classes of proteins in the tomato stromal proteome had mol % values ranging from 0.1 to 37 (Figure 5, Table 1.2). The rankings of these 62 proteins were compared to their Arabidopsis homologs (Peltier et al. 2006). Although of varying abundance and rankings, 17 of the 23 most abundant proteins in Arabidopsis were detected in tomato's top two abundance classes (Table 1.S6). This includes the four sets of tomato proteins had two or more paralogs in tomato: RuBisCo small subunit (RBCS-1, RBCS-2A, RBCS-3B), RuBisCo activase (RCA1, RCA2), elongation factor Tu (EFTuA, EFTuB), and fructose-bisphosphate aldolase (FBA2, FBA3) relative to single proteins in Arabidopsis (Table 1.2). An additional six abundant Arabidopsis proteins were detected but at lower abundance levels in the tomato stroma (Table 1.S6). Twenty-one tomato proteins that were in the top-two protein cohorts were not detected by Peltier et al. (2006) (Table 1.S2A). The new stromal proteins included: KIROLA-like protein, a

macrophage migration inhibitory factor, two polyphenol oxidases (with no Arabidopsis orthologs), and one lumenal protein TL19 (Table 1.2).

Reciprocally, of the 23 most abundant stromal proteins reported by Peltier et al. (2006), all but one (a ROC4-like protein with no tomato ortholog) were detected in the tomato stromal proteome but their relative rankings (by mol %) were significantly different (Table 1.S6). While the RuBisco large subunit (RBCL) was the most abundant protein in both studies, there was a striking difference in the abundance of the RuBisCo small subunits. Peltier et al. (2006) reported the abundance a RBCS protein pool, which ranked 2 in abundance. In contrast, the analogous tomato RBCS pool would rank 23 in the tomato stromal proteome (Table 1.S6). Furthermore, some tomato proteins, such as 2-CYS-Prx1, 2-CYS-Prx2, CPN20, and LOX2, were not even in the top 100 most-abundant proteins of the tomato stromal proteome. Collectively, these data indicate the mechanisms that dictate stromal protein abundance are significantly different in these plant species.

Comparisons of tomato stromal proteome with Arabidopsis chloroplast proteins reported in PPDB, SUBA4 or plprot showed that 103 stromal proteins were not previously detected (Table 1.3). A majority (67%) of the novel proteins were reproducibly detected (in >40% of acetone and/or gel samples) and 97% of the novel proteins were predicted to reside within the chloroplasts by two or more algorithms (Table 1.3). The abundance of the novel stromal proteins ranged from 0.47 mol % to $<5 \times 10^{-5}$ mol %. and totaled 1.1 mol % of the stromal proteome. Strikingly, four of the most abundant proteins were defense-associated proteins (PPOE, PPOF, AIG2-like, and KIROLA) and collectively these proteins accounted for >83% of the mass of the novel proteins. Most

novel stromal proteins were not abundant and were likely identified due to the enhanced accuracy and resolution of the Orbitrap Fusion MS.

Thirty-two of the novel proteins had roles in RNA biogenesis, protein biogenesis, redox, or stress responses and 25 proteins have roles in cellular metabolism spanning amino acid to secondary metabolism (Table 1.3). Unknown proteins and proteins with uncharacterized functions dominated, representing 31% of the novel proteins. Finally, 12 proteins did not have orthologs in Arabidopsis including: three tomato polyphenol oxidases (PPO-F, PPO-E, and PPO-A) (Newman et al. 1993; Tran et al. 2012), YCF23, a methyltransferase, a transcription factor (SAP-like BP-73), and 32 unknown/uncharacterized proteins.

Functional comparisons of the tomato leaf stromal and fruit plastid proteomes

While the proteomes of tomato fruit are well-characterized (Sant'Ana and Lefsrud 2018), few studies have focused on the plastids of tomato fruit or leaves (Barsan et al. 2010; Barsan et al. 2012; Tamburino et al. 2017). Barsan et al. (2010, 2012) identified 1,932 proteins in plastids undergoing the chloroplast to chromoplast transition associated with fruit ripening (Table 1.S7). A core of 430 proteins were shared with the leaf stromal proteome and the proteomes of mature-green, breaker and red fruit plastids with reflecting shared housekeeping and biochemical functions. In addition, 550 proteins were unique to the leaf stromal proteome (Figure 6, Table 1.S7). Of the 81 chloroplast-genome encoded proteins, 44 were detected in the leaf stromal proteome (Table 1.S8A). When the leaf stromal and fruit plastid proteomes were considered collectively, they provide empirical evidence for 56 of the chloroplast-genome encoded proteins (Table 1.S6; Table 1.S8A).

To infer function, stromal proteins were assigned MapMan function bins using Mercator (Lohse et al. 2014). The four of the five largest bins (>59 proteins) were associated with well-known plastid functions - photosynthesis, protein synthesis, amino acid metabolism, and RNA (Figure 7A, Table 1.S7). There was a surprising lack of correlation of numbers of proteins and the relative protein mass (based on mol %) for the top five bins (Figure 7B). For example, approximately 64% of the stromal protein mass was associated with the 124 proteins in the photosystem bin. In contrast, the 59 proteins in the RNA and the 88 proteins in the amino acid metabolism bins were 3.3% and 0.85% of the proteome, respectively. Subsequent manual curation of the proteins in the not-assigned bin allowed specific or general functions to be assigned of these 298 proteins, leaving 36 proteins as uncharacterized or unknown and 52 enzymes with unknown functions (Table 1.S9). The manually curated stromal proteins were grouped into 11 functional categories (Table 1.4); tables S8-S18 provide the identity of proteins in each group. Below I highlight several of these functional groups.

Photosynthetic complexes

As over 60% of the stromal proteome mass is associated with the MapMan photosynthesis bin and many of these proteins are stromal localized or peripherally associated with the thylakoid membrane, we explored the abundance of the nuclear- and chloroplast-genome encoded proteins of five major multimeric complexes: photosystem I-Light Harvesting Complex I (PSI-LHCI), PSII-LHCII, cytochrome b6f, ATP synthase, and NADH dehydrogenase (NDH) complexes. We also report proteins involved in complex stability and assembly (Table 1.S9B-F) and provide a visual interpretation of relative subunit abundance for each complex (Figure S1).

Photosynthesis initiates with the absorbance of light energy by light-harvesting complex proteins (LHCII) and photosystem II (PSII) (Buchanan et al. 2015). The vast majority of PSII-associated proteins are integral-membrane proteins and were not detected. The chloroplast genome-encoded PSBA-E (D1), PSBB (CP43), PSBC (CP47), PSBD (D2), and PSBE (Cytb559) were detected infrequently, at low levels and with non-molar ratios (Table 1.S9B). Three other nuclear-genome encoded PSII subunits (PSBR, PSBS, and PSB33) and six LHCII subunits were also detected. While the amounts of five of the LHCII proteins (LHCB13, 1A, 1B, 3C, and CP29.1) were low (< 0.001 mol %) and sporadically identified, LHCB9 was 4-fold more abundant and detected in all samples analyzed, suggesting a looser association with the thylakoid membranes. The most abundant proteins associated with PSII were the lumenal oxygen-evolving proteins (PSBO1, PSBO2, PSBP, and PSBQ) and the extrinsic PSB27-H1, PSB27-H2 and PSB28 proteins. Dozens of proteins important for PSII protein and pigment assembly, stability or repair are known in Arabidopsis (de Luna-Valdez et al. 2019; Li et al. 2019; Liu and Last 2017; Lu 2016; Sato et al. 2017). We detected 29 of these orthologous proteins, as well as thio/disulfide-modulating proteins critical for PSII assembly/maintenance and protein processing/turnover, which are described elsewhere (Table 1.4).

Linking PSI and PSII, the cytochrome b6/f complex has eight subunits (Malone et al. 2019). We detected the lumenal PETC (Reiske subunit) and plastocyanin (PETE) at significantly higher levels than the chloroplast genome-encoded integral membrane proteins PETA and PETB (Table 1.S8C). None of the remaining thylakoid membrane-embedded components (PETD, PETG, PETL, PETM, and PETN), nor cytochrome assembly factor (YCF5) were detected (Figure S1). Two cytochrome b6/f complex

assembly/stability factors were detected: HCF164 and LIR1 (Yang et al. 2016; Lennartz et al. 2001) (Table 1.S8C).

PSI and its light-harvesting complex LHCI is an asymmetric assemblage of 15 PSI proteins, LHCA proteins, and PSI assembly proteins (Table 1.S8D) (Amunts et al. 2010). We detected 11 PSI subunits including six integral membrane proteins (PSAA, PSAB, PSAC, PSAG, PSAK, and PSAL) and extrinsic proteins exposed on the stromal side (PSAC, PSAD, PSAE) and lumen side (PSAF, PSAN) (Figure S1). Of the PSI-associated light-harvesting complex proteins, the tomato LHCAs most similar to AtLHCA1 and AtLHCA2 were not detected, but two AtLHCA3-like (LHCA8A, LHCA8B) and one AtLHCA4 (LHCA11) were detected. Finally, we detected five proteins likely involved with PSI assembly including: YCF3, YCF3-interacting factor, PPD1, PSA2, and PSA3 (Fristedt et al. 2014; Liu et al. 2012; Naver et al. 2001; Nellaepalli et al. 2018; Shen et al. 2017); notably, the chloroplast genome-encoded YCF4 was not detected. Of the PSI-LHC proteins detected, abundance varied within a 66-fold range with the assembly factors PPD1 and PSA3 being most abundant (Table 1.S8D).

The large NAD(P)H-dehydrogenase-like complex (NDH) associates with two PSI complexes and is active in photorespiration. The NDH complex and PGR5 and PGR-like proteins are also associated with cyclic electron flow to preferentially contribute to ATP synthesis (Yamamoto and Shikanai 2019; Munekage et al. 2002). PGR5 and PGRL1A were detected, as were many subunits of the NDH complex and several NDH assembly proteins (Table 1.S8D). NDH is the largest complex with 29 proteins organized into subcomplexes (Shikanai 2016). Nine NDH subunits were detected including the chloroplast genome-encoded and stroma-facing NDHH, NDHI and NDHJ of subcomplex A (Table 1.S8D, Figure S1). Other nuclear genome-encoded subunits of subcomplex A

(NDHM, NDHN and NDHO), subcomplex E (NDHS, NDHU, NDUV), and PIFI (post-illumination chlorophyll fluorescence-increase protein) were also detected (Shikanai 2016; Wang and Portis 2007) as were five of the seven proteins critical for subcomplex A assembly (CRR1, CRR6, CRR7, CRR9, and CRR41). All subunits of stroma-exposed subcomplex B (PNSB1-PNSB5) and lumenal subcomplex L (PNSL1-PNSL5) were detected; whereas, none of the proteins in the thylakoid membrane-associated subcomplexes SubL nor SubM were detected. Based on mol % values, the subunits for the NDHH subcomplexes A, B and L are not detected in equimolar ratios. Finally, the minor LHCA proteins (similar to AtLHCA5 and AtLHCA6) that mediate the PSI-NDH super-complex formation were not detected (Peng et al. 2009). Collectively, these NDH complex and associated proteins represented 0.4 mol% of the stromal proteome (Table 1.S8D).

The ATP synthase complex is composed of eight different subunits (Hahn et al. 2018). All subunits of the extrinsic CF1 complex (α, β, δ, ε, and γ), which are peripheral thylakoid membrane proteins, were detected (Table 1.S8F). While α (ATPA), β (ATPB), δ (ATPD), ε (ATPE), and γ (ATPC) are present in a 3:3:1:1:1 ratio in CF1, their abundance in the tomato stroma did not reflect this stoichiometry. ATPB was 23-, 15-, 18-, and 68-fold more abundant than ATPA, ATPD, ATPE, and ATPC. While the integral membrane subunits a (ATPH) and c (ATPI) were not detected, the b (ATPF) and b' (ATPG) subunits, which are tethered to ATPH, were detected at substantially lower levels than ATPB. ATPB was 3051- and 796-fold more abundant than ATPF and ATPG, respectively (Table 1.S8E; Figure S1). Finally, four ATP synthase biogenesis proteins were detected (e.g., ALB4, BFA1, BFA2, and PAB) (Mao et al. 2015; Trösch et al. 2015; Zhang et al. 2016; Zhang et al. 2018). In contrast, tomato orthologs of the Arabidopsis

assembly proteins P11 (Solyc02g093690) and P12 (Solyc02g031770) were not detected (Duan et al. 2020).

Of critical importance to photosynthesis is the biogenesis and maintenance of the thylakoid membranes, in which the photosynthetic complexes are imbedded. In addition, proteins associated with plastid fission, chloroplast differentiation, and plastoglobules are important for chloroplast structure and function (Table 1.S10). Of the 51 proteins in this group, 19 were fibrillins (Laizet et al. 2004). Ten different types of fibrillins were detected in the stromal proteome with two paralogs for FBN2 and FBN7; only FBN11 (Solyc03g083420) was not detected. The FBNs of plastoglobules (FBN1, FBN2A-B, FBN4, FBN7A-B, FBN8) were most abundant representing 0.2 mol %. The other FBNs (FBN 3, FBN5, FBN6, FBN9, FBN10, and a FBN-like protein) were less abundant (0.04 mol %).

Photosynthetic metabolism in chloroplasts

The chloroplast is a metabolic hub that synthesizes a broad spectrum of molecules essential for plant growth, development and adaptation to stress (Buchanan et al. 2015; Rolland et al. 2012). A significant proportion of the stromal proteome is associated with the central (or primary) metabolic pathways of photosynthetic metabolism (Wise and Hooper 2006). These pathways include the Calvin cycle, TCA cycle, OPP pathway, major and minor carbohydrate metabolism, C1 metabolism, glycolysis, gluconeogenesis, and photorespiration (Table 1.4, Table 1.S11A-H). A total of 160 proteins associated with carbon metabolism were detected and, collectively, they constitute > 51 mol % of the stromal proteome. Notably, while 14 of these proteins were encoded by single-copy genes in Arabidopsis but by two paralogs in tomato; for example, the Calvin cycle, TCA

cycle, and major carbohydrate metabolism pathways having nine, five and five duplicated genes, respectively (Table 1.S10). The majority of the paralogous proteins accumulated to different levels in the tomato stroma. For example, the RuBisCo large subunit methyl transferase LMST2 was 48-fold more abundant than LMST1 (Table 1.S10).

Non-photosynthetic metabolism in plastids: Amino acids, nitrogen, sulfur, nucleotides, co-factors, and vitamins

Numerous non-photosynthetic central metabolic pathways are active within the plastid including nitrogen and sulfur metabolism and biosynthesis of nucleotides, co-factor and vitamins, amino acids, lipids and defense-associated oxylipins, as well as secondary metabolites and enzymes critical for turnover of xenobiotics (Table 1.S12-S15). We also detected ten enzymes with roles in other metabolic pathways and identified 52 enzymes that could not be reliably assigned to a pathway (Table 1.S9B-C).

The largest group of proteins associated with non-photosynthetic central metabolism were the enzymes that catalyze amino acid biosynthesis (Lancien et al. 2007). Accordingly, we detected 98 proteins with these functions (Table 1.S12A) and, collectively, these enzymes represented 0.99 mol % of the stromal proteome. Three enzymes (TSA, SK, and ASB2) involved with aromatic amino acid biosynthesis were not previously reported in proteomics studies (Table 3.1). Finally, three ACT domain proteins were detected. This regulatory domain is an amino acid-binding site for feedback-regulated amino acid metabolic enzymes; however, at the present time, the pathways these proteins participate are not known.

111

The chloroplast contributes to nitrogen and sulfur metabolism (Table 1.S12B) (Chan et al. 2013; Masclaux-Daubresse et al. 2010). Seven enzymes in nitrogen metabolism were detected with glutamine synthase 2 (GS2) being most abundant at 0.39 mol %. We detected 20 proteins associated with sulfur metabolism, which centers on Cys biosynthesis and catabolism. Cys is essential for protein biosynthesis and is a critical residue in enzyme active sites, protein tertiary structure, protein-protein interactions, redox sensitive enzyme activity, [Fe-S] groups, vitamins, and cofactors (Table 1.S12B). Proteins involved in sulfate catabolism (APS1, APR3, SiR), the synthesis of Cys (OASC), as well as Cys-derived methionine biosynthesis (GS, CBL), cystathione biosynthesis (CBX1A-C), and synthesis of the redox regulator glutathione (GSH1, GSH2) were detected. Finally, SAL1, a critical redox-responsive regulator of the retrograde stress signal PAP was detected (Chan et al. 2013); while the integral-membrane antiporters of PAPS/PAP (PAPST1 and PAPST2) that help to control the levels of cytosolic PAP were not detected (Ashykhmina et al. 2019).

Forty-five enzymes associated with nucleotide metabolism were detected (Table 1.S12C). Of these, six were detected for the first time, including an Appr-1-p processing domain protein (Kumaran 2005), a nucleoside diphosphate kinase (NDK3), and ribose-phosphate pyrophosphokinase 3 (PRS3) (Table 3.1). Surprisingly, we reproducibly detected two enzymes of pyrimidine biosynthesis dihydroorotate dehydrogenase (DHODH) and orotidine 5'-phosphate decarboxylase (ODCase), which catalyze tandem steps in pyrimidine biosynthesis in the stroma. While the tomato DHODH had no predicted targeting signals, it has been previously detected in plant mitochondria (Bellin et al. 2021). In contrast, the tomato ODCase has strong predictors for plastid

localization; although previous studies suggest it resides in the cytosol. The stromal localization of both proteins may provide new insights into pyrimidine metabolism.

Non-photosynthetic metabolism: Lipids and oxylipins

The central metabolic pathways for lipids and phytohormone biosynthesis are highly conserved (Li-Beisson et al. 2013; Wasternack and Song 2017). Fifty-four enzymes associated with lipid metabolism were identified in the stromal proteome totaling 0.51 mol % of the stromal proteome (Table 1.S13A). Enzymes for the synthesis of acetyl-CoA (ACS and the pyruvate dehydrogenase complex), the full complement of soluble enzymes required for lipid elongation, many lipases critical for lipid catabolism, and lipid-binding proteins were detected. The inner membrane-associated enzymes (palmitoyl-ACP, lysophosphatidic acid acyl transferase, PA phosphatase) and enzymes associated with lipid desaturation were not detected. An acyl carrier protein (ACP5) and the oleoyl-acyl carrier protein thioesterase 2 (FATA) were not previously reported in the Arabidopsis proteomics databases (Table 3.1; Table 1.S13A). In addition, several enzymes associated with early steps of the oxylipin pathway were also detected (Table 1.S13A). The oxylipin pathways is responsible for the synthesis of jasmonic acid (JA), which is critical for plant defense and development, numerous oxylipins with roles in defense signaling including the HPL branch that produces C6 volatiles. While many of these enzymes are membrane associated and, therefore, not detected, we detected two lipoxygenases (LOXC and LOXF), allene oxide synthase (AOS) and allene oxide cyclase (AOC), as well as HPL.

Isoprenoid metabolism, retrograde signals, and other metabolic pathways

With over 35,000 different compounds derived from the isoprenoid pathway in plants (Kirby and Keasling 2009), isoprenoids are the largest and most diverse group of natural products. The plastid-derived isoprenoid metabolites (heme, chlorophylls, carotenoids, ABA, gibberellins, strigolactones, plastoquinones, phylloquinones, tocopherols, and terpenoid volatiles) are derived from the five-carbon isopentenyl diphosphate (IPP) and DMAPP, which are primarily synthesized by the MEP pathway (Zhou and Pichersky 2020). Seventy-nine proteins associated with isoprenoid production were detected in the stromal proteome (Table 1.S14A-C). All enzymes of the plastidial MEP pathway, as well as two IPP isomerases, were detected ranging from 0.0002 to 0.12 mol % (DXS2 and MCS, respectively). DXS, which creates the substrates for the MEP pathway and thiamine biosynthesis, is encoded by two paralogs in tomato with DXS1 14-fold more abundant than DXS2 in leaf chloroplasts (Table 1.S14A), which consistent with DXS1 and DXS2 RNA levels in leaves and fruit (Paetzold et al. 2010). The MCS is a light- and stress-induced enzyme that controls levels of MEcPP, which is a retrograde signal used for communicating plastid status to regulate nuclear genes dictating the balance of growth and development and stress responses (de Souza et al. 2017). Additional enzymes detected included three cis-prenyl transferases, two geranylgeranyl pyrophosphate synthases (GGPPS), a GGPPS small subunit (SSU-II), and three terpene synthases (Table 1.S14A). While Barja et al. (2021) and Zhou and Pichersky (2020) reported three plastidial GGPP synthases (SIG1-3) with similar kinetic parameters, only SIG2 and SIG3 were detected in our leaf stromal proteome. The absence of SIG1 protein (Solyc11g011240) was consistent with low levels of SIG1 mRNAs, relative to SIG2 and SIG3 (Barja et al. 2021). It is noteworthy that SSU-I

114

(Solyc07g064660), which is known to modify SIG1-3 activity was not detected (Zhou and Pichersky 2020).

GGPP is used for the synthesis of carotenoids, which are important for stabilization of the photosynthetic apparatus, light capture, and photoprotection (Stanley and Yuan 2019). The carotenoid-derived apocarotenoids are important for synthesis of the plant hormone abscisic acid and signaling molecule strigolactone, as well as producing a suite of volatiles important in development and stress signaling (e.g., β-cyclocitral). Fifteen enzymes associated with carotenoid metabolism were detected, although the rating-limiting leaf phytoene synthase 1 (PSY1), orange chaperones, and carotenoid-cleavage enzymes were not detected (Table 1.S14B).

GGPP is also used to synthesize tocopherols, chlorophylls, plastoquinones, and phylloquinones (Tables 1.S14B). Tocopherols scavenge singlet oxygen derived from photosynthesis and three enzymes in tocopherol metabolism (VTE1, VTE3, and VTE4) and two regulatory kinases (ABCK1 and ABCK3) were detected (Tables 1.S14B). In addition, the plastoquinione biosynthesis enzyme, solanesyl diphosphate synthase, was detected. The tetrapyrrole pathway yields hemes, the chlorophylls essential for the light-harvesting antennae of PSI and PSII, and a chlorophyll intermediate protochlorophyllide (PChlide) with a critical role in chloroplast-nuclear communication. We detected 33 enzymes associated with tetrapyrrole biosynthesis and catabolism (Table 1.S14C). The complete tetrapyrrole pathway was represented with the exception of the membrane-bound chlorophyllide a oxygenase and uroporphyrinogen III methylase. Tomato also has expanded its tetrapyrrole protein complement with two UROD and three POR paralogs (Table 1.S14C) (Gabruk and Mysliwa-Kurdziel 2020).

PChlide is a photosensitizer that critical in retrograde signaling. In the light, PChlide transfers its excitation energy to oxygen, creating the highly reactive singlet oxygen ($^1O_2$). To limit $^1O_2$ production and photosensitivity, FLU controls PChlide levels (op den Camp et al. 2003). We detected two paralogous FLU proteins (FLU1 and FLU2); neither have been studied to date and it is unclear if they are functionally redundant (Table 1.S14C). However, FLU1 is 5-5-fold more abundant than FLU2 in the chloroplast stroma. In Arabidopsis, the EXECUTER proteins (AtEX1 and AtEX2) have critical but distinct roles in perception of $^1O_2$ and triggering the reprogramming of nuclear gene expression for stress adaptation (Dogra et al. 2017; Duan et al. 2019; Lee et al. 2007). In tomato, EX2 is 8-fold more abundant than EX1 (Table 1.S14C). It is unclear if this reflects differences in the roles of the tomato EX proteins, the tightness of association with the thylakoid membranes or location within the grana margins of the thylakoid. Finally, we detected SAFEGUARD1, which acts at the thylakoid grana margins and suppresses $^1O_2$ production (Wang et al. 2020a). The tomato SAFEGUARD1 is 2-fold more abundant than EX2 (Table 1.S14C).

Redox regulation: Damage control to cellular homeostasis

Chloroplasts use redox-regulatory systems to limit cellular damage from ROS and adapt plant metabolism to fluctuating light/dark cycles and environmental insults, such as abiotic stress or pathogen/pest attack (Yoshida et al. 2019; Cejudo et al. 2019; Fichman and Mittler 2020; Exposito-Rodriguez et al. 2017). Chloroplast redox regulation is dependent on the electron transport chain of the thylakoid's photosynthetic complexes to produce reducing power, which is transferred from ferredoxin (Fd) to a thioredoxin (Trx) via Fd-Trx reductase (FTR). The diversity of proteins with Trx motifs and Trx-like motifs and down-stream redox proteins provides flexibility and specificity in responses. The

tomato stromal proteome identified 54 redox-regulation proteins including two FTRs, 22 proteins with thioredoxin domains, four peroxiredoxins, seven glutathione peroxidases, five superoxide dismutases, eleven proteins in the ascorbate/glutathione cycle, and three proteins with single cystathionine β-synthase (CBX) domains (Table 1.S16). The abundance of the redox proteins had a 958-fold range with Trx-m4.1 (0.49 mol %) as the most abundant protein. The tomato redox systems are distinguished from the model plant Arabidopsis by the facts that: (1) the tomato Trx-m4 family is expanded (three paralogs), (2) there are two NTRC proteins (with one detected), (3) there are two Fe-SOD2 paralogs, (4) the 2-CYS-Prx's collectively are the most abundant peroxiredoxin in the tomato stroma, but their abundance is significantly lower than in Arabidopsis, and (3) the CBX1 protein family with probable roles regulation of redox signaling is expanded (three paralogs) (Table 1.S16, Table 3.1) (Cheng et al. 2014).

Protein homeostasis

A protein's destiny is highly regulated to assure its activity occurs in the correct cellular compartment at the appropriate time. Approximately 3000 plastid-localized proteins are encoded by nuclear genes, translated on cytosolic ribosomes and imported into this organelle (Thomson et al. 2020), while the remaining 81 proteins are translated on chloroplast ribosomes (Daniell et al. 2006; Kahlau et al. 2006). All chloroplast-localized proteins must be folded, post-translationally modified, transported to their sub-compartment within the chloroplast, associated with their cofactors, assembled into their multimeric complexes, and ultimately be targeted for proteolytic turnover. Protein homeostasis is carefully regulated to ensure metabolic responses are coordinated with light/dark cycles and can adapt to the stresses imposed by photosystem-generated ROS and the environment. With the powers of genetics, we have been able to dissect and

identify many of the processes that fine tune the "life and death" of a protein. Not surprisingly over 316 proteins associated with protein homeostasis were detected in the tomato stroma (Table 1.S17).

The plastid's 50S and 30S ribosome complexes are essential for synthesizing chloroplast genome-encoded proteins. Importantly, perturbations in translation are perceived and communicated to the nucleus (via GUN1) to coordinate plastid biogenesis and mediate adaptation to stress (Marino et al. 2019; Wu et al. 2019). We detected 31 RPL subunits, 23 RPS subunits, 5 plastid specific ribosomal proteins (PRSPs), as well as 28 proteins were associated with rRNA, tRNA, or ribosomal protein modifications (Table 1.S17A). The ribosomal protein subunits were not detected at equimolar levels. Six subunits were particularly abundant including the chloroplast-genome encoded RPS19, RPS15 and RPL23 and nuclear-genome encoded RPL12A, RPL12B and RPS1A. In addition, 26 amino-acyl tRNA synthases and 20 proteins associated with translational initiation, elongation, termination or regulation were identified. The abundance of EF-TuB (1.93 mol %) rivaled that of RPS19 (1.56 mol %). Seven of the tRNA synthases lacked an identifiable transit peptide, while 14 and 3 had predicted chloroplast or mitochondrial transit peptides, respectively (Table 1.S17A). If similar to Arabidopsis, many of these proteins will have dual localization in the chloroplast and mitochondrion or cytosol (Duchene et al. 2005).

Import of proteins that are translated in the cytosol into plastids is a regulated and disruption of import provides a retrograde signal to mediate stress adaptation (Wu et al. 2019). For imported proteins, there are several routes for entry into the chloroplast including the canonical import via the outer and inner membranes (TOC and TIC complexes) and inter-organellar channels (Armbruster et al. 2009; Cline and Dabney-

118

Smith 2008; Nakai 2018; Thomson et al. 2020). We identified 30 proteins involved in subcellular targeting (Table 1.S17B). For most stromal proteins, transit peptides engage with the plastid's translocation machinery TOC/TIC and affiliated chaperones to import proteins into the stroma (Table 1.S17B); as TIC/TOC are membrane complexes, only a few of these proteins were detected at low levels. The presequence proteases (PREP1, SPP, TOP1) that remove the N-terminal transit peptide from imported proteins (Table 1.S17E) and ten other proteins critical for translocating proteins to the thylakoid membrane or lumen were also identified (Table 1.S17B).

Upon reaching their destination within the chloroplast, proteins must establish and maintain their secondary, tertiary, and quaternary structures to preserve their function or remove their structures to facilitate proteolysis. The chloroplast has an impressive array of proteins to facilitate protein folding and refolding with 60 different proteins identified in the tomato stroma (Table 1.S17C). This included: 30 chaperones or chaperonins; three ATP-dependent chaperones of the Clp protease (CLPC1, CLPC2, CLPD), CLPB, 19 peptidyl-prolyl cis/trans isomerases, and seven protein disulfide isomerases. Three of these proteins (DJC65, DJC73 and FKBP17-1) were not previously detected (Table 3.1). Proteins are further post-translationally modified by chemical moiety addition/removal or by proteolytic processing. The tomato stromal proteome contained 36 modification enzymes in five functional categories: kinases, phosphatases, methylases, acetylases, deformylases, and peptide methionine sulfoxide reductases (Table 1.S17D). Two PDFs and 13 N-terminal peptidases that modify the N-terminus of stromal-localized proteins to influence function or stability were detected (Table 1.S17D-E) (Gibbs et al. 2016; Walling 2006). Unique to tomato are the wound-induced LAPs (LAP-A1 and LAP-A2) that control

the expression of nuclear genes associated with the wound- and stress-responses (Fowler et al. 2009; Scranton et al. 2013).

The chloroplast also has a robust complement of oligopeptidases and endoproteases to mediate protein turnover (Kmiec et al. 2014; Nishimura et al. 2017). These proteinases and proteolytic complexes are located within envelope, stroma, lumen, or thylakoid membranes. We detected a total of 52 proteins associated with proteolysis (Table 1.S17E). These proteins constituted 1 mol% of the tomato stromal proteome with the abundance of individual proteins spanning > 5000-fold range. While these proteins primarily remove damaged or unfolded proteins from the chloroplast, it is also clear that peptidase activity is critical for chloroplast signaling, as evidenced by the requirement of FtsH2 protease-mediated turnover of EX1 for signaling $^1O_2$ damage (Wang et al. 2016) and role of chloroplast peptides in defense signaling (Kmiec et al. 2018).

The stroma-localized Clp complex is well characterized structurally and known to have a critical role in protein homeostasis and proteome remodeling (Nishimura et al. 2017). We detected all subunits of the stromal Clp complex (Table 1.S17E) including the proteolytically active (ClpP1, P3, P4, P5, and P6) subunits, inactive (ClpR1, R2, R3, and R4) subunits, the three Clp protease chaperones (ClpC1, ClpC2, and ClpD), as well as the ClpS, ClpF, ClpT1, and ClpT2 proteins that help deliver or provide substrate specificity to the Clp protease (Nishimura et al. 2017). The ClpC1 and ClpC2 chaperones are the most abundant of the Clp protease subunits with ClpC1 being 3-fold more abundant than ClpC2 (0.32 mol% vs 0.11 mol %).

Little is known of the function of tomato's chloroplast DEG proteases; therefore function is inferred from their Arabidopsis orthologs (Table 1.S17E) (Nishimura et al.

2017). We detected two stromal DEG2 paralogs in tomato, and three lumenal DEGs (DEG1, DEG5 and DEG8), but the stromal DEG7 (Solyc02g091410) was not detected. The filamentation temperature-sensitive H (FtsH) proteases are associated with membranes, turnover proteins damaged by the ROS generated during photosynthesis, and thermotolerance. While the thylakoid-localized FtsH1, FtsH6, FtsH8, and FtsH9 and inner envelope FtsH12 were not detected, four out of nine chloroplast-localized FtsH proteins (thylakoid-localized FtsH2 and FtsH5, and inner envelope-localized FtsH7 and FtsH11) were detected (Table 1.S17E). Notably, FtsH6 and FtsH2 have different roles in tomato chloroplasts, with FtsH6 acting in thermotolerance (Sun et al. 2006), FtsH2 is critical in retrograde signaling. FtsH2 controls the turnover of D1 (a reaction center protein of PSII) and the $^1O_2$ sensor EX1 at the margins of the grana; these events are correlated with chloroplast-nuclear communication (Wang et al. 2016). Finally, three C-terminal processing peptidases (CTPA1-3) and two subunits of the EGY (ethylene-dependent gravitropism-deficient and yellow-green) protease were detected.

The replication and transcriptional hub of the chloroplast

The proteomes of nucleoids and transcriptionally active chromosomes (pTAC) from plastids have been characterized in Arabidopsis and maize (Melonek et al. 2016). The protein composition of these structures is influenced by the differentiation state of plastids and/or environmental factors. Based on orthologous relationships to the Arabidopsis and maize proteins (Huang et al. 2013b; Melonek et al. 2016), 58 nucleoid- and TAC-associated proteins were detected (Table 1.S18A). This included all plastid-encoded RNA polymerase (PEP) subunits, 20 PEP-associated proteins, nine DNA replication and repair proteins, four redox proteins, ten RNA biogenesis enzymes, two kinases, and six other proteins with diverse functions. Surprisingly, we did not detect the

seven sigma factors (SigA-F) that interact with PEP. Collectively, the nucleoid/pTAC proteins detected in the tomato stroma constituted 1.07 mol % of the proteome ranging from 0.39 mol % (Fe-SOD2.1) to 0.0001 mol % (DNA topoisomerase) (Table 1.S17A).

We detected numerous proteins of the conserved nucleoid core including: the MURE-like protein and all but three (pTAC9, pTAC11 and pTAC13) of the 18 pTACs (Melonek et al. 2016) (Table 1.S17A). The tomato genome does not encode a pTAC11-like protein (WHIRLY3) (Akbudak and Filiz 2019); in contrast, the tomato genes encoding a pTAC9-like protein (OSB2, Solyc09g007430) and a pTAC13-like protein (Solyc09g011830) were present. We detected pTAC7, pTAC10, pTAC12, and pTAC14, as well as the FNL1 and FNL2 kinases, that are known to interact with one another to regulate the activity of PEP (Huang et al. 2013a; Chang et al. 2017; Gao et al. 2012). While the function of pTAC17 is unknown, we detected two tomato pTAC17s; the tomato pTAC17A was the most abundant pTAC protein identified (0.16 mol %) and was 80-fold more abundant than pTAC17B.

In addition to the proteins associated with transcriptionally active nucleoids, we detected proteins involved with plastid DNA replication chromatin assembly, and recombination and, transcription factors, RNA processing and binding, and signaling (Table 1.S17B-E). Based on their Arabidopsis orthologs, there were 82 proteins important for post-transcriptional control (Table 1.S17D). While there is substantial evidence for nuclear transcription factors being dual-localized in Arabidopsis, only 12 transcription factors and regulators were detected (Table 1.S17A and 1.S17B) (Krause et al. 2012; Krupinska et al. 2020). We did detect three histone proteins, with two H3-2 proteins and one H2B.1 (Table 1.S17B).

Discussion

Globally tomato cultivation comprises of 4.7 million hectares annually and is a $2.2 billion industry in the US. Tomato has emerged as model plant to study fruit development, plant wounding, herbivory, and pathogen attack (Klee and Giovannoni 2011; Campos et al. 2014; Sant'Ana and Lefsrud 2018). The tomato chromoplast proteome has been studied in detail along with the metabolic shifts associated with the transition of chloroplasts to chromoplasts (Barsan et al. 2010; Barsan et al. 2012; Suzuki et al. 2015; Li et al. 2020; Luna et al. 2020). However, surprisingly, the chloroplast proteome of tomato leaves is understudied (Tamburino et al. 2017). Given the importance of plastids as biochemical hubs and in generating signals to environmental stress (Unal et al. 2020; Yang et al. 2021; de Souza et al. 2017; Dogra et al. 2017), an understanding of the chloroplast proteome is needed. The dynamics of the tomato chloroplast proteome has the potential to provide deep insights into this organelle that can ultimately be used the development of technologies to improve crop yield by regulating protective metabolites and proteins.

Here we focused on establishing the tomato stromal proteome due to our long-term interest in elucidating the role of the stroma-localized tomato leucine aminopeptidase A (LAP-A) in regulating tomato defense (Fowler et al. 2009; Narváez-Vásquez et al. 2008). LapA is induced by systemin, JA, ABA, herbivory, and wounding (Chao et al. 1999). LAP-A is involved in the upregulation of nuclear genes in the late branch of wound signaling downstream of JA perception and accumulation, but not the early branch of this defense pathway (Fowler et al. 2009). Furthermore, alteration in LAP-A abundance promotes downregulation a set of nuclear stress-response genes (Scranton et al. 2013). Given LAP-A's plastid location and ability to modulate nuclear genes that encode

123

proteins localized to non-plastid subcellular compartments, LAP-A is likely to generate or modulate one or more signals to up- and downregulate gene expression.

Acting within the stroma, LAP-A has the potential to influence protein homeostasis due to LAP-A's aminopeptidase and chaperone activities (Gu and Walling 2000; Gu et al. 1999; Scranton et al. 2012). By stabilizing or destabilizing stromal proteins, LAP-A may generate a signal that emanates from the chloroplast to enable communication with the nucleus and, thereby, deploy adaptations to cope with ROS, mechanical damage, herbivory, and pathogen attack. To understand its global impact on tomato defense and chloroplast-to-nucleus signaling, multi-omics approaches are being pursued including characterization of the MeJA- and LAP-A-dependent proteome, metabolome and transcriptome. Foundational for identification of the MeJA- and LAP-A-dependent proteome is an understanding of the unperturbed stromal proteome, which we present here.

The 1254-member leaf stromal proteome Atlas was curated from 2158 detected proteins using rigorous criteria. Proteins that were detected once with 1 PSM, identified with a single peptide or sporadically identified (in less than 40% of the samples analyzed) were discarded. However, proteins in these categories were retained if empirical evidence for plastid localization had been reported in an Arabidopsis database (PPDB, SubA4, or plprot), in the literature or if the tomato chloroplast protein Atlas, which predicted protein residences in plastids. As prediction of protein localization is most accurate when the results of multiple machine-learning algorithms are considered (Hooper et al. 2017; Richly and Leister 2004), the Atlas compiled data from five algorithms (TargetP, ChloroP, Predotar, WolfPsort, and Yloc) to predict tomato protein localization. The value of the Atlas was verified by the fact that 91% of the proteins in the

tomato stromal proteome was predicted to be plastid localized by the Atlas. In conjunction with PPDB and SubA4, the Atlas enabled identification of >350 proteins that copurified with tomato stromal proteins (Bhattacharya et al. 2020). The co-isolating proteins (CIPs) may reflect the close association of tomato chloroplasts with other organelles or, alternatively, possible dual localization of proteins (Andersson et al. 2007; Barton et al. 2018; Exposito-Rodriguez et al. 2017; Gao et al. 2016; Higa et al. 2014; Islam and Takagi 2010; Mehrshahi et al. 2013; Mullineaux et al. 2020; Oikawa et al. 2019; Hooper et al. 2017; Nakai 2018; Thomson et al. 2020).

Considerable time and energy were invested in accurately annotating the tomato stroma-localized proteins. We found that gene/protein annotations of ITAG 2.4 and at Sol Genomics were outdated or inaccurate. Therefore, protein identities were determined by reciprocal BlastP searches of the tomato and Arabidopsis deduced proteomes and from the literature. Enabling this initiative were MapMan bin descriptors, which provided an initial functional categorization of the stromal proteins. However, with 298 proteins initially classified as "non-assigned", manual curation was critical for assessing the full functional diversity captured in the tomato stromal proteome. After manual curation, only 36 and 52 proteins remained as unknown/uncharacterized or as enzymes with unknown functions, respectively. The proteins with known functions were curated into 10 functional categories (Table 1.4). The result was a detailed compendium that should enable other investigators interested in the dynamics of the soluble chloroplast proteome. As plastids are now recognized as a critical hubs to sense and transmit signals to notify organellar networks of deviations from plastidial and cellular homeostasis (de Souza et al. 2017; Unal et al. 2020; Wang et al. 2020b; Fernandez and Burch-Smith 2019), our knowledge of the tomato stromal proteome should enable

125

researchers address fundamental questions in plastid biology and enable those interested in the role that chloroplasts play in tomato-pathogen and -pest interactions. Importantly, for the Walling lab, the stromal proteome provides the underpinnings of our ongoing studies to elucidate the LAP-A- and MeJA-dependent stromal proteomes, and correlate these data with corresponding metabolomes and transcriptomes.

The tomato stromal proteome is an important contribution to the field, as few stromal proteomes are available to date and most have derived from studies of the model plant Arabidopsis thaliana (Olinares et al. 2010; Peltier et al. 2006). Given the advances in the sensitivity and accuracy in mass spectrometry and the development of a high-yielding method for isolating tomato chloroplasts and stroma (Bhattacharya et al. 2020), we unambiguously identified 1,254 proteins. This is marked increase from the size of the initial stromal proteome of Arabidopsis (241 proteins) (Peltier et al. 2006). Finally, our proteome provided empirical evidence for the plastid location of 550 tomato proteins that were not previously detected in tomato chromoplast or chloroplast proteomes (Barsan et al. 2010; Barsan et al. 2012; Tamburino et al. 2017), as well as 103 tomato proteins had not been previously reported as stroma localized in Arabidopsis databases (Sun et al. 2009).

As chloroplasts act as stress sensors and regulate numerous signal transduction pathways via anterograde and retrograde signals, we identified key processes and proteins that are associated with biogenic and operational retrograde signaling (de Souza et al. 2017; Marino et al. 2019). As LAP-A controls defense processes after chloroplast biogenesis is complete, it is likely that LAP-A may controls one or more operational retrograde signal. Numerous proteins that are associated with the synthesis of plastidial metabolites known to be retrograde signals were identified in the tomato

126

stromal proteome including proteins associated with sulfur (PAP, 3'-phosphoadenosine 5'-phosphate), carotenoid (β-cyclocitral), isoprenoid (MEcPP, 2-C-methyl-D-erythritol 2,4cyclodiphosphate), and fatty acid metabolism. In addition, a robust complement of proteins associated the generation and dissipation of reactive oxygen species (ROS) or serving as photosensitizers (tetrapyrroles, FLU, EX1, and EX2) may also be critical in LAP-A's plastid-nuclear communication. It is noteworthy, unlike Arabidopsis, tomato has two FLU proteins and therefore signaling may be distinct.

Finally, given the fact LAP-A is both an aminopeptidase and a chaperone, an understanding of LAP-A's role in stromal protein homeostasis will be important elucidate. Over 300 proteins associated with protein homeostasis were identified in tomato's stromal proteome. Not surprisingly, ~80 of these proteins were associated with the plastid's translational machinery. The proteins synthesized within the chloroplast and proteins synthesized in the cytosol and subsequently imported into the chloroplasts require proper folding, modification, assembly, and insertion into their appropriate plastidial subcompartment. Once damaged by ROS, chloroplast proteins must be unfolded and degraded. LAP-A may assist with one or more of these processes. As seen in Chapter 3, LAP-A interacts with subunits of the major proteolytic complex of the stroma – the Clp protease suggesting that LAP-A's chaperone activity may help target substrates to Clp or may degrade Clp generated peptides. Either interaction may be result in LAP-A-dependent signals to active defense genes. The tomato stromal proteome provides a superb frame of reference to unravel the LAP-A-dependent changes after wounding and herbivory at the transcript, protein, and metabolite level.

References

Abdallah F, Salamini F, Leister D (2000) A prediction of the size and evolutionary origin of the proteome of chloroplasts of Arabidopsis. Trends in Plant Science 5 (4):141-142. doi:https://doi.org/10.1016/S1360-1385(00)01574-0

Akbudak MA, Filiz E (2019) Whirly (Why) transcription factors in tomato (Solanum lycopersicum L.): genome-wide identification and transcriptional profiling under drought and salt stresses. Molecular Biology Reports 46 (4):4139-4150. doi:10.1007/s11033-019-04863-y

Almagro Armenteros JJ, Salvatore M, Emanuelsson O, Winther O, Von Heijne G, Elofsson A, Nielsen H (2019) Detecting sequence signals in targeting peptides using deep learning. Life Science Alliance 2 (5):e201900429. doi:10.26508/lsa.201900429

Andersson MX, Goksor M, Sandelius AS (2007) Optical manipulation reveals strong attracting forces at membrane contact sites between endoplasmic reticulum and chloroplasts. Journal of Biological Chemistry 282 (2):1170-1174. doi:10.1074/jbc.M608124200

Andon NL, Hollingworth S, Koller A, Greenland AJ, Yates JR, 3rd, Haynes PA (2002) Proteomic characterization of wheat amyloplasts using identification of proteins by tandem mass spectrometry. Proteomics 2 (9):1156-1168. doi:10.1002/1615-9861(200209)2:9<1156::aid-prot1156>3.0.co;2-4

Armbruster U, Hertle A, Makarenko E, Zühlke J, Pribil M, Dietzmann A, Schliebner I, Aseeva E, Fenino E, Scharfenberg M, Voigt C, Leister D (2009) Chloroplast Proteins without Cleavable Transit Peptides: Rare Exceptions or a Major Constituent of the Chloroplast Proteome? Molecular Plant 2 (6):1325-1335. doi:https://doi.org/10.1093/mp/ssp082

Ashykhmina N, Lorenz M, Frerigmann H, Koprivova A, Hofsetz E, Stührwohldt N, Flügge U-I, Haferkamp I, Kopriva S, Gigolashvili T (2019) PAPST2 Plays Critical Roles in Removing the Stress Signaling Molecule 3′-Phosphoadenosine 5′-Phosphate

from the Cytosol and Its Subsequent Degradation in Plastids and Mitochondria. The Plant Cell 31 (1):231-249. doi:10.1105/tpc.18.00512

Baginsky S, Siddique A, Gruissem W (2004) Proteome analysis of tobacco bright yellow-2 (BY-2) cell culture plastids as a model for undifferentiated heterotrophic plastids. J Proteome Res 3 (6):1128-1137. doi:10.1021/pr0499186

Barja MV, Ezquerro M, Beretta S, Diretto G, Florez-Sarasa I, Feixes E, Fiore A, Karlova R, Fernie AR, Beekwilder J, Rodriguez-Concepcion M (2021) Several geranylgeranyl diphosphate synthase isoforms supply metabolic substrates for carotenoid biosynthesis in tomato. New Phytologist 231 (1):255-272. doi:10.1111/nph.17283

Barsan C, Sanchez-Bel P, Rombaldi C, Egea I, Rossignol M, Kuntz M, Zouine M, Latche A, Bouzayen M, Pech JC (2010) Characteristics of the tomato chromoplast revealed by proteomic analysis. J Exp Bot 61 (9):2413-2431. doi:10.1093/jxb/erq070

Barsan C, Zouine M, Maza E, Bian W, Egea I, Rossignol M, Bouyssie D, Pichereaux C, Purgatto E, Bouzayen M, Latche A, Pech JC (2012) Proteomic analysis of chloroplast-to-chromoplast transition in tomato reveals metabolic shifts coupled with disrupted thylakoid biogenesis machinery and elevated energy-production components. Plant Physiol 160 (2):708-725. doi:10.1104/pp.112.203679

Barton KA, Wozny MR, Mathur N, Jaipargas EA, Mathur J (2018) Chloroplast behaviour and interactions with other organelles in Arabidopsis thaliana pavement cells. Journal of Cell Science 131 (2). doi:10.1242/jcs.202275

Bayer RG, Stael S, Csaszar E, Teige M (2011) Mining the soluble chloroplast proteome by affinity chromatography. Proteomics 11 (7):1287-1299. doi:10.1002/pmic.201000495

Bellin L, Melzer M, Hilo A, Garza Amaya DL, Keller I, Meurer J, Möhlmann T (2021) Pyrimidine nucleotide availability is essential for efficient photosynthesis, ROS scavenging, and organelle development. Cold Spring Harbor Laboratory. doi:10.1101/2021.01.22.427776

Berardini TZ, Reiser L, Li D, Mezheritsky Y, Muller R, Strait E, Huala E (2015) The Arabidopsis Information Resource: Making and mining the "gold standard" annotated reference plant genome. genesis 53 (8):474-485. doi:10.1002/dvg.22877

Bhattacharya O, Ortiz I, Walling LL (2020) Methodology: an optimized, high-yield tomato leaf chloroplast isolation and stroma extraction protocol for proteomics analyses and identification of chloroplast co-localizing proteins. Plant Methods 16 (1). doi:10.1186/s13007-020-00667-5

Briesemeister S, Rahnenführer J, Kohlbacher O (2010) YLoc--an interpretable web server for predicting subcellular localization. Nucleic acids research 38 (Web Server issue):W497-W502. doi:10.1093/nar/gkq477

Buchanan BB, Gruissem W, Jones RL (2015) Biochemistry & molecular biology of plants.

Campos ML, Kang J-H, Howe GA (2014) Jasmonate-Triggered Plant Immunity. Journal of Chemical Ecology 40 (7):657-675. doi:10.1007/s10886-014-0468-3

Carter C, Pan S, Zouhar J, Avila EL, Girke T, Raikhel NV (2004) The vegetative vacuole proteome of Arabidopsis thaliana reveals predicted and unexpected proteins. Plant Cell 16 (12):3285-3303. doi:10.1105/tpc.104.027078

Cejudo FJ, Ojeda V, Delgado-Requerey V, González M, Pérez-Ruiz JM (2019) Chloroplast Redox Regulatory Mechanisms in Plant Adaptation to Light and Darkness. Frontiers in plant science 10 (380). doi:10.3389/fpls.2019.00380

Chan KX, Wirtz M, Phua SY, Estavillo GM, Pogson BJ (2013) Balancing metabolites in drought: the sulfur assimilation conundrum. Trends in Plant Science 18 (1):18-29. doi:10.1016/j.tplants.2012.07.005

Chang SH, Lee S, Um TY, Kim J-K, Do Choi Y, Jang G (2017) pTAC10, a Key Subunit of Plastid-Encoded RNA Polymerase, Promotes Chloroplast Development. Plant Physiology 174 (1):435-449. doi:10.1104/pp.17.00248

Chao WS, Gu YQ, Pautot V, Bray EA, Walling LL (1999) Leucine aminopeptidase RNAs, proteins, and activities increase in response to water deficit, salinity, and the

wound signals systemin, methyl jasmonate, and abscisic acid. Plant Physiology 120 (4):979-992

Chen H, Boutros PC (2011) VennDiagram: a package for the generation of highly-customizable Venn and Euler diagrams in R. BMC Bioinformatics 12 (1):35. doi:10.1186/1471-2105-12-35

Cheng F, Zhou Y-H, Xia X-J, Shi K, Zhou J, Yu J-Q (2014) Chloroplastic thioredoxin-f and thioredoxin-m1/4 play important roles in brassinosteroids-induced changes in CO(2) assimilation and cellular redox homeostasis in tomato. Journal of Experimental Botany 65 (15):4335-4347. doi:10.1093/jxb/eru207

Cline K, Dabney-Smith C (2008) Plastid protein import and sorting: different paths to the same compartments. Current opinion in plant biology 11 (6):585-592. doi:10.1016/j.pbi.2008.10.008

Daniell H, Lee S-B, Grevich J, Saski C, Quesada-Vargas T, Guda C, Tomkins J, Jansen RK (2006) Complete chloroplast genome sequences of Solanum bulbocastanum, Solanum lycopersicum and comparative analyses with other Solanaceae genomes. Theoretical and Applied Genetics 112 (8):1503-1518. doi:10.1007/s00122-006-0254-x

de Luna-Valdez LA, Villaseñor-Salmerón CI, Cordoba E, Vera-Estrella R, León-Mejía P, Guevara-García AA (2019) Functional analysis of the Chloroplast GrpE (CGE) proteins from Arabidopsis thaliana. Plant Physiology and Biochemistry 139:293-306. doi:https://doi.org/10.1016/j.plaphy.2019.03.027

de Souza A, Wang JZ, Dehesh K (2017) Retrograde Signals: Integrators of Interorganellar Communication and Orchestrators of Plant Development. In: Merchant SS (ed) Annual Review of Plant Biology, Vol 68, vol 68. Annual Review of Plant Biology. pp 85-108. doi:10.1146/annurev-arplant-042916-041007

Dogra V, Duan JL, Lee KP, Lv SS, Liu RY, Kim CH (2017) FtsH2-Dependent Proteolysis of EXECUTER1 Is Essential in Mediating Singlet Oxygen-Triggered Retrograde Signaling in Arabidopsis thaliana. Frontiers in Plant Science 8. doi:10.3389/fpls.2017.01145

Drakakaki G, van de Ven W, Pan S, Miao Y, Wang J, Keinath NF, Weatherly B, Jiang L, Schumacher K, Hicks G, Raikhel N (2012) Isolation and proteomic analysis of the SYP61 compartment reveal its role in exocytic trafficking in Arabidopsis. Cell Res 22 (2):413-424. doi:10.1038/cr.2011.129

Duan JL, Lee KP, Dogra V, Zhang SY, Liu KW, Caceres-Moreno C, Lv SS, Xing WM, Kato Y, Sakamoto W, Liu RY, Macho AP, Kim C (2019) Impaired PSII Proteostasis Promotes Retrograde Signaling via Salicylic Acid. Plant Physiology 180 (4):2182-2197. doi:10.1104/pp.19.00483

Duan Z, Li K, Zhang L, Che L, Lu L, Rochaix J-D, Lu C, Peng L (2020) F-Type ATP Synthase Assembly Factors Atp11 and Atp12 in Arabidopsis. Frontiers in Plant Science 11. doi:10.3389/fpls.2020.522753

Duchene AM, Giritch A, Hoffmann B, Cognat V, Lancelin D, Peeters NM, Zaepfel M, Marechal-Drouard L, Small ID (2005) Dual targeting is the rule for organellar aminoacyl-tRNA synthetases in Arabidopsis thaliana. Proceedings of the National Academy of Sciences 102 (45):16484-16489. doi:10.1073/pnas.0504682102

Elias JE, Haas W, Faherty BK, Gygi SP (2005) Comparative evaluation of mass spectrometry platforms used in large-scale proteomics investigations. Nature methods 2 (9):667-675. doi:10.1038/nmeth785

Emanuelsson O, Brunak S, von Heijne G, Nielsen H (2007) Locating proteins in the cell using TargetP, SignalP and related tools. Nat Protoc 2 (4):953-971

Emanuelsson O, Nielsen H, Brunak S, von Heijne G (2000) Predicting subcellular localization of proteins based on their N-terminal amino acid sequence. J Mol Biol 300 (4):1005-1016. doi:10.1006/jmbi.2000.3903

Emanuelsson O, Nielsen H, Von Heijne G (1999) ChloroP, a neural network-based method for predicting chloroplast transit peptides and their cleavage sites. Protein Science 8 (5):978-984.

Exposito-Rodriguez M, Laissue PP, Yvon-Durocher G, Smirnoff N, Mullineaux PM (2017) Photosynthesis-dependent H2O2 transfer from chloroplasts to nuclei

provides a high-light signalling mechanism. Nature Communications 8. doi:10.1038/s41467-017-00074-w

Fernandez JC, Burch-Smith TM (2019) Chloroplasts as mediators of plant biotic interactions over short and long distances. Current opinion in plant biology 50:148-155. doi:https://doi.org/10.1016/j.pbi.2019.06.002

Ferro M, Salvi D, Brugière S, Miras S, Kowalski S, Louwagie M, Garin J, Joyard J, Rolland N (2003) Proteomics of the chloroplast envelope membranes from Arabidopsis thaliana. Molecular & cellular proteomics : MCP 2 (5):325-345. doi:10.1074/mcp.M300030-MCP200

Fichman Y, Mittler R (2020) Rapid systemic signaling during abiotic and biotic stresses: is the ROS wave master of all trades? The Plant Journal 102 (5):887-896. doi:10.1111/tpj.14685

Fowler JH, Aromdee DN, Pautot V, Holzer FM, Walling LL (2009) Leucine aminopeptidase regulates defense and wound signaling downstream of jasmonic acid. Plant Cell 21 (4):1239-1251. doi:10.1105/tpc.108.065029

Friso G, Giacomelli L, Ytterberg AJ, Peltier JB, Rudella A, Sun Q, Wijk KJ (2004) In-depth analysis of the thylakoid membrane proteome of Arabidopsis thaliana chloroplasts: new proteins, new functions, and a plastid proteome database. Plant Cell 16 (2):478-499. doi:10.1105/tpc.017814

Fristedt R, Williams-Carrier R, Merchant SS, Barkan A (2014) A Thylakoid Membrane Protein Harboring a DnaJ-type Zinc Finger Domain Is Required for Photosystem I Accumulation in Plants. Journal of Biological Chemistry 289 (44):30657-30667. doi:10.1074/jbc.m114.587758

Gabruk M, Mysliwa-Kurdziel B (2020) The origin, evolution and diversification of multiple isoforms of light-dependent protochlorophyllide oxidoreductase (LPOR): focus on angiosperms. Biochemical Journal 477 (12):2221-2236. doi:10.1042/bcj20200323

Gao HB, Metz J, Teanby NA, Ward AD, Botchway SW, Coles B, Pollard MR, Sparkes I (2016) In vivo quantification of peroxisome tethering to chloroplasts in tobacco

epidermal cells using optical tweezers. Plant Physiology 170 (1):263-272. doi:10.1104/pp.15.01529

Gao Z-P, Chen G-X, Yang Z-N (2012) Regulatory role of Arabidopsis pTAC14 in chloroplast development and plastid gene expression. Plant Signaling & Behavior 7 (10):1354-1356. doi:10.4161/psb.21618

Gibbs DJ, Bailey M, Tedds HM, Holdsworth MJ (2016) From start to finish: amino-terminal protein modifications as degradation signals in plants. New Phytologist 211 (4):1188-1194. doi:10.1111/nph.14105

Gu Y-Q, Chao WS, Walling LL (1996a) Localization and post-translational processing of the wound-induced leucine aminopeptidase proteins of tomato. Journal of Biological Chemistry 271 (42):25880-25887. doi:10.1074/jbc.271.42.25880

Gu Y-Q, Walling LL (2000) Specificity of the wound-induced leucine aminopeptidase (LAP-A) of tomato: Activity on dipeptide and tripeptide substrates. European Journal of Biochemistry 267 (4):1178-1187.

Gu YQ, Holzer FM, Walling LL (1999) Overexpression, purification and biochemical characterization of the wound-induced leucine aminopeptidase of tomato. European Journal of Biochemistry 263 (3):726-735

Gu YQ, Pautot V, Holzer FM, Walling LL (1996b) A complex array of proteins related to the multimeric leucine aminopeptidase of tomato. Plant Physiology (Rockville) 110 (4):1257-1266

Hahn A, Vonck J, Mills DJ, Meier T, Kühlbrandt W (2018) Structure, mechanism, and regulation of the chloroplast ATP synthase. Science 360 (6389):eaat4318. doi:10.1126/science.aat4318

Higa T, Suetsugu N, Kong SG, Wada M (2014) Actin-dependent plastid movement is required for motive force generation in directional nuclear movement in plants. Proceedings of the National Academy of Sciences of the United States of America 111 (11):4327-4331. doi:10.1073/pnas.1317902111

Hofmann K, Stoffel W (1993) TMbase - A database of membrane spanning protein segments

Hooper CM, Castleden IR, Tanz SK, Aryamanesh N, Millar AH (2017) SUBA4: the interactive data analysis centre for Arabidopsis subcellular protein locations. Nucleic Acids Research 45 (D1):D1064-D1074. doi:10.1093/nar/gkw1041

Horton P, Park KJ, Obayashi T, Fujita N, Harada H, Adams-Collier CJ, Nakai K (2007) WoLF PSORT: protein localization predictor. Nucleic Acids Res 35 (Web Server issue):W585-587. doi:10.1093/nar/gkm259

Huang C, Yu Q-B, Lv R-H, Yin Q-Q, Chen G-Y, Xu L, Yang Z-N (2013a) The Reduced Plastid-Encoded Polymerase-Dependent Plastid Gene Expression Leads to the Delayed Greening of the Arabidopsis fln2 Mutant. PLoS ONE 8 (9):e73092. doi:10.1371/journal.pone.0073092

Huang MS, Friso G, Nishimura K, Qu X, Olinares PDB, Majeran W, Sun Q, van Wijk KJ (2013b) Construction of Plastid Reference Proteomes for Maize and Arabidopsis and Evaluation of Their Orthologous Relationships; The Concept of Orthoproteomics. Journal of Proteome Research 12 (1):491-504. doi:10.1021/pr300952g

Huerta-Cepas J, Szklarczyk D, Heller D, Hernández-Plaza A, Forslund SK, Cook H, Mende DR, Letunic I, Rattei T, Lars, Christian, Bork P (2019) eggNOG 5.0: a hierarchical, functionally and phylogenetically annotated orthology resource based on 5090 organisms and 2502 viruses. Nucleic Acids Research 47 (D1):D309-D314. doi:10.1093/nar/gky1085

Initiative TAG (2000) Analysis of the genome sequence of the flowering plant Arabidopsis thaliana. Nature 408 (6814):796-815. doi:10.1038/35048692

Ishihama Y, Oda Y, Tabata T, Sato T, Nagasu T, Rappsilber J, Mann M (2005) Exponentially modified protein abundance index (emPAI) for estimation of absolute protein amount in proteomics by the number of sequenced peptides per protein. Molecular & cellular proteomics : MCP 4 (9):1265-1272. doi:10.1074/mcp.M500061-MCP200

Islam MS, Takagi S (2010) Co-localization of mitochondria with chloroplasts is a light-dependent reversible response. Plant Signaling & Behavior 5 (2):146,147-146,147. doi:10.4161/psb.5.2.10410

Jarvis P, López-Juez E (2013) Biogenesis and homeostasis of chloroplasts and other plastids. Nature Reviews Molecular Cell Biology 14 (12):787-802. doi:10.1038/nrm3702

Kahlau S, Aspinall S, Gray JC, Bock R (2006) Sequence of the Tomato Chloroplast DNA and Evolutionary Comparison of Solanaceous Plastid Genomes. Journal of Molecular Evolution 63 (2):194-207. doi:10.1007/s00239-005-0254-5

Kirby J, Keasling JD (2009) Biosynthesis of Plant Isoprenoids: Perspectives for Microbial Engineering. Annual Review of Plant Biology 60 (1):335-355. doi:10.1146/annurev.arplant.043008.091955

Klee HJ, Giovannoni JJ (2011) Genetics and control of tomato fruit ripening and quality attributes. Annual review of genetics 45:41-59. doi:10.1146/annurev-genet-110410-132507

Kleffmann T, Hirsch-Hoffmann M, Gruissem W, Baginsky S (2006) plprot: a comprehensive proteome database for different plastid types. Plant & cell physiology 47 (3):432-436. doi:10.1093/pcp/pcj005

Kleffmann T, Russenberger D, von Zychlinski A, Christopher W, Sjölander K, Gruissem W, Baginsky S (2004) The Arabidopsis thaliana chloroplast proteome reveals pathway abundance and novel protein functions. Curr Biol 14 (5):354-362. doi:10.1016/j.cub.2004.02.039

Kmiec B, Branca RMM, Berkowitz O, Li L, Wang Y, Murcha MW, Whelan J, Lehtiö J, Glaser E, Teixeira PF (2018) Accumulation of endogenous peptides triggers a pathogen stress response in Arabidopsis thaliana. The Plant Journal 96 (4):705-715. doi:doi:10.1111/tpj.14100

Kmiec B, Teixeira PF, Glaser E (2014) Shredding the signal: targeting peptide degradation in mitochondria and chloroplasts. Trends in Plant Science 19 (12):771-778. doi:10.1016/j.tplants.2014.09.004

Krause K, Oetke S, Krupinska K (2012) Dual Targeting and Retrograde Translocation: Regulators of Plant Nuclear Gene Expression Can Be Sequestered by Plastids. International Journal of Molecular Sciences 13 (9):11085-11101. doi:10.3390/ijms130911085

136

Krupinska K, Blanco NE, Oetke S, Zottini M (2020) Genome communication in plants mediated by organelle–n-ucleus-located proteins. Philosophical Transactions of the Royal Society B: Biological Sciences 375 (1801):20190397. doi:10.1098/rstb.2019.0397

Kumaran D (2005) Structure and mechanism of ADP-ribose-1"-monophosphatase (Appr-1"-pase), a ubiquitous cellular processing enzyme. Protein Science 14 (3):719-726. doi:10.1110/ps.041132005

Laizet Yh, Pontier D, Mache R, Kuntz M Subfamily Organization and Phylogenetic Origin of Genes Encoding Plastid Lipid-Associated Proteins of the Fibrillin Type. In, 2004.

Lancien M, Lea PJ, Azevedo RA (2007) Amino Acid Synthesis in Plastids. In: The Structure and Function of Plastids. Springer Netherlands, pp 355-385. doi:10.1007/978-1-4020-4061-0_18

Lee KP, Kim C, Landgraf F, Apel K (2007) EXECUTER1- and EXECUTER2-dependent transfer of stress-related signals from the plastid to the nucleus of Arabidopsis thaliana. Proceedings of the National Academy of Sciences 104 (24):10270-10275. doi:10.1073/pnas.0702061104

Li-Beisson Y, Shorrosh B, Beisson F, Andersson MX, Arondel V, Bates PD, Baud S, Bird D, Debono A, Durrett TP, Franke RB, Graham IA, Katayama K, Kelly AA, Larson T, Markham JE, Miquel M, Molina I, Nishida I, Rowland O, Samuels L, Schmid KM, Wada H, Welti R, Xu C, Zallot R, Ohlrogge J (2013) Acyl-Lipid Metabolism. The Arabidopsis Book 11:e0161. doi:10.1199/tab.0161

Li Y, Chen Y, Zhou L, You S, Deng H, Chen Y, Alseekh S, Yuan Y, Fu R, Zhang Z, Su D, Fernie AR, Bouzayen M, Ma T, Liu M, Zhang Y (2020) MicroTom Metabolic Network: Rewiring Tomato Metabolic Regulatory Network throughout the Growth Cycle. Molecular Plant 13 (8):1203-1218. doi:10.1016/j.molp.2020.06.005

Li Y, Liu B, Zhang J, Kong F, Zhang L, Meng H, Li W, Rochaix J-D, Li D, Peng L (2019) OHP1, OHP2, and HCF244 Form a Transient Functional Complex with the Photosystem II Reaction Center. Plant Physiology 179 (1):195-208. doi:10.1104/pp.18.01231

Liu J, Last RL (2017) A chloroplast thylakoid lumen protein is required for proper photosynthetic acclimation of plants under fluctuating light environments. Proceedings of the National Academy of Sciences 114 (38):E8110-E8117. doi:10.1073/pnas.1712206114

Liu J, Yang H, Lu Q, Wen X, Chen F, Peng L, Zhang L, Lu C (2012) PSBP-DOMAIN PROTEIN1, a Nuclear-Encoded Thylakoid Lumenal Protein, Is Essential for Photosystem I Assembly in Arabidopsis. The Plant Cell 24 (12):4992-5006. doi:10.1105/tpc.112.106542

Lohse M, Nagel A, Herter T, May P, Schroda M, Zrenner R, Tohge T, Fernie AR, Stitt M, Usadel B (2014) Mercator: a fast and simple web server for genome scale functional annotation of plant sequence data. Plant, cell & environment 37 (5):1250-1258. doi:10.1111/pce.12231

Lu Y (2016) Identification and Roles of Photosystem II Assembly, Stability, and Repair Factors in Arabidopsis. Frontiers in Plant Science 7. doi:10.3389/fpls.2016.00168

Luna E, Flandin A, Cassan C, Prigent S, Chevanne C, Kadiri CF, Gibon Y, Petriacq P (2020) Metabolomics to Exploit the Primed Immune System of Tomato Fruit. Metabolites 10 (3). doi:10.3390/metabo10030096

Lundquist PK, Mantegazza O, Stefanski A, Stuhler K, Weber APM (2017) Surveying the Oligomeric State of Arabidopsis thaliana Chloroplasts. Molecular Plant 10 (1):197-211. doi:10.1016/j.molp.2016.10.011

Majeran W, Friso G, Asakura Y, Qu X, Huang MS, Ponnala L, Watkins KP, Barkan A, van Wijk KJ (2012) Nucleoid-Enriched Proteomes in Developing Plastids and Chloroplasts from Maize Leaves: A New Conceptual Framework for Nucleoid Functions. Plant Physiology 158 (1):156-189. doi:10.1104/pp.111.188474

Mao J, Chi W, Ouyang M, He B, Chen F, Zhang L (2015) PAB is an assembly chaperone that functions downstream of chaperonin 60 in the assembly of chloroplast ATP synthase coupling factor 1. Proceedings of the National Academy of Sciences 112 (13):4152-4157. doi:10.1073/pnas.1413392111

Marino G, Naranjo B, Wang J, Penzler JF, Kleine T, Leister D (2019) Relationship of GUN1 to FUG1 in chloroplast protein homeostasis. Plant Journal 99 (3):521-535. doi:10.1111/tpj.14342

Masclaux-Daubresse C, Daniel-Vedele F, Dechorgnat J, Chardon F, Gaufichon L, Suzuki A (2010) Nitrogen uptake, assimilation and remobilization in plants: challenges for sustainable and productive agriculture. Annals of Botany 105 (7):1141-1157. doi:10.1093/aob/mcq028

Mehrshahi P, Stefano G, Andaloro JM, Brandizzi F, Froehlich JE, DellaPenna D (2013) Transorganellar complementation redefines the biochemical continuity of endoplasmic reticulum and chloroplasts. Proceedings of the National Academy of Sciences of the United States of America 110 (29):12126-12131. doi:10.1073/pnas.1306331110

Melonek J, Oetke S, Krupinska K (2016) Multifunctionality of plastid nucleoids as revealed by proteome analyses. Biochimica Et Biophysica Acta-Proteins and Proteomics 1864 (8):1016-1038. doi:10.1016/j.bbapap.2016.03.009

Millar AH, Whelan J, Small I (2006) Recent surprises in protein targeting to mitochondria and plastids. Current opinion in plant biology 9 (6):610-615. doi:10.1016/j.pbi.2006.09.002

Mullineaux PM, Exposito-Rodriguez M, Laissue PP, Smirnoff N, Park E (2020) Spatial chloroplast-to-nucleus signalling involving plastid–nuclear complexes and stromules. Philosophical Transactions of the Royal Society B: Biological Sciences 375 (1801):20190405. doi:10.1098/rstb.2019.0405

Munekage Y, Hojo M, Meurer J, Endo T, Tasaka M, Shikanai T (2002) PGR5 Is Involved in Cyclic Electron Flow around Photosystem I and Is Essential for Photoprotection in Arabidopsis. Cell 110 (3):361-371. doi:10.1016/s0092-8674(02)00867-x

Nakai M (2018) New Perspectives on Chloroplast Protein Import. Plant and Cell Physiology 59 (6):1111-1119. doi:10.1093/pcp/pcy083

Narváez-Vásquez J, Tu CJ, Park SY, Walling LL (2008) Targeting and localization of wound-inducible leucine aminopeptidase A in tomato leaves. Planta 227:341-351

Naver H, Boudreau E, Rochaix JD (2001) Functional studies of Ycf3: its role in assembly of photosystem I and interactions with some of its subunits. The Plant cell 13 (12):2731-2745. doi:10.1105/tpc.010253

Nellaepalli S, Ozawa S-I, Kuroda H, Takahashi Y (2018) The photosystem I assembly apparatus consisting of Ycf3–Y3IP1 and Ycf4 modules. Nature Communications 9 (1). doi:10.1038/s41467-018-04823-3

Nishimura K, Kato Y, Sakamoto W (2017) Essentials of Proteolytic Machineries in Chloroplasts. Molecular Plant 10 (1):4-19. doi:10.1016/j.molp.2016.08.005

Oikawa K, Hayashi M, Hayashi Y, Nishimura M (2019) Re-evaluation of physical interaction between plant peroxisomes and other organelles using live-cell imaging techniques. Journal of Integrative Plant Biology 61 (7):836-852. doi:10.1111/jipb.12805

Olinares PDB, Ponnala L, van Wijk KJ (2010) Megadalton Complexes in the Chloroplast Stroma of Arabidopsis thaliana Characterized by Size Exclusion Chromatography, Mass Spectrometry, and Hierarchical Clustering. Molecular & Cellular Proteomics 9 (7):1594-1615. doi:10.1074/mcp.M000038-MCP201

op den Camp RGL, Przybyla D, Ochsenbein C, Laloi C, Kim C, Danon A, Wagner D, Hideg É, Göbel C, Feussner I, Nater M, Apel K (2003) Rapid Induction of Distinct Stress Responses after the Release of Singlet Oxygen in Arabidopsis. The Plant Cell 15 (10):2320-2332. doi:10.1105/tpc.014662

Paetzold H, Garms S, Bartram S, Wieczorek J, Urós-Gracia E-M, Rodríguez-Concepción M, Boland W, Strack D, Hause B, Walter MH (2010) The Isogene 1-Deoxy-D-Xylulose 5-Phosphate Synthase 2 Controls Isoprenoid Profiles, Precursor Pathway Allocation, and Density of Tomato Trichomes. Molecular Plant 3 (5):904-916. doi:10.1093/mp/ssq032

Peltier JB, Cai Y, Sun Q, Zabrouskov V, Giacomelli L, Rudella A, Ytterberg AJ, Rutschow H, van Wijk KJ (2006) The oligomeric stromal proteome of Arabidopsis thaliana chloroplasts. Molecular & cellular proteomics : MCP 5 (1):114-133. doi:10.1074/mcp.M500180-MCP200

Peltier JB, Emanuelsson O, Kalume DE, Ytterberg J, Friso G, Rudella A, Liberles DA, Soderberg L, Roepstorff P, von Heijne G, van Wijk KJ (2002) Central functions of the lumenal and peripheral thylakoid proteome of Arabidopsis determined by experimentation and genome-wide prediction. Plant Cell 14 (1):211-236

Peng L, Fukao Y, Fujiwara M, Takami T, Shikanai T (2009) Efficient Operation of NAD(P)H Dehydrogenase Requires Supercomplex Formation with Photosystem I via Minor LHCI in Arabidopsis. The Plant Cell 21 (11):3623-3640. doi:10.1105/tpc.109.068791

Petsalaki EI, Bagos PG, Litou ZI, Hamodrakas SJ (2006) PredSL: a tool for the N-terminal sequence-based prediction of protein subcellular localization. Genomics Proteomics Bioinformatics 4 (1):48-55. doi:10.1016/S1672-0229(06)60016-8

Ploscher M, Reisinger V, Eichacker LA (2011) Proteomic comparison of etioplast and chloroplast protein complexes. Journal of Proteomics 74 (8):1256-1265. doi:10.1016/j.jprot.2011.03.020

Rappsilber J, Ryder U, Lamond AI, Mann M (2002) Large-scale proteomic analysis of the human spliceosome. Genome Res 12 (8):1231-1245. doi:10.1101/gr.473902

Reumann S, Babujee L, Ma C, Wienkoop S, Siemsen T, Antonicelli GE, Rasche N, Lüder F, Weckwerth W, Jahn O (2007) Proteome Analysis of Arabidopsis Leaf Peroxisomes Reveals Novel Targeting Peptides, Metabolic Pathways, and Defense Mechanisms. The Plant Cell 19 (10):3170-3193. doi:10.1105/tpc.107.050989

Richly E, Leister D (2004) An improved prediction of chloroplast proteins reveals diversities and commonalities in the chloroplast proteomes of Arabidopsis and rice. Gene 329:11-16

Rolland N, Curien G, Finazzi G, Kuntz M, Marechal E, Matringe M, Ravanel S, Seigneurin-Berny D (2012) The biosynthetic capacities of the plastids and integration between cytoplasmic and chloroplast processes. Annual review of genetics 46:233-264. doi:10.1146/annurev-genet-110410-132544

Rosenberg LA, Padgett PE, Assmann SM, Walling LL, Leonard RT (1997) Identification of mRNAs and proteins in higher plants using probes from the Band 3 anion transporter of mammals. Journal of Experimental Botany 48 (309):857-868

Sant'Ana DVP, Lefsrud M (2018) Tomato proteomics: Tomato as a model for crop proteomics. Scientia Horticulturae 239:224-233. doi:https://doi.org/10.1016/j.scienta.2018.05.041

Sato R, Kono M, Harada K, Ohta H, Takaichi S, Masuda S (2017) FLUCTUATING-LIGHT-ACCLIMATION PROTEIN1, Conserved in Oxygenic Phototrophs, Regulates H+ Homeostasis and Non-Photochemical Quenching in Chloroplasts. Plant and Cell Physiology 58 (10):1622-1630. doi:10.1093/pcp/pcx110

Sato S, Nakamura Y, Kaneko T, Asamizu E, Tabata S (1999) Complete structure of the chloroplast genome of Arabidopsis thaliana. DNA Res 6 (5):283-290. doi:10.1093/dnares/6.5.283

Schubert M, Petersson UA, Haas BJ, Funk C, Schroder WP, Kieselbach T (2002) Proteome map of the chloroplast lumen of Arabidopsis thaliana. Journal of Biological Chemistry 277 (10):8354-8365. doi:10.1074/jbc.M108575200

Scranton M, Fowler JH, Girke T, Walling LL (2013) Microarray analysis of tomato's early and late wound response reveals new regulatory targets for leucine aminopeptidase A. PLoS One 8 (10):e77889

Scranton M, Yee A, Park SY, Walling LL (2012) Plant leucine aminopeptidases moonlight as molecular chaperones. Journal of Biological Chemistry 287:18408-18417. doi:10.1074/jbc.M111.309500

Shen J, Williams-Carrier R, Barkan A (2017) PSA3, a Protein on the Stromal Face of the Thylakoid Membrane, Promotes Photosystem I Accumulation in Cooperation with the Assembly Factor PYG7. Plant Physiology 174 (3):1850-1862. doi:10.1104/pp.17.00524

Shikanai T (2016) Chloroplast NDH: A different enzyme with a structure similar to that of respiratory NADH dehydrogenase. Biochimica et Biophysica Acta (BBA) - Bioenergetics 1857 (7):1015-1022. doi:10.1016/j.bbabio.2015.10.013

Siddique MA, Grossmann J, Gruissem W, Baginsky S (2006) Proteome analysis of bell pepper (Capsicum annuum L.) chromoplasts. Plant and Cell Physiology 47 (12):1663-1673

Small I, Peeters N, Legeai F, Lurin C (2004) Predotar: A tool for rapidly screening proteomes for N-terminal targeting sequences. Proteomics 4 (6):1581-1590. doi:10.1002/pmic.200300776

Stanley L, Yuan Y-W (2019) Transcriptional Regulation of Carotenoid Biosynthesis in Plants: So Many Regulators, So Little Consensus. Frontiers in Plant Science 10 (1017). doi:10.3389/fpls.2019.01017

Sun A-Q, Yi S-Y, Yang J-Y, Zhao C-M, Liu J (2006) Identification and characterization of a heat-inducible ftsH gene from tomato (Lycopersicon esculentum Mill.). Plant Science 170 (3):551-562. doi:10.1016/j.plantsci.2005.10.010

Sun Q, Zybailov B, Majeran W, Friso G, Olinares PD, van Wijk KJ (2009) PPDB, the Plant Proteomics Database at Cornell. Nucleic Acids Res 37 (Database issue):D969-974. doi:10.1093/nar/gkn654

Suzuki M, Takahashi S, Kondo T, Dohra H, Ito Y, Kiriiwa Y, Hayashi M, Kamiya S, Kato M, Fujiwara M, Fukao Y, Kobayashi M, Nagata N, Motohashi R (2015) Plastid Proteomic Analysis in Tomato Fruit Development. PLOS ONE 10 (9):e0137266. doi:10.1371/journal.pone.0137266

Tamburino R, Vitale M, Ruggiero A, Sassi M, Sannino L, Arena S, Costa A, Batelli G, Zambrano N, Scaloni A, Grillo S, Scotti N (2017) Chloroplast proteome response to drought stress and recovery in tomato (Solanum lycopersicum L.). BMC plant biology 17 (1):40. doi:10.1186/s12870-017-0971-0

Thimm O, Bläsing O, Gibon Y, Nagel A, Meyer S, Krüger P, Selbig J, Müller LA, Rhee SY, Stitt M (2004) MAPMAN: a user-driven tool to display genomics data sets onto diagrams of metabolic pathways and other biological processes. Plant J 37 (6):914-939. doi:10.1111/j.1365-313x.2004.02016.x

Thomson SM, Pulido P, Jarvis RP (2020) Protein import into chloroplasts and its regulation by the ubiquitin-proteasome system. Biochemical Society Transactions 48:71-82. doi:10.1042/bst20190274

143

Trösch R, Töpel M, Flores-Pérez Ú, Jarvis P (2015) Genetic and Physical Interaction Studies Reveal Functional Similarities between ALBINO3 and ALBINO4 in Arabidopsis. Plant Physiology 169 (2):1292-1306. doi:10.1104/pp.15.00376

Unal D, García-Caparrós P, Kumar V, Dietz K-J (2020) Chloroplast-associated molecular patterns as concept for fine-tuned operational retrograde signalling. Philosophical Transactions of the Royal Society B: Biological Sciences 375 (1801):20190443. doi:10.1098/rstb.2019.0443

Von Zychlinski A, Kleffmann T, Krishnamurthy N, Sjölander K, Baginsky S, Gruissem W (2005) Proteome Analysis of the Rice Etioplast. Molecular & Cellular Proteomics 4 (8):1072-1084. doi:10.1074/mcp.m500018-mcp200

Walling LL (2006) Recycling or regulation? The role of amino-terminal modifying enzymes. Current opinion in plant biology 9 (3):227-233

Wang D, Portis AR (2007) A Novel Nucleus-Encoded Chloroplast Protein, PIFI, Is Involved in NAD(P)H Dehydrogenase Complex-Mediated Chlororespiratory Electron Transport in Arabidopsis. Plant Physiology 144 (4):1742-1752. doi:10.1104/pp.107.103218

Wang L, Kim C, Xu X, Piskurewicz U, Dogra V, Singh S, Mahler H, Apel K (2016) Singlet oxygen- and EXECUTER1-mediated signaling is initiated in grana margins and depends on the protease FtsH2. Proceedings of the National Academy of Sciences 113 (26):E3792-E3800. doi:10.1073/pnas.1603562113

Wang L, Leister D, Guan L, Zheng Y, Schneider K, Lehmann M, Apel K, Kleine T (2020a) The Arabidopsis SAFEGUARD1 suppresses singlet oxygen-induced stress responses by protecting grana margins. Proceedings of the National Academy of Sciences 117 (12):6918-6927. doi:10.1073/pnas.1918640117

Wang Y, Selinski J, Mao C, Zhu Y, Berkowitz O, Whelan J (2020b) Linking mitochondrial and chloroplast retrograde signalling in plants. Philosophical Transactions of the Royal Society B: Biological Sciences 375 (1801):20190410. doi:10.1098/rstb.2019.0410

Wang YQ, Yang Y, Fei Z, Yuan H, Fish T, Thannhauser TW, Mazourek M, Kochian LV, Wang X, Li L (2013) Proteomic analysis of chromoplasts from six crop species

reveals insights into chromoplast function and development. J Exp Bot 64 (4):949-961. doi:10.1093/jxb/ers375

Wasternack C, Song SS (2017) Jasmonates: biosynthesis, metabolism, and signaling by proteins activating and repressing transcription. Journal of Experimental Botany 68 (6):1303-1321. doi:10.1093/jxb/erw443

Wise RR, Hooper JK (2006) The Structure and Function of Plastids. Advances in Photosynthesis and Respiration, vol 23. Springer, Dordrecht, Netherlands

Wu GZ, Meyer EH, Richter AS, Schuster M, Ling QH, Schottler MA, Walther D, Zoschke R, Grimm B, Jarvis RP, Bock R (2019) Control of retrograde signalling by protein import and cytosolic folding stress. Nature Plants 5 (5):525-538. doi:10.1038/s41477-019-0415-y

Yamamoto H, Shikanai T (2019) PGR5-Dependent Cyclic Electron Flow Protects Photosystem I under Fluctuating Light at Donor and Acceptor Sides. Plant Physiology 179 (2):588-600. doi:10.1104/pp.18.01343

Yang F, Xiao K, Pan H, Liu J (2021) Chloroplast: The Emerging Battlefield in Plant–Microbe Interactions. Frontiers in plant science 12 (218). doi:10.3389/fpls.2021.637853

Yoshida K, Yokochi Y, Hisabori T (2019) New Light on Chloroplast Redox Regulation: Molecular Mechanism of Protein Thiol Oxidation. Frontiers in plant science 10:1534-1534. doi:10.3389/fpls.2019.01534

Zhang L, Duan Z, Zhang J, Peng L (2016) BIOGENESIS FACTOR REQUIRED FOR ATP SYNTHASE 3 Facilitates Assembly of the Chloroplast ATP Synthase Complex in Arabidopsis. Plant Physiology:pp.00248.02016. doi:10.1104/pp.16.00248

Zhang L, Pu H, Duan Z, Li Y, Liu B, Zhang Q, Li W, Rochaix J-D, Liu L, Peng L (2018) Nucleus-Encoded Protein BFA1 Promotes Efficient Assembly of the Chloroplast ATP Synthase Coupling Factor 1. The Plant Cell 30 (8):1770-1788. doi:10.1105/tpc.18.00075

Zhou F, Pichersky E (2020) The complete functional characterisation of the terpene synthase family in tomato. New Phytologist 226 (5):1341-1360. doi:10.1111/nph.16431

Zybailov B, Rutschow H, Friso G, Rudella A, Emanuelsson O, Sun Q, van Wijk KJ (2008) Sorting signals, N-terminal modifications and abundance of the chloroplast proteome. PLoS One 3 (4):e1994. doi:10.1371/journal.pone.0001994
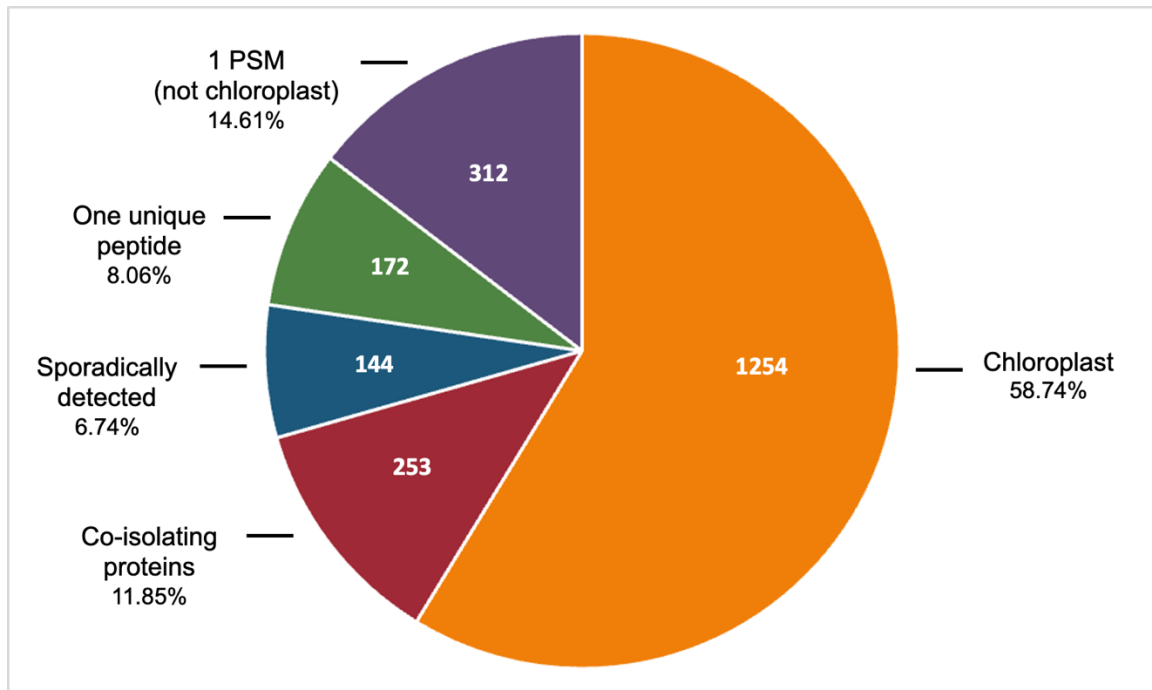
Figure 1.1 Classification of 1% FDR proteins identified in tomato chloroplast soluble extracts. The 2,135 proteins identified in the soluble extracts of tomato chloroplasts includes 1,254 chloroplast proteins, 253 co-isolating proteins (CIPs) that were reproducibly detected and 628 proteins that were removed from consideration because they were detected with one PSM, with one unique peptide, or sporadically (in less than 40% of the acetone or PAGE samples).
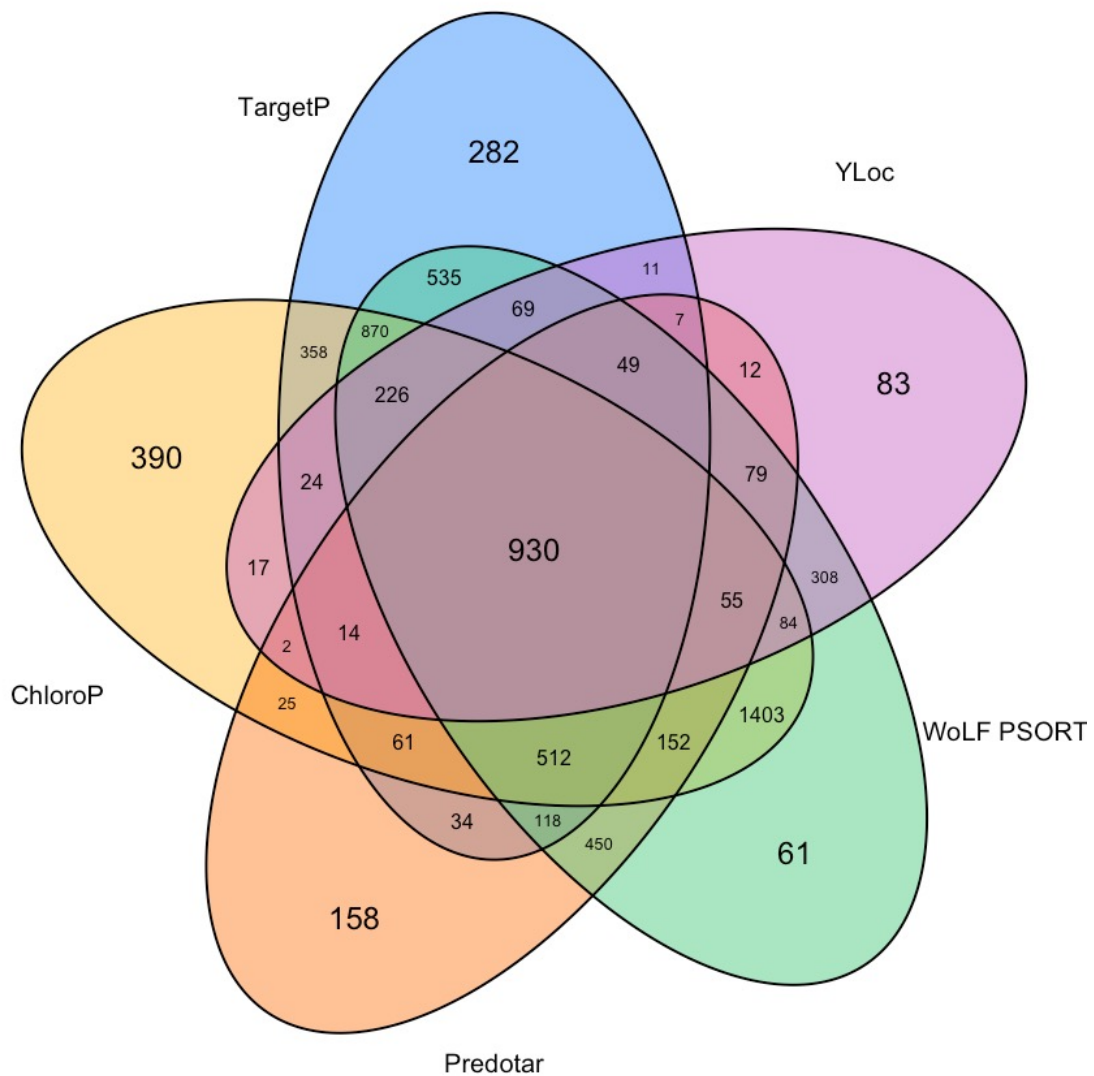
Figure 1.2 Source of proteins assigned to the tomato Atlas. A total of 7,379 nuclear-genome encoded proteins were predicted to be chloroplast localized by one or more of five subcellular localization programs: WoLF PSORT, Predotar, ChloroP, TargetP, and YLoc. The 87 plastid-genome encoded proteins, which are part of the Atlas, are not displayed.

Figure 1.3 Overlap of the tomato chloroplast protein Atlas with the three Arabidopsis protein databases. A four-way Venn diagram compares the overlap of the tomato protein Atlas with Arabidopsis thaliana homologs present in plprot, SUBA4, and PPDB.
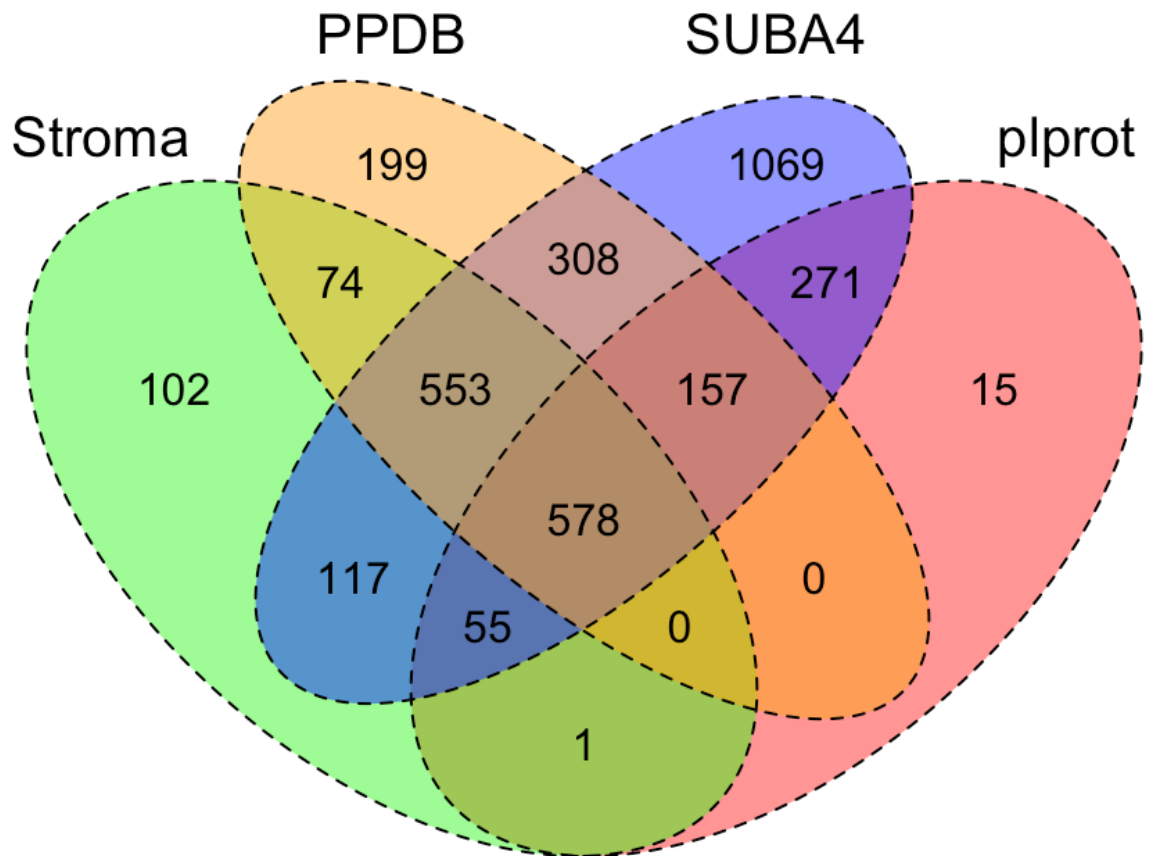
Figure 1.4 Comparison of the tomato stromal proteome with Arabidopsis thaliana proteins with chloroplast localization present in the plprot, SUBA4 and PPDB databases. A core of 518 proteins with one Arabidopsis ortholog was detected in all three databases. Sixty proteins in the tomato stromal proteome had multiple Arabidopsis orthologs in all three databases.
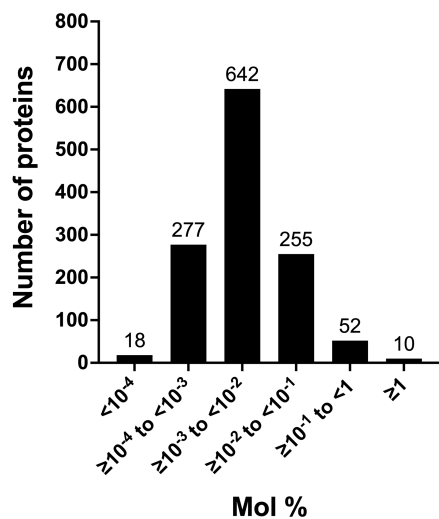
Figure 1.5 Abundance classes of leaf stromal proteins. The abundance of the 1,254 proteins of the leaf stromal proteome was determined by calculating the emPAI and mol percent of the proteome. Six protein classes were defined by their relative abundance. The numbers of proteins in each emPAI class are provided above the bar.
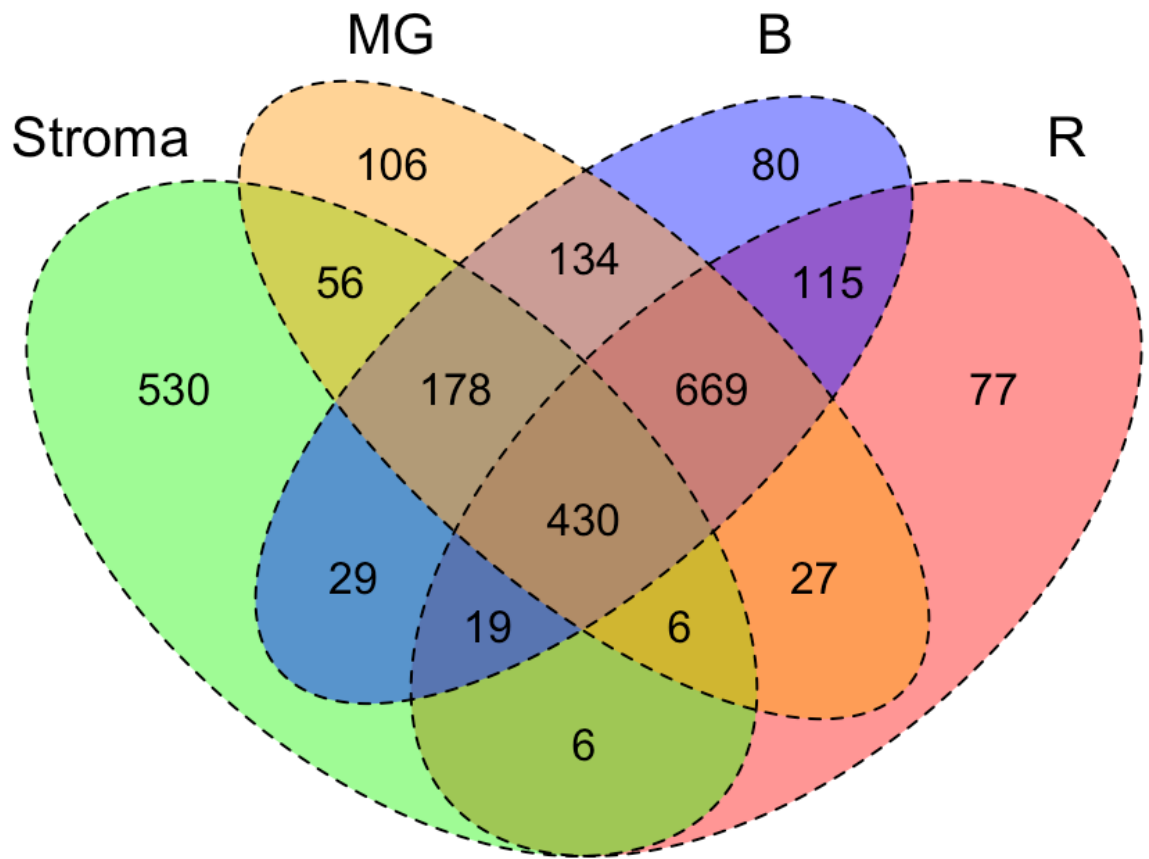
Figure 1.6 Intersection of the tomato stromal proteome with fruit plastid proteomes. A four-way Venn diagram illustrates the overlap of the leaf stromal proteome with three tomato plastid proteomes from fruit in the mature green (MG), breaker and 10-d post breaker (B), and red (R) stages of fruit development.

A

B

153
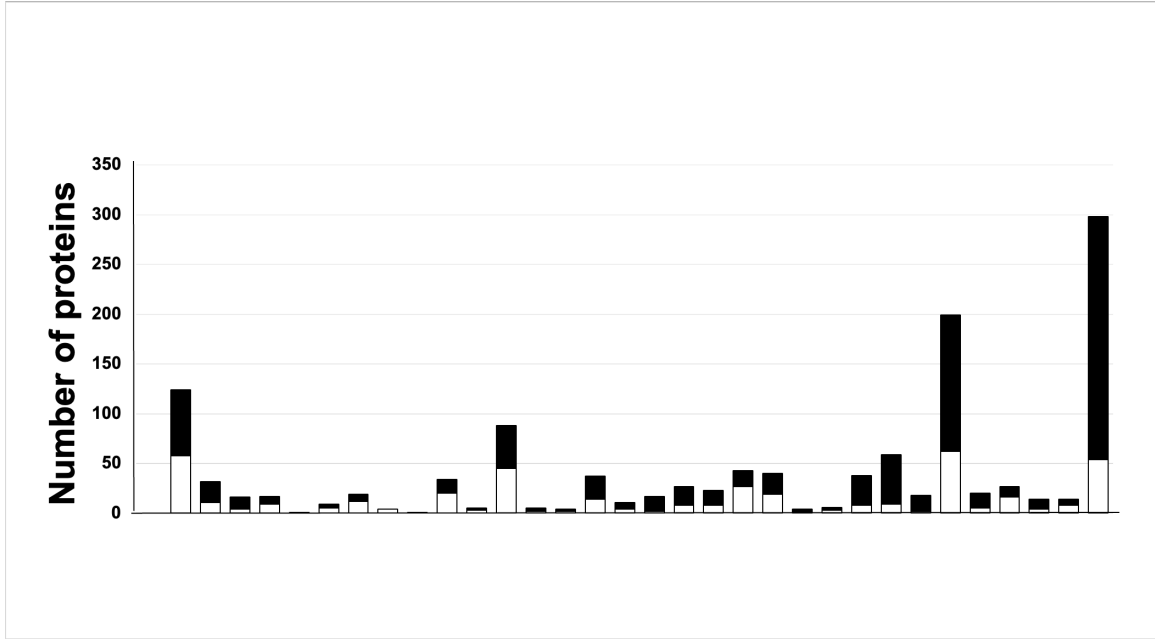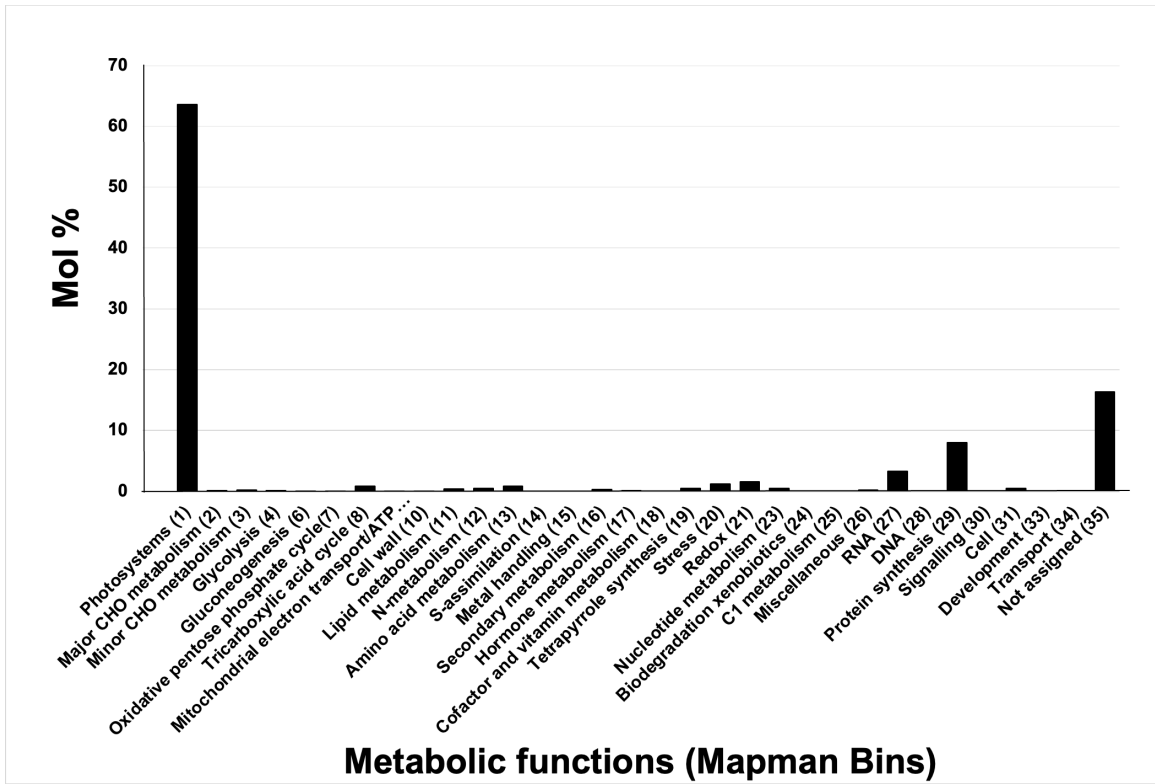
Figure 1.7 Functions and abundance of proteins detected in the tomato stromal proteome. The 1,254 proteins of the tomato stromal proteome were categorized into MapMan functional categories. Mapman bin numbers are within parentheses. A) The 430 proteins shared with the fruit plastid proteomes (white) and 844 proteins detected only in the leaf stromal proteome (black) are displayed. No stromal proteins were associated with fermentation (Bin 5), polyamine metabolism (Bin 22) or microRNA and natural antisense RNA (Bin 22) bins; for this reason, these bins are not displayed. B) The abundance of the proteins in each Mapman bin is displayed as Mol % of the stromal proteome.

Chapter 2

Leucine aminopeptidase and MeJA regulate primary and secondary metabolites in an array of biochemical pathways

Abstract

Tomatoes are model plants to study plant defense. Jasmonic acid (JA) is a key regulator of development, wounding and defense responses to pathogens and herbivores. In tomato and a subset of the Solanaceae, leucine aminopeptidase A (LAP-A) is a key regulator of the late branch of wound signaling acting downstream of JA perception and synthesis. LAP-A is plastid stroma-localized protein with bifunctional with aminopeptidase and chaperone activities. LAP-A is implicated in creating or perpetuating a retrograde signal essential for defense against herbivores. Using wild-type (wild-type) plants and LapA mutant plants that silence LAP-A (LapA-SI) and overexpress LAP-A (LapA-OX), changes in metabolites after methyl jasmonate (MeJA) treatments were determined. Using targeted and untargeted mass spectrometry techniques, metabolites were identified and quantified to reveal plant metabolites that were MeJA and/or LAP-A dependent. The discovery of primary and secondary metabolites regulated by LAP-A and methyl jasmonate (MeJA) in this study has shed light on the role of LAP-A in plant defense. Amino acids, osmolytes, nucleotides, steroidal glycoalkaloids (SGAs), and flavonoids are a few of the essential metabolites regulated by LAP-A and MeJA.

Introduction

The advances in speed and accuracy of gas chromatography-mass spectrometry (GC-MS) and liquid chromatography-mass spectrometry (LC-MS) technologies over the past two decades has fueled an explosive increase in our understanding of the diversity of plant metabolites (Allwood and Goodacre 2010; Sumner et al. 2015; Alseekh and Fernie 2021; Enfissi et al. 2021). It is currently estimated that the plant kingdom produces over 200,000 different metabolites. While no one technology can provide a comprehensive understanding of a plant's metabolome, deployment of both targeted and untargeted approaches to metabolite identification has revealed the chemical complexity of plants throughout development and in response to abiotic and biotic stresses. Integrating metabolite profiles with single-nucleotide polymorphisms, transcriptomes, proteomes, and epigenome data sets have allowed a comprehensive understanding of regulatory networks that link metabolites to their metabolic and regulatory pathways (Alseekh and Fernie 2021; Enfissi et al. 2021; Scossa et al. 2021; Soltis and Kliebenstein 2015). Integrative omics approaches have facilitated discovery of candidate gene(s) and firmly established genotype-phenotype relationships critical for the improvement of important plant traits (Das et al. 2021; Li et al. 2020).

Solanum lycopersicum (tomato) is a major horticultural crop in the US and world (USDA 2017). Valued for its unique flavor, antioxidants and high nutritional value, tomato fruit are a staple in many cuisines across the world. Therefore, it is not surprising that tomato has emerged as model system to understand fruit development, maturation and ripening at the genome, proteome and metabolome level (Li et al. 2020; Sant'Ana and Lefsrud 2018; Fortuny et al. 2021). There are numerous metabolomics, and more

156

recently multi-omics studies, of fruit development in cultivated and wild tomatoes with an increasing emphasis on understanding the impact of environmental fluctuations that will be imposed by climate change (Moing et al. 2020; Li et al. 2020; Tohge et al. 2020).

The ability of tomato fruits, shoots and roots to protect themselves from the continuous challenges imposed by environmental fluctuations (e.g., changes in light intensity, temperature, salinity, and water deficit) and attacks by pathogens and herbivores is critical for an abundant and nutritious crop. Therefore, it is not surprising that tomatoes have also emerged as a model system for the understanding of the mechanisms of plant defense and its associated metabolites (Chaudhary et al. 2019; Luna et al. 2020; Mandal et al. 2020; Paupiere et al. 2020; Soltis and Kliebenstein 2015; Perez-Fons et al. 2019). For tomatoes, secondary metabolites within leaf trichomes from wild tomato species have been intensively investigated at the metabolomic and transcriptomic levels, as many of these metabolites provide broad-spectrum resistance to herbivores (Kortbeek et al. 2021; Fan et al. 2016; Ekanayaka et al. 2015; Bleeker et al. 2012). While some of these metabolites are constitutively expressed, many secondary metabolites are regulated by jasmonates, which are essential oxylipins that regulate plant defense against pathogens and herbivores, as well as having an essential role in plant growth and development (Howe et al. 2018; Wei et al. 2021; De Geyter et al. 2012; Cabianca et al. 2021).

When the transcriptome and metabolome studies are paired with comparisons of wild-type (wild-type) and defense gene mutants, significant insights into the metabolic pathways and their regulatory programs have been revealed (Li et al. 2020; Yan et al. 2014; Chen et al. 2006; Schuman et al. 2018). For example, comparisons of the responses of Arabidopsis jaz mutants (jasmonate-zim domain proteins, which negatively

regulate JA-induced responses) and wild-type (wild-type) plants to methyl jasmonate (MeJA) treatments revealed the magnitude of changes to the JA-regulated transcriptome and metabolome (Yan et al. 2014).

In tomato, a second layer of control in jasmonate signaling is imposed by the multi-functional, chloroplast-localized leucine aminopeptidase A (LAP-A) (Scranton et al. 2013; Fowler et al. 2009). LAP-A is present in a subset of the Solanaceae (Chao et al. 2000). LAP-A is an aminopeptidase and a molecular chaperone that has the potential to modulate protein stability and activity within the chloroplast stroma (Gu et al. 1999; Gu and Walling 2002; Scranton et al. 2012). Transgenic tomato lines that silence LAP (LapA-SI) and ectopically express LAP-A (LapA-OX) were used to interrogate the impact of LAP-A on tomato immunity. LapA-SI plants are more susceptible to caterpillar (Manduca sexta) feeding, while LapA-OX plants are more resistant than wild-type plants (Fowler et al. 2009). Well correlated with foliage consumption was the fact that the masses of M. sexta larvae were 2-fold larger after 11 days of feeding on LapA-SI plants than wild-type plants. The supplementation of artificial diets with LAP-A does not deter herbivore growth and development suggesting that LAP-A's mode of action is dependent on other defense proteins within the insect gut or its ability to upregulate the expression of nuclear-encoded genes that encode antinutritive proteins in vivo (e.g., proteinase inhibitors (PINs) and polyphenol oxidase (PPO)) (Fowler et al. 2009). LAP-A regulates JA-responsive genes by acting downstream of the biosynthesis and perception of JA (Fowler et al. 2009). Finally, LAP-A is a negative regulator of other stress-responsive genes, such as pathogenesis-related proteins and stress-response chaperones (Scranton et al. 2013).

The magnitude of LAP-A's ability to reprogram the tomato transcriptome, proteome and metabolome is yet to be revealed. A first step to understanding the LAP-dependent metabolome is presented here. To garner insights into the MeJA- and/or LAP-A-dependent metabolome, we performed a targeted and untargeted metabolomics studies to compare wild-type, LapA-SI and LapA-OX plant responses to MeJA (a proxy for wounding). These analyses identified changes in primary and secondary metabolites at three times after MeJA treatment (0, 8, 12, and 24 h). As metabolite levels can be controlled at the transcriptional, post-transcriptional, translational or post-translational level (Kosmacz et al. 2020), we investigated the regulation of a subset of LapA-regulated metabolites. By leveraging current proteome data and performing qRT-PCR for selected biosynthetic and/or catabolic enzymes, we assessed if metabolite levels were correlated with changes in protein or mRNA levels of key biosynthetic enzymes. We focused on a subset of genes that encoded enzymes responsible for the biosynthesis of the LapA-regulated metabolites which included steroidal glycoalkaloids (SGAs), flavonoids and a subset of amino acids.

Results

With the goal of identifying the MeJA- and LAP-A-dependent metabolomes of tomato leaves, targeted and untargeted LC-MS metabolomics analyses were performed on leaves from wild-type, LapA-SI, and LapA-OX tomatoes at 0, 8, 12, and 24 h after MeJA treatments. A central carbon panel of metabolites was used to identify the targeted metabolites. In silico databases were used to identify the untargeted metabolites after careful consideration of mass spectral peak matches to annotated compounds. A total of 209 annotated metabolites were identified, with targeted metabolomics of polar, primary metabolites identifying 78 metabolites (Table 2.1) and

untargeted metabolomics identifying 131 annotated metabolites and 3,828 unknown metabolites (Table 2.2). Metabolites that accumulated in a MeJA- or LAP-A-dependent manner were identified using two-tailed Welch's t tests on $\log_2$-transformed individual metabolites and had adjusted P-values < 0.05. Of the 209 metabolites with annotated functions, 135 were MeJA regulated, 60 were LAP-A regulated, and 57 were regulated by both (Tables 2.1- 2.2).

There were 15 functional categories covered in the targeted metabolomics analyses and 29 functional categories covered in the untargeted metabolomics analyses (Fig 2.1). Primary metabolites were mostly identified in targeted metabolomics; secondary metabolites and lipids were mostly identified in untargeted metabolomics. Primary metabolites are directly required for plant growth and secondary metabolites mediate plant-environment interactions, but recent research shows that primary metabolites respond to environmental stresses and secondary metabolites are also regulators of plant growth (Erb and Kliebenstein 2020; Trovato et al. 2021). In addition, some secondary metabolites are derived primarily from amino acids, such as the true alkaloids that are derived from Phe, Tyr, and Trp (Parthasarathy et al. 2021). Polar and semipolar amino acid (aa) functional category (37 metabolites (47%)) dominated the targeted metabolites (Fig 2.1A). Eight amino acids were also identified in the untargeted metabolomics (Fig 2.1B).

Amino acid metabolism is regulated by LAP-A and MeJA

Of the 37 metabolites in the amino acid (aa) functional category, a total of 18 metabolites classified as proteinogenic aa, derived from aa, or nonproteinogenic aa were regulated by both MeJA and LAP-A (Table 2.3A-B; Fig 2.1A). The proteinogenic aa pathways that were detected included the hydrophobic (Met, Phe, Trp), branched chain

(Ile, Val, Leu), basic (Lys, Arg), and uncharged (Thr, Asn) amino acids (Table 2.3, Fig 2.2). In addition, there were eight nonpolar proteinogenic amino acids (aa) identified in the untargeted metabolomics data analyses (Table 2.4A-B). Three aromatic aa (Phe, Trp, and Tyr) and Leu were LAP-A and MeJA regulated (Table 2.4A-B, Fig 2.2). Phe, Trp and Leu were identified in both the targeted and untargeted metabolite analyses and showed the good experimental reproducibility. There were two isomers of Phe detected in the untargeted analysis; one of the isomers had the same trend as seen with Phe in the targeted metabolomics analyses (Table 2.2).

A total of three nonproteinogenic aa (α-aminobutyric acid (AABA/2ABA), γ-aminobutyric acid (GABA) and kynurenine) were identified (Fig 2.3A-C). AABA was the only nonproteinogenic aa regulated by LAP-A and upregulated by MeJA (Table 2.3; Fig 2.3A). GABA was downregulated and kynurenine was upregulated by MeJA treatments in all three genotypes, respectively (Table 2.3; Fig 2.3B-C). Literature has shown GABA accumulates in response to biotic (insects and pathogens), abiotic stresses (salinity, heat shock, and wounding), and interacts with defense-related hormones such as JA, SA, and ethylene (Tarkowski et al. 2020). There were 17 metabolites classified as aa-derived; these were intermediates in aa biosynthesis pathways, aa degradation pathways or modified aa (Table 2.3). Seven of the compounds derived from aa were regulated by MeJA and LAP-A (Table 2.3). For example, pipecolic acid and 5-aminovaleric acid are derived from Lys and involved in plant defense (Adam et al. 2018); these metabolites will be discussed further in the section, "Lys biosynthesis and its catabolites are LAP-A and MeJA regulated."

161

The Asp, Lys, Thr and Met amino acid pathway

Asp is catabolized to provide the precursors for the synthesis of Ile, Thr, and Met (Fig 2.4). MeJA treatments of wild-type, LapA-SI and LapA-OX plants suppressed Asp accumulation at all timepoints in a LAP-independent manner (Fig 2.5; Table 2.3). In contrast, Lys and Met increased in response to MeJA in all three genotypes and Thr was upregulated by MeJA in wild-type and LapA-OX plants but were not MeJA regulated in LapA-SI plants (Fig. 2.2). At 0 h, Lys and Thr levels were significantly higher in LapA-SI than wild-type plants. In contrast, at 24 h Met levels were lower in LapA-SI plants than wild-type and a similar trend is seen in LapA-OX.

Given the decline in Asp and increases in Lys, Thr and Met, we correlated transcript levels for several genes that encode enzymes for Asp catabolism and Lys, Thr and Met biosynthesis. RNA levels measured using qRT-PCR in wild-type, LapA-SI and LapA-OX plants after MeJA treatments. Using Asp as the initial substrate, aspartokinase 2 and aspartate-semialdehyde dehydrogenase (ASDH) act sequentially to synthesize L-aspartate-4-seminaldehyde, which is the substrate at the branch point of Lys versus Thr and Met synthesis (Fig 2.4, Fig 2.6). While neither of these Asp-derived metabolites were detected, MeJA induced the levels of aspartokinase2 transcripts in all three genotypes from 8 to 24 h in a LapA-independent manner (Fig 2.6A). In contrast, the MeJA regulation of ASDH RNAs was more complex; MeJA did not significantly impact ASDH RNAs in LapA-SI or LapA-OX plants, but a significant increase in ASDH RNAs were detected in wild-type plants at 12 h after MeJA treatment (Fig 2.6B). The bifunctional aspartokinase/homoserine dehydrogenase 1 (AK-HSDH1) produces L-homoserine, which is the first committed step for synthesis of Thr and Met (Fig 2.6).

162

MeJA strongly suppressed AK-HSDH1 RNA levels by 8 h in all three genotypes. In addition, LAP-A negatively regulated the levels of AK-HSDH1 RNAs, as this RNA was more abundant in at 0 h in LapA-SI versus wild-type plants (Fig 2.6C). Homoserine kinase (HSK) phosphorylates homoserine (Fig 2.6D). HSK transcripts were more abundant in LapA-SI and LapA-OX plants after MeJA treatment, and a similar trend was seen in wild-type (Fig 2.6D; Fig 2.7). LAP-A influenced HSK RNA levels as evidenced by LapA-OX plants having 1.54-fold more HSK RNAs than wild-type plants at 8 h after MeJA treatments (Fig 2.6D).

O-phospho-L-homoserine is the branch point for Thr and Met biosynthesis (Fig. 2.7). For Met biosynthesis, O-phospho-L-homoserine is used to produce L-cystathione, a Met precursor (Fig 2.2A, Fig 2.7). L-cystathione was strongly downregulated by MeJA in all three genotypes (Fig 2.5, Fig 2.7), while Met levels gradually increased. While LAP-A positively regulated Met levels after MeJA treatment, it did not influence L-cystathione levels.

Thr is 1.76-fold more abundant in LapA-SI at 0 h compared to wild-type and trends for higher levels at 8 and 24 h were also seen suggesting that LAP-A is a negative regulator of Thr in healthy plants (Fig 2.2, 2.4, 2.7). By 8 h, MeJA increased levels of Thr in wild-type and LapA-OX plants, while this MeJA regulation was not clearly seen in LapA-SI plants. The synthesis of the branched chain amino acid Ile initiates with Thr (Fig 2.2, Fig 2.7). In all genotypes, Ile levels rose across the 24-h MeJA time course, reaching peak levels at 24 h. At 24 h, Ile was 1.43-fold more abundant in wild-type compared to LapA-SI plants suggesting LAP-A is a positive regulator of Ile biosynthesis (Fig 2.2, Fig 2.7).

Threonine synthase (TS) uses O-phospho-L-homoserine to produce Thr. While TS RNA levels did not change significantly in wild-type and LapA-OX plants after MeJA (Fig 2.7, Fig 2.8A), TS RNAs declined in LapA-SI at 8 and 12 h after MeJA treatment and rose by 24 h (Fig 2.8A). At 12 h, the LapA-SI and wild-type TS levels were significantly different with TSbeing 1.9-fold more abundant in wild-type plants; similar trends were also noted at 8 and 12 h in LapA-OX plants. These data indicate that LAP-A regulated TS transcript abundance at 12 h post MeJA treatment (Fig 2.8A).

Two enzymes (Threonine deaminase 1/Thr dehydratase1 and Threonine deaminase 2/Thr dehydratase 2) are responsible for first step in threonine catabolism (Fig 2.7, Fig 2.8B-C). While both TD1 and TD2 RNAs are induced after MeJA treatment in all three genotypes, their transcript abundances at 24 h have a 1098-fold difference, with TD2 being the most abundant (Fig 2.8B-C); the MeJA induction of TD1 and TD2 was previously documented (Chen et al. 2007; Gonzales-Vigil et al. 2011). Neither TD1 nor TD2 RNA levels were LAP-A dependent.

Cystathione is further catabolized (in several steps) to produce Met and pyruvate (Fig 2.4). The methyltransferase encoded by Solyc01g009180.3 catalyzes the final step for Met biosynthesis converting L-homocysteine (which is derived from L-cystathionine) to Met (Fig 2.7, Fig 2.8D). While Met levels increased in response to MeJA, the methyltransferase RNA levels were unchanged after MeJA treatment in LapA-SI, wild-type and LapA-OX plants; although a trend for RNA increases was observed (Fig. 2.8D). Surprisingly, based on the proteome profile of LapA-SI, wild-type, and LapA-OX plants treated with MeJA at 0 and 24 h, LAP-A suppressed this methyltransferase (Bhattacharya, Ortiz and Walling, unpublished results). These data suggest the complex and multilevel regulation of Met in tomato.

The last step for pyruvate biosynthesis from L-cystathionine is mediated by both the inducible (CHRDi) and constitutive (CHRD) plastid-lipid associated proteins. The CHRDi and CHRD transcripts were influenced by MeJA treatments in all genotypes (Fig. 2.7; Fig 2.8E-F). CHRD RNAs were less abundant than CHRDi transcripts and they were suppressed by MeJA in all three genotypes. In contrast, CHRDi RNAs increased over 50-fold in all three genotypes after MeJA treatments; reaching peak levels at 24 h. At this time the CHRDi transcripts were 277-fold more abundant than CHRD RNAs. Pyruvate is a substrate for numerous biochemical reactions, including the synthesis of the branched chain amino acids Leu and Val (see below).

Lys catabolites and Lys-derived compounds are LAP-A and MeJA regulated.

Like Thr and Met, Lys is produced from L-aspartate-4-semialdehyde in four biochemical steps (Fig. 2.4). As noted above, Lys levels were induced by MeJA (Fig 2.2G; Fig 2.9A) and LAP-A appears to be a negative regulator of Lys accumulation, since Lys was 1.6-fold higher in LapA-SI plants than wild-type in untreated leaves (0 h) (Fig. 2.2G, Fig 2.9B). In addition, four Lys-derived compounds (pipecolic acid, 5-aminovaleric acid, N-acetyllysine, and trimethyllysine) were detected (Table 2.3). MeJA upregulates N-acetyllysine and trimethyllysine. 1.8- and 2.7-fold, respectively, 24 h after MeJA treatments (Fig. 2.10). Both trimethyllysine and N-acetyllysine were upregulated by LAP-A in healthy plants. In addition, N-acetyllysine was also LAP-A upregulated at 8 and 12 h MeJA treatment (Fig 2.10). Trimethyllysine and N-acetyllysine are important post-translational modifications of Lys. Therefore, it is possible that their detection is due to protein turnover. However, in addition to its importance in epigenetic regulation of gene expression, trimethyllysine is important for the biosynthesis of carnitine (Maas et al. 2020). The role of carnitine in plant biology is understudied but its role as an osmolyte

165

and in fatty-acid trafficking seems likely (Jacques et al. 2018). N-acetyllysine is also a post-translational protein modification first detected in histones, but it now understood to be present in array of proteins and particularly enriched in chloroplast proteins (Fang et al. 2015). While N^{ε}-acetyl-β-lysine and N^{α}-acetyl-β-lysine are osmolytes in some microbes (Sowers et al. 1990; Jiang et al. 2015); this role has yet to be demonstrated in plants.

The other two lysine-derived metabolites (5-aminovaleric acid/ 5-aminopentanoate and pipecolic acid/ pipecolate) are linked to plant defense (Adam et al. 2018) and their biosynthetic pathway is provided in Figure 2.9A. The production of N-hydroxy-pipecolic acid from Lys is important for Arabidopsis thaliana immunity and systemic acquired resistance (Chen et al. 2018; Hartmann and Zeier 2018). Four metabolites associated with this pathway were detected (Lys, Ala (a by-product), 5-aminovaleric acid, and pipecolic acid) and three were significantly regulated by LAP-A and MeJA. While Ala levels were not influenced by LAP-A or MeJA (Table 2.2), Lys, pipecolic acid and 5-aminovaleric acid levels were all upregulated in response to MeJA treatments in wild-type, LapA-SI and LapA-OX plants (Fig.2.4, Fig 2.9B). Pipecolic acid levels were significantly higher in LapA-SI lines relative to wild-type plants prior to MeJA treatments (Fig 2.9B; Table 2.3A). Also, 5-aminovaleric acid had a 1.3-fold higher relative abundance in LapA-SI relative to wild-type plants treated with MeJA at 12 h (Fig 2.9A; Table 2.3A). However, the downstream and biologically active N-hydroxy-pipecolic acid has reported in tomato.

5-aminovaleric acid is produced by two pathways. 5-aminovaleric acid is produced from 5-aminopentanal (not shown) and from 6-amino-2-oxohexanoate/ketocaproic acid (KAC) (Fig 2.9A) (Shimizu et al. 2019). KAC reacts spontaneously with H_2O_2 to form 5-

aminovaleric acid. The generation of 5-aminovaleric acid from KAC has the potential to modulate the levels of this defense-metabolite precursor, to potentially control its flux into the pipecolic acid pathway. As neither of the 5-aminovaleric acid precursors were detected, we cannot infer the substrate used to produce 5-aminovaleric acid in LapA-SI and after MeJA treatments. Finally, 5-aminovaleric acid and 2-oxoglutarate are used for glutamate biosynthesis; Glu was upregulated in all the genotypes or after MeJA treatments (Table 2.3B; Fig 2.S1).

While the production of 5-aminovaleric acid is spontaneous, the production of KAC, pipecolic acid and N-hydroxy-pipecolic acid biosynthesis is controlled by the enzymes AGD2-like defense response protein1 (ALD1), SAR-deficient4 (SARD4), and Flavin-containing monooxygenases (FMO1), respectively (Fig 2.9A). The levels of these transcripts in wild-type, LapA-SI and LapA-OX plants after MeJA treatments were assessed. While the ALD1 transcripts were not regulated, there was a strong trend for their increase 24 h after MeJA treatment (Fig 2.9C).

Pipecolic acid levels were induced in all three genotypes after MeJA treatment and pipecolic acid levels were elevated at 0 h in LapA-SI relative to wild-type plants (Fig. 2.9B). SARD4 generates pipecolic acid from 2,3-de-hydropipecolic acid (2,3-DP) (Fig 2.9) SARD4 RNAs increased significantly at 24 h post treatment in wild-type plants. SARD4 RNAs were elevated in wild-type plants at 24 h, relative to LapA-OX and LapA-SI plants. Furthermore, SARD4 protein levels were elevated in wild-type relative to LapA-SI plants after a 16-h MeJA treatment (Bhattacharya, Ortiz and Walling, unpublished results). These data strongly suggest that LAP-A regulates both SARD4 transcript and protein levels after MeJA treatment (Fig 2.9C). In contrast, in untreated LapA-SI and wild-type plants, pipecolic acid is at higher levels in LapA-SI than wild-type

plants (Fig. 2.9B), suggesting a complex mechanism of regulation. Finally, FMO1 uses

pipecolic acid to form the SAR-inducing N-hydroxy-pipecolic acid (Fig 2.9A). After MeJA

treatments, FMO1 transcripts declined significantly (Fig 2.9C). While neither FMO1 nor

N-hydroxypipecolic acid were detected in our proteomics or metabolite studies,

respectively, these data suggest that production of N-hydroxypipecolic acid is regulated

in MeJA treated plants to antagonize the SAR signal and will be discussed further in the

Discussion section.

LAP-A regulation of osmolytes

In addition to their responses to defense signals, LapA mRNAs and proteins

accumulate in response to water deficit stress and salinity (Chao et al. 1999). In

response to these environmental stresses, plants accumulate osmolytes (proline,

sugars, and polyamines) to adapt to the osmotic stress (Sharma et al. 2019). In this

study, we detected five osmolytes that were MeJA regulated: N-acetylputrescine,

proline, and three hexoses (Tables 2.1 and 2.2). The polyamine N-acetylputrescine is

the only polyamine detected in our analyses (Table 2.1, Fig 2.1A, Fig 2.S2); polyamines

are known for their roles in development, as well as abiotic and biotic stress responses

(Chen et al. 2019; Liu et al. 2019). N-acetylputrescine accumulates after MeJA

treatments in all three genotypes (Fig 2.11A). N-acetylputrescine is synthesized from

putrescine via N-acetyltransferase AtNATA1(Lou et al. 2016) (Fig 2.S2); the tomato

NATA1 (Solyc10g084640) RNAs are induced by MeJA within 0.5 h (Roche and Walling,

unpublished results). N-acetylputrescine is thought to sequester putrescine (lou et al

2016). More recently, Lou et al. (2020) showed N-acetylputrescine can also be

synthesized from N-acetylornithine using arginine decarboxylase in Arabidopsis;

however, it is unclear if this pathway is active in other plants. Production of N-

acetylputrescine lowers levels of putrescine and its derivatives (spermidine and spermine) and causes a decline in H_2O_2 (Lou et al 2016) (Chen et al. 2019; Liu et al. 2019). This blocks pathogen-associated molecular pattern (PAMP)-triggered immunity's SA-regulated defenses that work in synergy with H_2O_2. To date the role of N-acetylputrescine as an osmolyte has not be investigated in plants to date.

In contrast to N-acetylputrescine, MeJA suppresses Pro accumulation in a LAP-independent manner in wild-type and LapA-SI plants and a similar trend is seen in LapA-OX plants (Fig 2.11B). This contrasts with Bali et al. (2018) who showed MeJA treatment of mature tomato plants increased Pro. Finally, sugars are also important osmolytes; sugar levels declined in tobacco after herbivory due to hormonal crosstalk between JA and ethylene (Machado et al. 2017). Three sugar metabolite levels also declined in this study after MeJA treatment in wild-type and both mutant lines (Fig 2.11C- E).

Trends indicate LAP-A may downregulate purines and pyrimidines

Together the purines (12.8%) and pyrimidines (5.1%) represented the second largest group of targeted metabolites detected in our study (Fig 2.1A). Purines and pyrimidines are the building blocks for DNA and RNA and they influence all areas of normal cellular metabolism. As such, the purine and pyrimidine metabolic pathways are tightly controlled in plants via de novo synthesis, salvage, degradation, modification, and reutilization (Fig 2.12) (Kafer et al. 2004; Bellin et al. 2021).

Of the fourteen purines and pyrimidines detected in the targeted metabolomics and two purines detected in the untargeted metabolomics, three were MeJA regulated with p values < 0.05 (Table 2.5; Figure 2.12). In addition, several of these metabolites had trends that suggested MeJA and/or LAP-A may be a regulator; however, due to sample variation these values did not meet the statistical criteria required for strongly

establishing this regulation. The purines (guanine, adenine, hypoxanthine, and xanthine) and their metabolites or precursors (xanthosine, guanosine, adenosine, cGMP, dAMP) were detected (Fig 2.S2). While trends for MeJA up-regulation (hypoxanthine, guanine, adenosine, adenine) or down-regulation (guanosine, AMP, xanthine) were detected, only xanthosine showed statistically significant regulation by MeJA. After MeJA treatments, xanthosine, a precursor of xanthine, reached a peak at 8 h and subsequently declined at 12 and 24 h. (Fig. 2.12G). In addition, the higher levels of LAP-A in LapA-OX plants suppressed xanthosine levels relative to wild-type plants, and a similar trend was seen in LapA-SI plants. Interrogation of our MeJA-responsive proteome showed that LAP-A suppressed the levels inosine 5'-monophosphate dehydrogenase, which generates xanthosine (Bhattacharya, Ortiz and Walling, unpublished results).

Only a few metabolites associated with pyrimidine metabolism were detected (cytidine, uridine, 3-ureido-proprionic acid, and β-alanine) (Fig. 2.S3). Cytidine and uridine were not significantly regulated by MeJA or LAP-A; however, at 8 h after MeJA treatment LapA-SI lines displayed a strong trend for higher levels of both metabolites than wild-type and LapA-OX plants. In addition, while there was variation, there was a trend for the levels of uridine to increase over time in all three genotypes after MeJA treatment.

3-ureido-proprionic acid and β-Ala are both uracil catabolic products. 3-ureido-proprionic acid was induced in all three genotypes by 8 h after MeJA treatment and was LAP-A independent. Consistent with these results, our proteomics data has shown that MeJA induces dihydropyrimidinase protein levels, which catalyzes the production of 3-ureido-proprionate from dihydrouracil. Finally, while cytidine levels were not modulated by MeJA or LAP-A based on our statistical analyses, there was a strong trend for MeJA

increasing cytidine levels after 8 h of MeJA treatments. The enzyme that converts CMP to cytidine (5'-nucleotidase/ CMP phosphatase) was also detected in our proteomics study and there is no evidence that the enzyme was regulated by either LAP-A or MeJA.

Untargeted metabolite profiles: Fatty acids and lipids are MeJA and LAP-A regulated

The chemically diverse secondary metabolites were identified in our untargeted metabolomics analyses (Table 2.2). This included 131 lipids and secondary metabolites with annotated metabolic functions and 3,828 unclassified compounds (Table 2.2). The top four annotated lipid and fatty acid molecules identified were phosphatidylcholine (PC) (14.8%), sterols (9.4%), phosphatidyl ethanolamines (PE) (9.4%), and monogalactosyldiacylglycerol (MGDG) (7%) (Fig 2.1B). Sixty-seven lipids and fatty acids were regulated by LAP-A and/or MeJA (Table 2.2; Table 2.9). It makes sense MeJA regulates many fatty acids because JA is fatty acid derived. It is noteworthy that the bulk of fatty acid metabolism and LAP-A are co-localized in the chloroplast (Cook et al. 2021; Gu et al. 1996; Narvaez-Vasquez et al. 2008). Analysis of metabolites in tomato fruits treated with MeJA has shown that lipids are the most differentially regulated class of molecules in fruit relative to the primary and secondary metabolites detected and identified (Rivero Meza et al. 2021). Due to our focus on other metabolites for this chapter, the lipids and fatty acids that are MeJA- and/or LAP-A-regulated will be intensively pursued and included in the manuscript that will be submitted for publication.

A few obvious and noteworthy molecules deserve a call-out. We detected jasmonic acid and the JA precursor linoleic acid (Table 2.2). Not surprisingly, JA increased with MeJA treatments in all three genotypes, whereas linoleic acid remained unchanged throughout the MeJA treatment.

171

LAP-A regulation of pseudoalkoids

Unlike alkaloids from other species, which are derived from amino acid precursors, Solanaceous alkaloids are often termed pseudoalkaloids since they are derived from cholesterol (Parthasarathy et al. 2021). A total of 7 alkaloids (~5%) were detected in the untargeted annotated metabolites (Fig 2.1B). Three steroidal glycoalkaloids (SGAs) with known roles in plant immunity were detected including: tomatidine derivatives, dehydrotomatine, and tomatine (Table 2.7; Fig 2.13).

The recently elucidated pathway for SGA biosynthesis is illustrated in Figure 2.13 (Akiyama et al. 2019; Sonawane et al. 2018; You and van Kan 2021). The biosynthesis of tomatine and dehydrotomatine involves several reactions including oxidation, isomerization, and reduction to convert cholesterol to secondary metabolites dehydrotomatidine (tomatidenol), tomatidine, α-tomatine, and dehydrotomatine (Fig 2.13A) (Akiyama et al. 2019; Sonawane et al. 2018). While cholesterol was not detected, a cholesterol-like metabolite was detected and its abundance was similar in wild-type, LapA-SI and LapA-OX plants and these levels did not change significantly after MeJA treatment (Fig 2.13). The precursor of tomatidine, α-tomatine, and tomatidenol was not detected. However, a fragment of dehydrotomatine was detected. While this metabolite was not significantly modulated by MeJA, the dehydrotomatine fragments were more abundant in LapA-SI plants relative to wild-type plants at 0 h and 24 h (Table 2.7; Fig 2.13B); there is also a trend for elevated levels of this fragment at 12 h. These data suggest that LAP-A suppresses synthesis of dehydrotomatine at these times.

Four polar isomers of tomatidine were detected (Table 2.7). MeJA regulated tomatidine isomer 1 with significant increases by 12 h and a decline by 24 h in all three genotypes (Table 2.7; Fig 2.13). In addition, the levels of this metabolite were 2.38-fold

higher wild-type compared to LapA-SI at 0 h, indicating that LAP-A likely regulates tomatidine levels in healthy plants (Table 2.7A; Fig 2.13B). Finally, the levels of α-tomatine were inferred from a tomatine fragment. The tomatine fragment levels were not LAP-A nor MeJA regulated; however, a trend for increases in this metabolite at 12 h was seen in wild-type, LapA-SI and LapA-OX plants (Table 2.7).

As the enzymes involved in SGA biosynthesis in tomato have been recently elucidated (You and van Kan 2021) and LAP-A was implicated in regulating levels of dehydrotomatine and tomatidine isomer 1, we assessed the levels of GAME (GLYCOCALKAOID METABOLISM ENZYME) transcript levels in LapA-SI, wild-type and LapA-OX lines after MeJA treatments. GAME11/6/4/12 catalyze the conversion of cholesterol to tomatidenol (Fig 2.14A- D). In all three genotypes, MeJA suppresses the levels of these GAME11/6/4/12 transcripts. Several comparisons support the premise that LAP-A regulates GAME6, 4 and 12; for example, GAME4 and GAME12 RNAs are more abundant in wild-type versus LapA-SI plants at 0 h and GAME12 RNAs were more abundant in LapA-OX than wild-type 12 h after MeJA treatment. In contrast, GAME11 appears to be LAP-A independent. LapA upregulates GAME25 acting on the biosynthetic step from tomatidenol to tomatidine (Fig 2.14E). MeJA suppresses GAME1/17/18 transcript levels responsible in the biosynthesis step of tomatidenol to dehydrotomatine and biosynthesis step of tomatidine to α-tomatine (Fig 2.14G- I).

Conversion of tomatidenol to tomatidine is controlled by GAME25 and S5αR2. While S5αR2 RNAs increased in response to MeJA, no evidence for LAP-A regulation was noted (Fig 2.14E-F). In contrast, GAME25 RNAs were both MeJA and LAP-A regulated, and temporal responses were different in the wild-type, LapA-SI and LapA-OX lines. GAME25 RNAs were strongly down-regulated after MeJA treatments in the LapA-

SI line (8 h) and at a later time point in LapA-OX line (12 h), whereas in wild-type plants GAME25 RNAs did not change until 24 h after MeJA treatments and these RNAs increased. LAP-A regulation of was clearly demonstrated in comparisons of LapA-SI vs wild-type and LapA-OX vs wild-type plants. Finally, GAME1/17/18 convert tomatidenol to dehydrotomine, as well as tomatidine to α-tomatine. All three RNAs were negatively regulated by MeJA (Fig 2.14G-I). In both LapA-SI and LapA-OX plants, GAME17 RNAs were less abundant than in wild-type plants.

Flavonoids: a complex story in LAP-A and MeJA regulation

Flavonoids and flavonoid glycosides were a substantial part of the untargeted metabolites that were discovered. These amino acid-derived defense metabolites are ubiquitous and are well characterized in many species (Parthasarathy et al. 2021) (Fig 2.1B). Some flavonoids have established roles in plant immunity (Fig 2.15) (Slimestad et al. 2008). There are 4 flavonoids and 9 flavonoid glycosides identified in this untargeted metabolomics dataset (Fig 2.16A-E; Table 2.8). Three classes of flavonoids were detected: (1) kaempferol isomers and kaempferol glucosides, (2) quercetin, quercetin glucosides and rutin (Ilixathin, a quercetin metabolite), and (3) luteolin glycosides (Table 2.8A-B). Three kaempferol isomers had different responses to MeJA (Fig 2.16A-C). Isomer 2 was not significantly regulated by MeJA or LAP-A. In contrast, isomer 3 was down regulated by MeJA in LapA-OX plants, and similar trends were seen in wild-type and LapA-SI lines. The kaempferol isomer 1 was MeJA responsive in wild-type and LapA-SI lines with RNAs reaching peak levels at 24 h. Futhermore, LAP-A regulation was observed for isomer 1. At 12 h, isomer 1 was 1.43-fold higher in wild-type than LapA-SI. In addition, isomer 1 was significantly higher in LapA-OX than wild-type plants

at 0 h and a trend suggests isomer 1 was more abundant in wild-type than LapA-SI plants at 0 h.

In addition, two flavonoid glycosides were regulated by MeJA (Fig 2.16D-E). Kaempferal-3-O-glc-1-3-rham-1-6-glucoside was downregulated by MeJA. In contrast, a flavonoid glycoside (with no common name) was upregulated by both MeJA and LAP-A. The powerful antioxidant quercetin, four quercetin glycosides, and quercetin-derived rutin, with antinutritive impacts on herbivores, were detected (Table 2.8A-B). (Demkura et al. 2009; Li et al. 2021; Muhlemann et al. 2018; Slimestad et al. 2008; Tohge et al. 2020). Levels of these six quercetin metabolites were similar in wild-type, LapA-SI and LapA-OX and they did not change in response to MeJA. Similarly, the luteolin glycoside was neither LAP-A nor MeJA regulated (Table 2.8).

To assess whether the changes in kaempferol levels were correlated with its synthesis from (+)-dihydro kaempferol by flavonol synthases, the levels of flavanol synthase RNAs were quantified by qRT-PCR (Fig 2.15, Fig 2.17) (Martens and Mithöfer 2005). One flavonol synthase (Solyc01g090140) was up-regulated by MeJA reaching peak levels in all three genotypes at 12 h. In contrast, the second flavonol synthease (Solyc11g013111) encoded a more abundant RNA, which was strongly down-regulated at 8, 12 and 24 h after MeJA treatment in all gentoypes (Fig 2.17).

Three Kaempferol 4'-O-methyltransferase/kaempferide 7-O-methyltransferase genes are involved in methylation of kaempferide/kaempferol using S-adenosylmethionine (SAM) as a cofactor (Figs. 2.15, 2.17). While the RNAs encoded by Solyc06g064500 and Solyc01g068545 were down-regulated by MeJA in wild-type, LapA-SI and LapA-OX plants Solyc10g047520 RNAs were not significantly altered after MeJA treatments in all three genotypes (Fig 2.15).

S-adenosylhomocysteine (SAH) and S-adenosylmethione (SAM) are important cofactors for flavonoid metabolism, as well as a wide variety of other metabolic functions, which will be covered further in Chapter 3. Metabolites S-adenosylmethionine (SAM) and S-adenosylhomocysteine (SAH) are substrates and byproducts, respectively, for both kaemferol methyltransferases (Fig 2.16). Both SAM and SAH levels declined after MeJA treatment in all three genotypes (Fig 2.16E-F).

Discussion

Given LAP-A's ability to up and down-regulate different sets of nuclear-encoded genes (Scranton et al. 2013; Fowler et al. 2009), LAP-A must produce or modulate levels of one or more retrograde signals to control nuclear gene expression. To date, we do not know if the LAP-A signal is a protein, peptide or metabolite. The Walling lab is taking a multi-omics approach to discover the magnitude of change in macromolecules that is caused by LAP-A deficiencies or excess, with the goal of identifying the pathways influenced by LAP-A, which may lead to the identity of the LAP-A dependent signals. The Walling lab is analyzing the LapA-dependent transcriptome (Roche and Walling, unpublished results), proteome (Bhattacharya, Ortiz and Walling, unpublished results; Chapter 1) and metabolome (Chapters 2 and 3). As LAP-A acts down stream of JA perception, metabolites that are either LAP-A or LAP-A and MeJA regulated are candidates for this putative regulator or they reflect a LAP-A dependent response.

Targeted and untargeted metabolomics analyses of compounds in LapA-SI, wild-type, and LapA-OX leaves treated for different times with MeJA identified of 78 primary metabolites and 131 secondary metabolites and lipids/ fatty acids (Fig 2.1). Primary metabolites are involved in tomato's response to environmental factors aside from their essential role in plant growth and development (Steinbrenner et al. 2011; Zeiss et al.

176

2018). Secondary metabolites often have roles in defense, abiotic stress tolerance, flavor and fragrance (Pott et al. 2019; War et al. 2020). Examination of these data sets allowed us to discover metabolites that were regulated by MeJA and the plastid-localized LAP-A in tomato.

Of the 209 metabolites with annotated functions detected in this study, 65% were MeJA and/or LAP-A regulated. Of these metabolites, 78 were MeJA regulated and 57 were regulated by both LAP-A and MeJA. The fact that 95% of the metabolites that were influenced by LAP-A levels were also MeJA responsive is not surprising given the fact that LAP-A regulates JA-responsive genes by acting downstream of the biosynthesis and perception of JA (Fowler et al. 2009).

LAP-A is a negative regulator of amino acid levels in the absence of MeJA

Of the MeJA- and MeJA/LAP-A-regulated metabolites, the largest primary metabolite group (37 compounds) identified was associated with amino acid biosynthesis and catabolism or compounds derived from amino acids (Fig 2.1A). Most amino acid biosynthesis pathways are localized in plastids. Given LAP-A's colocalization with aa biosynthetic/catabolic proteins in the plastid stroma, it is not surprising that LAP-A has an impact on these pathways. One frequent pattern of LAP-A regulation was seen in eightamino acids (Phe, Val, Trp, Leu, Lys, Arg, Thr, and Asn). For these amino acids, LAP-A exerted its effect at 0 h prior to MeJA treatments (Fig 2.2). In addition, evidence of LAP-A regulation was observed for Met and Ile after 24 h MeJA treatment (Fig 2.2, Fig 2.7); here, LAP-A upregulated at 24 h MeJA treatment. For these reasons, we further examined into the metabolic pathways of Ile, Thr, and Met biosynthesis by assessing if selected enzymes associated with this pathway were MeJA regulated at the level of protein accumulation (0 and 16 h post MeJA treatment) from our proteomics study

(Bhattacharya, Ortiz and Walling, unpublished results) or at the RNA level by qPCR (0-24 h after MeJA treatment) (Fig 2.5-2.8). LAP-A was shown to upregulate HSK and TS in the biosynthesis of Lys, Thr, and Met (Fig 2.6- 2.8). The LAP-A downregulation of the amino acids is at 0 h and the transcripts that encode enzymes for the biosynthesis of metabolites were upregulated by LAP-A (TS and HSK) after MeJA treatments except for AK-HSDH1.

The transcript abundance for HSK, TD1, TD2, and CRDi increased after MeJA correlating with Thr, Met and Ile metabolite abundance after MeJA treatment as well (Fig 2.5- 2.8). The LAP-A suppression of AK-HSDH1 at 0 h correlated with LAP-A suppression of Thr and Leu at 0 h (Fig 2.4- 2.7). However, MeJA downregulated AK-HSDH1 and MeJA upregulated Thr and Leu. In addition, the LAP-A upregulation of TS at 12 h after MeJA treatment does not correlate with LAP-A suppression of Thr metabolite at 0 h.

MeJA and LAP-A regulate pipecolic acid and, potentially, the mobile SAR signal

Two Lys-derived metabolites, pipecolic acid and 5-aminovaleric acid, are plant defense regulators (Bernsdorff et al. 2016; Chen et al. 2018; Hartmann and Zeier 2018; Hartmann et al. 2018) (Fig 2.9). Pipecolic acid and N-hydroxypipecolic acid and their biosynthetic gene RNAs (ALD1, SARD4, and FMO1) are induced by SA via a MPK3/MPK6- and WRKY33-regulated pathway (Wang et al. 2018); the responses of pipecolic acid and N-hydroxypipecolic acid in response to wounding and MeJA is, to date, uninvestigated territory. Based on JA-SA cross talk (Wang et al. 2021), it might be assumed that these metabolites would be down regulated by MeJA and LAP-A.

While SA regulation of pipecolic acid is established in Arabidopsis (Chen et al. 2018; Hartmann et al. 2018; Orlovskis and Reymond 2020), we show for the first time that both

MeJA and LAP-A regulate 5-aminovaleric acid and pipecolic acid in tomato; N-hydroxypipecolic acid was not detected. Pipecolic acid and 5-aminovaleric acid are derived from the same precursor (KAC; Fig. 2.9) and therefore it was possible that increased production of 5-aminovaleric acid might divert the intermediate and negatively impact pipecolic acid production. 5-aminovaleric acid is produced spontaneously with H_2O_2 and KAC. H_2O_2 levels are known to rise after wounding of tomato foliage (Orozco-Cárdenas et al. 2001). In addition, in Chapter 3, we show that LAP-A is a negative regulator of H_2O_2 as H_2O_2 levels are significantly higher in LapA-SI plants over wild-type plants after wounding. Here we showed that increases in H_2O_2 were well correlated with increases in 5-aminovaleric acid. In all cases, 5-aminovaleric acid was higher in LapA-SI lines at 0, 12 and 24 h after MeJA treatment (Fig 2.9B). What was surprising is that 5-aminovaleric acid was also elevated in LapA-OX plants at 8, 12 and 24 h relative to wild-type plants; the reason for this is currently not known, but it suggests a more complex regulatory program where LAP-A is an activator in the absence of MeJA but is a repressor in the presence of MeJA.

Furthermore, pipecolic acid is also induced by wounding in all three genotypes and LAP-A negatively regulates levels of this metabolite prior to mechanical damage. These data indicate that after wounding, 5-aminovaleric acid and pipecolic acid are not reciprocally regulated and, therefore, 5-aminovaleric acid does not impact the flux of KAC into pipecolic acid. Pipecolic acid influences defense because its product N-hydroxypipecolic acid has a role in systemic acquired resistance and may be the mobile SAR signal (Hartmann and Zeier 2019; Huang et al. 2020). N-hydroxypipecolic acid is induced after pathogen infection of both monocots and dicots, including tomato, (Schnake et al. 2020). The regulation of pipecolic acid and, presumably, N-

hydroxypipecolic acid, by wounding was unanticipated. We followed the responses of three genes (ALD1, SARD4 and FMO1) that are important N-hydroxy-pipecolic acid production (Joglekar et al. 2018; Chen et al. 2018; Hartmann and Zeier 2018; Hartmann et al. 2018). Both ALD1 and SARD4 transcripts are relatively unchanged from 0 to 12 h and trends indicate that ALD1 and SARD4 transcripts are at higher levels at 24 hrs in all three genotypes or solely in wild-type plants, respectively. The tomato SARD4 RNAs were at significantly lower levels in LapA-SI and LapA-OX lines at 24 h; indicating that, similar to 5-aminovaleric acid, LAP-A may be both a repressor in the absence of MeJA and an activator in the presence of MeJA (Fig 2.9C). This is a novel finding. In contrast, FMO1 RNAs declined in all genotypes after MeJA treatment. This suggests that while MeJA does not down-regulate pipecolic acid or 5-aminovaleric acid, MeJA may interfere with the generation of the putative mobile signal of SAR, N-hydroxypipecolic acid. In the future, a targeted metabolomics approach might be able to detect N-hydroxy-pipecolic acid in tomato foliage.

LAP-A is a regulator of pseudoalkaloids

SGAs are a class of alkaloids unique to Solanaceous plants and these metabolites were regulated by MeJA and LAP-A. Following dehydrotomatine and tomatidine isomer 1 levels after MeJA treatments of wild-type, LapA-SI and LapA-OX plants showed that LAP-A is a negative regulator of dehydrotomatine at 0 h; whereas LAP-A is a positive regulator of tomatidine isomer 1 at 0 h (Table 2.7, Fig 2.11). MeJA regulated all GAME genes examined; LAP-A regulated a subset of these transcripts. GAME11/6/4/12 and GAME 1/17/18 that are associated with the conversion of cholesteral to dehydrotomatidine and tomatidine/dehydrotomatidine to α-tomatine/dehydrotomatine are all negatively regulated by MeJA. Of these genes, GAME1, GAME4, GAME6, and

GAME12 were LAP-A regulated. Similar to other genes described in sections above, LAP-A is an activator in the absence of MeJA, as evidenced by comparisons of LapA-SI and wild-type at 0 h . Furthermore, comparisons of transcript levels between wild-type and LapA-OX indicated that LAP-A can also be a repressor in the presence of LAP-A. These patterms are also observed with GAME25. In contrast, only S5αR2 is the only gene, whose transcripts increased after MeJA treatments in all genotypes and there was no evidence for LAP-A regulation.

LAP-A also regulated transcripts GAME6, GAME4, GAME12, GAME25, GAME1, and GAME18. All of these are responsible for the biosynthesis from cholesterol to dehydrotomatidine/ tomatidenol, dehydrotomatine, tomatidine, and tomatine (Akiyama et al. 2019; Cárdenas et al. 2015; Cárdenas et al. 2016; Kazachkova et al. 2021; Kozukue et al. 2004; Montero-Vargas et al. 2018; Sonawane et al. 2018; You and van Kan 2021). LAP-A and MeJA appear to regulate both branches of SGA biosynthesis (dehydrotomatine synthesis vs α-tomatine synthesis). However, it appears that neither LAP-A nor MeJA impact the final levels of the toxic α-tomatine, which is known to deter herbivory. However, we propose that LAP-A does regulate the biosynthesis of α-tomatine for plant defense responses by downregulating dehydrotomatine which is in a different SGA branch from tomatine. LAP-A may pull the biosynthesis of SGA toward the -tomatine branch in this manner. Chloroplast-localized LAP-A regulates many of the nuclear localized GAME genes and several alkaloids that are synthesized in the cytosol supports the premise that LAP-A has retrograde signaling functions to regulate GAME transcripts and their derived metabolites.

LAP-A is a positive regulator of the flavonol keampferol.

A total of 13 flavonoids and flavonoid glycosides were identified in the untargeted metabolomics dataset. Many of these molecules (eg., quercetin, quercetin glycosides and derivatives, and a luteolin glycoside) were neither MeJA nor LAP-A regulated. However, of the flavonoids related to keampferol, kaempferol isomer 1 was LAP-A regulated. Specifically, comparisons of keampferal levels at 0 h (wild-type vs LapA-OX) and 12 h (LapA-SI vs wild-type) post-MeJA treatment indicated that LAP-A enhances the levels of isomer 1 (Table 2.8, Fig 2.14). Whereas, the level of kaempferol isomer 3 was downregulated by MeJA. In tomato, two flavonol synthases are responsible for kaempferol biosynthesis, Neither were LAP-A regulated; however, they had reciprocal responses to MeJA. The flavonol synthase gene with the most abundant transcript being downregulated (Solyc01g068545) and the gene encoding the less abundant transcript being induced by MeJA (Solyc10g047520) (Fig 2.12, Fig 2.15). At the present time the significance of correlation of two RNAs with the levels of the kaempferol isomer 1 and 3 levels is not clear. Two additional flavonoid glycosides that were detected both up- and down-regulation by MeJA. And one flavonoid glycoside is an unknown common name. While downstream kaempferol metabolites were not detected, SAM and SAH which are cofactors for kaempferol modifications were detected. Neither SAM nor SAH were LAP-A regulated but they were both strongly down-regulated by MeJA treatments. Both SAM and SAH are involved in myriad chemical reactions in planta and their role in redox regulation is further pursued in Chapter 3.

Future Directions

There are several metabolites that show MeJA or MeJA and LAP-A regulation that have not yet been examined in depth at this time. Each metabolite requires an in-depth investigation of anabolic and catabolic pathways and to discern links to already investigated pathways (Tables 2.1 and 2.2). These untapped data sets will provide additional insights into the impact of LAP-A and/or MeJA on the tomato leaf metabolome. I will interrogate the remaining metabolites for their regulatory programs after MeJA treatment. Of interest are the 67 of lipids, 12 sterols, and 4 terpenes. In addition, while the identity of the 3,828 metabolites that were detected but remain unidentified, I will determine how many are LAP-A or MeJA regulated and if similar or distinct programs of regulation are revealed.

The emergence of our transcriptomes of wild-type, LapA-SI and LapA-OX plants prior to and after MeJA treatments will provide an important resource to understanding the importance of the compared to wild-type plants. The Walling lab has previously used UCR's Multi-Omics Comparison Analysis (MOCA) programs designed by Manhoi Hur to correlate transcript and metabolite levels in cassava. We will use MOCA to correlate tomato transcripts with foliar metabolites. Despite the deep metabolomics datasets for tomato fruit (Moing et al. 2020), these data for tomato leaves especially in response to wounding or MeJA treatments are limited (Li et al. 2020; Chen et al. 2006). These comparisons may provide evidence-based knowledge of a subset of unclassified metabolites that could enhance or understanding of wounding and LAP-A action.

The studies presented here clearly indicates that LAP-A is a modulator of a substantial number of metabolites with a variety of functions. These molecules are

synthesized both in the plastid and in other subcellular compartments. As LAP-A is chloroplast localized and it's the ability of LAP-A to modulate metabolites prior to and after wounding supports our premise that LAP-A regulates diverse responses within tomato leaves. Both LAP-A and MeJA impact metabolites associated with biotic and abiotic stress responses, as well as molecules associated with growth and development. Finally, although metabolites that are regulated by LAP-A have been identified, their role as a putative retrograde signal remains unclear. Further, correlations with LAP-dependent proteomes and transcriptomes are needed to infer these regulatory roles, which must then be tested using transgenic or editing strategies.

Methods

Plant growth and treatments

Solanum lycopersicum UC82 (wild-type), LapA-SI, and LapA-OX plants were grown to 4-weeks old in a growth chamber with an 18-h (28°C)/6-h (22°C) light/ dark cycle (300 µE). For exogenous methyl jasmonate (MeJA) (Cat #392707, Sigma-Aldrich) treatments, shoots were excised with a razor blade. The shoots were incubated in flasks with 10 µM MeJA and 0.005% ethanol in a closed (Chao et al. 1999). Leaves were harvested at each time point of 0, 8, 12 and 24 h post-MeJA treatments. The leaves of three plants for each genotype were pooled together. Leaves were flash frozen with liquid nitrogen and stored at -80ºC until tissue was processed. There were three biological replications of the MeJA time course.

Sample preparation for LC-MS metabolomics

Leaf samples were freeze dried for removal of water from tissue in a benchtop freeze dryer. Freeze-dried leaf samples were homogenized using an OMNI Bead Ruptor (Perkin Elmer) at processing force of 6 ms for 3 cycles of 10-sec agitation and 10-sec

dwell time. Approximately 10 mg of dried leaves were transferred to a 2-mL Eppendorf tube and 100 µL/mg extraction solvent added (30:30:20:20 acetonitrile: methanol, water, and isopropanol (ACN: MeOH, H2O, IPA)). Samples were vortexed for 90 min at 4°C then centrifuged for 15 min at 16,000 x g at 4°C. The supernatant was transferred to a 2-mL glass vial (Cat# 10803-884, VWR). A pooled quality control sample of an equimolar mix of homogenized tissue samples of different genotypes and time points was prepared to check the quality of samples.

LC-MS metabolomics - untargeted

LC-MS metabolomics analysis was performed at the UC Riverside Metabolomics Core Facility as described previously (Rothman et al. 2019). Briefly, anaysis was performed on a Synapt G2-Si quadrupole time-of-flight mass spectrometer (Waters) coupled to an I-class UPLC system (Waters). Separations were carried out on a CSH phenyl-hexyl column (2.1 x 100 mm, 1.7 µM) (Waters). The mobile phases were (A) water with 0.1% formic acid and (B) acetonitrile with 0.1% formic acid. The flow rate was 250 µL/min and the column was held at 40°C. The injection volume was 1 µL. The gradient was as follows: 0 min, 1% B and 99% A; 1 min, 1% B and 99% A; 8 min, 40% B and 60% A; 24 min, 100% B; 26.5 min, and 100% B; 27 min, 1% B and 99% A.

The MS was operated in positive ion mode (50 to 1200 m/z) with a 100 msec scan time. MS/MS was acquired in data-dependent fashion. Source and desolvation temperatures were 150°C and 600°C, respectively. Desolvation gas was set to 1100 L/h and cone gas to 150 L/h. All gases were nitrogen except the collision gas, which was argon. Capillary voltage was 1 kV.

A quality control sample, generated by pooling equal aliquots of each sample, was analyzed periodically to monitor system stability and performance. Samples were

analyzed in random order. Leucine enkephalin was infused and used for mass correction.

LC-MS metabolomics - targeted

Targeted metabolomics of polar, primary metabolites was performed at the UC Riverside Metabolomics Core Facility as described previously (Vliet et al. 2019). Briefly, analysis was performed on a TQ-XS triple quadrupole mass spectrometer (Waters) coupled to an I-class UPLC system (Waters). Separations were carried out on a ZIC-pHILIC column (2.1 x 150 mm, 5 µM) (EMD Millipore). The mobile phases were (A) water with 15 mM ammonium bicarbonate adjusted to pH 9.6 with ammonium hydroxide and (B) acetonitrile. The flow rate was 200 µL/min and the column was held at 50°C. The injection volume was 1 µL. The gradient was as follows: 0 min, 90% B and 10% A; 1.5 min, 90% B and 10% A; 16 min, 20% B and 80% A; 18 min, 1% B and 99% A; 22 min, 1% B and 99% A; 23 min, 90% B and 10% A; and 33 min, 90% B and 10% A.

The MS was operated in selected reaction monitoring mode. Source and desolvation temperatures were 150°C and 600°C, respectively. Desolvation gas was set to 1100 L/h and cone gas to 150 L/h. Collision gas was set to 0.15 mL/min. All gases were nitrogen except the collision gas, which was argon. Capillary voltage was 1 kV in positive ion mode and 2 kV in negative ion mode. A quality control sample, generated by pooling equal aliquots of each sample, was analyzed periodically to monitor system stability and performance. Samples were analyzed in random order.

Data processing and analysis

Untargeted data processing (peak picking, alignment, deconvolution, integration, normalization, and spectral matching) was performed in Progenesis Qi software (Nonlinear Dynamics). Data were normalized to total ion abundance. Features with a CV

greater than 30% across QC injections were removed (Barupal et al. 2019; Dunn et al. 2011). To aid in the identification of features that belong to the same metabolite, features were assigned a cluster ID using RAMClust (Broeckling et al. 2014). An extension of the metabolomics standard initiative guidelines was used to assign annotation level confidence (Schymanski et al. 2014; Sumner et al. 2007). Annotation level 1 indicates an MS and MS/MS match or MS and retention time match to an in-house database generated with authentic standards. Level 2a indicates an MS and MS/MS match to an external database. Level 2b indicates an MS and MS/MS match to the Lipiblast in-silico database (Kind et al. 2013) or an MS match and diagnostic evidence, such as the dominant presence of an m/z 85 fragment ion for acylcarnitines. Level 3 indicates an MS match, though some additional evidence is required, such as adducts were detected to sufficiently deduce the neutral mass or the retention time is in the expected region. Several mass spectral metabolite databases were searched against Metlin, Mass Bank of North America, and an in-house database. Targeted data processing was performed with the open-source Skyline software (Rothman et al. 2019).

Chemical Structure and Metabolic Pathway Drawings

Chemical structures, substructures, and reactions were drawn using software Marvin 17.21.0 (ChemAxon, www.chemaxon.com). A pathway genome database (Plant Metabolics Network (PMN)) on www.plantcyc.org was used to draw the tomato metabolic pathway figures (Caspi et al. 2018; Karp et al. 2011; Karp et al. 2016).

RNA isolation and Real-time quantitative PCR

RNA was isolated from frozen leaf tissue samples (see Plant Growth and Treatments above) using the hot-phenol method (Pautot et al. 2001). The genomic DNA was removed from RNA samples using RQ1 DNase digestion (Cat# M6101, Promega). A

total of 2 μg RNA was used for cDNA synthesis with Superscript III Reverse Transcriptase (Cat# 18080093, ThermoFisher). The cDNA templates were diluted 10 times with water for qRT-PCR. A total reaction volume of 25 μL using iQ SYBR Green Supermix (Cat# 170-8884, BioRad), with 200 nM of primers (Table 2.10) was added to 96-well plates in the BioRad MyIQ instrument. Two reference genes, UBI3 and eIF, were used to normalize the relative transcript level of each gene (Table 2.10). The primers were designed using Geneious Prime® 2021.1.1 The qRT-PCR reaction efficiency and the fractional cycle number at threshold (CT) was calculated using Real-time PCR Miner version 4.0 (Zhao and Fernald 2005).

Statistics

To analyze the effects of MeJA treatments, two-tailed Welch's t tests on log_2-transformed individual metabolites identified in samples in comparisons between MeJA-treatments in genotypes (LapA-SI, wild-type, and LapA-OX) to assess statistical significance and corrected for multiple comparisons with a Benjamini-Hochberg (BH)-corrected adjusted P-value. To analyze the effects of silencing LapA or overexpression of LapA, two-tailed Welch's t tests on log_2-transformed individual metabolites identified in samples in comparisons between wild-type to LapA-SI and comparisons between wild-type to LapA-OX to assess statistical significance and corrected for multiple comparisons with a Benjamini-Hochberg (BH)-corrected adjusted P-value. R stats package with TukeyHSD functions was utilized. Bar graphs were drawn using software GraphPad Prism v. 9.1.2 for MacOS. The standard error of the mean (SEM=$(\sigma/\sqrt{n})$) was utilized for error bars.

References

Adam AL, Nagy ZA, Katay G, Mergenthaler E, Viczian O (2018) Signals of Systemic Immunity in Plants: Progress and Open Questions. Int J Mol Sci 19 (4). doi:10.3390/ijms19041146

Akiyama R, Lee HJ, Nakayasu M, Osakabe K, Osakabe Y, Umemoto N, Saito K, Muranaka T, Sugimoto Y, Mizutani M (2019) Characterization of steroid 5α-reductase involved in α-tomatine biosynthesis in tomatoes. Plant Biotechnol (Tokyo) 36 (4):253-263. doi:10.5511/plantbiotechnology.19.1030a

Allwood JW, Goodacre R (2010) An Introduction to Liquid Chromatography-Mass Spectrometry Instrumentation Applied in Plant Metabolomic Analyses. Phytochemical Analysis 21 (1):33-47. doi:10.1002/pca.1187

Alseekh S, Fernie AR (2021) Using Metabolomics to Assist Plant Breeding. In: Tripodi P (ed) CROP BREEDING: Genetic Improvement Methods, vol 2264. Methods in Molecular Biology. pp 33-46. doi:10.1007/978-1-0716-1201-9_3

Bali S, Kaur P, Kohli SK, Ohri P, Thukral AK, Bhardwaj R, Wijaya L, Alyemeni MN, Ahmad P (2018) Jasmonic acid induced changes in physio-biochemical attributes and ascorbate-glutathione pathway in Lycopersicon esculentum under lead stress at different growth stages. Science of The Total Environment 645:1344-1360. doi:https://doi.org/10.1016/j.scitotenv.2018.07.164

Barupal DK, Zhang Y, Fan S, Hazen SL, Tang WHW, Cajka T, Irvin MR, Arnett DK, Kind T, Kaddurah-Daouk R, Fiehn O (2019) The circulating lipidome is largely defined by sex descriptors in the GOLDN, GeneBank and the ADNI studies. bioRxiv:731448. doi:10.1101/731448

Bellin L, Melzer M, Hilo A, Garza Amaya DL, Keller I, Meurer J, Möhlmann T (2021) Pyrimidine nucleotide availability is essential for efficient photosynthesis, ROS scavenging, and organelle development. bioRxiv:2021.2001.2022.427776. doi:10.1101/2021.01.22.427776

Bernsdorff F, Doring AC, Gruner K, Schuck S, Brautigam A, Zeier J (2016) Pipecolic Acid Orchestrates Plant Systemic Acquired Resistance and Defense Priming via Salicylic Acid-Dependent and -Independent Pathways. Plant Cell 28 (1):102-129. doi:10.1105/tpc.15.00496

Bleeker PM, Mirabella R, Diergaarde PJ, VanDoorn A, Tissier A, Kant MR, Prins M, de Vos M, Haring MA, Schuurink RC (2012) Improved herbivore resistance in cultivated tomato with the sesquiterpene biosynthetic pathway from a wild relative. Proceedings of the National Academy of Sciences 109 (49):20124-20129. doi:10.1073/pnas.1208756109

Broeckling CD, Afsar FA, Neumann S, Ben-Hur A, Prenni JE (2014) RAMClust: A Novel Feature Clustering Method Enables Spectral-Matching-Based Annotation for Metabolomics Data. Analytical Chemistry 86 (14):6812-6817. doi:10.1021/ac501530d

Cabianca A, Müller L, Pawlowski K, Dahlin P (2021) Changes in the Plant β-Sitosterol/Stigmasterol Ratio Caused by the Plant Parasitic Nematode Meloidogyne incognita. Plants 10 (2):292

Cárdenas PD, Sonawane PD, Heinig U, Bocobza SE, Burdman S, Aharoni A (2015) The bitter side of the nightshades: Genomics drives discovery in Solanaceae steroidal alkaloid metabolism. Phytochemistry 113:24-32. doi:10.1016/j.phytochem.2014.12.010

Cárdenas PD, Sonawane PD, Pollier J, Vanden Bossche R, Dewangan V, Weithorn E, Tal L, Meir S, Rogachev I, Malitsky S, Giri AP, Goossens A, Burdman S, Aharoni A (2016) GAME9 regulates the biosynthesis of steroidal alkaloids and upstream isoprenoids in the plant mevalonate pathway. Nat Commun 7:10654. doi:10.1038/ncomms10654

Caspi R, Billington R, Fulcher CA, Keseler IM, Kothari A, Krummenacker M, Latendresse M, Midford PE, Ong Q, Ong WK, Paley S, Subhraveti P, Karp PD (2018) The MetaCyc database of metabolic pathways and enzymes. Nucleic Acids Res 46 (D1):D633-d639. doi:10.1093/nar/gkx935

Chao WS, Gu YQ, Pautot V, Bray EA, Walling LL (1999) Leucine aminopeptidase RNAs, proteins, and activities increase in response to water deficit, salinity, and the wound signals systemin, methyl jasmonate, and abscisic acid. Plant Physiology 120 (4):979-992. doi:10.1104/pp.120.4.979

Chao WS, Pautot V, Holzer FM, Walling LL (2000) Leucine aminopeptidases: the ubiquity of LAP-N and the specificity of LAP-A. Planta 210 (4):563-573. doi:10.1007/s004250050045

Chaudhary J, Khatri P, Singla P, Kumawat S, Kumari A, Vinaykumar R, Vikram A, Jindal SK, Kardile H, Kumar R, Sonah H, Deshmukh R (2019) Advances in Omics Approaches for Abiotic Stress Tolerance in Tomato. Biology-Basel 8 (4). doi:10.3390/biology8040090

Chen D, Shao Q, Yin L, Younis A, Zheng B (2019) Polyamine Function in Plants: Metabolism, Regulation on Development, and Roles in Abiotic Stress Responses. Frontiers in Plant Science 9 (1945). doi:10.3389/fpls.2018.01945

Chen H, Gonzales-Vigil E, Wilkerson CG, Howe GA (2007) Stability of plant defense proteins in the gut of insect herbivores. Plant Physiol 143 (4):1954-1967. doi:10.1104/pp.106.095588

Chen H, Jones AD, Howe GA (2006) Constitutive activation of the jasmonate signaling pathway enhances the production of secondary metabolites in tomato. FEBS Letters 580 (11):2540-2546. doi:https://doi.org/10.1016/j.febslet.2006.03.070

Chen YC, Holmes EC, Rajniak J, Kim JG, Tang S, Fischer CR, Mudgett MB, Sattely ES (2018) N-hydroxy-pipecolic acid is a mobile metabolite that induces systemic disease resistance in Arabidopsis. Proc Natl Acad Sci U S A 115 (21):E4920-e4929. doi:10.1073/pnas.1805291115

Cook R, Lupette J, Benning C (2021) The Role of Chloroplast Membrane Lipid Metabolism in Plant Environmental Responses. Cells 10 (3):706

Das PP, Rana S, Muthamilarasan M, Kannan M, Ghazi IA (2021) Omics Approaches for Understanding Plant Defense Response. In: Kumar A, Kumar R, Shukla P, Pandey MK (eds) Omics Technologies for Sustainable Agriculture and Global Food Security Volume 1. Springer Singapore, Singapore, pp 41-83. doi:10.1007/978-981-16-0831-5_3

De Geyter N, Gholami A, Goormachtig S, Goossens A (2012) Transcriptional machineries in jasmonate-elicited plant secondary metabolism. Trends in Plant Science 17 (6):349-359. doi:https://doi.org/10.1016/j.tplants.2012.03.001

Demkura PV, Abdala G, Baldwin IT, Ballaré CL (2009) Jasmonate-Dependent and -Independent Pathways Mediate Specific Effects of Solar Ultraviolet B Radiation on Leaf Phenolics and Antiherbivore Defense   Plant Physiology 152 (2):1084-1095. doi:10.1104/pp.109.148999

Dunn WB, Broadhurst D, Begley P, Zelena E, Francis-McIntyre S, Anderson N, Brown M, Knowles JD, Halsall A, Haselden JN, Nicholls AW, Wilson ID, Kell DB, Goodacre R (2011) Procedures for large-scale metabolic profiling of serum and plasma using gas chromatography and liquid chromatography coupled to mass spectrometry. Nat Protoc 6 (7):1060-1083. doi:10.1038/nprot.2011.335

Ekanayaka EAP, Celiz MD, Jones AD (2015) Relative Mass Defect Filtering of Mass Spectra: A Path to Discovery of Plant Specialized Metabolites. Plant Physiology 167 (4):1221-1232. doi:10.1104/pp.114.251165

Enfissi EMA, Drapal M, Perez-Fons L, Nogueira M, Berry HM, Almeida J, Fraser PD (2021) New plant breeding techniques and their regulatory implications: An opportunity to advance metabolomics approaches. Journal of Plant Physiology 258. doi:10.1016/j.jplph.2021.153378

Erb M, Kliebenstein DJ (2020) Plant Secondary Metabolites as Defenses, Regulators, and Primary Metabolites: The Blurred Functional Trichotomy. Plant Physiology 184 (1):39-52. doi:10.1104/pp.20.00433

Fan PX, Miller AM, Schilmiller AL, Liu XX, Ofner I, Jones AD, Zamir D, Last RL (2016) In vitro reconstruction and analysis of evolutionary variation of the tomato acylsucrose metabolic network. Proceedings of the National Academy of Sciences of the United States of America 113 (2):E239-E248. doi:10.1073/pnas.1517930113

Fang X, Chen W, Zhao Y, Ruan S, Zhang H, Yan C, Jin L, Cao L, Zhu J, Ma H, Cheng Z (2015) Global analysis of lysine acetylation in strawberry leaves. Frontiers in Plant Science 6 (739). doi:10.3389/fpls.2015.00739

Fortuny AP, Bueno RA, da Costa JHP, Zanor MI, Rodriguez GR (2021) Tomato fruit quality traits and metabolite content are affected by reciprocal crosses and heterosis. Journal of Experimental Botany 72 (15):5407-5425. doi:10.1093/jxb/erab222

Fowler JH, Narvaez-Vasquez J, Aromdee DN, Pautot V, Holzer FM, Walling LL (2009) Leucine Aminopeptidase Regulates Defense and Wound Signaling in Tomato Downstream of Jasmonic Acid. Plant Cell 21 (4):1239-1251. doi:10.1105/tpc.108.065029

Gonzales-Vigil E, Bianchetti CM, Phillips GN, Jr., Howe GA (2011) Adaptive evolution of threonine deaminase in plant defense against insect herbivores. Proc Natl Acad Sci U S A 108 (14):5897-5902. doi:10.1073/pnas.1016157108

Gu YQ, Chao WS, Walling LL (1996) Localization and post-translational processing of the wound-induced leucine aminopeptidase proteins of tomato. Journal of Biological Chemistry 271 (42):25880-25887

Gu YQ, Holzer FM, Walling LL (1999) Overexpression, purification and biochemical characterization of the wound-induced leucine aminopeptidase of tomato. European Journal of Biochemistry 263 (3):726-735

Gu YQ, Walling LL (2002) Identification of residues critical for activity of the wound-induced leucine aminopeptidase (LAP-A) of tomato. European Journal of Biochemistry 269 (6):1630-1640. doi:10.1046/j.1432-1327.2002.02795.x

Hartmann M, Zeier J (2018) l-lysine metabolism to N-hydroxypipecolic acid: an integral immune-activating pathway in plants. Plant J 96 (1):5-21. doi:10.1111/tpj.14037

Hartmann M, Zeier J (2019) N-hydroxypipecolic acid and salicylic acid: a metabolic duo for systemic acquired resistance. Current Opinion in Plant Biology 50:44-57. doi:https://doi.org/10.1016/j.pbi.2019.02.006

Hartmann M, Zeier T, Bernsdorff F, Reichel-Deland V, Kim D, Hohmann M, Scholten N, Schuck S, Brautigam A, Holzel T, Ganter C, Zeier J (2018) Flavin Monooxygenase-Generated N-Hydroxypipecolic Acid Is a Critical Element of Plant Systemic Immunity. Cell 173 (2):456-469.e416. doi:10.1016/j.cell.2018.02.049

Howe GA, Major IT, Koo AJ (2018) Modularity in Jasmonate Signaling for Multistress Resilience. Annual Review of Plant Biology 69 (1):387-415. doi:10.1146/annurev-arplant-042817-040047

Huang W, Wang Y, Li X, Zhang Y (2020) Biosynthesis and Regulation of Salicylic Acid and N-Hydroxypipecolic Acid in Plant Immunity. Mol Plant 13 (1):31-41. doi:10.1016/j.molp.2019.12.008

Jacques F, Rippa S, Perrin Y (2018) Physiology of L-carnitine in plants in light of the knowledge in animals and microorganisms. Plant Sci 274:432-440. doi:10.1016/j.plantsci.2018.06.020

Jiang K, Xue Y, Ma Y (2015) Identification of Nα-acetyl-α-lysine as a probable thermolyte and its accumulation mechanism in Salinicoccus halodurans H3B36. Scientific Reports 5 (1):18518. doi:10.1038/srep18518

Joglekar S, Suliman M, Bartsch M, Halder V, Maintz J, Bautor J, Zeier J, Parker JE, Kombrink E (2018) Chemical Activation of EDS1/PAD4 Signaling Leading to Pathogen Resistance in Arabidopsis. Plant Cell Physiol 59 (8):1592-1607. doi:10.1093/pcp/pcy106

Kafer C, Zhou L, Santoso D, Guirgis A, Weers B, Park S, Thornburg R (2004) Regulation of pyrimidine metabolism in plants. Frontiers in Bioscience-Landmark 9:1611-1625

Karp PD, Latendresse M, Caspi R (2011) The pathway tools pathway prediction algorithm. Stand Genomic Sci 5 (3):424-429. doi:10.4056/sigs.1794338

Karp PD, Latendresse M, Paley SM, Krummenacker M, Ong QD, Billington R, Kothari A, Weaver D, Lee T, Subhraveti P, Spaulding A, Fulcher C, Keseler IM, Caspi R (2016) Pathway Tools version 19.0 update: software for pathway/genome informatics and systems biology. Brief Bioinform 17 (5):877-890. doi:10.1093/bib/bbv079

Kazachkova Y, Zemach I, Panda S, Bocobza S, Vainer A, Rogachev I, Dong Y, Ben-Dor S, Veres D, Kanstrup C, Lambertz SK, Crocoll C, Hu Y, Shani E, Michaeli S, Nour-Eldin HH, Zamir D, Aharoni A (2021) The GORKY glycoalkaloid transporter is indispensable for preventing tomato bitterness. Nature Plants. doi:10.1038/s41477-021-00865-6

Kind T, Liu KH, Lee DY, DeFelice B, Meissen JK, Fiehn O (2013) LipidBlast in silico tandem mass spectrometry database for lipid identification. Nat Methods 10 (8):755-758. doi:10.1038/nmeth.2551

193

Kortbeek RWJ, Galland MD, Muras A, van der Kloet FM, André B, Heilijgers M, van Hijum SAFT, Haring MA, Schuurink RC, Bleeker PM (2021) Natural variation in wild tomato trichomes; selecting metabolites that contribute to insect resistance using a random forest approach. BMC Plant Biology 21 (1):315. doi:10.1186/s12870-021-03070-x

Kosmacz M, Sokołowska EM, Bouzaa S, Skirycz A (2020) Towards a functional understanding of the plant metabolome. Current Opinion in Plant Biology 55:47-51. doi:https://doi.org/10.1016/j.pbi.2020.02.005

Kozukue N, Han JS, Lee KR, Friedman M (2004) Dehydrotomatine and alpha-tomatine content in tomato fruits and vegetative plant tissues. J Agric Food Chem 52 (7):2079-2083. doi:10.1021/jf0306845

Li Y, Chen Y, Zhou L, You S, Deng H, Chen Y, Alseekh S, Yuan Y, Fu R, Zhang Z, Su D, Fernie AR, Bouzayen M, Ma T, Liu M, Zhang Y (2020) MicroTom Metabolic Network: Rewiring Tomato Metabolic Regulatory Network throughout the Growth Cycle. Molecular Plant 13 (8):1203-1218. doi:https://doi.org/10.1016/j.molp.2020.06.005

Li Z, Peng R, Yao Q (2021) SlMYB14 promotes flavonoids accumulation and confers higher tolerance to 2,4,6-trichlorophenol in tomato. Plant Science 303:110796. doi:https://doi.org/10.1016/j.plantsci.2020.110796

Liu C, Atanasov KE, Tiburcio AF, Alcázar R (2019) The Polyamine Putrescine Contributes to H2O2 and RbohD/F-Dependent Positive Feedback Loop in Arabidopsis PAMP-Triggered Immunity. Frontiers in Plant Science 10 (894). doi:10.3389/fpls.2019.00894

Lou YR, Ahmed S, Yan J, Adio AM, Powell HM, Morris PF, Jander G (2020) Arabidopsis ADC1 functions as an N(δ) -acetylornithine decarboxylase. J Integr Plant Biol 62 (5):601-613. doi:10.1111/jipb.12821

Lou YR, Bor M, Yan J, Preuss AS, Jander G (2016) Arabidopsis NATA1 Acetylates Putrescine and Decreases Defense-Related Hydrogen Peroxide Accumulation. Plant Physiol 171 (2):1443-1455. doi:10.1104/pp.16.00446

Luna E, Flandin A, Cassan C, Prigent S, Chevanne C, Kadiri CF, Gibon Y, Petriacq P (2020) Metabolomics to Exploit the Primed Immune System of Tomato Fruit. Metabolites 10 (3). doi:10.3390/metabo10030096

Maas MN, Hintzen JCJ, Porzberg MRB, Mecinović J (2020) Trimethyllysine: From Carnitine Biosynthesis to Epigenetics. International Journal of Molecular Sciences 21 (24):9451

Machado RAR, Baldwin IT, Erb M (2017) Herbivory-induced jasmonates constrain plant sugar accumulation and growth by antagonizing gibberellin signaling and not by promoting secondary metabolite production. New Phytologist 215 (2):803-812. doi:https://doi.org/10.1111/nph.14597

Mandal S, Ji W, McKnight TD (2020) Candidate Gene Networks for Acylsugar Metabolism and Plant Defense in Wild Tomato Solanum pennellii. The Plant cell 32 (1):81-99. doi:10.1105/tpc.19.00552

Martens S, Mithöfer A (2005) Flavones and flavone synthases. Phytochemistry 66 (20):2399-2407. doi:https://doi.org/10.1016/j.phytochem.2005.07.013

Moing A, Pétriacq P, Osorio S (2020) Special Issue on "Fruit Metabolism and Metabolomics". Metabolites 10 (6):230

Montero-Vargas JM, Casarrubias-Castillo K, Martínez-Gallardo N, Ordaz-Ortiz JJ, Délano-Frier JP, Winkler R (2018) Modulation of steroidal glycoalkaloid biosynthesis in tomato (Solanum lycopersicum) by jasmonic acid. Plant Science 277:155-165. doi:https://doi.org/10.1016/j.plantsci.2018.08.020

Muhlemann JK, Younts TL, Muday GK (2018) Flavonols control pollen tube growth and integrity by regulating ROS homeostasis during high-temperature stress. Proceedings of the National Academy of Sciences 115 (47):E11188-E11197

Narvaez-Vasquez J, Tu C-J, Park S-Y, Walling LL (2008) Targeting and localization of wound-inducible leucine aminopeptidase A in tomato leaves. Planta 227 (2):341-351. doi:10.1007/s00425-007-0621-0

Orlovskis Z, Reymond P (2020) Pieris brassicae eggs trigger interplant systemic acquired resistance against a foliar pathogen in Arabidopsis. New Phytol. doi:10.1111/nph.16788

Orozco-Cárdenas ML, Narváez-Vásquez J, Ryan CA (2001) Hydrogen Peroxide Acts as a Second Messenger for the Induction of Defense Genes in Tomato Plants in Response to Wounding, Systemin, and Methyl Jasmonate. The Plant Cell 13 (1):179-192

Parthasarathy A, Borrego EJ, Savka MA, Dobson RCJ, Hudson AO (2021) Amino acid-derived defense metabolites from plants: A potential source to facilitate novel antimicrobial development. J Biol Chem 296:100438. doi:10.1016/j.jbc.2021.100438

Paupiere MJ, Tikunov Y, Schleiff E, Bovy A, Fragkostefanakis S (2020) Reprogramming of Tomato Leaf Metabolome by the Activity of Heat Stress Transcription Factor HsfB1. Frontiers in Plant Science 11. doi:10.3389/fpls.2020.610599

Pautot V, Holzer FM, Chaufaux J, Walling LL (2001) The induction of tomato leucine aminopeptidase genes (LapA) after Pseudomonas syringae pv. tomato infection is primarily a wound response triggered by coronatine. Mol Plant Microbe Interact 14 (2):214-224. doi:10.1094/mpmi.2001.14.2.214

Perez-Fons L, Bohorquez-Chaux A, Irigoyen ML, Garceau DC, Morreel K, Boerjan W, Walling LL, Becerra Lopez-Lavalle LA, Fraser PD (2019) A metabolomics characterisation of natural variation in the resistance of cassava to whitefly. BMC Plant Biology 19 (1):518. doi:10.1186/s12870-019-2107-1

Pott DM, Osorio S, Vallarino JG (2019) From Central to Specialized Metabolism: An Overview of Some Secondary Compounds Derived From the Primary Metabolism for Their Role in Conferring Nutritional and Organoleptic Characteristics to Fruit. Front Plant Sci 10:835. doi:10.3389/fpls.2019.00835

Rivero Meza SL, de Castro Tobaruela E, Benedetti Pascoal G, Louro Massaretto I, Purgatto E (2021) Post-Harvest Treatment with Methyl Jasmonate Impacts Lipid Metabolism in Tomato Pericarp (Solanum lycopersicum L. cv. Grape) at Different Ripening Stages. Foods 10 (4). doi:10.3390/foods10040877

Rothman JA, Leger L, Kirkwood JS, McFrederick QS (2019) Cadmium and Selenate Exposure Affects the Honey Bee Microbiome and Metabolome, and Bee-Associated Bacteria Show Potential for Bioaccumulation. Appl Environ Microbiol 85 (21):e01411-01419. doi:10.1128/AEM.01411-19

Sant'Ana DVP, Lefsrud M (2018) Tomato proteomics: Tomato as a model for crop proteomics. Scientia Horticulturae 239:224-233. doi:https://doi.org/10.1016/j.scienta.2018.05.041

Schnake A, Hartmann M, Schreiber S, Malik J, Brahmann L, Yildiz I, von Dahlen J, Rose LE, Schaffrath U, Zeier J (2020) Inducible biosynthesis and immune function of the systemic acquired resistance inducer N-hydroxypipecolic acid in monocotyledonous and dicotyledonous plants. Journal of Experimental Botany 71 (20):6444-6459. doi:10.1093/jxb/eraa317

Schuman MC, Meldau S, Gaquerel E, Diezel C, McGale E, Greenfield S, Baldwin IT (2018) The Active Jasmonate JA-Ile Regulates a Specific Subset of Plant Jasmonate-Mediated Resistance to Herbivores in Nature. Frontiers in Plant Science 9 (787). doi:10.3389/fpls.2018.00787

Schymanski EL, Jeon J, Gulde R, Fenner K, Ruff M, Singer HP, Hollender J (2014) Identifying Small Molecules via High Resolution Mass Spectrometry: Communicating Confidence. Environmental Science & Technology 48 (4):2097-2098. doi:10.1021/es5002105

Scossa F, Alseekh S, Fernie AR (2021) Integrating multi-omics data for crop improvement. Journal of Plant Physiology 257:153352. doi:10.1016/j.jplph.2020.153352

Scranton M, Yee A, Park SY, Walling LL (2012) Plant leucine aminopeptidases moonlight as molecular chaperones. Journal of Biological Chemistry 287:18408-18417. doi:10.1074/jbc.M111.309500

Scranton MA, Fowler JH, Girke T, Walling LL (2013) Microarray Analysis of Tomato's Early and Late Wound Response Reveals New Regulatory Targets for Leucine Aminopeptidase A. PLOS ONE 8 (10):e77889. doi:10.1371/journal.pone.0077889

Sharma A, Shahzad B, Kumar V, Kohli SK, Sidhu GPS, Bali AS, Handa N, Kapoor D, Bhardwaj R, Zheng B (2019) Phytohormones Regulate Accumulation of Osmolytes Under Abiotic Stress. Biomolecules 9 (7). doi:10.3390/biom9070285

Shimizu Y, Rai A, Okawa Y, Tomatsu H, Sato M, Kera K, Suzuki H, Saito K, Yamazaki M (2019) Metabolic diversification of nitrogen-containing metabolites by the expression of a heterologous lysine decarboxylase gene in Arabidopsis. The Plant Journal 100 (3):505-521. doi:10.1111/tpj.14454

Slimestad R, Fossen T, Verheul MJ (2008) The Flavonoids of Tomatoes. Journal of Agricultural and Food Chemistry 56 (7):2436-2441. doi:10.1021/jf073434n

Soltis NE, Kliebenstein DJ (2015) Natural Variation of Plant Metabolism: Genetic Mechanisms, Interpretive Caveats, and Evolutionary and Mechanistic Insights. Plant Physiology 169 (3):1456-1468. doi:10.1104/pp.15.01108

Sonawane PD, Heinig U, Panda S, Gilboa NS, Yona M, Kumar SP, Alkan N, Unger T, Bocobza S, Pliner M, Malitsky S, Tkachev M, Meir S, Rogachev I, Aharoni A (2018) Short-chain dehydrogenase/reductase governs steroidal specialized metabolites structural diversity and toxicity in the genus Solanum. Proc Natl Acad Sci U S A 115 (23):E5419-e5428. doi:10.1073/pnas.1804835115

Sowers KR, Robertson DE, Noll D, Gunsalus RP, Roberts MF (1990) N epsilon-acetyl-beta-lysine: an osmolyte synthesized by methanogenic archaebacteria. Proc Natl Acad Sci U S A 87 (23):9083-9087. doi:10.1073/pnas.87.23.9083

Steinbrenner AD, Gómez S, Osorio S, Fernie AR, Orians CM (2011) Herbivore-Induced Changes in Tomato (Solanum lycopersicum) Primary Metabolism: A Whole Plant Perspective. Journal of Chemical Ecology 37 (12):1294-1303. doi:10.1007/s10886-011-0042-1

Sumner LW, Amberg A, Barrett D, Beale MH, Beger R, Daykin CA, Fan TW, Fiehn O, Goodacre R, Griffin JL, Hankemeier T, Hardy N, Harnly J, Higashi R, Kopka J, Lane AN, Lindon JC, Marriott P, Nicholls AW, Reily MD, Thaden JJ, Viant MR (2007) Proposed minimum reporting standards for chemical analysis Chemical Analysis Working Group (CAWG) Metabolomics Standards Initiative (MSI). Metabolomics 3 (3):211-221. doi:10.1007/s11306-007-0082-2

Sumner LW, Lei Z, Nikolau BJ, Saito K (2015) Modern plant metabolomics: advanced natural product gene discoveries, improved technologies, and future prospects. Natural Product Reports 32 (2):212-229. doi:10.1039/C4NP00072B

Tarkowski ŁP, Signorelli S, Höfte M (2020) γ-Aminobutyric acid and related amino acids in plant immune responses: emerging mechanisms of action. Plant, cell & environment 43 (5):1103-1116

Tohge T, Scossa F, Wendenburg R, Frasse P, Balbo I, Watanabe M, Alseekh S, Jadhav SS, Delfin JC, Lohse M, Giavalisco P, Usadel B, Zhang Y, Luo J, Bouzayen M, Fernie AR (2020) Exploiting Natural Variation in Tomato to Define Pathway Structure and Metabolic Regulation of Fruit Polyphenolics in the Lycopersicum Complex. Molecular Plant 13 (7):1027-1046. doi:https://doi.org/10.1016/j.molp.2020.04.004

Trovato M, Funck D, Forlani G, Okumoto S, Amir R (2021) Editorial: Amino Acids in Plants: Regulation and Functions in Development and Stress Defense. Frontiers in Plant Science 12 (2287). doi:10.3389/fpls.2021.772810

USDA (2017) National Agricultural Statistics Service - Vegetables 2016 Summary (Washington, DC: USDA). https://wwwnassusdagov/ Publications/Todays_Reports/reports/vegean17pdf

Vliet SMF, Dasgupta S, Sparks NRL, Kirkwood JS, Vollaro A, Hur M, Zur Nieden NI, Volz DC (2019) Maternal-to-zygotic transition as a potential target for niclosamide during early embryogenesis. Toxicol Appl Pharmacol 380:114699. doi:10.1016/j.taap.2019.114699

Wang Y, Mostafa S, Zeng W, Jin B (2021) Function and Mechanism of Jasmonic Acid in Plant Responses to Abiotic and Biotic Stresses. International Journal of Molecular Sciences 22 (16):8568

Wang Y, Schuck S, Wu J, Yang P, Döring A-C, Zeier J, Tsuda K (2018) A MPK3/6-WRKY33-ALD1-Pipecolic Acid Regulatory Loop Contributes to Systemic Acquired Resistance. The Plant Cell 30 (10):2480-2494. doi:10.1105/tpc.18.00547

War AR, Buhroo AA, Hussain B, Ahmad T, Nair RM, Sharma HC (2020) Plant defense and insect adaptation with reference to secondary metabolites. Co-Evolution of Secondary Metabolites:795-822

Wei X, Vrieling K, Kim HK, Mulder PPJ, Klinkhamer PGL (2021) Application of methyl jasmonate and salicylic acid lead to contrasting effects on the plant's metabolome and herbivory. Plant Science 303:110784. doi:https://doi.org/10.1016/j.plantsci.2020.110784

Yan H, Yoo M-J, Koh J, Liu L, Chen Y, Acikgoz D, Wang Q, Chen S (2014) Molecular Reprogramming of Arabidopsis in Response to Perturbation of Jasmonate Signaling. Journal of Proteome Research 13 (12):5751-5766. doi:10.1021/pr500739v

You Y, van Kan JAL (2021) Bitter and sweet make tomato hard to (b)eat. New Phytologist 230 (1):90-100. doi:https://doi.org/10.1111/nph.17104

Zeiss DR, Mhlongo MI, Tugizimana F, Steenkamp PA, Dubery IA (2018) Comparative Metabolic Phenotyping of Tomato (Solanum lycopersicum) for the Identification of Metabolic Signatures in Cultivars Differing in Resistance to Ralstonia solanacearum. International Journal of Molecular Sciences 19 (9). doi:10.3390/ijms19092558

Zhao S, Fernald RD (2005) Comprehensive algorithm for quantitative real-time polymerase chain reaction. J Comput Biol 12 (8):1047-1064. doi:10.1089/cmb.2005.12.1047

A

Targeted: Primary metabolites

Category	Number of metabolites
Amino acid	37
Purine	10
Pyrimidine	4
Oxidative stress	4
Electron carrier	4
Urea cycle	3
Methylation	3
TCA cycle	2
Sugar	2
Phospholipid turnover	2
Choline	2
B Vitamin	2
Sugar alcohol	1
Polyamine	1
Alkaloid	1

Number of metabolites

B

Untargeted: Lipids and secondary metabolites

Category	Number of metabolites
PC	19
Sterol	12
PE	12
MGDG	9
Flavonoid glycoside	9
Amino Acid	8
Alkaloid	7
DG	6
Lyso PC	5
Oxylipin	4
Oxidized PC	4
Hexosyl ceramide	4
Flavonoid	4
Lyso PE	3
Ceramide	3
Terpene	2
Terpene glycoside	2
Purine	2
Polyphenol	2
Ox stress	2
Hydroxycinammic acid	2
Fatty acid	2
DGDG	2
Vitamin K	1
TG	1
Sphingoid	1
MG	1
Glycoside	1
Coumarin	1

Number of metabolites

Figure 2.1 Metabolites classified by functional categories.
A) The 78 primary metabolites detected were classified into 15 functional categories. B) The 131 lipids and secondary metabolites were classified into 29 functional categories.
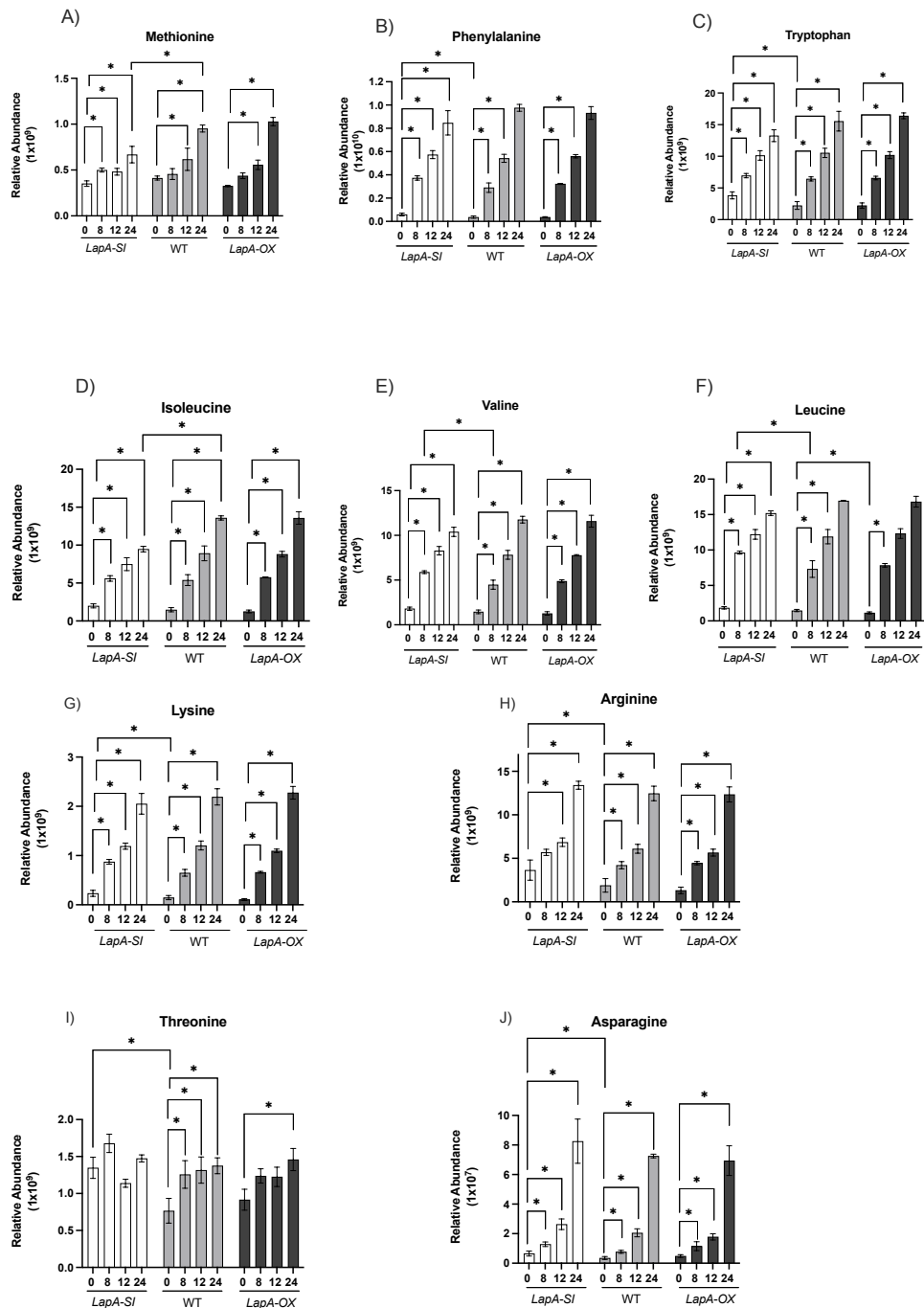
Figure 2.2 Changes in proteinogenic amino acid metabolite abundance at 0, 8, 12, and 24 h after MeJA treatments in WT, LapA-SI and LapA-OX plants . Subset of metabolites involved in amino acid biosynthesis pathways were LAP-A and MeJA regulated. A) Met, B) Phe, C) Trp, D) Ile, E) Val, F) Leu, G) Lys, H) Arg, I) Thr, and J) Asn. Asterisks represent statistically different values at adjusted P-value ≤ 0.05.

201
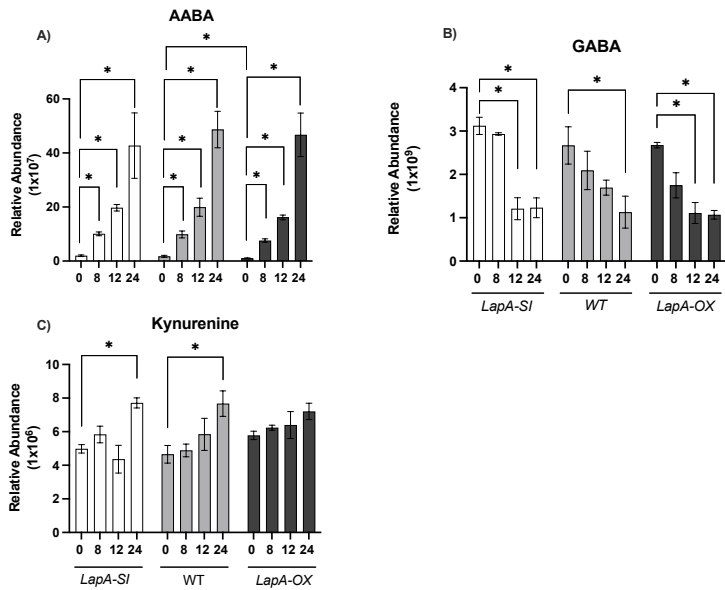
Figure 2.3 Nonproteinogenic amino acids regulated by LAP-A and/ or MeJA in WT, LapA-SI and LapA-OX plants. Three nonproteinogenic amino acids were differentially regulated after MeJA treatements . A) α-aminobutyric acid/2-aminobutyric acid (AABA), B) γ-aminobutyric acid (GABA), and C) the Trp-derived kynurenine. Asterisks represent statistically different values at adjusted P-value ≤ 0.05.
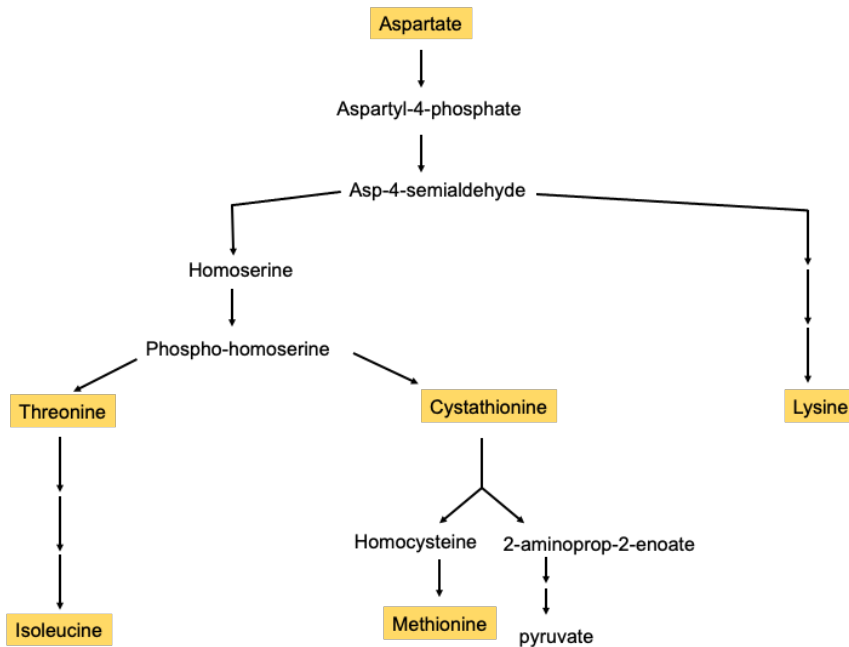
Figure 2.4. The catabolism of Asp and pathway biosynthesis of Threonine, Met, Leu, and Ile metabolites. Metabolites in yellow represent detected metabolites.
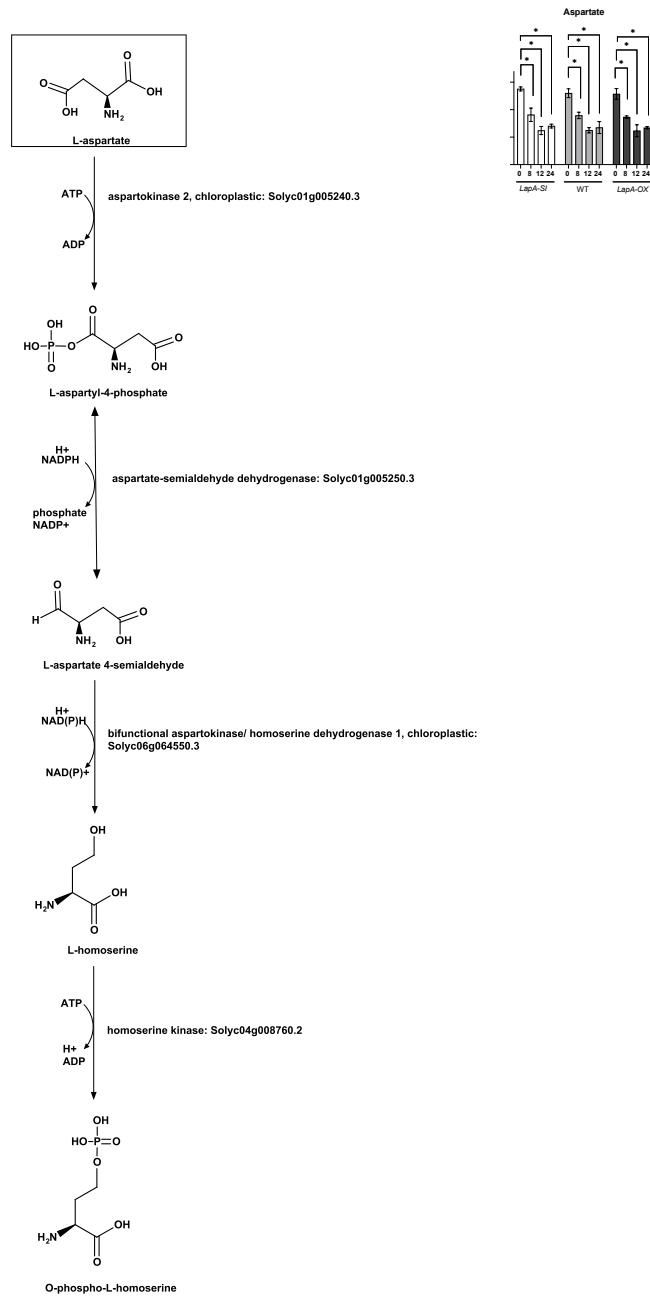
Figure 2.5 Relative Asp abundance in WT, LapA-SIand LapA-OX lines 0, 8, 12 and 24 h after MeJA treatment. Asp participates as a substrate in the homoserine biosynthesis pathway. The substrates, enzymes, byproducts, and products are shown. The final product of this pathway, O-phospho-L-homoserine, feeds into biosynthetic pathways for both Thr and Met. A double arrow indicates a reversible chemical reaction. Enzyme names and SolycIDs are listed on respective reactions. Asterisks represent statistically different values at adjusted P-value ≤ 0.05.
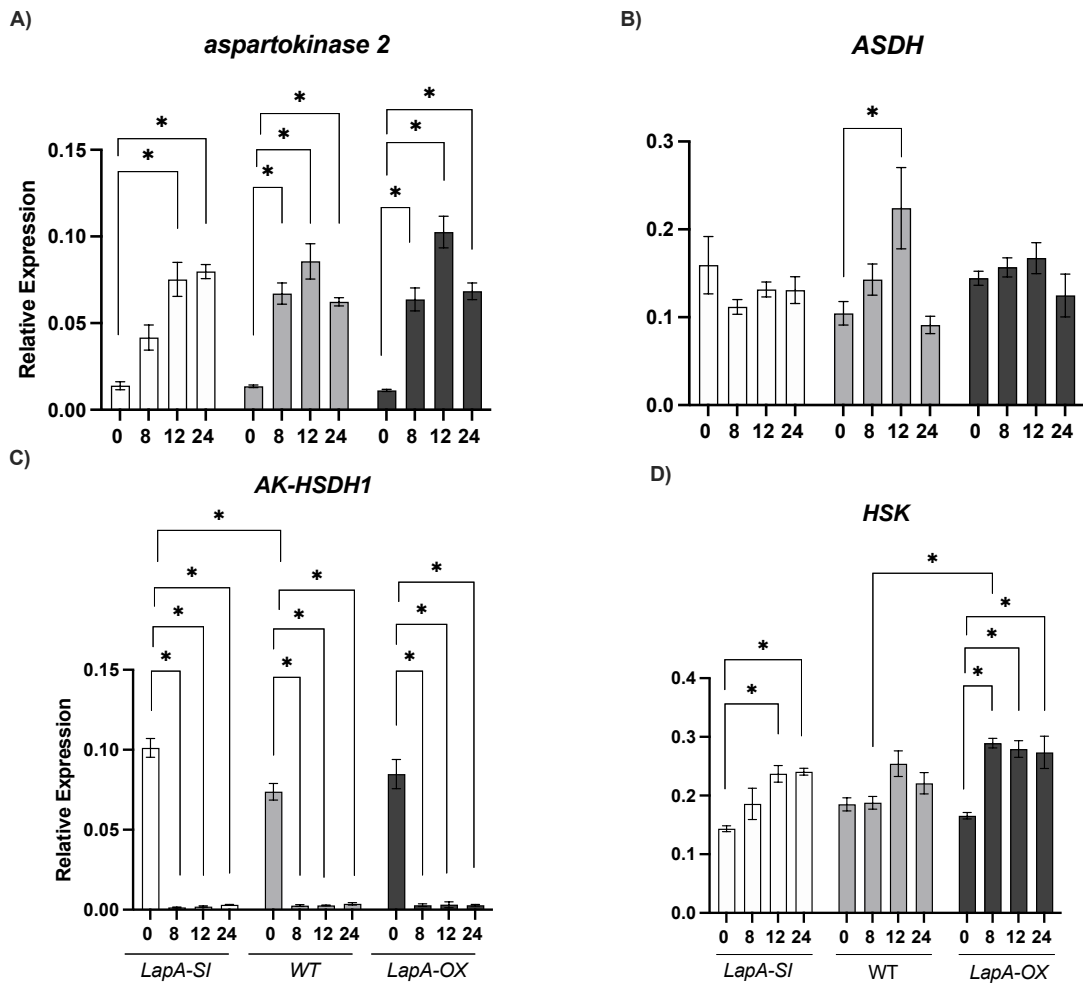
Figure 2.6 Relative transcript levels for genes that encode enzymes represented in the pathways upstream of Thr, Met, and Ile after MeJA treatments of WT, LapA-SI and LapA-OX plants. A) aspartokinase 2, B) aspartate-semialdehyde dehydrogenase (ASDH), (C) bifunctional aspartokinase/ homoserine dehydrogenase 1 (AK-HSDH1), D) homoserine kinase (HSK), Asterisks represent statistically different values at adjusted P-value ≤ 0.05.
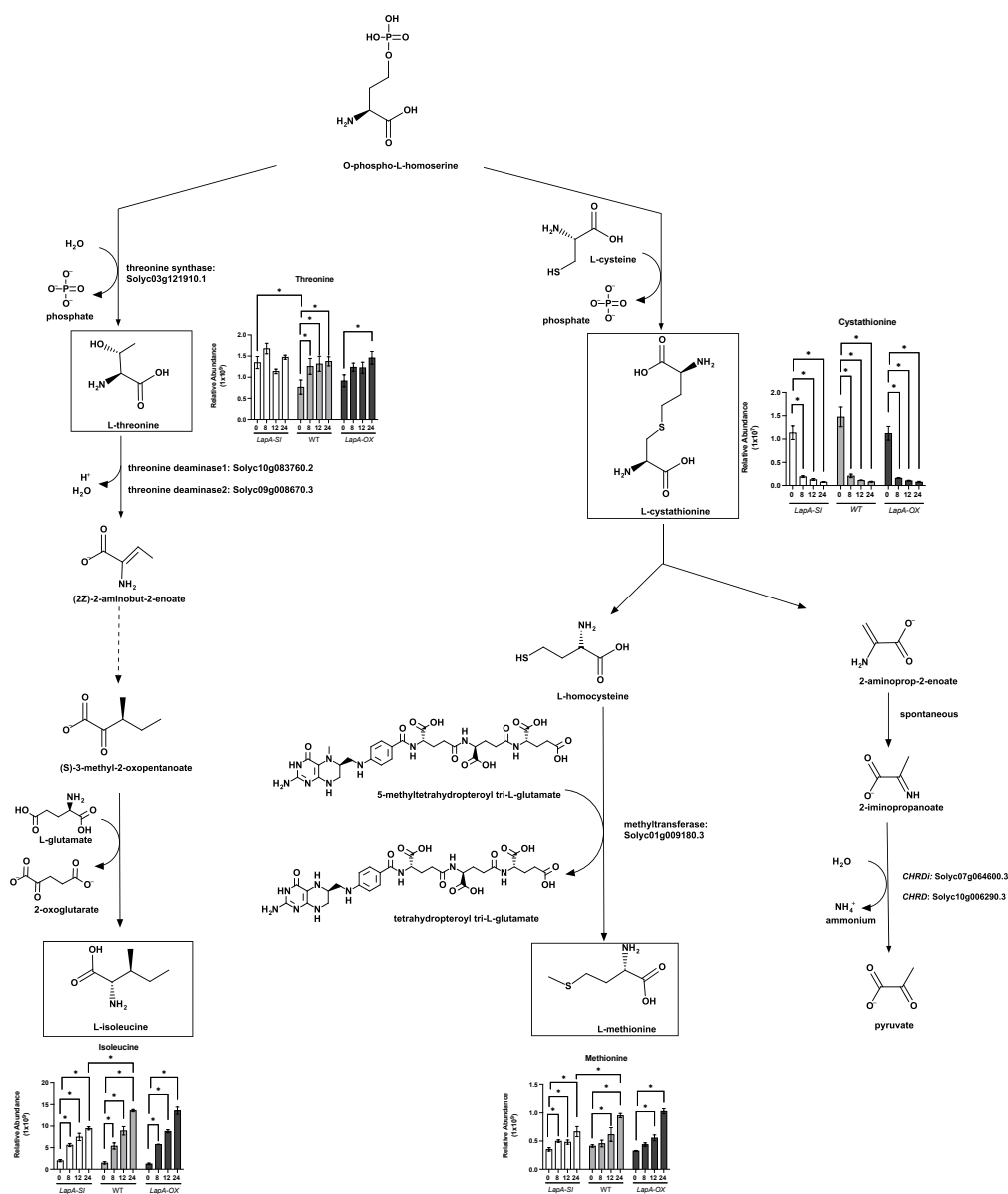
Figure 2.7 Relative Thr, Ile, Cystathionine and Met abundance in LapA-SI, WT and LapA-OX lines after MeJA treatment. The branched pathway that utilizes O-phospho-L-homoserine as the substrate for cystathionine and Thr biosynthesis is shown. Thr is a substrate for the Ile biosynthesis. Cystathionine feeds into biosynthetic pathways of Met and pyruvate. Changes in metabolites detected in these pathways are shown. A dashed arrow indicates several biochemical reactions are required and not shown for simplicity. Enzyme names and SolycIDs are listed on respective reactions. Asterisks represent statistically different values at adjusted P-value ≤ 0.05.

205
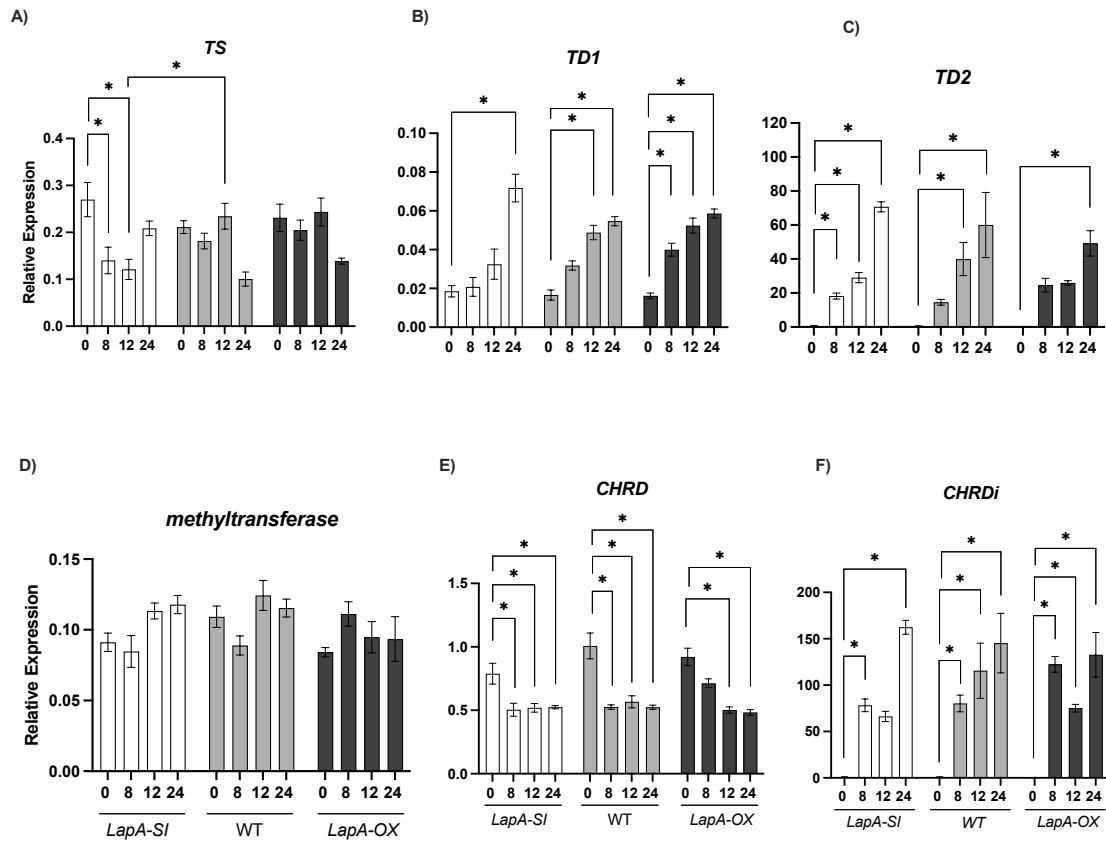
Figure 2.8 Relative transcript levels for genes that encode enzymes represented in the biosynthesis pathways of Thr, Met, and Ile in WT, si in WT, LapA-SI and LapA-OX lines after MeJA treatments. A) threonine synthase (TS), B) threonine dehydratase 1/Thr deaminase 1 (TD1), C) threonine dehydratase 2/The deaminase 2 (TD2), D) methyltransferase, E) constitutive plastid-lipid associated protein (CHRD), F) inducible plastid-lipid associated protein (CHRDi). Asterisks represent statistically different values at adjusted P-value ≤ 0.05.
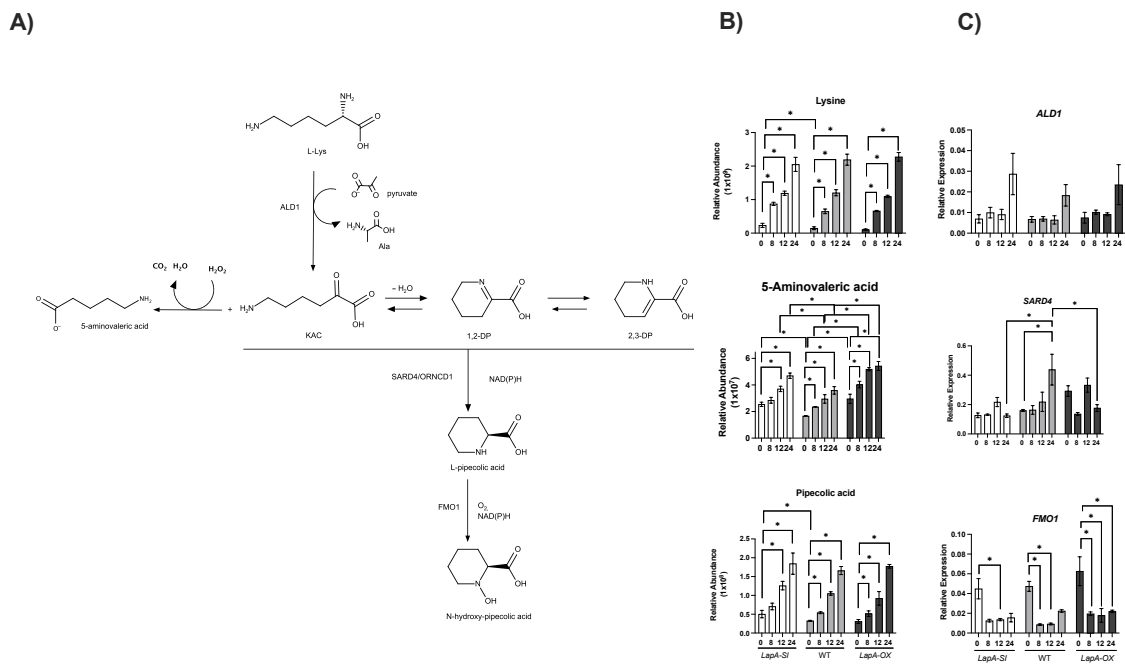
Figure 2.9 Pathways and metabolite abundance in for production of pipecolic acid 5-aminovaleric acid in LapA-SI, WT and LapA-OX lines 0, 8, 12 and 24 h after MeJA treatment. A) Diagram of the N-hydroxy-pipecolic acid biosynthesis pathway based on the Arabidopsis literature including the spontaneous production of 5-aminovaleric acid in the presence of hydrogen peroxide. B) Relative abundance of Lys, 5-aminovaleric acid, and pipecolic acid. C) Transcript levels of genes associated wth N- hydroxy-pipecolic acid production. Aminotransferase AGD2-like defense response protein (ALD1), reductase SAR-deficient 4 (SARD4), and flavin-dependent monooxygenase1 (FMO1). Dehydropipecolic acid (DP) intermediates and ε-amino-α-ketocaproic acid (KAC) are substrates for L-pipecolic acid generation but were not detected. Asterisks represent statistically different values at adjusted P-value ≤ 0.05.
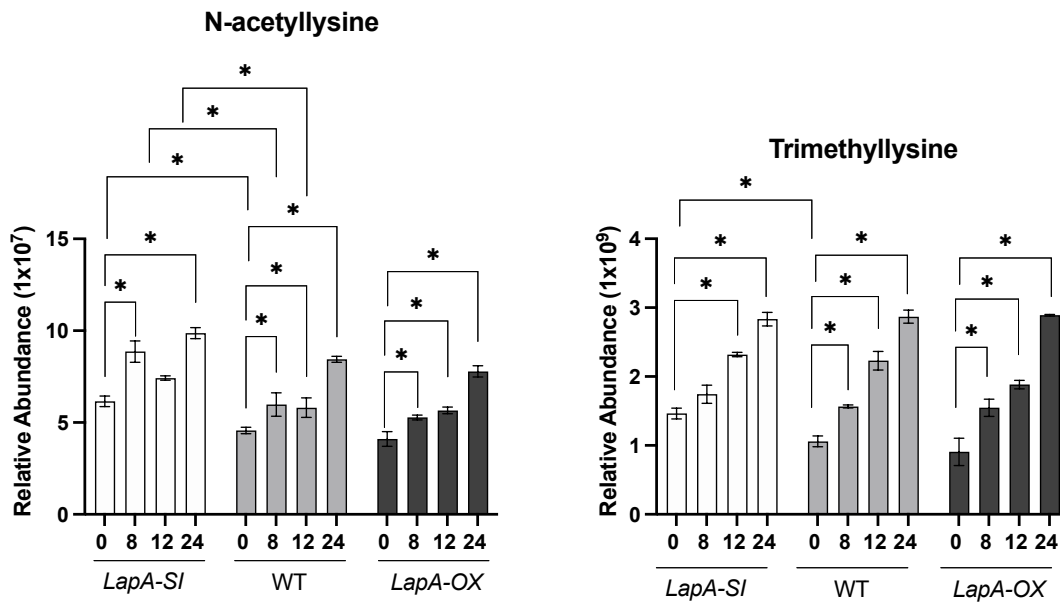
Figure 2.10 Relative abundance of Lys-derived amino acids N-acetyllysine and trimethyllysine in WT, LapA-SI and LapA-OX plants after MeJA treatments. Asterisks represent statistically different values at adjusted P-value ≤ 0.05.
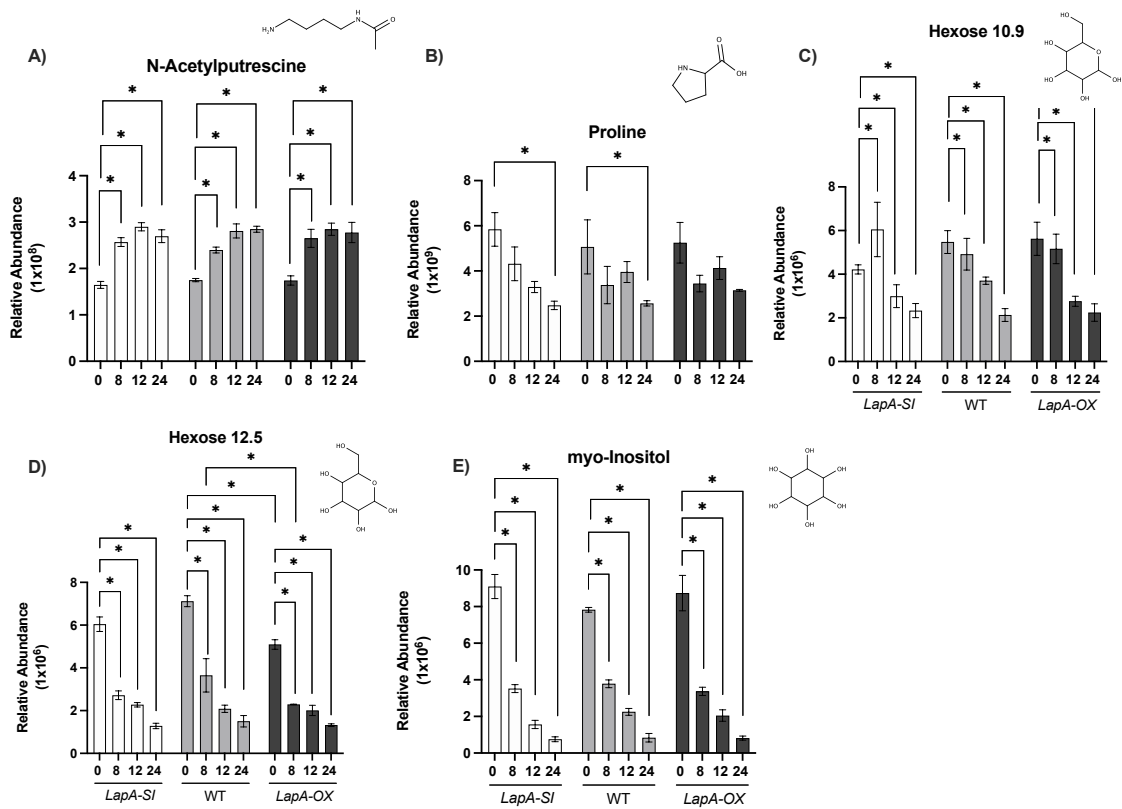
Figure 2.11 Relative osmolyte abundance in LapA-SI, WT and LapA-OX lines 0, 8, 12 and 24 h after MeJA treatment. A) polyamine N-acetylputrescine. B) Proline. C) hexose 10.9 profile. D) hexose 12.5 profile. E) myo-inositol (sugar alcohol). Asterisks represent statistically different values at adjusted P-value ≤ 0.05.
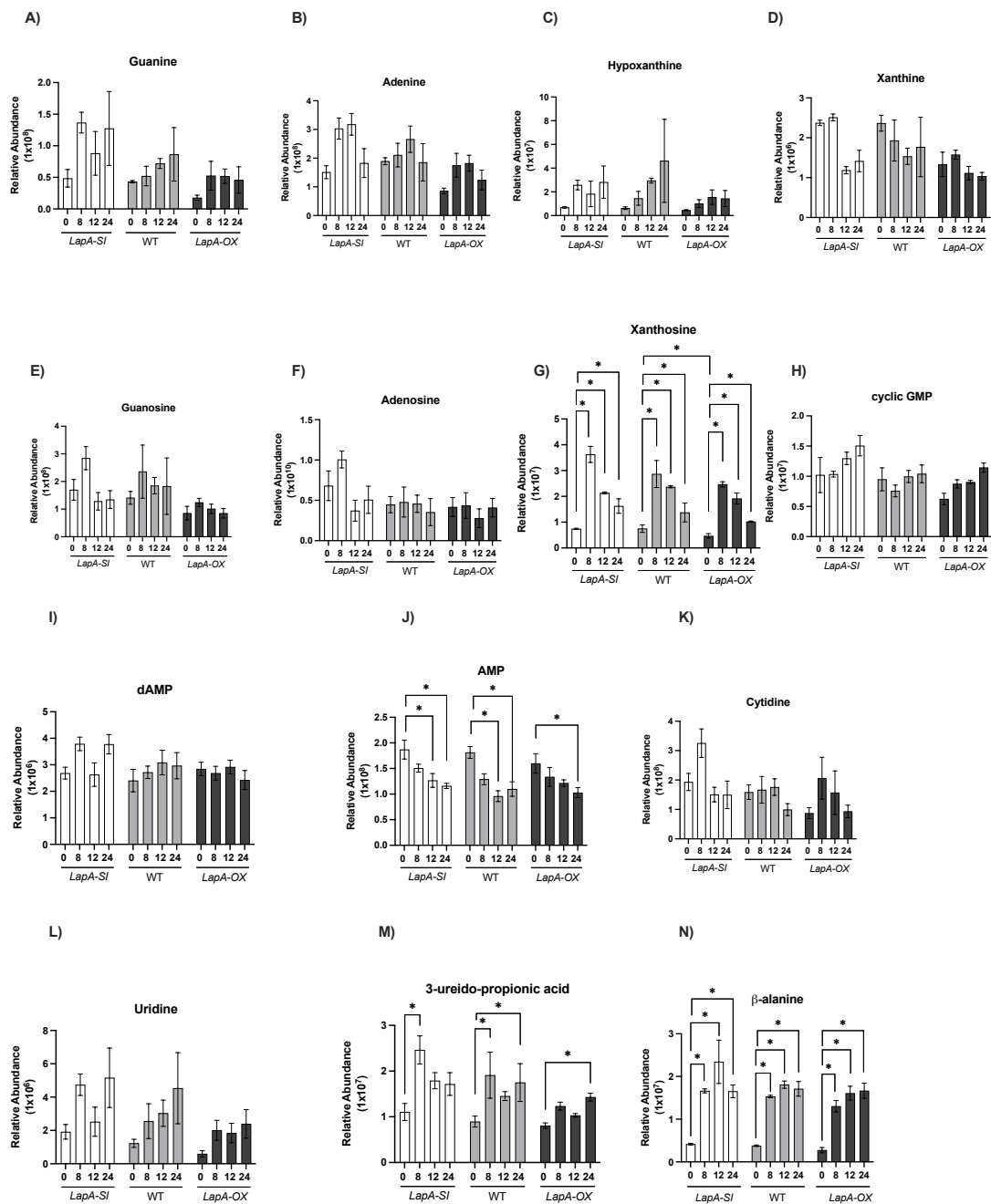
Figure 2.12 Relative purine and pyrimidine abundance in LapA-SI, WT and LapA-OX lines 0, 8, 12 and 24 h after MeJA treatment. A) Guanine. B) Adenine, C) Hypoxanthine, D) Xanthine, E) Guanosine, F) Adenosine, G) Xanthosine, H) cyclic GMP, I) dAMP, J) AMP, K) Cytidine, L) Uridine, M) 3-ureido-propionic acid, N) beta-alanine. Asterisks represent statistically different values at adjusted P-value ≤ 0.05
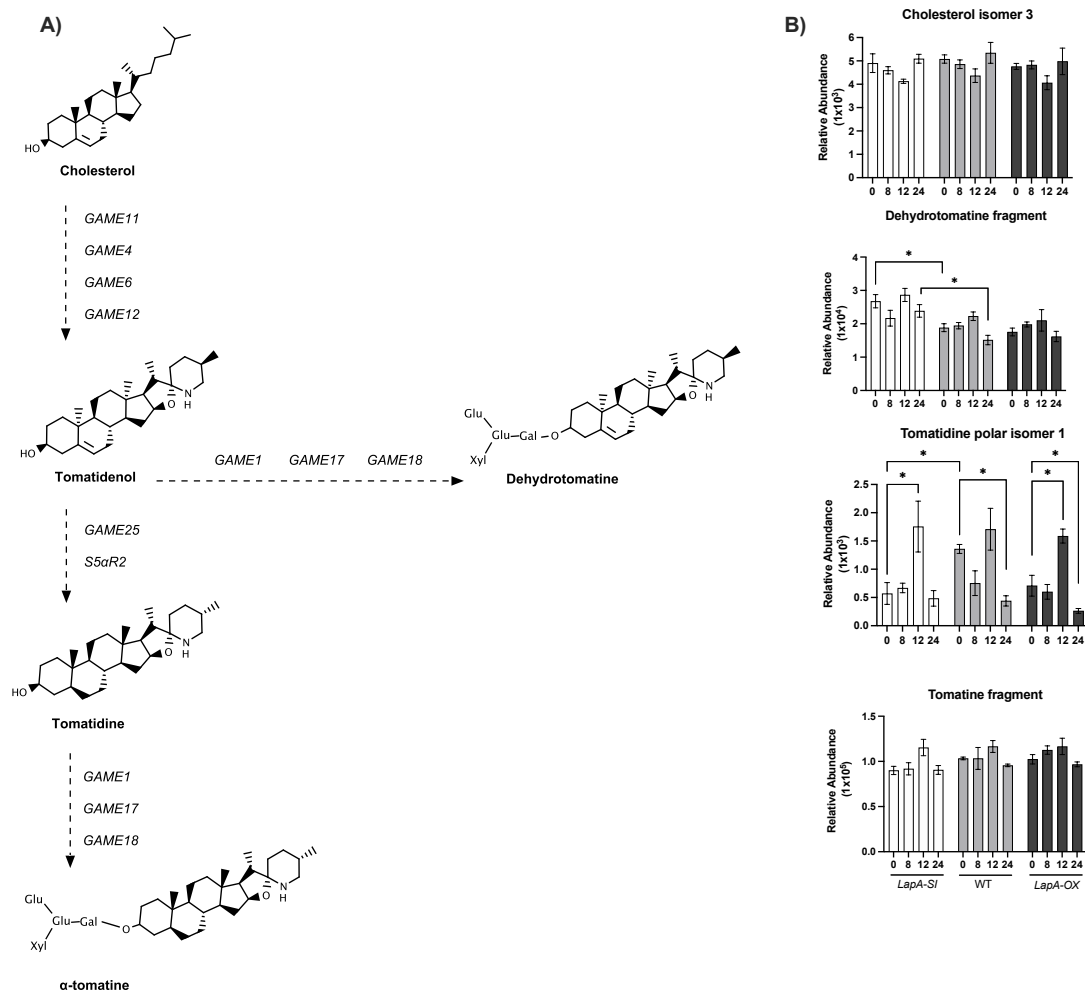
Figure 2.13 Relative metabolite abundance represented in steroidal glycoalkaloid (SGA) biosynthesis pathway beginning with cholesterol in WT, LapA-SI and LapA-OX plants after MeJA treatment. A) Biosynthetic pathway of SGA metabolites and names enzymes. B) Relative metabolite levels of Cholesterol isomer 3, dehydrotomatine fragment, tomatidine polar isomer 1, and tomatine fragment metabolites in LapA-SI, WT, and LapA-OX treated with MeJA at 0, 8, 12, and 24 h. Asterisks represent statistically different values at adjusted P-value ≤ 0.05.
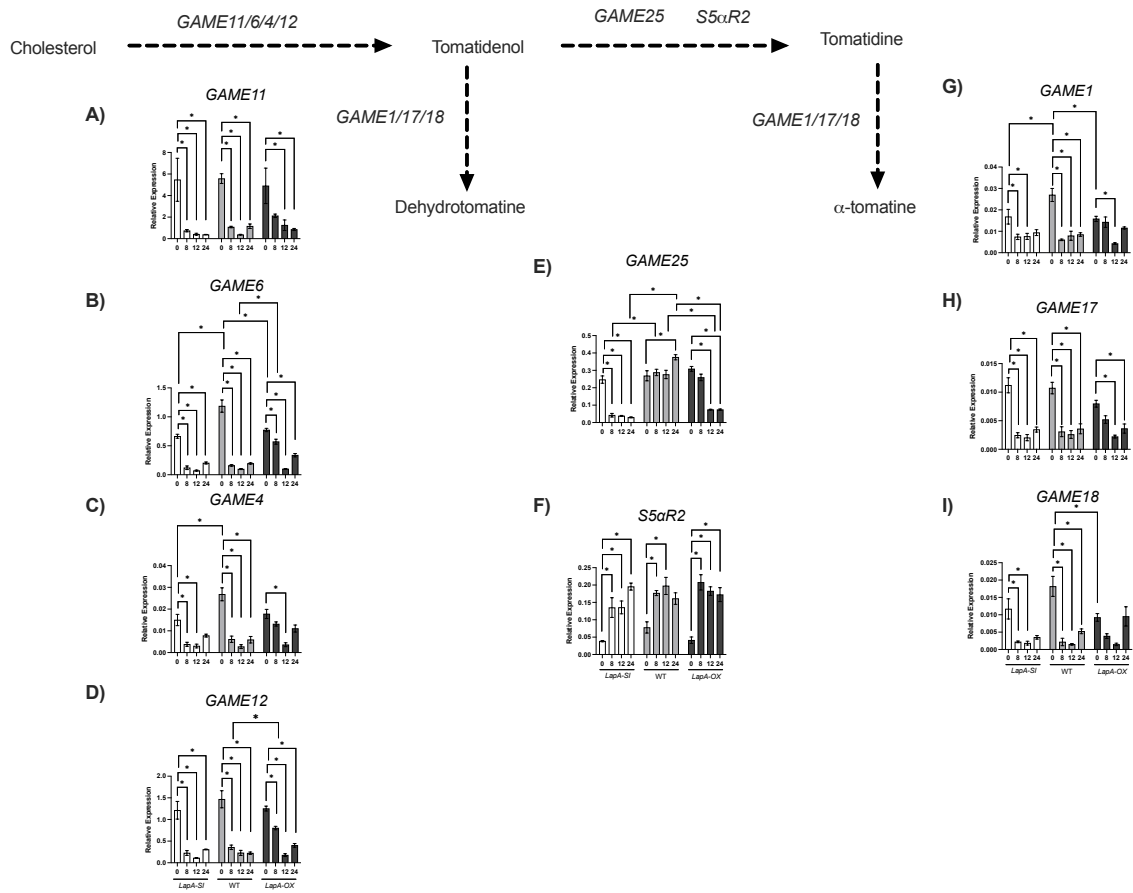
Figure 2.14 Relative transcript levels for genes encoding SGA biosynthesis pathway genes in *LapA-SI,* WT and *LapA-OX* lines after MeJA treatment. A) GAME11, B) GAME6, C) GAME4, D) GAME12, E) GAME25, F) S5αR2, G) GAME1, H) GAME17, I) GAME18. Asterisks represent statistically different values at adjusted P-value ≤ 0.05.
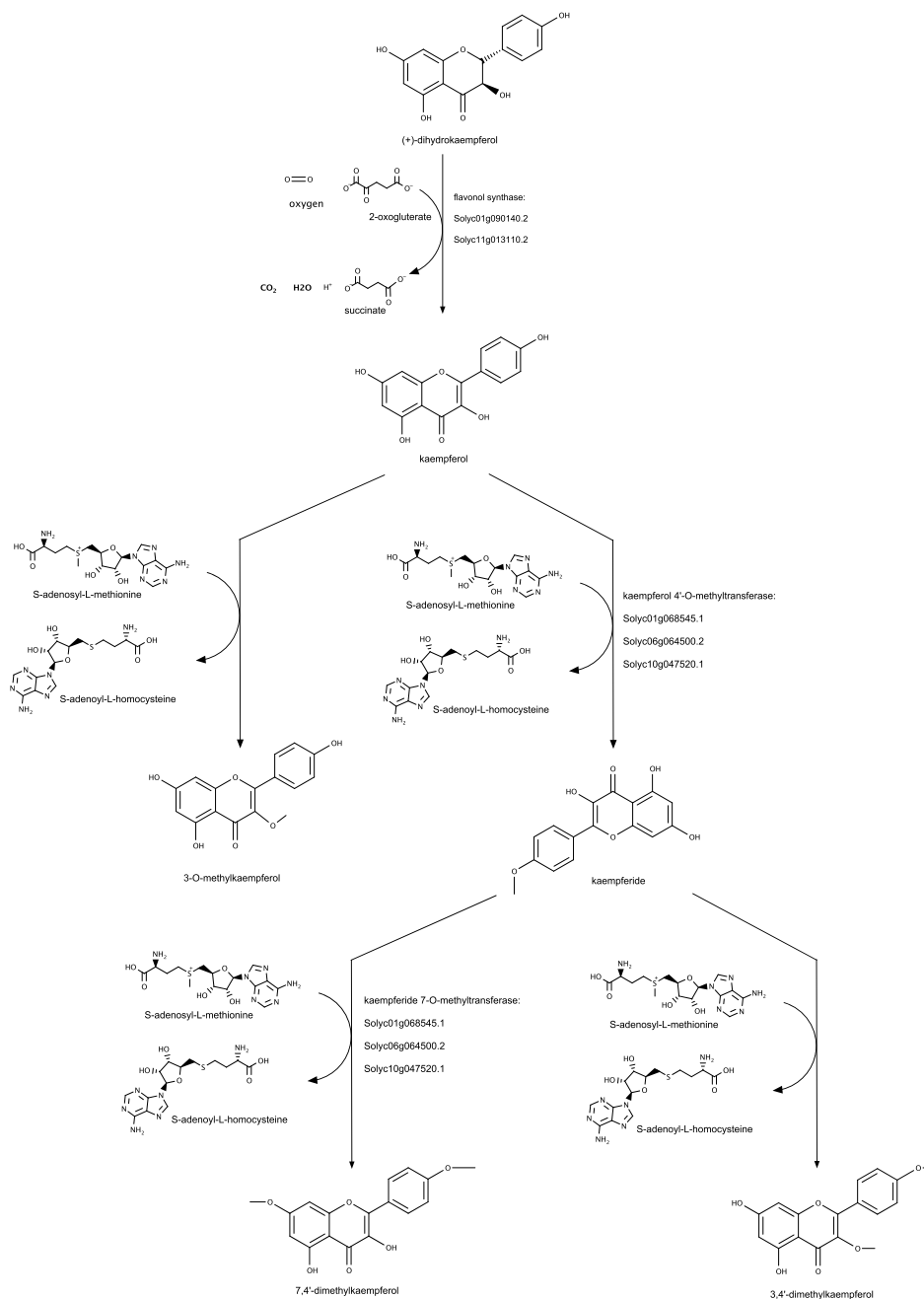
Figure 2.15 Flavonoid biosynthesis pathway. The pathway for kaempferol and kaempferal-derived. Metabolite (3'O-methylkaempferol, 7,4'-dimethylkaempferol, and 3,4'-dimethylkaempferol) biosynthesis is displayed. Biosynthetic enzymes (flavonol synthase, kaempferol 4'-O-methyltransferase, and kaemferide 7-O-methyltransferase) are also shown.
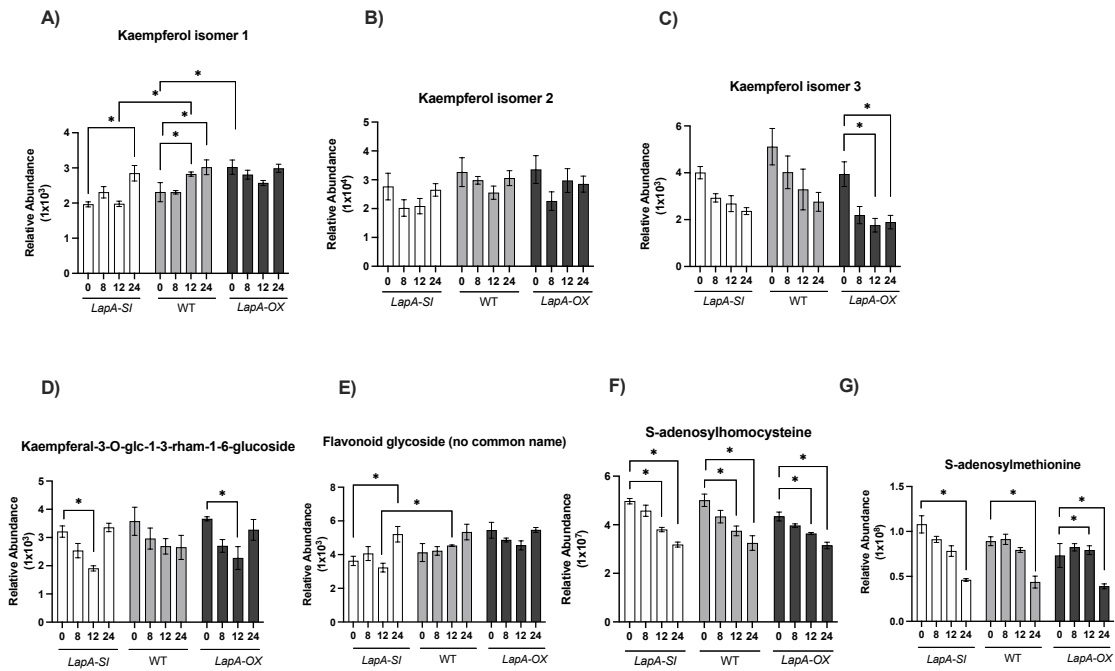
Figure 2.16 Relative abundance of kaempferol metabolites, glycosylated flavonoids, and the cofactors for flavonoid biosynthesis from LapA-SI, WT, and LapA-OX after MeJA treatment. A) kaempferol isomer 1 B) kaempferol isomer 2 C) kaempferol isomer 3 D) kaemferal-3-O-glc-1-3-rham-1-6-glucoside E) flavonoid glycoside (no common name) F) S-adenosyl homocysteine G) S-adenosylmethionine. Asterisks represent statistically different values at adjusted P-value ≤ 0.05.
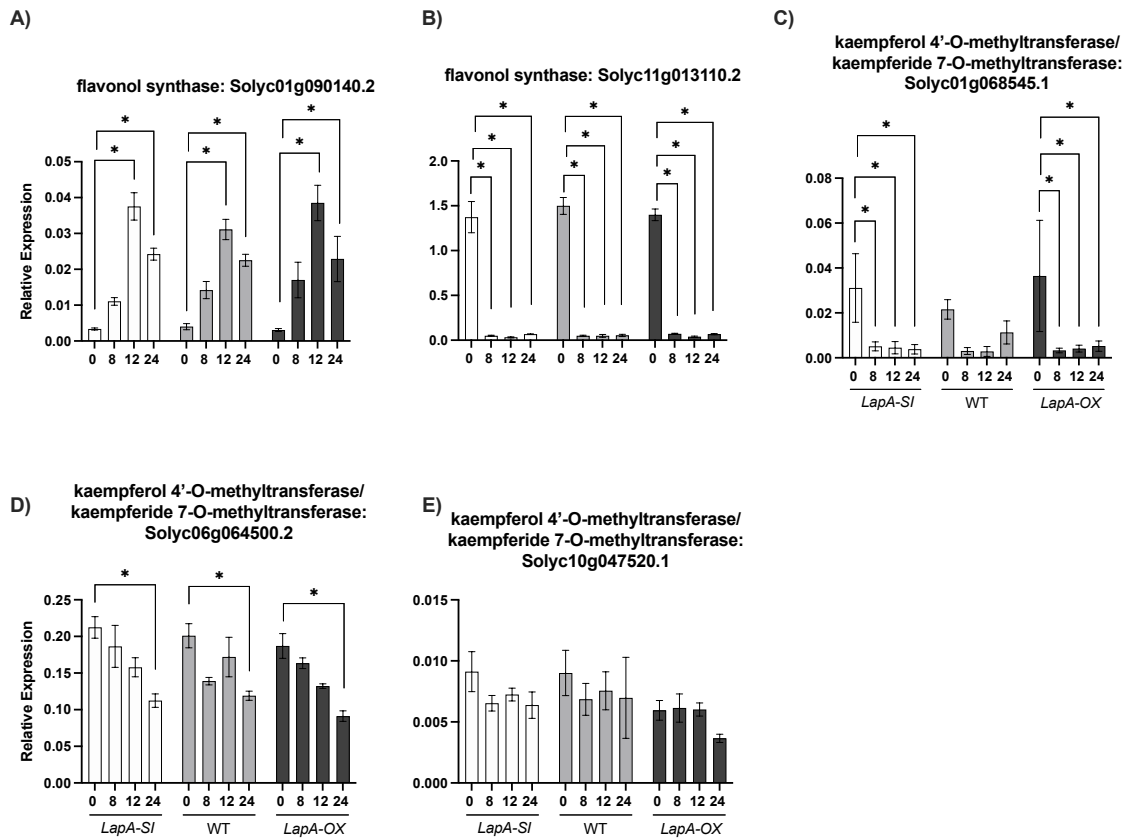
Figure 2.17 Transcript levels for genes involved in kaempferol biosynthesis in LapA-SI, WT and LapA-OX lines after MeJA treatment. A) flavonol synthase: Solyc01g090140.2, B) flavonol synthase: Solyc11g013110.2, C) kaempferol 4'-O-methyltransferase/ kaempferide 7-O-methyltransferase: Solyc01g068545.1, D) kaempferol 4'-O-methyltransferase/ kaempferide 7-O-methyltransferase: Solyc06g064500.2, E) kaempferol 4'-O-methyltransferase/ kaempferide 7-O-methyltransferase: Solyc10g047520.1 Asterisks represent statistically different values at adjusted P-value ≤ 0.05.
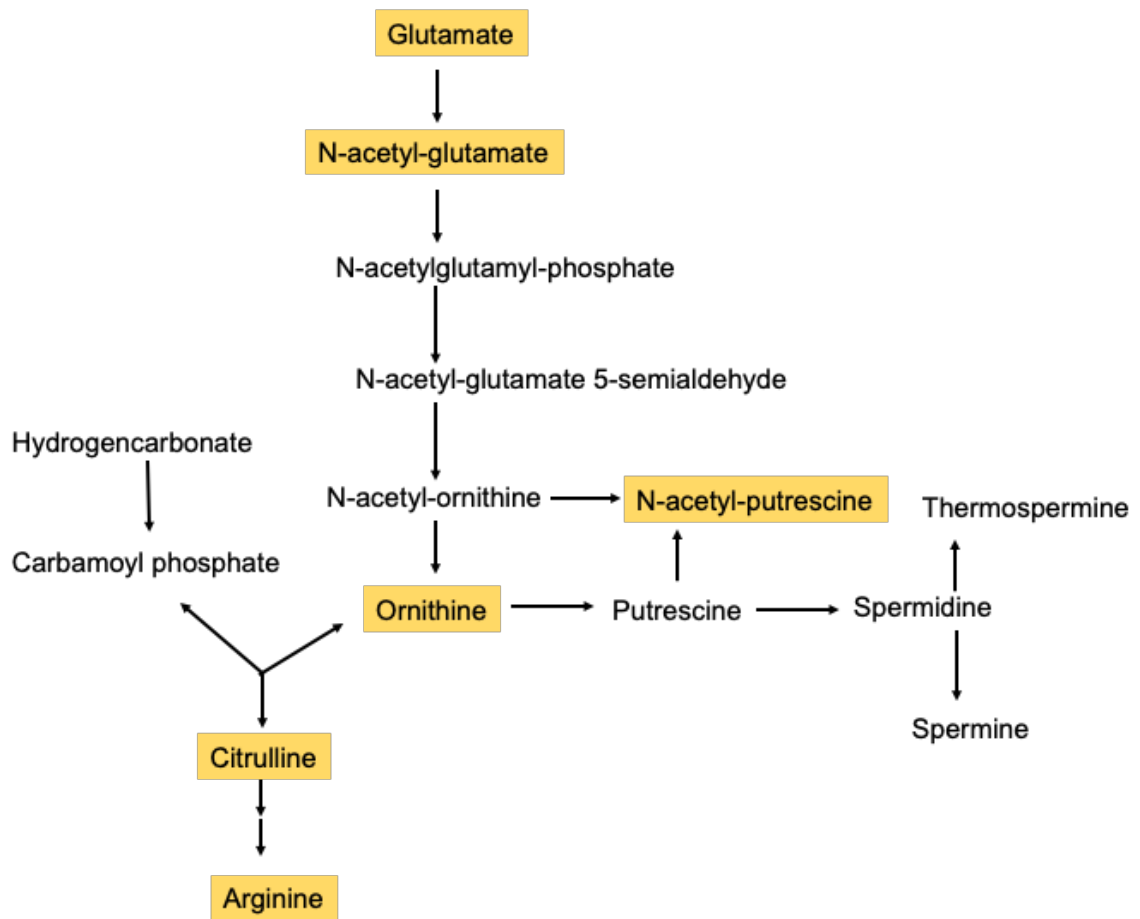
Figure 2.S1 Schematic of arginine, ornithine, cirtrulline and polyamine biosynthetic pathway. Yellow boxes represent metabolites identified.
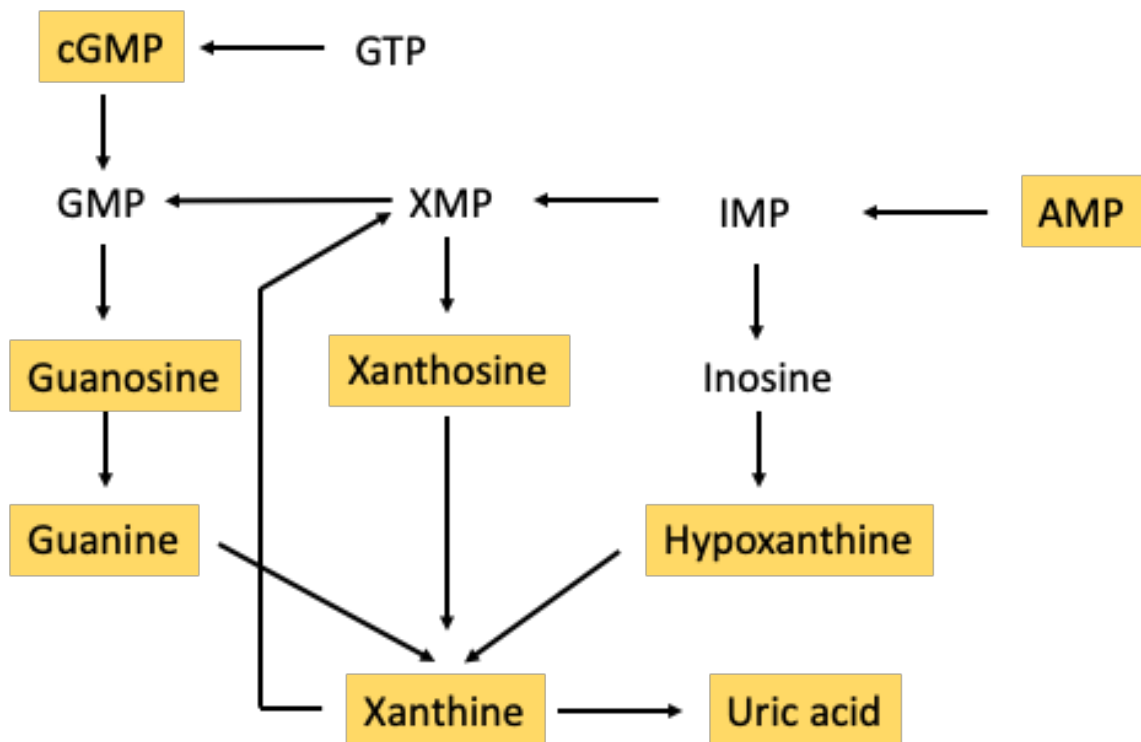
Figure 2.S2 Schematic of the purine biosynthesis pathway. Yellow boxes represent metabolites identified.
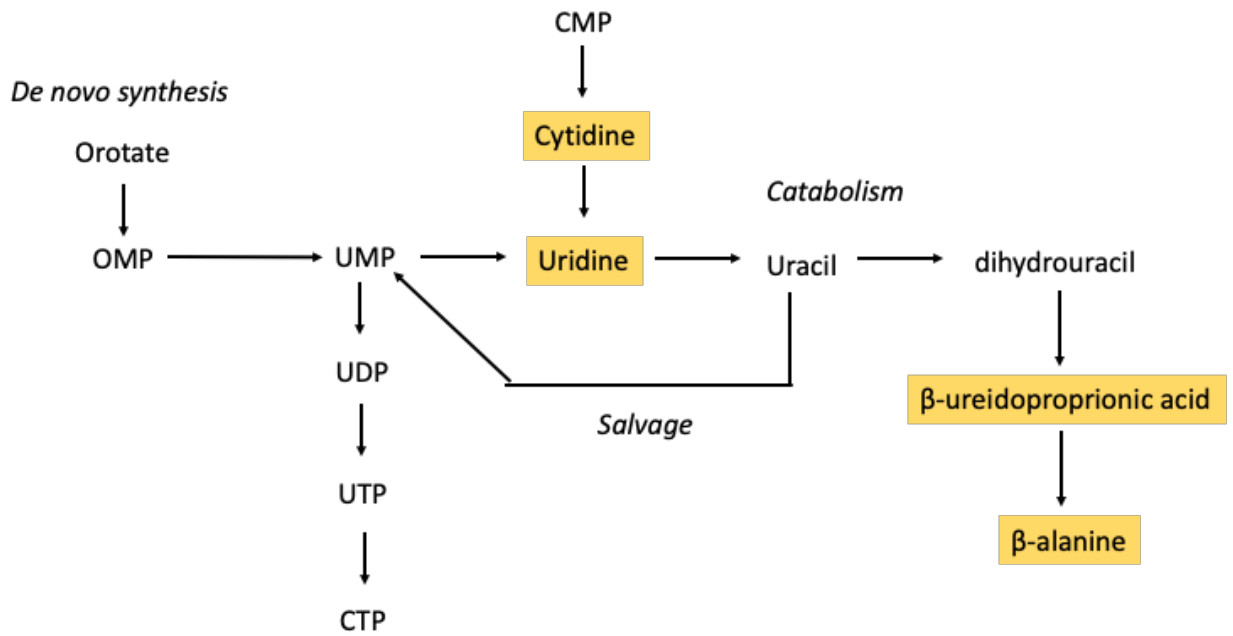
Figure 2.S3 Schematic of the pathways for de novo synthesis, catabolism and salvage of several pyrimidines. The yellow boxes represent metabolites identified.

Chapter 3: LAP's role in redox homeostasis and sulfur assimilation

Abstract

Leucine aminopeptidase A (LapA) is a jasmonate-responsive, late wound response gene in tomato. Using wild-type and transgenic plants that suppress (LapA-SI) or ectopically express (LapA-OX) LapA, we showed that LAP-A up- and downregulates defense and stress-response gene RNAs, respectively. Here we report the use of these genotypes in biochemical and metabolomics analyses to identify putative LAP-mediated retrograde signal(s) and LAP-A interacting proteins. In time-course experiments that simultaneously measured the levels of H_2O_2 and glutathione, as well as glutathione redox status, LAP-A was revealed as a regulator of H_2O_2 and the ratio of reduced to oxidized glutathione after wounding; LAP-A did not modulate glutathione levels after wounding. As H_2O_2 is an established mediator of retrograde signaling and several proteins that control reactive oxygen species (ROS) levels or repair ROS damage to macromolecules were identified, redox-dependent model for LAP-A's role in regulating H_2O_2 levels after wounding is proposed.

Introduction

In tomato, there are three Leucine aminopeptidase (Lap) genes encoding plastid-localized proteins (Walling 2013). LapN encodes a protein with a neutral pI, is constitutively expressed and is present in most plants (Chao et al. 1996; Chao et al. 1999; Chao et al. 2000; Tu et al. 2003). LapA1 and LapA2 encode two highly related LAP-A proteins with acidic pIs and are coordinately regulated by jasmonates, wounding and ABA (Chao et al. 1999; Gu et al. 1996a; Gu et al. 1996b). LAP-A and LAP-N proteins all have dual activities serving as aminopeptidases (cleaving N-terminal amino acids from peptides and proteins) and molecular chaperones (Gu et al. 1999; Gu and Walling 2002; Scranton et al. 2012). However, LapA distinguishes itself from LapN, as LapA regulates wound signaling and resistance to herbivory (Chao et al. 2000; Fowler et al. 2009). LapA-SI and Lap-OX plants are more susceptible and more resistant to caterpillar feeding in comparison to wild-type plants, respectively (Fowler et al. 2009). The chloroplast-localized LAP-A positively regulates anti-nutritive, nuclear-encoded defense genes that are expressed during the late phase of wound signaling in tomato (eg., Pin1, Pin2, and PPO) (Fowler et al. 2009; Gu et al. 1999; Gu and Walling 2002; Scranton et al. 2012); interestingly, LAP-A does not modulate tomato's early wound-response genes. LAP-A also negatively regulates a set of defense/stress-response genes such as the pathogenesis-related protein genes (PR1-c and PR1-a) and two chaperone genes (TAS14 and Dhn3) (Scranton et al. 2013).

As LAP-A is unique to the Solanaceae, the LAP-A-dependent signal(s) and its mechanism to influence nuclear gene expression may be novel. Initially we thought, LAP-A may modulate levels of a phytohormone associated with wound signaling (Chao et al. 1999; Fowler et al. 2009; Doares et al. 1995; Orozco-Cárdenas et al. 2001;

Orozco-Cárdenas and Ryan 2002; PenaCortes et al. 1996), as the chloroplast initiates synthesis of several phytohormones (e.g., jasmonic acid (JA), salicylic acid (SA), abscisic acid (ABA), gibberellic acid (GA), cytokinins, and brassinosteroids) (Wasternack and Feussner 2018; Li et al. 2019). However, we know that the levels of JA, JA-Ile, SA, SA-glucose, and ABA are similar in wild-type, LapA-SI and LapA-OX plants after wounding (Scantron et al 2013). These data suggest that the LAP-A-dependent signal(s) does not regulate phytohormone levels.

Evidence is accumulating to suggest that LAP-A induces or modulates the levels of a novel regulator or one of the known biogenic or operational retrograde signals that were identified in barley, mustard, pea, and Arabidopsis (Oelmüller et al. 1986; Sullivan and Gray 1999; Susek et al. 1993; Pogson et al. 2008; de Souza et al. 2017). Whether the signal is novel or corresponds to an established retrograde signaling molecule, LAP-A must act post-translationally within the plastid to generate or modulate this signal. Given its dual activities as an aminopeptidase and chaperone, LAP-A could directly regulate levels or activity of a protein or peptide or act indirectly to regulate a metabolite to control expression of the LapA-dependent nuclear genes. Since H_2O_2 and LAP-A both regulate the late branch of wound signaling in tomato, LAP-A may have a role in modulating H_2O_2 levels in tomato and we test this hypothesis here.

At times cross-species comparisons of gene function provide profound insights into regulatory programs and gene function. For this reason, our attention was drawn to the human LAP ortholog and its link to sulfur metabolism. In the lens of human eyes, LAP controls reactive oxygen species (ROS) formation (Taylor 1985). The human LAP catabolizes the dipeptide Cys-Gly, which is a breakdown product of the tripeptide glutathione (GSH, γ-Glu-Cys-Gly) (Cappiello et al. 2004; Habib et al. 1996). In the lens,

221

excess Cys-Gly leads to oxidative damage. Mammalian LAP cleaves Cys-Gly to eliminate this oxidative stressor and to regenerate the essential amino acid Cys. For these reasons, we interrogated LAP-A's potential link to both H_2O_2 and sulfur metabolism.

GSH acts as an antioxidant to maintain H_2O_2 at a threshold limit enabling plants to survive and, yet, generating sufficient H_2O_2 to initiate chloroplast-to-nucleus (retrograde) signaling (Foyer and Noctor 2016; Aslam et al. 2021; de Souza et al. 2017). GSH-mediated ROS detoxification involves a series of enzymes in the ascorbate-glutathione cycle (AsA-GSH cycle) [i.e. ascorbate peroxidase (APX), glutathione reductase (GR), mono- dehydroascorbate reductase (MDHAR) and dehydroascorbate reductase (DHAR)], and their associated metabolites (i.e. ascorbate (AsA) and GSH) to catabolize H_2O_2 (Hasanuzzaman et al. 2020).

As GSH is abundant, reaching millimolar levels in many plant cell subcellular compartments (Choudhury et al. 2018; Noctor et al. 2012), GSH is a Cys reservoir. GSH is catabolized to γ-Glu and Cys-Gly by γ–glutamyl transpeptidase (GGT) (Ferretti et al. 2009; Martin and Slovin 2000). The catabolism of Cys-Gly is imperative to release free Cys for GSH metabolism and other metabolic pathways, and to reduce levels of Cys-Gly, which can cause oxidative damage to cells (Del Bello et al. 1999; Del Corso et al. 2002; Dominici et al. 1999; Enoiu et al. 2000). However, while the mechanism of Cys-Gly hydrolysis is known in humans (Cappiello et al. 2004; Habib et al. 1996), it has remained elusive in plants. Our previous studies suggested a link of tomato's LAP-A and GSH catabolism. In vitro His_6-LAP cleaves Cys-Gly (Fig 3.1) but it does not hydrolyze the tripeptide GSH (Scranton 2013). In addition, the cytosolic LAP1 of Arabidopsis also cleaves Cys-Gly (Scranton 2013; Kumar et al. 2015). These data suggested a role of

LAP-A in regenerating Cys from Cys-Gly in vivo and providing a potential link of LAP-A to GSH and H_2O_2 level control.

For the reasons above, we hypothesized LAP-A has a role in GSH turnover, H_2O_2 production and, specifically, hydrolysis of Cys-Gly. Our previous studies also support this link to H_2O_2. We know that LAP-A only regulates genes expressed in the late phase of the wound-response (Fowler et al. 2009) and that H_2O_2 is a positive regulator of this branch of signaling in tomato (Orozco-Cárdenas et al. 2001). For these reasons, biochemical and metabolomics assays were done to compare LAP-A's impact on the levels of GSH, Cys-Gly and H_2O_2, as well as GSH redox status using control and wounded wild-type (wild-type), LapA-silenced (LapA-SI) and LapA-overexpressing (LapA-OX) plants.

To further interrogate the role of LAP-A's potential link to ROS and sulfur metabolism, we identified suite of ROS-responsive genes in tomato and determined their response to H_2O_2 in wild-type, LapA-SI and LapA-OX lines (Table 3.1). By integrating these data with our current proteome (Chapter 1) (Table 3.2) and metabolomics data from Chapter 2 (Tables 2.1- 2.2), we revealed LAP-A's role in ROS, defense and retrograde signaling. Finally, the identification of LAP-A and LAP-N protein interactors has shed light on several protein functions unique and shared between both forms of LAP. We focused on analyzing the plastid-localized LAP-A interactors here, using the LAP-N interactors to remove non-specific interactions. Link of these interactors to H_2O_2, defense and protein homeostasis is discussed.

Results

To rigorously assess the link of LAP-A to H_2O_2, Cys-Gly, and GSH, we assessed the

levels of H_2O_2 and thiols in wild-type, LapA-SI, LapA-OX plants from the same samples

of wounded or control leaf tissue (Fig 3.2). This is a novel approach initially pioneered by

a former graduate student in the Walling lab, Missy Scranton (Scranton 2013). Samples

were processed and split into three aliquots to measure thiols, glutathione redox status,

and H_2O_2 levels. Thiol extraction and quantification of Cys, Cys-Gly, γ-Glu-Cys, and GSH

were based on the High-Performance Liquid Chromatography (HPLC) methods of

Queval and Noctor (2007). The ratio of reduced and oxidized GSH and H_2O_2 was

assessed biochemically with methods adapted from Queval et al. (2008) and Rao et al.

(2000). The advantage of integrating the thiol measurements, GSH redox status and

H_2O_2 levels from one sample was it was time efficient and limited biological variation (Fig

3.2).

LAP-A regulates H_2O_2

With the goal of determining the LAP-A-dependent changes in H_2O_2, GSH and

GSH catabolite levels, and GSH redox status, we assessed levels of these key

metabolites in leaves from wild-type, LapA-SI, and LapA-OX tomatoes at 0, 1, 8, 12, and

24 h after wounding (Fig 3.3). The wounding time course revealed that H_2O_2 levels in

wild-type, LapA-SI and LapA-OX increased after damage with peak levels attained at 8-

12 h. LAP-A regulation of H_2O_2 was demonstrated at two time points. H_2O_2 levels were

significantly higher in LapA-SI compared to wild-type plants at 8 h post wounding and

strong trends for elevated H_2O_2 were also seen at 4 and 12 h after wounding. In addition,

LAP-A levels were significantly lower in LapA-OX relative to wild-type at 24 h.

Collectively, these data suggest that LAP-A suppresses wound-induced H_2O_2, which is

known to be a critical signal in modulating the late-branch of wound signaling in tomato (Orozco-Cárdenas et al. 2001). In addition, H_2O_2 is a known retrograde signal in Arabidopsis (Exposito-Rodriguez et al. 2017).

LAP-A does not control GSH or Cys-Gly levels in vivo

GSH is a critical antioxidant for maintaining redox homeostasis and H_2O_2 levels in plants subcellular compartments (Aslam et al. 2021; Noctor et al. 2012). The mammalian LAP, Arabidopsis LAP1 and tomato LAP-A are able to hydrolyze the GSH catabolite Cys-Gly (Fig 3.1) (Cappiello et al. 2004; Habib et al. 1996; Scranton 2013). If LAP-A mediated Cys-Gly turnover, LAP-A may control the free Cys pool that required for GSH and Met biosynthesis and the levels of GSH and GSSG may be altered in LapA mutants relative to wild-type plants. Using a targeted metabolomics approach, we measured the levels of monobromobimane (mBB)-conjugated GSH, Cys-Gly, γGlu-Cys, and Cys after wounding in the three genotypes (Fig. 3.4). GSH increased significantly after wounding in LapA-SI and LapA-OX compared to wild-type leaves; these increases were not LAP-A dependent. There was also a trend of elevated level of Cys-Gly in LapA-SI. At 24 h after wounding, Cys levels increased significantly in LapA-SI leaves compared wild-type (Fig 3.4C). However, this reciprocal response was not observed in LapA-OX leaves compared to wild-type. The GSH precursor γGlu-Cys was significantly reduced in all three genotypes within one h after mechanical wounding; this regulation was LAP-A independent (Fig 3.4D).

GSH and GSSG levels in response to wounding were determined biochemically using a spectrophotometric glutathione reductase assay described by Queval and Noctor (2007) (Fig 3.5). While LAP-A did not modulate total GSH or total GSSG levels, wounding modulated the GSH/GSSG ratio. In all three genotypes, the GSH and GSSG

levels increased after wounding as observed in Fig. 3.4A. Strong trends suggest that the GSH/GSSG ratio increased after wounding at 1, 8 and 12 h and declined by 24 h. However, this regulation was LAP-independent.

The untargeted metabolomics analyses of MeJA-regulated metabolites also detected mBB-conjugated GSH and GSSG (Fig. 3.6; Chapter 2; Table 2.2). Unlike wounding (Fig. 3.5), GSH and GSSG declined significantly in response to MeJA treatments in all three genotypes (Fig 3.4A), this regulation was LAP-A independent. These data indicate that while MeJA treatments are often used as a proxy for wounding, these treatments have profoundly different affects in GSH and GSSG levels in tomato plants.

Redox regulation in wild-type, LapA-SI, and LapA-OX plants

Given the fact that LAP-A modulates H_2O_2 levels, it was important to understand the impacts of H_2O_2 on the expression of putative ROS-responsive genes in tomato. Using Arabidopsis orthologs, putative ROS-responsive genes and genes encoding proteins important for ROS homeostasis were identified (Table 3.1) (Scranton, 2013). The levels of five putative ROS-responsive genes were chosen for further analysis to determine their responses to H_2O_2 in wild-type, LapA-SI, and LapA-OX plants.

For the H_2O_2 treatment, excised shoots were treated with glucose and glucose oxidase and (catalase plus glucose and glucose oxidase) treatments served as a control, catalase is known to catabolize H_2O_2 to O_2 and H_2O (Orozco-Cárdenas et al. 2001). We demonstrated that catalase decreased H_2O_2 levels under our experimental conditions (Fig. 3.7A). We assessed RNA levels for genes associated with the ascorbate-GSH cycle (MDHAR1), H_2O_2 production from superoxide radical (O_2^-) (Fe-SOD2), GSH catabolism (GGT1), reduction of ROS-damaged proteins (GRX1), as well

as a gene that is induced by the ROS produced by the plasma-membrane bound NADPH-oxidase (Asparaginase 2) (Sagi et al. 2004). GGT1 and Asparinginase2 RNAs were not regulated by H_2O_2 or catalase (Fig. 3.7) these gene products are non-plastid localized. GGT1 encodes gamma-glutamyltransferase that catabolizes GSH to γ-Glu and Cys-Gly. GGT1 transcripts were upregulated in Arabidopsis after GSH treatments (Destro et al. 2011). The fact that GGT1 RNAs were not modulated by H_2O_2 or LAP-A was consistent with the levels of Cys-Gly in wild-type, LapA-SI and LapA-OX plants (Fig 3.7, Fig 3.4).

In contrast, three of the genes (MDHAR1, Fe-SOD2, and GRX1) encoded chloroplast-localized proteins and were detected in the stromal proteome (Chapter 1). None of these RNAs were modulated by H_2O_2; although there was a strong trend for MDHAR1 RNA increases in LapA-SI plants. (Fig 3.7). Surprisingly, all three transcripts increased in LapA-SI plants after catalase treatments (Fig 3.7, Table 3.1). For Fe-SOD2 and GRX1, RNA levels in LapA-SI plants was significantly higher than in wild-type plants after catalase treatment.

LAP-A's role in sulfate assimilation

Sulfur metabolism plays an important role in the regulation of ROS-scavenging systems by controlling the levels of Cys, an essential precursor of GSH (Fig. 3.8). Limitation in sulfur supply in plants results in lower levels of GSH and plant development is negatively affected (Jahan et al. 2019). Importantly, GSH levels and the reduced/oxidized ratio of GSH control plant defense and abiotic-stress responses (Choudhury et al. 2018; Diaz-Vivancos et al. 2015; Zhu et al., 2021; Aslam et al. 2021).

Sulfate is used for the production of a variety of Cys-derived primary metabolism compounds (eg., GSH and Met) (Fig. 3.8) and in secondary metabolism to produce

PAPS, which is a sulfur donor for key metabolic pathways and is the precursor for PAP (Fig 3.9). PAP is a known retrograde signal that coordinates chloroplast, nuclear and mitochondrial genome activities (Chan et al. 2016; Estavillo et al. 2011). To garner insights into LAP-A's role into early steps in sulfate assimilation (Fig 3.8), we examined the impact of LAP-A on RNAs from three ATP sulfurylase (APS) and sulfate adenylyltransferase (APR) genes and, as well as a Cys biosynthesis gene Serine acetyltransferase1 (SAT1) after H_2O_2 and catalase treatments. SAT1 uses Ser and acetyl coA to produce O-acetyl-L-serine, a precursor for the Cys that used with H_2S to produce Cys by OAS (O-acetylserine sulfhydrylase) (Fig 3.8) (Gotor et al. 2015). SAT1 RNAs were not regulated by LAP-A nor H_2O_2 (Fig 3.10B). This was mostly consistent with Cys levels after wounding in exception that Cys levels were higher in LapA-SI after wounding (Fig 3.4C).

The regulatory steps of sulfate assimilation to sulfite include the transport of sulfate into cells and the plastid and subsequent conversion to adenosine 5'-phosphosulfate by the cytosolic and plastidial ATP sulfurylase/sulfate adenylyltransferases (APSs) (Fig 3.9). APS is used for both primary and secondary metabolism. In primary metabolism, adenosine 5'-phosphosulfate is reduced to sulfite by 5'-adenylylsulfate reductase (APR) (Bohrer et al. 2015; Jez 2019). Three APR genes that encode plastid-localized APR proteins in tomato were identified; two APR3-like genes (Solyc02g080640.2.1 and Solyc02g032860.2.1) and one APR2 gene (Solyc03g031620.2.1). Support for plastid localization of these proteins was provided by their identification in the tomato chloroplast Atlas and/or stromal proteome in Chapter 1 (Table 3.1) APR3B RNA (Solyc02g032860.2.1) levels were not influenced by H_2O_2 or catalase treatments nor by the presence/absence of LAP-A (Fig 3.10B). In contrast, APR3A RNAs

228

(Solyc02g080640.4.1) were positively regulated by LAP-A in untreated controls and after catalase treatments (Fig 3.10C). In contrast, APR2 RNAs declined after H_2O_2 and catalase treatments in wild-type and LapA-OX plants but were not responsive to either treatment in LapA-SI plants (Fig 3.10D). LAP-A was a positive regulator of APR2 RNA at 0 h, as wild-type plants had higher levels of APR2 RNA than LapA-SI; a similar trend was seen in LapA-OX plants.

LAP-A and LAP-N protein interactors

Our targeted and untargeted metabolomics studies, in conjunction with our methyl jasmonate-regulated proteomes of wild-type, LapA-SI and LapA-OX plants, indicate that LAP-A has a significant impact on the wound- and MeJA-regulated metabolomes and proteomes. Insights into the LAP-A-dependent mechanism used to control these metabolites and proteins may be revealed by identifying the proteins that interact with LAP-A.

To this end, LAP-A interacting proteins were identified using an affinity purification assay. We used proteins from MeJA-treated wild-type leaves, as LAP-A acts downstream of JA perception. In addition, since wounding disrupts cellular and organellar integrity and damage-associated proteins and metabolites are known to be important in defense signaling, it is possible that LAP-A would interact with proteins from non-plastidial cell compartments, as well as proteins localized in chloroplasts. Putative LAP-A interactors were bound to resin immobilized His-tagged LAP-A-wild-type and LAP-A-R431A because the latter protein is a catalytically inactive mutant. The use of a LAP-A catalytically inactive mutant assured us that we would not lose substrates that would possibly be cleaved and released due to active LAP-A in wild-type protein extracts.

Leaf protein extracts (in three technical replicates) were poured over the column with immobilized His-tagged LAP-A (wild-type) or mutant (R431A) proteins. Total leaf proteins bound to nickel-affinity resin in the absence of immobilized wild-type or R431A LAP-A served as a control nonspecific binding to the nickel resin (Fig 3.11). LAP-A bound proteins were eluted and concentrated using a Stratagene resin. Proteins were digested with trypsin and subjected to nanoLC-MS/MS. LAP-A interactors were identified by using semi-tryptic peptides to enhance specificity. Peptides were matched to the deduced tomato proteome and methyl jasmonome. Proteins that bound to two of three replicates for LAP-A or R341A LAP-A were given the status of putative interactor.

Of the 299 putative interactors that bound to wild-type and/or R431A LAP-A, 86 were identified in the stromal proteome (Table 3.3). The tomato chloroplast Atlas (Chapter 1) identified 114 (38%) interactors. We used two recent algorithms (DeepLoc and TargetP 2.0) to predict the subcellular location of the LAP-A interactors (Almagro Armenteros et al. 2019; Almagro Armenteros et al. 2017). DeepLoc and TargetP 2.0 identified 69 and 63 plastid-localized proteins, respectively. Collectively, these programs identified three additional proteins that were not present in the tomato chloroplast Atlas, indicating that the Atlas is a robust predictor of plastidial localization. LAP-A interactors had diverse functions (Fig. 3.12). The top three Mapman functional groups included protein biosynthesis with 50 proteins (16.7%), protein homeostasis with 29 proteins (9.7%), and carbohydrate metabolism with 17 proteins (5.7%). Subsequent manual curation of proteins resolved identity of the putative LAP-A specific interactors in the "non-assigned" Mapman bin; evidence for each interactor in the chloroplast protein Atlas, stromal proteome, and methyl jasmonome was also determined (Table 3.3; Chapter 1, Bhattacharya, Ortiz and Walling, unpublished).

To further delimit LAP-A interactors, we determined the proteins that interact with tomato's LAP-N. Like LAP-A, LAP-N is plastid localized and has both aminopeptidase and chaperone activity. However, LAP-N has a distinct substrate specificity and is not induced in response to JA, ABA, or wounding. Therefore, it was expected that LAP-N should interact with a distinct set of proteins. A comparison of the complement of LAP-N and LAP-N interactors would help define the proteins that are uniquely associated with these related LAPs and those that are shared.

Despite the high sequence conservation between the LAP-A and LAP-N proteins in the C-terminal catalytic domain, these enzymes have different substrate specificities based on aminopeptidase assays but both enzymes are potent molecular chaperones (Gu et al. 1999; Gu and Walling 2000, 2002; Scranton et al. 2012). LAP-N interactors were identified using the methods developed for LAP-A. We used a LAP-N catalytic site mutant K357E, that like LAP-A R341E, abolished catalysis but retained its hexameric structure (Scranton et al. 2012). There were 652 putative wild-type LAP-N and/or K357E LAP-N interactors (Table 3.4). As anticipated, the complement of LAP-N interactors was distinct from LAP-A, with only 68 proteins that were bound by both enzymes (Fig. 3.13). While the LAP-N interactors have not yet been thoroughly characterized, it was clear that the relative affinities of the interactors for LAP-A and LAP-N identified were different. High-affinity interactors were identified based on their ability to bind in all three biological replicates using a wild-type or catalytically inactive LAP (Tables 3.3- 3.4). Over 38% and 22% of the LAP-N and LAP-A interactors, respectively, bound in all three replicate samples for wild-type and mutant proteins (Fig 3.14). In addition, the high-affinity proteins that bound only to the wild-type LAP-A or LAP-N were less frequent than proteins only binding the mutant enzymes or to both enzymes.

231

Using the LAP-N and LAP-A interactor datasets, we identified 231 LAP-A-specific interactors (Figure 3.13). As LAP-A resides within the chloroplast stroma, we focused on the 86 interactors that were LAP-A specific and co-localized with LAP-A in the chloroplast (Table 3.3C). The LAP-A specific interactors had a wide array of functions. Given LAP-A's role as an aminopeptidase and molecular chaperone, in controlling H_2O_2 and having a role in chloroplast-nuclear communication (Gu et al. 1999; Gu and Walling 2002; Scranton 2013; Fowler et al. 2009), we focused on proteins involved with protein turnover, folding, and modification, as well as redox, stress responses, and sulfur metabolism (Table 3.3C).

LAP-A interacts with proteins associated with ROS homeostasis.

Given LAP-A's role in controlling H_2O_2 after wounding, interactors involved in ROS homeostasis were examined including a glutaredoxin, two thioredoxins, and glutathione reductase. The cytosolic GR1 and plastidial GR2 proteins were LAP-A interactors (Table 3.3C-D; Table 3.4). GRs catalyze the reduction of glutathione disulfide (GSSG) to GSH to maintain cellular redox status (Fig. 3.8). However, GSH and GSSG levels and the GSH:GSSG ratios were not LAP-A dependent, suggesting that the GR-LAP-A interaction may not impact GSH metabolism or redox state and its significance is not clear at the present time (Fig. 3.5-3.6). Another link to GSH redox status was the fact that the cytosolic ascorbate peroxidase (APX1) was a LAP-A and LAP-N interactor. The significance of the LAPs interacting with the cytosolic protein is unclear.

When ROS levels rise, proteins that are oxidatively damaged can be post-translationally modified by GSH (glutathionylation). Glutathionylation may prevent irreversible inactivation of a protein by ROS and/or modulate a protein's activity (Rouhier et al. 2008). Glutaredoxins remove GSH to return these proteins to their active forms.

Four GRXs (GRXC1, GRX1, GRX4, and GRX-like) were detected in the stromal proteome (Chapter 1, Table S1.2). Two of these plastidial GRXs and two cytosolic GRXs were detected as LAP interactors. The chloroplast-localized GRX4 protein interacted with only with LAP-A (Table 3.3C-D; Table 3.4). Whereas the chloroplast-localized GRX1 and GRX3 only interacted with LAP-N (Tables 3.2, 3.4; Chapter 1, Tables S1.2, S.1.3). These data stress the likely specificity of LAP-A vs LAP-N interactors; this must be confirmed by further molecular analyses. Whether the LAPs enhance or deter GRX activity remains to be determined.

Two chloroplast thioredoxins detected in the tomato stromal proteome were LAP-A interactors: NTRC1 and CDSP32 (Trx-L1) (Fig. S1.2; Table 3.3C). CDSP32 is a drought-induced gene in Nicotiana; in Arabidopsis it is induced by heat stress, but not by ABA or drought stress (Pant et al. 2020). Its regulation in tomato is currently unknown. In Arabidopsis, AtTRXL1 interacts with over 400 proteins, is degraded by the Clp protease, and it is protected from degradation by the chaperone CPN60 (Pant et al. 2020). AtTRXL1 and the Nicotiana CDSP32 have a role in defense and thermotolerance by regulating the activity of malate dehydrogenase activity. AtTRXL1 is also important for regenerating methionine sulfoxide reductase (MSR4), which reduces Met sulfoxide to Met; Met sulfoxide is readily produced in response to ROS (Romero et al. 2004). MSR4 was also identified as a LAP-A-specific interactor (Table 3.3C).

LAP-A specifically interacts with NADPH thioredoxin reductase-C (NTRC1). Unlike Arabidopsis, the tomato genome contains two NTRC genes; however only the NTRC1 protein was detected in the stromal proteome (Tables S1.2, S1.16). AtNTRC has a key role in controlling redox status and dissipation of H_2O_2. It acts through 2-CysPrxA and B (2-Cys peroxiredoxin) (Muthuramalingam et al. 2009). In addition, fructose-1,6-

bisphosphatase (FBPase), a known NTRC interactor in Arabidopsis is a LAP partner (Table 3.4), we propose a LAP-A dependent redox model (Fig 3.15). However, our current data and analyses suggest that LAP-A directly interacts with NTRC1 (3/3 samples) and, interestingly, 2-CysPrx is an LAP-N interactor.

NTRC1 provides the reducing power for regenerating 2-CysPrx, which is a redox-dependent molecular hub in the chloroplast (Muthuramalingam et al. 2009). 2-CysPrx acts as a peroxidase, chaperone, thiol oxidase, and a modulator of cell signaling. 2-CysPrxs catabolize H_2O_2, lipid hydroperoxides, and peroxynitrates to limit cell damage (Ishiga et al. 2012; Rey et al. 2005; Stenbaek et al. 2008). 2-CysPrx is a redox sensor that changes its form (dimer, decamer, and high molecular weight (HMW) oligomers) and activity (peroxidase vs chaperone vs inactive aggregate) dependent on the redox status and pH of the chloroplast (Dietz et al. 2006).

We hypothesize that LAP-A influences this pathway via NTRC1 (Table 3.3); the net outcome of LAP-A action must be to control H_2O_2 (Fig 3.15). As LAP-A-deficient LapA-SI plants accumulate more H_2O_2 than wild-type plants, LAP-A must enable NTRC1's reduction of 2-CysPrx to control the H_2O_2 burst that occurs in response to wounding. We propose that LAP-A enhances amount of bioactive 2-CysPrx (reduced form) to: (1) control H_2O_2 levels (2) limit protein and lipid damage, (3) limit accumulation of insoluble protein aggregates that cause plant cell death, and (4) regulate key redox sensitive chloroplast enzymes (Table 3.3). In Arabidopsis, known 2-CysPrx-binding partners include: NTRC (Muthuramalingam et al. 2009), thioredoxins (Trx-x, Trx-m, and CDSP32), FBPase, athe cyclophilin Cyp20-3 (Konig et al. 2002; Collin et al. 2003; Broin and Rey 2003; Laxa et al. 2007; Rey et al. 2005). Interestingly, FBPase, CDSP32 and NTRC were identified as LAP-A interacting proteins indicating the specificity of LAP-A's

interactions; tomato does not have a Cyp20-3 ortholog (Chapter 1, Table S1.6). These data suggest that LAP-A may play a role in this redox hub via its interaction with NTRC1.

LAP-A and sulfur metabolism

Several proteins linked to primary and secondary sulfur metabolism interacted with LAP-A. Amongst the chloroplast localized, LAP-A-specific interactors was APS (ATP sulfurylase) that uses sulfate to produce adenosine 5'-phosphate (Table 3.2, 3.3; Fig. 3.8). APS (Solyc03g005260) is a moderately abundant protein (0.02% mol %) detected in the tomato stroma (Chapter 1, Table 1.S2). APS interacted in all three LAP-A and one R431A binding assays. It is possible the Arg to Ala substitution in the LAP-A catalytic site negatively affects LAP-A's binding with APS. APS is of particular interest because it's the first enzyme reaction for sulfate conversion to adenosine 5'-phosphosulfate (Fig 3.8), which is used for the synthesis of Cys and PAPS/PAP (Fig 3.9). While APR2 and APR3A RNAs were wound and LAP-A regulated, they were not detected as a LAP-A or LAP-N partner. Unfortunately, the metabolites between adenosine 5'-phosphosulfate and Cys, as well as PAPS and PAP secondary sulfur metabolism was hard to predict.

Cys is used to synthesize cystathionine. For synthesis of Met and S-adenosylmethionine (SAM), cystathionine β-lyase catabolizes cystathionine to produce L-homocysteine, the precursor of Met (Fig 3.8). Cystathionine β-lyase interacts with both LAP-A and LAP-N (Table 3.3D). The impact of LAPs on cystathionine β-lyase stability and or activity would be important to assess in the future. Since Met levels increase after wounding, we postulate that LAPs might enhance cellular cystathionine β-lyase activity (Fig 3.8, Chapter 2, Table 2.1).

Met is catabolized to S-adenosylmethionine (SAM), which is used in numerous biochemical processes including polyamine, ethylene, transulfurylation reactions (Met

salvage) and transmethylation (eg., DNA, RNA, proteins, and lipids). SAM synthesis occurs in the cytosol. Surprisingly, two of the four SAM synthase proteins, (Solyc09g008280.2.1 and Solyc10g083970.1.1) interacted with LAP-A and LAP-N (Table 3.3). Transcripts for these interactors were down-regulated by SA, ABA and brassinosteroids and these transcripts were inversely regulated by water-deficit stress (Heidari et al. 2020). These SAMs were not MeJA regulated based on our methyl jasmonome (Bhattacharya, Ortiz and Walling, unpublished results). While SAMs are cytosolic and synthesize SAM from Met, the discovery of two SAM synthase proteins as LAP-A and LAP-N interactors is intriguing since the metabolite S-adenosylmethionine is down-regulated after MeJA treatment (Chapter 2, Table 2.1; Fig 3.8). Collectively, these data imply that LAPs might interfere with SAM synthesis from Met. Alternatively, other metabolic pathways are consuming SAM after wounding. The first option is supported by the fact that Met was upregulated after wounding and upregulated by LAP-A at 24 h post-MeJA treatment (Chapter 2). Neither LAP-A nor LAP-N interacted with the enzymes critical for Met recycling via S-adenosylhomocysteine and L-homocysteine or for polyamine biosynthesis.

LAP-A interacts with proteins involved in protein turnover and modification.

Of the chloroplast localized proteases, LAP interactions were found with subunits of the stromal proteolytic complex CLP and for oligopeptidase A (aka, OOP or TOP). OOP is critical for catabolizing transit peptides after their cleavage from their preproteins. LAP-A may further catabolize these peptides based on its aminopeptidase activity or LAP-A chaperone activity could be important for OOP stability and function. LAP-A also interacted with four CLP subunits; ClpC2, ClpP4, ClpR1 and ClpR4. While the interactions with ClpR1 and ClpP4 were LAP-A specific interactors, ClpC2 and ClpR4

bound both LAP-A and LAP-N. This suggests there may have a second mode of action of LAP action. We propose that, via interactions with ClpC2, LAP-A and/or LAP-N may direct substrates to the Clp proteolytic complex for turnover; alternatively, the LAPs may interfere with substrate delivery and promote target protein stabilization. Given the LAP-A specific interactions with Clp and OOP is possible that LAP-A forms a novel mega complex with OOP and (perhaps) the Clp protease to promote the turnover of newly imported proteins or their transit peptides. Finally, we predict that LAP-A may change the quality and quantity of Clp-derived peptides; these peptides serve as the mobile retrograde signal. Peptides exported from mitochondria make up the mitochondrial unfolded-protein response (UPR) (Vogtle and Meisinger 2012). A graduate student in the Walling lab (Paul Roche) is investigating the LAP-A dependent Bioactive Peptide Model hypothesis.

Discussion

Based on time-course analysis of H_2O_2 accumulation after wounding, we conclude that LAP-A regulated H_2O_2 production (Fig 3.3). LAP-A is critical for the expression of genes in the late branch of wound signaling (Fowler et al. 2009) and previous studies showed that H_2O_2 amplifies the late wound-signaling branch (Orozco-Cárdenas et al. 2001). Based on the stromal location of LAP-A, our data suggests that wound-generated H_2O_2 is chloroplast derived. This conclusion contrasts with the conclusions of Orozco-Cárdenas et al. (2001) who demonstrated using chemical inhibitors that the plasma-membrane bound NADPH oxidase and SOD were responsible for generating H_2O_2. As H_2O_2 is sufficiently long lived and mobile, H_2O_2 derived from the apoplast was reasoned to be the regulator of the late branch of wound signaling. We challenge that long-standing dogma.

We suggest LAP-A may enhance the functionality of the main redox hub of the chloroplast that involves NTRC and 2-CysPrx. Unlike Arabidopsis tomato has two NTRC genes. LAP-A specifically interacted with NTRC1, but not NTRC2 (Solyc04g016010). NTRC2 RNAs are not influenced by MeJA treatments, whereas NTRC1 transcripts are downregulated by MeJA within 30 min after treatment (Roche and Walling, unpublished results). If NTRC1 protein levels also decline after MeJA treatment the NTRC/2CysPrx hub would be compromised resulting in a H_2O_2 burst. It is possible that LAP-A stabilizes the remaining NTRC1 protein enabling H_2O_2 scavenging to continue. A model for LAP-A action is based on its ability to interact with NTRC is derived from the Arabidopsis literature (Muthuramalingam et al. 2009) (Fig 3.14); however, there are a small number of papers examining NTRC and ROS after pathogen infection in tomato and tobacco and they support this general model.

Under non-stress conditions, NTRC reduces the inactive 2-CysPrx dimer (with a disulfide bond between its two subunits) and 2-CysPrx assembles into an active decamer (Puerto-Galán et al. 2015). The reduced 2-CysPrx decamer can catabolize H_2O_2 and other hydroperoxides (eg., hydroperoxylipids and peroxynitiles) (Peltier et al. 2006; Konig et al. 2002). While catabolizing hydroperoxides, a transient 2-CysPrx sulfenic intermediate is formed and it is slowly resolved to reform the dimer's disulfide bond and, at this time, the decamer disassembles into inactive dimers. The decameric form (the active peroxidase) is associated with the thylakoid membranes, where it appears to scavenge electrons and catabolize H_2O_2. Under highly oxidative conditions, 2-CysPrx becomes over-oxidized to the sulfinic and sulfonic forms. The sulfinic form can be reduced by sulfiredoxin (SRX) and disulfide bridges in the dimer form and the redox cycle can reinitiate. The sulfinic decamer can make a multimer, which is an active

chaperone; the chaperone binds FBPase to regulate its activity. The over-oxidized sulfonic form is non-reversibly damaged and to date there is no mechanism to return the sulfonic 2-CysPrx to the sulfinic or sulfenic forms.

We propose that LAP-A/NTRC1 interaction promotes the ability of NTRC1 to reduce its substrates. 2-CysPrx and FBPase are NTRC1 interactors; NTRC1 is a LAP-A target. We propose that the wound-induced LAP-A binds NTRC to either promotes NTRC's reduction of the sulfhydryl bonds in the inactive 2-CysPrx dimer or to extend the life time of NTRC1 after MeJA treatments or wounding. We propose that in LapA-SI plants, LAP-A levels are diminished and, therefore, NTRC1 activity is diminished, causing a decline in active 2-CysPrx dimers and impairing efficient H_2O_2 scavenging and promoting the generation of a transient ROS signal, promoting protein and lipid damage, promoting insoluble protein aggregates, and altering the regulator of key redox responsive enzymes (eg., FBPase). At the present time, it is unclear if LAP-A's aminopeptidase and/or chaperone activity is required to modulate NTRC.

Given the ability of LAP-A to cleave Cys-Gly and the importance of recycling Cys-Gly to retrieve Cys and to alleviate the oxidative damage induced by this dipeptide, we had proposed the wild-type, LapA-SI and LapA-OX plants would have distinctly different levels of Cys, Cys-Gly and GSH levels. This proposed role for LAP-A was also consistent with the importance of GSH in scavenging H_2O_2. We anticipated that LapA-SI plants would have lower levels of GSH and Cys and higher levels of Cys-Gly and H_2O_2. While Lap-A modulated H_2O_2 levels, it did not control the levels of reduced (GSH) or oxidized (GSSG) glutathione after wounding, nor did it influence the GSH:GSSG ratio (Fig 3.4-3.6).

In these studies, we discovered an anomaly. MeJA is often used as proxy for mechanical wounding, since there is a substantial overlap in MeJA- and wound-induced cellular responses. Surprisingly, we observed that MeJA and wounding impacted GSH and GSSG levels in completely different ways. We observed an increase in GSH and GSSG levels after wounding (Chapter 2, Table 2.2, Fig. 3.5). In contrast, after MeJA treatments GSH and GSSR levels declined (Fig 3.6). Wound induced increases of H_2O_2 in tomato is well established (Orozco-Cárdenas et al. 2001).

Since H_2O_2 was regulated by LAP-A and increased after wounding, we monitored the RNAs from a set of putative ROS-response genes (MDHAR1, SOD2, and GRX1) (Table 3.1, Fig 3.7). Although catalase catabolized H_2O_2 in vitro, catalase treatments did not dissipate the H_2O_2 increases in these RNA (Fig 3.7, 3.10). Instead, catalase caused increases in all three of these transcripts. While a simple explanation is not clear, it is possible that there may be a feedback loop. In response to higher levels of H_2O_2, genes are induced but at modest levels. In the total absence of H_2O_2 (e.g., the catalase treatment), genes are hyperinduced.

LAP-A influences S metabolism. LAP-A upregulated genes encoding two key enzymes in sulfur assimilation (APR and APS) (Table 3.1- 3.2). Both APR3A and APR2 RNAs were upregulated by LAP-A (Table 3.1- 3.3, Fig. 3.10). APR3 reduces its substrate adenosine 5'-phosphosulfate to sulfite using GSH (Fig 3.8) (Bekturova et al. 2021; Cohen et al. 2020). Although APR's main substrate is adenosine 5'-phosphosulfate, APR also reduces 3'-phosphoadenosine 5'-phosphate (PAP) using sulfite and an oxidized thioredoxin protein (Setya et al. 1996; Gutierrez-Marcos et al. 1996). PAP is a key retrograde operational signal (Estavillo et al. (2011). Unfortunately, the compounds PAP and PAPS were not detected in wild-type, LapA-SI, and LapA-OX

leaves after MeJA treatment. The regulation of APR by LAP-A may result in different PAPS and PAP levels. Again, this model is extrapolated from Arabidopsis.

The final link to PAP is its regulation by oxidative stress. SAL1 catabolizes PAP Estavillo et al. (2011) and increases in ROS cause damage and inactivate the chloroplast SAL1 allowing PAP accumulation (Chan et al. 2016). When PAP levels rise in the chloroplast, PAP moves to the nucleus to regulate nuclear gene expression. SAL1-PAP retrograde signaling pathway regulates JA-mediated signaling and secondary metabolite glucosinolate pathways in Arabidopsis (Ishiga et al. 2017). This is another enticing link of LAP-A's influence on sulfur assimilation.

Finally, there were other LAP-A interactors that are worth investigation in the future because of their association with the metabolites regulated in Chapter 2. In particular, 11 LAP-A interactors were associated with lipid metabolism and a variety of lipids were LAP-A and/or MeJA regulated (Chapter 2; Table 2.2). We will look further into LAP-A's links to lipid metabolism in the near future.

Methods

Plant growth conditions

Solanum lycopersicum L. UC82 (wild-type, wild-type), LapA-SI, and LapA-OX were previously described (Fowler et al. 2009). Plants were grown in a growth chamber with an 18-h (28°C)/6-h (22°C) light dark cycle (300 μE)/. Four- to five-week-old wild-type, LapA-SI, and LapA-OX plants with three leaves per plant were used for plant treatments.

Wounding of tomato leaves

Four- to-five-week-old tomato plants (wild-type, LapA-SI, and LapA-OX) were used for wound time course experiments. Plants were wounded by crushing leaflets with a pair of needle-nosed pliers. Wounded leaves were collected at 0, 1, 8, 12, and 24 h post-

wounding. For each treatment's time point, leaves of three plants were pooled for analysis. Fresh leaf tissue (500 mg) was flash frozen in liquid nitrogen and stored at -80°C. Five biological replicate experiments were used for liquid chromatography-mass spectrometry (LC-MS) and thiol analyses.

H_2O_2 plant treatments

H_2O_2 and control treatments of tomato shoots were performed (Orozco-Cárdenas et al. 2001). Briefly, excised shoots from four-week-old plants (wild-type, LapA-SI, and LapA-OX) were placed in flasks with 10 mM phosphate buffer (PB) (pH 6.0) (control) or in 10 mM PB with 50 mM glucose (Glu) and 25 U/mL glucose oxidase (GO; Cat #G7141, Sigma-Aldrich). As a negative control, plants were also placed in a 10 mM PB with 50 mM Glu, 25 U/mL GO, and 25 U/mL catalase (CAT; Cat #C1345, Sigma-Aldrich). Leaves were harvested at 0 and 8 h after treatment. The leaves from three plants were pooled together and the sample fresh weight was weighed at 500 mg. Harvested leaf tissue was flash frozen with liquid nitrogen and stored at -80°C until use. Three biological replicates and three technical replicates of the experiment were performed for quantitative real-time polymerase chain reactions (qRT-PCR) analysis.

Methyl jasmonate treatments

For methyl jasmonate (MeJA) (Cat #392707, Sigma-Aldrich) treatment for identifying LAP-A and LAP-N interactors, three wild-type, LapA-SI and LapA-OX plants that were four-weeks-old were excised at the base of the shoot and placed in flasks with 10 µM MeJA for 24 h as previously described (Chao et al. 1999). Leaves from three plants were harvested and pooled. Harvested leaf tissue was flash frozen with liquid nitrogen and stored at -80°C until use for protein isolation and affinity purification. There was not a time course experiment conducted in this study.

Sample preparation for thiols, H₂O₂, GSH, and GSSG Measurements

Frozen wounded leaf tissue (500 mg) was ground in liquid nitrogen with a cold mortar and pestle. Four samples were processed at a time. Due to the number of samples and need for simultaneous processing, this was a two-person procedure. Under my direction, Dr. Maria Irigoyen or Ms. Diana Medina-Yerena helped to prepare the samples for thiol quantification for LC-MS. The protocols for measuring H_2O_2, GSH, GSSG and other thiol metabolites were described in (Queval et al. 2008; Queval and Noctor 2007; Rao et al. 2000). Methods were adapted to assay all metabolites from a single sample using microtiter plate assay. Methods were first developed in Scranton (2013) and modified and deployed here for wound time course samples (n=3).

Metabolites were extracted from ground leaves with minor modifications (Queval and Noctor 2007). Six volumes of 0.2 M HCl (3 mL) were added to each tissue sample in 15-mL tubes and gently mixed. Four samples were processed simultaneously (Fig 3.3). HCl extracts were incubated on ice for 5 min. The 3-mL volume was split into three 0.8-mL aliquots of the HCl extract by transferring to 1.5-mL tubes. Extracts were centrifuged at 14,000 g for 20 min at 4°C. Each cleared supernatant was transferred to a 1.5-mL tube. The three 0.8-mL aliquots were used for three assays to quantify reactive oxygen species (ROS; luminol assay), glutathione redox status (glutathione reductase activity assay), and relative thiol levels (LC-MS). Each 0.8-mL HCl aliquot was once again transferred to a 15-mL tube. All samples were brought to pH 5-6 with the addition of 50 µl of 0.2 M NaH_2PO_4 (pH 5.6) and approximately 400-500 µL of 0.2 M NaOH.

The four samples for the glutathione reductase enzymology assay were processed immediately (see below). At the same time, four samples were processed by Dr. Maria Irigoyen or Ms. Diana Medina-Yerena for thiol quantification for LC-MS (see below). The

four samples for the luminol assay were immediately flash frozen in liquid nitrogen, stored at -80 °C and processed within 48 h.

Glutathione reductase assay for total and oxidized glutathione

Total and oxidized GSH were determined immediately using a glutathione reductase assay (Queval and Noctor 2007) and modifications described in (Scranton 2013). Briefly, for each sample, two 0.2-ml aliquots were removed from the neutralized HCl supernatant. Samples were split into two aliquots. One of the two aliquots were spiked with GSH. Aliquots were again split into two more for a total of four aliquots. Two of the four aliquots were incubated with 1 µl of 2-vinylpyridine (VPD; Cat #132292, Sigma) for 20 min at room temperature (RT); the other aliquot served as the non-VPD treatment Three 20-µl aliquots of VPD- and non VPD-treated supernatants for each sample were added to a 96-well CoStar clear-bottom plate wells with 0.11 mL Buffer B (0.2 M NaH$_2$PO$_4$, pH 7.2, 10 mM EDTA, 10 mM NADPH). The reaction was started by the addition of 0.2 U glutathione reductase (GR; Cat #G3664, Sigma) in Buffer B with 2.4 mM 5,5'-dithiobis (2- nitrobenzoate) (DTNB; Cat #D8130, Sigma) for a total volume of 50 µl. The reaction was monitored at 405 nm for 5 min with shaking between each reading using a Victor2 1420 Multilabel Counter (PerkinElmer Life Sciences, Waltham, MA).

LC-MS thiol quantification

Each sample was immediately neutralized NaOH; NaOH (0.2 M) was added slowly in 100-µl amounts and shaken gently between additions up to an approximate total of 500-µl. When the tomato extract reached pH 5-6, it developed a clear color from a former pink color and pH was confirmed with pH paper. A yellow color is indicative of pH above 6 and samples were no longer good for the experiments and would need to be

discarded. The clear neutralized samples were immediately transferred to Dr. Maria Irigoyen or Ms. Diana Medina-Yerena.

For each neutralized extract, two technical replicates (0.2 mL aliquots each) were transferred into an amber 1.5-mL tube (Cat #05-408-134, Fisherbrand) from a method modified in (Queval and Noctor 2007). The thiols in each sample were derivatized with monobromobimane (mBB; Cat #69898, Sigma-Aldrich). The 0.340-mL volume reaction included 0.2 mL of extract with final concentrations of 1.76 mM mbb, 0.59 mM DTT and 147 mM 2-(cyclohexylamino)ethanesulfonic acid (CHES, pH 8.5, Cat #C2885, Sigma-Aldrich,) at room temperature for 15 min. The reaction was terminated with the addition of 10% v/v acetic acid (0.160 mL). The 0.5-mL samples were centrifuged at 10,000 g in a microfuge for 10 min at 4°C. The supernatant was filtered through a 0.25-µm hydrophilic polyethersulfone (PES) membrane filter screwed tightly onto the bottom of a 1-mL plastic syringe (Cat #SLGP033RS, Millipore Sigma) to clear excess salts from the reaction. Prior to sample application, the filter was washed with 1 mL of 10 mM CHES pH 8.5); this prevented sample volume loss. Approximately, 0.4 mL were recovered. A 0.160-mL aliquot of the filtered supernatant was transferred to a 2-mL amber glass vial with a conical glass insert with poly-support spring (Cat #82030-974, Cat #46610-762, VWR). The rest of the sample (approximately 0.2 mL) was transferred to another amber 1.5-mL tube and served as a backup. The cleared extracts were frozen in -80°C for no more than three weeks.

Derivatization of Thiol Standards

Pure 1.4 mM individual derivatized analytes (Cys, γ-Glu-Cys, Cys-Gly, GSH) (Cat # G4251, C7352, G0903, C0166, Sigma-Aldrich) were individually processed for standards (Table 3.5). The standard analytes were quantified prior to the quantification

of the thiols from the experimental samples. The analytes were quantified by LC-MS analysis.

LC-MS analysis

Targeted metabolomics of polar, primary metabolites in the processed thiol samples was performed at the UC Riverside Metabolomics Core Facility. Metabolites were fractionated and identified using an I-class UPLC system (Waters) coupled to a TQ-XS triple quadrupole mass spectrometer (Waters). Separations were carried out on the T3 column (2.1 x 150 mm, 5 µM) (Waters). The mobile phases were water (A) and acetonitrile (B), both with 0.1% formic acid. The flow rate was 250 µL/min and the column was held at 40°C. The injection volume was 3 µL. The gradient was as follows: 0 min, 1% B; 1 min, 1% B; 8 min, 35% B; 8.5 min, 100% B; 11 min, 100% B; 11.1 min, 1% B.

The MS was operated in selected reaction-monitoring mode. Source and desolvation temperatures were 150°C and 600°C, respectively. Desolvation gas was set to 1100 L /h and cone gas to 150 L/h. Collision gas was set to 0.15 mL/min. All gases were nitrogen, except the collision gas, which was argon. Capillary voltage was 1 kV in positive ion mode. Samples were analyzed in random order. Targeted data processing was performed with the open-source Skyline software (MacLean et al. 2010).

Luminol assay to quantify H_2O_2

Neutralized extracts for each sample were analyzed for hydrogen peroxide (H_2O_2) (Rao et al. 2000; Warm and Laties 1982; Queval et al. 2008) with minor modifications of (Scranton 2013) method. Neutralized extracts (0.8 mL) were thawed within 48 h after initial flash freezing. The samples were mixed thoroughly prior to use. A 0.5-mL sample was transferred to a fresh 1.5-mL tube. Each sample was treated with 1 U ascorbate

oxidase (Cat #A0157, Sigma) for 5 min at room temperature (Queval et al. 2008). Treated extracts were passed over a 1-mL syringe filled with 500 mg Dowex 1-X8 50-100 ion exchange resin (Cat #217417, Sigma). Extracts were eluted with 3 mL distilled water. Fifty µL of eluted extract was mixed with 850 µL of 0.2 M NH_4OH (pH 9.5) and 30 µM luminol (Cat #123072, Sigma). Luminescence was monitored after injection of 100 µl of 0.5 mM potassium ferricyanide in 0.2 M NH_4OH (pH 9.5) using Turner Biosystems 20/20n Luminometer (Promega, Madison, WI) at the UCR Genomics Core. Five biological replicates and three technical replicates were done.

RNA isolation and Quantitative real-time PCR

RNA was isolated from frozen leaf tissue samples previously treated with glucose, GO, or CAT using the hot-phenol method (Pautot et al. 2001). Genomic DNA was removed using RQ1 DNase (Cat# M6101, Promega). A total of 1 µg RNA was used for cDNA synthesis with ImpromII Reverse Transcriptase (Cat# A3803, Promega) and oligo-dT (25-mer) primers. cDNAs were diluted with water 10 times for the qRT-PCR reactions. These reactions were performed with the BioRad MyIQ instrument using iQ SYBR Green Supermix (Cat# 170-8884, BioRad), with 200 nM of primers and a total reaction volume of 25 µL. Two reference genes, Tip41 and eIF1a, were used to normalize the relative transcript level of each gene (Table 3.1). The primers were designed using Geneious Prime® 2021.1.1 The qRT-PCR reaction efficiency and the fractional cycle number at threshold (CT) was calculated using Real-time PCR Miner version 4.0 (Zhao and Fernald 2005). # biological and technical reps.

Statistics

Statistical analysis of metabolite levels and transcript levels was performed by Welch's t-test using at adjusted P-value ≤ 0.05 in software GraphPad Prism v. 9.1.2 for MacOS

(GraphPad Software, San Diego, CA, USA; www.graphpad.com) or R Studio. 2-way ANOVA test at adjusted P-value ≤ 0.05 in software GraphPad Prism v. 9.1.2 was done for analysis of GSH/GSSG ratio levels.

Protein Isolation and Affinity Purification

Frozen leaf tissue from 24-h MeJA-treated LapA-OX plants was ground in liquid nitrogen in a cold mortar and pestle. Proteins were extracted from ground leaves (700 mg) in a cold mortar and pestle using 3.5 mL of cold phosphate buffer (50 mM sodium phosphate monobasic, 300 mM NaCl, and 10 mM imidazole buffer, pH 8) and protease inhibitor (complete, mini, EDTA-free protease inhibitor cocktail tablet, Cat #11836170001, Roche). The homogenate was transferred to five 1-mL microfuge tubes and spun in a microcentrifuge at 10,000 g for 20 min at 4°C to remove debris. For each sample, the supernatants were collected, pooled, and transferred to a 15-mL tube. The Bradford method was used to determine protein concentrations using Bovine Serum Albumin (BSA) as a standard (Bio-Rad Protein Assay Kit I, Cat #5000001, Bio-Rad). Fresh protein homogenate (less than 12-h old) was used for the affinity purification assays. Proteins were assessed for integrity using 12% Sodium Dodecyl Sulfate- Polyacrylamide Gel Electrophoresis (SDS-PAGE) and Coomassie blue staining after 12-h incubation time.

His$_6$-tagged LAP-A, LAP-A-R431A, LAP-N, and LAP-N-K357E were overexpressed in Escherichia coli and purified as previously described (Gu et al. 1999). For the isolation of LAP-interacting proteins, there were three technical replicates (one leaf protein extraction and three columns) for each type of LAP protein incubated with leaf total proteins. The technical replicates were staggered to execute all replicates per experiment in one day and it required was a two people to execute; Dr. Maria Irigoyen

enabled these experiments. His$_6$-LAP proteins (20 ug) and 50 µL Ni-NTA resin (Cat #30210, Qiagen) were mixed in a microfuge tube and shaken gently at 4°C for an incubation period of 2 h. The excess non-bound His$_6$-LAP proteins were removed from resin-bound LAP by centrifugation in a microcentrifuge at 5,000g for 2 min. Leaf proteins (200 µg) were incubated with the resin-immobilized His$_6$-LAP proteins in a microcentrifuge with gentle shaking at 4°C for 2 hr. As a negative control, total leaf protein (200 µg) was incubated with 50 µL Ni-NTA resin.

A 3-mL plastic syringe column (Cat #309657, BD Mfr) was prepared for the affinity purification experiment. The syringe was fitted with a 3-way luer lock stopcock (Cat #50-822-022, Fisher scientific) and a piece of glass wool was inserted to prevent resin loss (Cat #11388, Fisher scientific). The resin-immobilized His$_6$-LAP proteins were transferred to the column and sealed. The column was shaken gently at 4°C for an incubation period of 2 h. Four sequential 4-mL wash steps with phosphate buffers with increasing imidazole concentrations (0-, 20-, 40-, and 80-mM imidazole) cleared non-bound protein. His$_6$-LAP proteins and their associated leaf proteins were eluted from the Ni-NTA resin with 250 mM imidazole buffer (1 mL) in two eluates. Samples were separated by SDS-PAGE and stained with Coomassie Blue (Figure 3.11).

Protein eluates were concentrated using StrataClean resin (hydroxylated silica particles; Cat #400714, Agilent). Each eluate (0.9 mL) was incubated with StrataClean (10 µL) for 20 min at room temperature in a microfuge tube with mixing gently for 30 seconds but not vigorous shaking. Samples were centrifuged at 5,000 g in a conventional table-top microcentrifuge for 2 min at room temperature. The unbound proteins in the flow-through fractions were discarded. Unbound protein was cleared again in wash steps by centrifugation at 5,000 g for 2 min. The two eluates for each

sample were combined in one microfuge tube for a final volume of 20 μL. Proteins bound to StrataClean resin were submitted to the UCR Proteomics core for endopeptidase digestion and nano LC-MS/MS analysis.

Protein sample preparation

Protein samples were resuspended in 100 μL trypsin solution (10 μg/mL trypsin, 50 mM ammonium bicarbonate (pH 8), 10% acetonitrile) and incubated at 37°C overnight. A MudPIT approach was employed to analyze the trypsin-treated samples and details are provided in Drakakaki et al. (2012). Samples were processed and analyzed on a sensitive nanoflow liquid chromatography system coupled to a high resolution Orbitrap Fusion mass spectrometer. A two-dimension nanoAcquity UPLC (Waters, Milford, MA) and an Orbitrap Fusion MS (Thermo Scientific, San Jose, CA) were configured to perform online 2D-nanoLC-MS/MS analysis. 2D-nanoLC was operated with a 2D-dilution method that is configured with nanoAcquity UPLC. The first dimension LC fractionation used 20 mM ammonium formate (pH 10) and acetonitrile. Five fractions were eluted using 13%, 18%, 21.5%, 27%, and 50% of acetonitrile. The second dimension nano-UPLC method was described previously (Drakakaki et al. 2012).

Orbitrap Fusion MS method was based on a data-dependent acquisition (DDA) survey using a nano ESI source. Orbitrap mass analyzer was used for the MS1 scan. For the MS2 scan, the Ion-Trap mass analyzer was used in a rapid scan mode. Only precursor ions with intensity 10,000 or higher were selected for MS2 scan. Sequence of individual MS2 scanning was from most-intense to least-intense precursor ions. Higher-energy CID (HCD) was used for fragmentation activation, quadrupole was used for precursor isolation and MS2 mass range was set auto/normal with first mass set at 120 m/z.

The raw MS files were processed and analyzed using Proteome Discoverer version 2.1 (Thermo Scientific, San Jose, CA). Sequest HT search engine was used to match all MS data to the deduced proteome of tomato (ITAG 4.0) and the tomato chloroplast protein Atlas (described in Chapter 1). Briefly, five protein localization algorithms were used to assemble a tomato plastid protein dataset (Atlas), which was used to predict subcellular localization of tomato proteins. The five protein localization algorithms included: TargetP version 1.1b (Emanuelsson et al. 2000), ChloroP version 1.1 (Emanuelsson et al. 1999), WoLF PSORT version 0.2 (Horton et al. 2007), YLoc (Briesemeister et al. 2010) and Predotar (Small et al. 2004). The search parameters were the following: trypsin with one missed cleavage, minimal peptide length of six amino acids, MS1 mass tolerance 20 ppm, MS2 mass tolerance 0.6 Da, and variable modifications included oxidation (M) and N-terminal acetylation.

Protein Identification and Analysis

Non-specific binding proteins were identified from the negative control samples (leaf protein non-specifically bound to Ni-NTA resin. Over 50 proteins were identified. These proteins were removed from the putative LAP-A and LAP-N interactor protein lists. The remaining proteins were used to identify putative LAP-A and LAP-N interactors. Proteins identified in at least two of the three technical replicates of each experiment were designated as putative LAP-interactors. Proteins were ranked and classified by their reproducibility and the number of peptides, and unique peptides used to identify the protein (Table 3.S1). The proteins functional categories were categorized using Mapman bins (Schwacke et al. 2019) and were manually curated.

The LAP-A interactors were localized in the chloroplast stroma based on comparing the tomato genes identified to those genes identified in the wild-type stromal

proteome from Chapter 1. Those proteins that overlap meant that they were localized in the chloroplast. The LAP-A interactors were also compared to the Methyl jasmonome to identify if proteins were regulated by LAP-A and/ or MeJA (unpublished results). The data analysis was performed in R Studio. The methyl jasmonome data acquired is unpublished and part of the dissertation of a graduate student (Oindrila Bhattacharya) in the Walling lab.

References

Almagro Armenteros JJ, Salvatore M, Emanuelsson O, Winther O, Von Heijne G, Elofsson A, Nielsen H (2019) Detecting sequence signals in targeting peptides using deep learning. Life Science Alliance 2 (5):e201900429. doi:10.26508/lsa.201900429

Almagro Armenteros JJ, Sønderby CK, Sønderby SK, Nielsen H, Winther O (2017) DeepLoc: prediction of protein subcellular localization using deep learning. Bioinformatics 33 (21):3387-3395. doi:10.1093/bioinformatics/btx431

Aslam S, Gul N, Mir MA, Asgher M, Al-Sulami N, Abulfaraj AA, Qari S (2021) Role of Jasmonates, Calcium, and Glutathione in Plants to Combat Abiotic Stresses Through Precise Signaling Cascade. Frontiers in Plant Science 12. doi:10.3389/fpls.2021.668029

Bekturova A, Oshanova D, Tiwari P, Nurbekova Z, Kurmanbayeva A, Soltabayeva A, Yarmolinsky D, Srivastava S, Tureckova V, Strnad M, Sagi M (2021) Adenosine 5' phosphosulfate reductase and sulfite oxidase regulate sulfite-induced water loss in Arabidopsis. Journal of experimental botany 72 (18):6447-6466. doi:10.1093/jxb/erab249

Bohrer AS, Yoshimoto N, Sekiguchi A, Rykulski N, Saito K, Takahashi H (2015) Alternative translational initiation of ATP sulfurylase underlying dual localization of sulfate assimilation pathways in plastids and cytosol in Arabidopsis thaliana. Frontiers in Plant Science 5. doi:10.3389/fpls.2014.00750

Briesemeister S, Rahnenfï¿½hrer Jr, Kohlbacher O (2010) YLoc—an interpretable web server for predicting subcellular localization. Nucleic Acids Research 38 (suppl_2):W497-W502. doi:10.1093/nar/gkq477

Broin M, Rey P (2003) Potato plants lacking the CDSP32 plastidic thioredoxin exhibit overoxidation of the BAS1 2-cysteine peroxiredoxin and increased lipid peroxidation in thylakoids under photooxidative stress. Plant Physiology 132 (3):1335-1343. doi:10.1104/pp.103.021626

Cappiello M, Lazzarotti A, Buono F, Scaloni A, D'Ambrosio C, Amodeo P, Mendez BL, Pelosi P, Del Corso A, Mura U (2004) New role for leucyl aminopeptidase in glutathione turnover. Biochemical Journal 378:35-44. doi:10.1042/bj20031336

Chan KX, Mabbitt PD, Phua SY, Mueller JW, Nisar N, Gigolashvili T, Stroeher E, Grassl J, Arlt W, Estavillo GM, Jackson CJ, Pogson BJ (2016) Sensing and signaling of oxidative stress in chloroplasts by inactivation of the SAL1 phosphoadenosine phosphatase. Proc Natl Acad Sci U S A 113 (31):E4567-4576. doi:10.1073/pnas.1604936113

Chao WS, Gu YQ, Holzer FM, Walling LL (1996) The wound-induced leucine aminopeptidase of the solanaceae: Gene activation during development and in response to stress. Plant Physiology 111 (2):511-511

Chao WS, Gu YQ, Pautot V, Bray EA, Walling LL (1999) Leucine aminopeptidase RNAs, proteins, and activities increase in response to water deficit, salinity, and the wound signals systemin, methyl jasmonate, and abscisic acid. Plant Physiology 120 (4):979-992. doi:10.1104/pp.120.4.979

Chao WS, Pautot V, Holzer FM, Walling LL (2000) Leucine aminopeptidases: the ubiquity of LAP-N and the specificity of LAP-A. Planta 210 (4):563-573. doi:10.1007/s004250050045

Choudhury FK, Devireddy AR, Azad RK, Shulaev V, Mittler R (2018) Rapid Accumulation of Glutathione During Light Stress in Arabidopsis. Plant and Cell Physiology 59 (9):1817-1826. doi:10.1093/pcp/pcy101

Cohen A, Hacham Y, Welfe Y, Khatib S, Avice JC, Amir R (2020) Evidence of a significant role of glutathione reductase in the sulfur assimilation pathway. Plant Journal 102 (2):246-261. doi:10.1111/tpj.14621

Collin V, Issakidis-Bourguet E, Marchand C, Hirasawa M, Lancelin JM, Knaff DB, Miginiac-Maslow M (2003) The Arabidopsis plastidial thioredoxins - New functions and new insights into specificity. Journal of Biological Chemistry 278 (26):23747-23752. doi:10.1074/jbc.M302077200

de Souza A, Wang JZ, Dehesh K (2017) Retrograde Signals: Integrators of Interorganellar Communication and Orchestrators of Plant Development. Annu Rev Plant Biol 68:85-108. doi:10.1146/annurev-arplant-042916-041007

Del Bello B, Paolicchi A, Comporti M, Pompella A, Maellaro E (1999) Hydrogen peroxide produced during gamma-glutamyl transpeptidase activity is involved in prevention of apoptosis and maintenance of proliferation in U937 cells. Faseb Journal 13 (1):69-79

Del Corso A, Vilardo PG, Cappiello M, Cecconi I, Dal Monte M, Barsacchi D, Mura U (2002) Physiological thiols as promoters of glutathione oxidation and modifying agents in protein S-thiolation. Archives of Biochemistry and Biophysics 397 (2):392-398. doi:10.1006/abbi.2001.2678

Destro T, Prasad D, Martignago D, Lliso Bernet I, Trentin AR, Renu IK, Ferretti M, Masi A (2011) Compensatory expression and substrate inducibility of γ-glutamyl transferase GGT2 isoform in Arabidopsis thaliana. Journal of experimental botany 62 (2):805-814

Diaz-Vivancos P, de Simone A, Kiddie G, Foyer CH (2015) Glutathione - linking cell proliferation to oxidative stress. Free Radical Biology and Medicine 89:1154-1164. doi:10.1016/j.freeradbiomed.2015.09.023

254

Dietz KJ, Jacob S, Oelze ML, Laxa M, Tognetti V, de Miranda SMN, Baier M, Finkemeier I (2006) The function of peroxiredoxins in plant organelle redox metabolism. Journal of Experimental Botany 57 (8):1697-1709. doi:10.1093/jxb/erj160

Doares SH, Syrovets T, Weiler EW, Ryan CA (1995) Oligogalacturonides and chitosan activate plant defensive genes through the octadecanoid pathway. Proc Natl Acad Sci U S A 92 (10):4095-4098. doi:10.1073/pnas.92.10.4095

Dominici S, Valentini M, Maellaro E, Del Bello B, Paolicchi A, Lorenzini E, Tongiani R, Comporti M, Pompella A (1999) Redox modulation of cell surface protein thiols in U937 lymphoma cells: The role of gamma-glutamyl transpeptidase-dependent H2O2 production and S-thiolation. Free Radical Biology and Medicine 27 (5-6):623-635. doi:10.1016/s0891-5849(99)00111-2

Emanuelsson O, Nielsen H, Brunak S, von Heijne G (2000) Predicting subcellular localization of proteins based on their N-terminal amino acid sequence. J Mol Biol 300 (4):1005-1016. doi:10.1006/jmbi.2000.3903

Emanuelsson O, Nielsen H, von Heijne G (1999) ChloroP, a neural network-based method for predicting chloroplast transit peptides and their cleavage sites. Protein Sci 8 (5):978-984. doi:10.1110/ps.8.5.978

Enoiu M, Aberkane H, Salazar JF, Leroy P, Groffen J, Siest G, Wellman M (2000) Evidence for the pro-oxidant effect of gamma-glutamyltranspeptidase-related enzyme. Free Radical Biology and Medicine 29 (9):825-833. doi:10.1016/s0891-5849(00)00370-1

Estavillo GM, Crisp PA, Pornsiriwong W, Wirtz M, Collinge D, Carrie C, Giraud E, Whelan J, David P, Javot H, Brearley C, Hell R, Marin E, Pogson BJ (2011) Evidence for a SAL1-PAP Chloroplast Retrograde Pathway That Functions in Drought and High Light Signaling in Arabidopsis   The Plant Cell 23 (11):3992-4012. doi:10.1105/tpc.111.091033

Exposito-Rodriguez M, Laissue PP, Yvon-Durocher G, Smirnoff N, Mullineaux PM (2017) Photosynthesis-dependent H2O2 transfer from chloroplasts to nuclei provides a high-light signalling mechanism. Nature Communications 8 (1):49. doi:10.1038/s41467-017-00074-w

Ferretti M, Destro T, Tosatto SCE, La Rocca N, Rascio N, Masi A (2009) Gamma-glutamyl transferase in the cell wall participates in extracellular glutathione salvage from the root apoplast. New Phytologist 181 (1):115-126. doi:10.1111/j.1469-8137.2008.02653.x

Fowler JH, Narvaez-Vasquez J, Aromdee DN, Pautot V, Holzer FM, Walling LL (2009) Leucine Aminopeptidase Regulates Defense and Wound Signaling in Tomato Downstream of Jasmonic Acid. Plant Cell 21 (4):1239-1251. doi:10.1105/tpc.108.065029

Foyer CH, Noctor G (2016) Stress-triggered redox signalling: what's in pROSpect? Plant, Cell & Environment 39 (5):951-964. doi:https://doi.org/10.1111/pce.12621

Gotor C, Laureano-Marin AM, Moreno I, Aroca A, Garcia I, Romero LC (2015) Signaling in the plant cytosol: cysteine or sulfide? Amino Acids 47 (10):2155-2164. doi:10.1007/s00726-014-1786-z

Gu YQ, Chao WS, Walling LL (1996a) Localization and post-translational processing of the wound-induced leucine aminopeptidase proteins of tomato. Journal of Biological Chemistry 271 (42):25880-25887

Gu YQ, Holzer FM, Walling LL (1999) Overexpression, purification and biochemical characterization of the wound-induced leucine aminopeptidase of tomato. European Journal of Biochemistry 263 (3):726-735. doi:10.1046/j.1432-1327.1999.00548.x

Gu YQ, Pautot V, Holzer FM, Walling LL (1996b) A complex array of proteins related to the multimeric leucine aminopeptidase of tomato. Plant Physiology 110 (4):1257-1266

Gu YQ, Walling LL (2000) Specificity of the wound-induced leucine aminopeptidase (LAP-A) of tomato - Activity on dipeptide and tripeptide substrates. European Journal of Biochemistry 267 (4):1178-1187. doi:10.1046/j.1432-1327.2000.01116.x

Gu YQ, Walling LL (2002) Identification of residues critical for activity of the wound-induced leucine aminopeptidase (LAP-A) of tomato. European Journal of Biochemistry 269 (6):1630-1640. doi:10.1046/j.1432-1327.2002.02795.x

Gutierrez-Marcos JF, Roberts MA, Campbell EI, Wray JL (1996) Three members of a novel small gene-family from Arabidopsis thaliana able to complement functionally an Escherichia coli mutant defective in PAPS reductase activity encode proteins with a thioredoxin-like domain and "APS reductase" activity. Proc Natl Acad Sci U S A 93 (23):13377-13382. doi:10.1073/pnas.93.23.13377

Habib GM, Barrios R, Shi ZZ, Lieberman MW (1996) Four distinct membrane-bound dipeptidase RNAs are differentially expressed and show discordant regulation with gamma-glutamyl transpeptidase. Journal of Biological Chemistry 271 (27):16273-16280. doi:10.1074/jbc.271.27.16273

Hasanuzzaman M, Bhuyan M, Zulfiqar F, Raza A, Mohsin SM, Al Mahmud J, Fujita M, Fotopoulos V (2020) Reactive Oxygen Species and Antioxidant Defense in Plants under Abiotic Stress: Revisiting the Crucial Role of a Universal Defense Regulator. Antioxidants 9 (8). doi:10.3390/antiox9080681

Heidari P, Mazloomi F, Nussbaumer T, Barcaccia G (2020) Insights into the SAM Synthetase Gene Family and Its Roles in Tomato Seedlings under Abiotic Stresses and Hormone Treatments. Plants 9 (5):586. doi:10.3390/plants9050586

Horton P, Park KJ, Obayashi T, Fujita N, Harada H, Adams-Collier CJ, Nakai K (2007) WoLF PSORT: protein localization predictor. Nucleic Acids Res 35 (Web Server issue):W585-587. doi:10.1093/nar/gkm259

Ishiga Y, Ishiga T, Wangdi T, Mysore KS, Uppalapati SR (2012) NTRC and chloroplast-generated reactive oxygen species regulate Pseudomonas syringae pv. tomato disease development in tomato and arabidopsis. Molecular plant-microbe interactions : MPMI 25 (3):294-306. doi:10.1094/MPMI-05-11-0130

Ishiga Y, Watanabe M, Ishiga T, Tohge T, Matsuura T, Ikeda Y, Hoefgen R, Fernie AR, Mysore KS (2017) The SAL-PAP Chloroplast Retrograde Pathway Contributes to Plant Immunity by Regulating Glucosinolate Pathway and Phytohormone Signaling. Mol Plant Microbe Interact 30 (10):829-841. doi:10.1094/mpmi-03-17-0055-r

Jahan B, Sehar Z, Masood A, Anjum NA, Khan MIR, Khan NA (2019) Sulfur Availability Potentiates Phytohormones-Mediated Action in Plants. Plant Signaling Molecules: Role and Regulation under Stressful Environments. doi:10.1016/b978-0-12-816451-8.00017-4

Jez JM (2019) Structural biology of plant sulfur metabolism: from sulfate to glutathione. Journal of Experimental Botany 70 (16):4089-4103. doi:10.1093/jxb/erz094

Konig J, Baier M, Horling F, Kahmann U, Harris G, Schurmann P, Dietz KJ (2002) The plant-specific function of 2-Cys peroxiredoxin-mediated detoxification of peroxides in the redox-hierarchy of photosynthetic electron flux. Proceedings of the National Academy of Sciences of the United States of America 99 (8):5738-5743. doi:10.1073/pnas.072644999

Kumar S, Kaur A, Chattopadhyay B, Bachhawat AK (2015) Defining the cytosolic pathway of glutathione degradation in Arabidopsis thaliana: role of the ChaC/GCG family of gamma-glutamyl cyclotransferases as glutathione-degrading enzymes and AtLAP1 as the Cys-Gly peptidase. Biochem J 468:73-85. doi:10.1042/bj20141154

Laxa M, Koenig J, Dietz K-J, Kandlbinder A (2007) Role of the cysteine residues in Arabidopsis thaliana cyclophilin CYP20-3 in peptidyl-prolyl cis-trans isomerase and redox-related functions. Biochemical Journal 401:287-297. doi:10.1042/bj20061092

Li N, Han X, Feng D, Yuan D, Huang L-J (2019) Signaling Crosstalk between Salicylic Acid and Ethylene/Jasmonate in Plant Defense: Do We Understand What They Are Whispering? International Journal of Molecular Sciences 20 (3):671

MacLean B, Tomazela DM, Shulman N, Chambers M, Finney GL, Frewen B, Kern R, Tabb DL, Liebler DC, MacCoss MJ (2010) Skyline: an open source document editor for creating and analyzing targeted proteomics experiments. Bioinformatics 26 (7):966-968. doi:10.1093/bioinformatics/btq054

Martin MN, Slovin JP (2000) Purified gamma-glutamyl transpeptidases from tomato exhibit high affinity for glutathione and glutathione S-conjugates. Plant Physiology 122 (4):1417-1426. doi:10.1104/pp.122.4.1417

Muthuramalingam M, Seidel T, Laxa M, de Miranda SMN, Gaertner F, Stroeher E, Kandlbinder A, Dietz K-J (2009) Multiple redox and non-redox interactions define 2-Cys Peroxiredoxin as a regulatory hub in the chloroplast. Molecular Plant 2 (6):1273-1288. doi:10.1093/mp/ssp089

Noctor G, Mhamdi A, Chaouch S, Han Y, Neukermans J, Marquez-Garcia B, Queval G, Foyer CH (2012) Glutathione in plants: an integrated overview. Plant Cell and Environment 35 (2):454-484. doi:10.1111/j.1365-3040.2011.02400.x

Oelmüller R, Levitan I, Bergfeld R, Rajasekhar VK, Mohr H (1986) Expression of nuclear genes as affected by treatments acting on the plastids. Planta 168 (4):482-492. doi:10.1007/bf00392267

Orozco-Cárdenas ML, Narváez-Vásquez J, Ryan CA (2001) Hydrogen Peroxide Acts as a Second Messenger for the Induction of Defense Genes in Tomato Plants in Response to Wounding, Systemin, and Methyl Jasmonate. The Plant Cell 13 (1):179-192

Orozco-Cárdenas ML, Ryan CA (2002) Nitric oxide negatively modulates wound signaling in tomato plants. Plant Physiol 130 (1):487-493. doi:10.1104/pp.008375

Pant BD, Oh S, Lee H-K, Nandety RS, Mysore KS (2020) Antagonistic Regulation by CPN60A and CLPC1 of TRXL1 that Regulates MDH Activity Leading to Plant Disease Resistance and Thermotolerance. Cell Reports 33 (11):108512. doi:https://doi.org/10.1016/j.celrep.2020.108512

Pautot V, Holzer FM, Chaufaux J, Walling LL (2001) The induction of tomato leucine aminopeptidase genes (LapA) after Pseudomonas syringae pv. tomato infection is primarily a wound response triggered by coronatine. Mol Plant Microbe Interact 14 (2):214-224. doi:10.1094/MPMI.2001.14.2.214

Peltier JB, Cai Y, Sun Q, Zabrouskov V, Giacomelli L, Rudella A, Ytterberg AJ, Rutschow H, van Wijk KJ (2006) The oligomeric stromal proteome of Arabidopsis thaliana chloroplasts. Molecular & Cellular Proteomics 5 (1):114-133. doi:10.1074/mcp.M500180-MCP200

PenaCortes H, Prat S, Atzorn R, Wasternack C, Willmitzer L (1996) Abscisic acid-deficient plants do not accumulate proteinase inhibitor II following systemin treatment. Planta 198 (3):447-451. doi:10.1007/bf00620062

Pogson BJ, Woo NS, Förster B, Small ID (2008) Plastid signalling to the nucleus and beyond. Trends Plant Sci 13 (11):602-609. doi:10.1016/j.tplants.2008.08.008

Puerto-Galán L, Pérez-Ruiz JM, Guinea M, Cejudo FJ (2015) The contribution of NADPH thioredoxin reductase C (NTRC) and sulfiredoxin to 2-Cys peroxiredoxin overoxidation in Arabidopsis thaliana chloroplasts. Journal of Experimental Botany. doi:10.1093/jxb/eru512

Queval G, Hager J, Gakière B, Noctor G (2008) Why are literature data for H2O2 contents so variable? A discussion of potential difficulties in the quantitative assay of leaf extracts. Journal of Experimental Botany 59 (2):135-146. doi:10.1093/jxb/erm193

Queval G, Noctor G (2007) A plate reader method for the measurement of NAD, NADP, glutathione, and ascorbate in tissue extracts: Application to redox profiling during Arabidopsis rosette development. Anal Biochem 363 (1):58-69. doi:10.1016/j.ab.2007.01.005

Rao MV, Lee H, Creelman RA, Mullet JE, Davis KR (2000) Jasmonic acid signaling modulates ozone-induced hypersensitive cell death. The Plant cell 12 (9):1633-1646. doi:10.1105/tpc.12.9.1633

Rey P, Cuine S, Eymery F, Garin J, Court M, Jacquot JP, Rouhier N, Broin M (2005) Analysis of the proteins targeted by CDSP32, a plastidic thioredoxin participating in oxidative stress responses. Plant Journal 41 (1):31-42. doi:10.1111/j.1365-313X.2004.02271.x

Romero HM, Berlett BS, Jensen PJ, Pell EJ, Tien M (2004) Investigations into the role of the plastidial peptide methionine sulfoxide reductase in response to oxidative stress in Arabidopsis. Plant Physiol 136 (3):3784-3794. doi:10.1104/pp.104.046656

Rouhier N, Lemaire SD, Jacquot JP (2008) The role of glutathione in photosynthetic organisms: emerging functions for glutaredoxins and glutathionylation. Annu Rev Plant Biol 59:143-166. doi:10.1146/annurev.arplant.59.032607.092811

Sagi M, Davydov O, Orazova S, Yesbergenova Z, Ophir R, Stratmann JW, Fluhr R (2004) Plant respiratory burst oxidase homologs impinge on wound responsiveness and development in Lycopersicon esculentum. The Plant cell 16 (3):616-628. doi:10.1105/tpc.019398

Schwacke R, Ponce-Soto GY, Krause K, Bolger AM, Arsova B, Hallab A, Gruden K, Stitt M, Bolger ME, Usadel B (2019) MapMan4: A Refined Protein Classification and Annotation Framework Applicable to Multi-Omics Data Analysis. Molecular Plant 12 (6):879-892. doi:https://doi.org/10.1016/j.molp.2019.01.003

Scranton MA (2013) Elucidation of the Role of Leucine Aminopeptidase A in the Wound Response Pathway in Tomato. UC Riverside.

Scranton MA, Fowler JH, Girke T, Walling LL (2013) Microarray Analysis of Tomato's Early and Late Wound Response Reveals New Regulatory Targets for Leucine Aminopeptidase A. Plos One 8 (10). doi:10.1371/journal.pone.0077889

Scranton MA, Yee A, Park S-Y, Walling LL (2012) Plant Leucine Aminopeptidases Moonlight as Molecular Chaperones to Alleviate Stress-induced Damage. Journal of Biological Chemistry 287 (22):18408-18417. doi:10.1074/jbc.M111.309500

Setya A, Murillo M, Leustek T (1996) Sulfate reduction in higher plants: molecular evidence for a novel 5'-adenylylsulfate reductase. Proc Natl Acad Sci U S A 93 (23):13383-13388. doi:10.1073/pnas.93.23.13383

Small I, Peeters N, Legeai F, Lurin C (2004) Predotar: A tool for rapidly screening proteomes for N-terminal targeting sequences. Proteomics 4 (6):1581-1590. doi:10.1002/pmic.200300776

Stenbaek A, Hansson A, Wulff RP, Hansson M, Dietz K-J, Jensen PE (2008) dNADPH-dependent thioredoxin reductase and 2-Cys peroxiredoxins are needed for the protection of Mg-protoporphyrin monomethyl ester cyclase. Febs Letters 582 (18):2773-2778. doi:10.1016/j.febslet.2008.07.006

Sullivan JA, Gray JC (1999) Plastid translation is required for the expression of nuclear photosynthesis genes in the dark and in roots of the pea lip1 mutant. Plant Cell 11 (5):901-910. doi:10.1105/tpc.11.5.901

Susek RE, Ausubel FM, Chory J (1993) Signal transduction mutants of arabidopsis uncouple nuclear CAB and RBCS gene expression from chloroplast development. Cell 74 (5):787-799. doi:https://doi.org/10.1016/0092-8674(93)90459-4

Taylor A (1985) Leucine aminopeptidase activity is diminished in aged hog, beef, and human lens. Prog Clin Biol Res 180:299-302

Tu CJ, Park SY, Walling LL (2003) Isolation and characterization of the neutral leucine aminopeptidase (LapN) of tomato. Plant Physiology 132 (1):243-255. doi:10.1104/pp.102.013854

Vogtle FN, Meisinger C (2012) Sensing mitochondrial homeostasis: the protein import machinery takes control. Devel Cell 23 (2):234-236. doi:10.1016/j.devcel.2012.07.018

Walling LL (2013) Leucyl Aminopeptidase (Plant). Handbook of Proteolytic Enzymes, Vols 1 and 2, 3rd Edition. doi:10.1016/b978-0-12-382219-2.00331-8

Warm E, Laties GG (1982) Quantification of hydrogen peroxide in plant extracts by the chemiluminescence reaction with luminol. Phytochemistry 21 (4):827-831. doi:https://doi.org/10.1016/0031-9422(82)80073-3

Wasternack C, Feussner I (2018) The Oxylipin Pathways: Biochemistry and Function. Annu Rev Plant Biol 69:363-386. doi:10.1146/annurev-arplant-042817-040440

Zhao S, Fernald RD (2005) Comprehensive algorithm for quantitative real-time polymerase chain reaction. J Comput Biol 12 (8):1047-1064. doi:10.1089/cmb.2005.12.1047

Zhu F, Zhang Q-P, Che Y-P, Zhu P-X, Zhang Q-Q, Ji Z-L Glutathione contributes to resistance responses to TMV through a differential modulation of salicylic acid and reactive oxygen species. Molecular Plant Pathology n/a (n/a). doi:https://doi.org/10.1111/mpp.13138

Zhu F, Zhang Q-P, Che Y-P, Zhu P-X, Zhang Q-Q, Ji Z-L (2021) Glutathione contributes to resistance responses to TMV through a differential modulation of salicylic acid and reactive oxygen species. Molecular Plant Pathology 22 (12):1668-1687. doi:https://doi.org/10.1111/mpp.13138
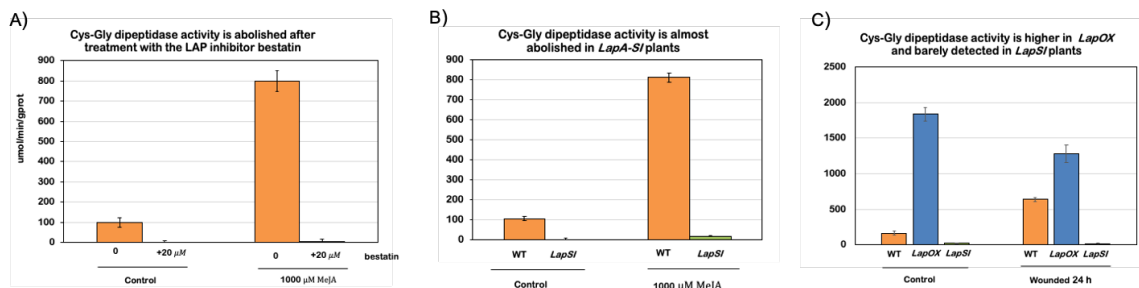
Figure 3.1 LAP-A is a Cys-Gly dipeptidase.
(A) Cys-Gly dipeptidase activity was measured from total soluble protein extracts from healthy or methyl jasmonate (MeJA) treated leaves of WT plants +/- the LAP inhibitor bestatin (20 µM). (B) Cys-Gly activity was measured control and MeJA- treated WT and LapSI leaves. (C) Cys-Gly dipeptidase activity was measured in total soluble protein extracts from healthy or wounded leaves of WT, LapSI, and LapOX plants. Cys-Gly dipeptidase experiments in total soluble protein extracts were conducted by Melissa Scranton (Scranton, 2013) and are provided here to provide perspective for the experiments in this Chapter.
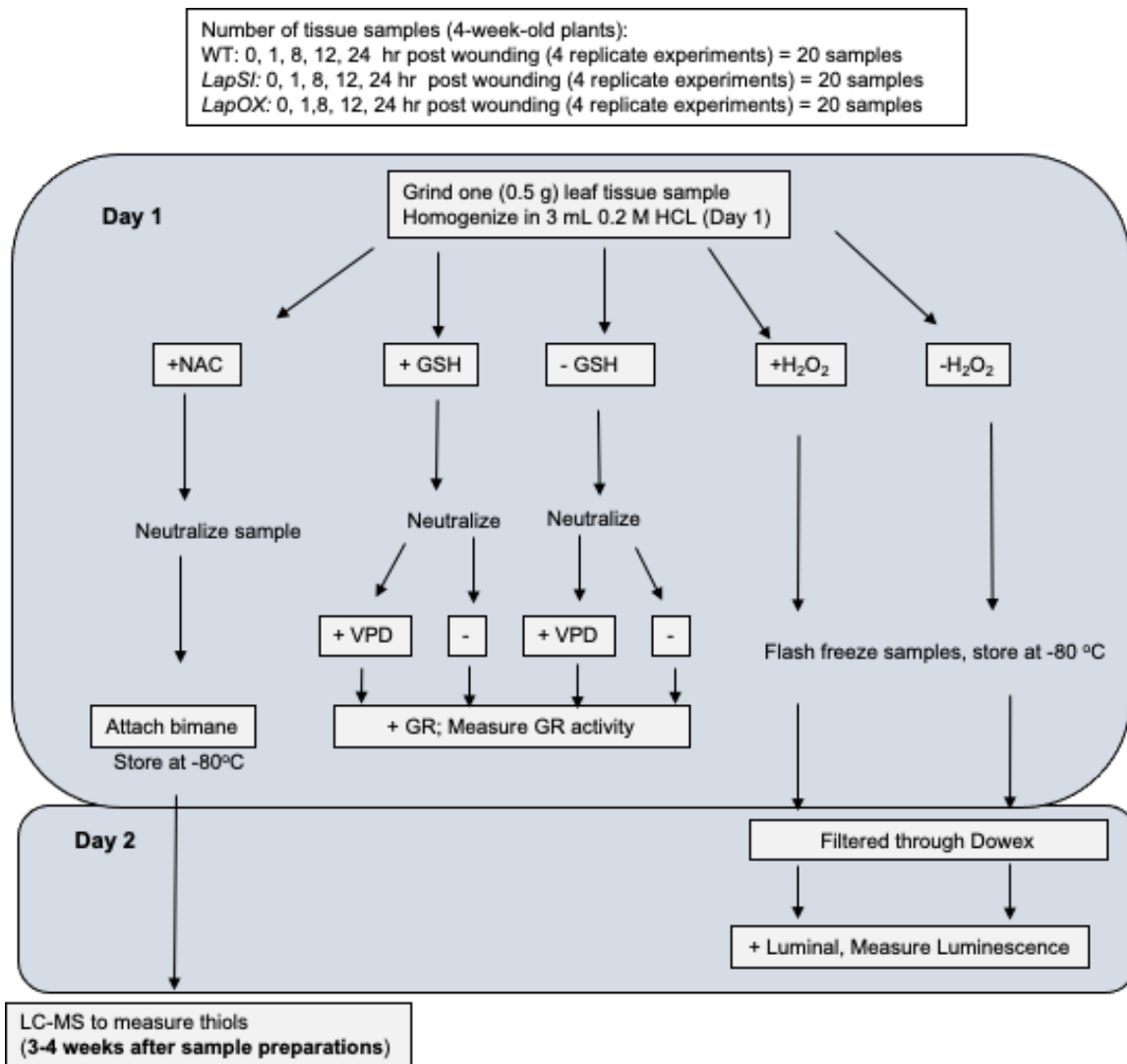
Figure 3.2 Flowchart of experiments to measure thiols in tomato leaves. Samples were taken from WT, LapA-SI, or LapA-OX at 0, 1, 8, 12, or 24 h post wounding. From a single tissue sample, metabolites were extracted and monobromobimane-conjugated thiols, glutathione (reduced (GSH) and oxidized (GSSG)), and H_2O_2 measurements were made. The experiment timeline is illustrated spanning two days for sample preparations. It took four weeks to process the 80 samples and submit them for analysis at the UCR Metabolomics Core using LC-MS. NAC (N-acetyl), VPD (2-vinylpryridine), GR (glutathione reductase).
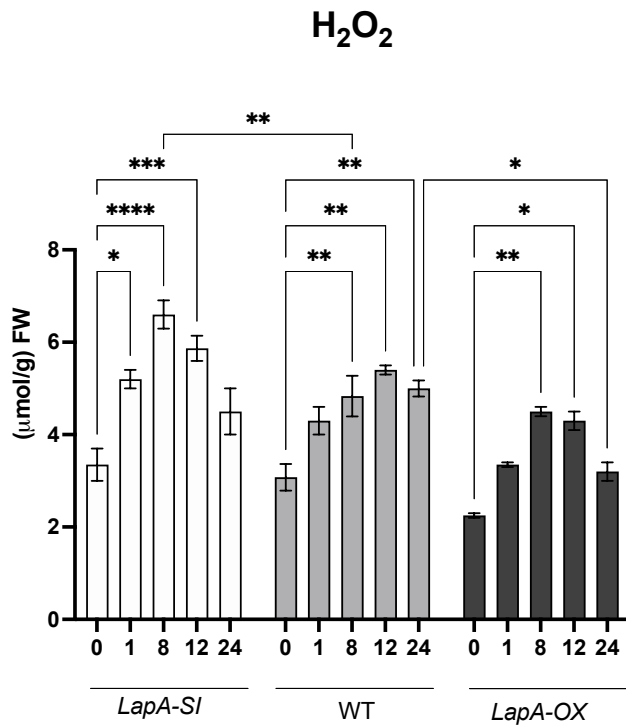
Figure 3.3 H_2O_2 levels in WT, LapA-SI, and LapA-OX leaves after wounding. The H_2O_2 (μmol/g FW) was quantified in leaves 0, 1, 8, 12, and 24 h after wounding of LapA-SI, WT, and LapA-OX plants using a luminescence assay (n=5). Significant differences in H_2O_2 levels within each genotype after treatment and between genotypes was determined by Welch's t-test analysis. Adjusted P-values between <0.05 (*), <0.035 (**), <0.0025 (***) and <0.0001 (****) are shown.
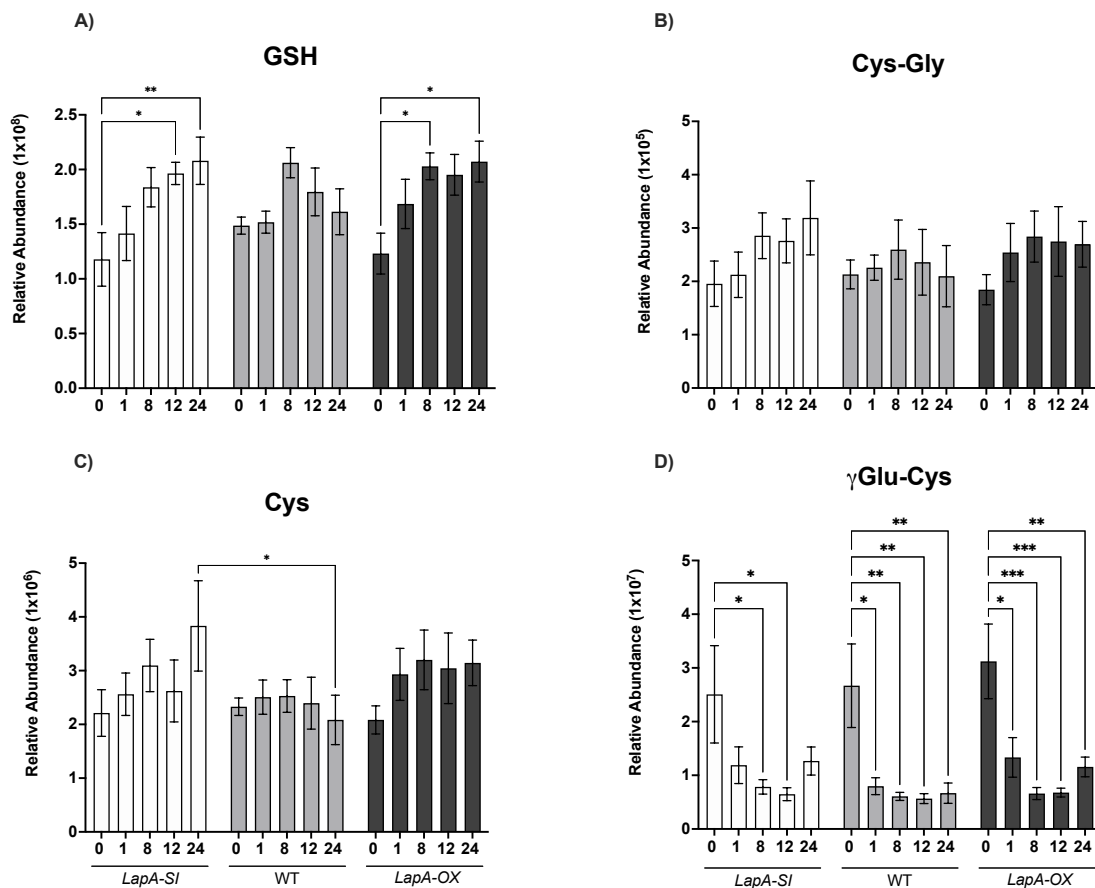
Figure 3.4. Thiol-containing compound levels in WT, LapA-SI, and LapA-OX leaves after wounding. Relative abundance of thiol-containing compounds, monobromobimane (mBB)-conjugated GSH, Cys-Gly, γGlu-Cys, and Cys from leaves at 0, 1, 8, 12, and 24 h after wounding of WT, LapA-SI and LapA-OX plants using the protocol outlined in Fig 3.3. mBB-conjugated thiols were quantified by targeted metabolomics using LC-MS. Thiol-containing compounds measured included (A) GSH, (B) Cys-Gly, (C) Cys, and (D) γGlu-Cys. Asterisks represent statistically different values at adjusted P-values between <0.05 (*) and <0.035 (**) <0.0025 (***) Welch's t-test.
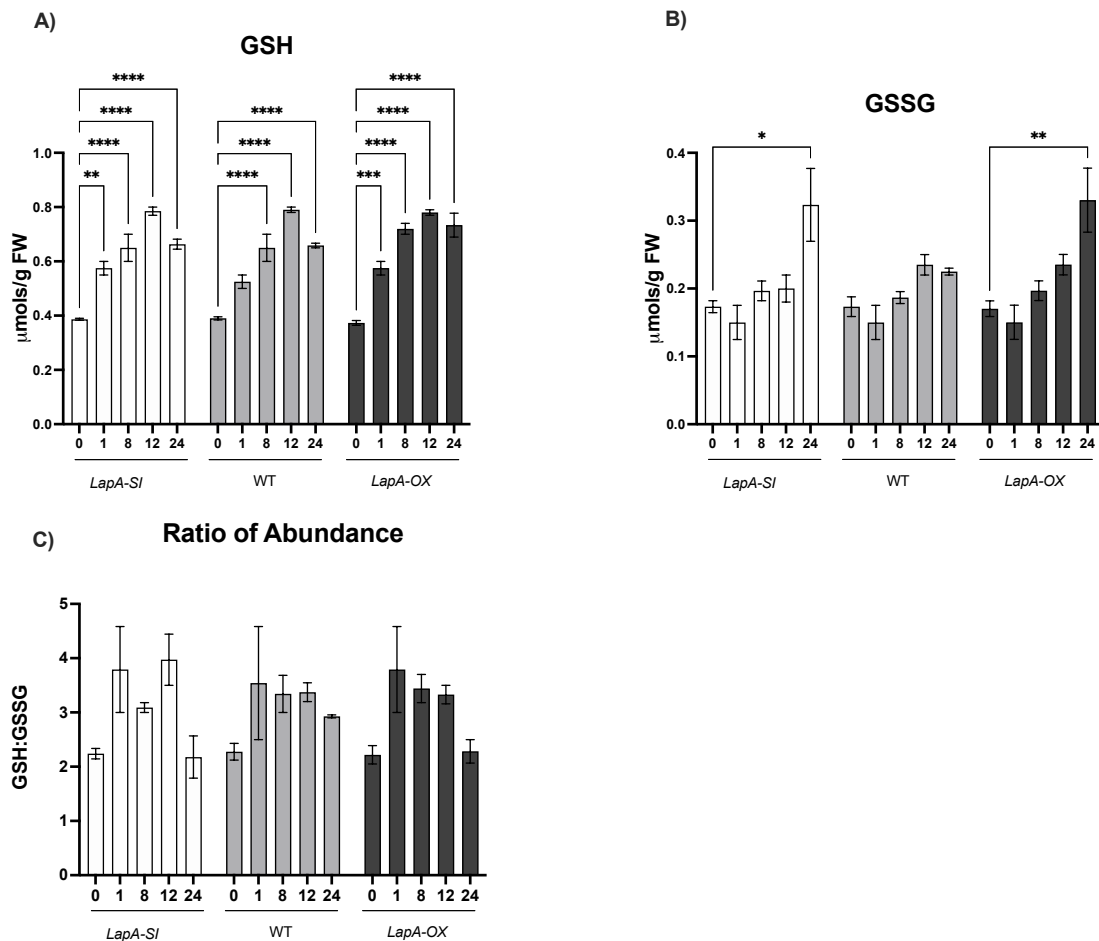
Figure 3.5 Glutathione abundance and GSH:GSSG ratio in WT, LapA-SI, and LapA-OX leaves after wounding. A) The total GSH levels and B) total GSSG levels were measured in leaves 0, 1, 8, 12, and 24 h after wounding in LapA-SI, WT, and LapA-OX plants using spectrophotometric assay (n=5). The sample preparation protocol is outlined in Fig 3.2. D) GSH:GSSG. Two-way ANOVA statistics was done. Asterisks represent statistically different values at adjusted P-values between <0.05 (*), <0.035 (**), <0.0025 (***) and <0.0001 (****) are shown.
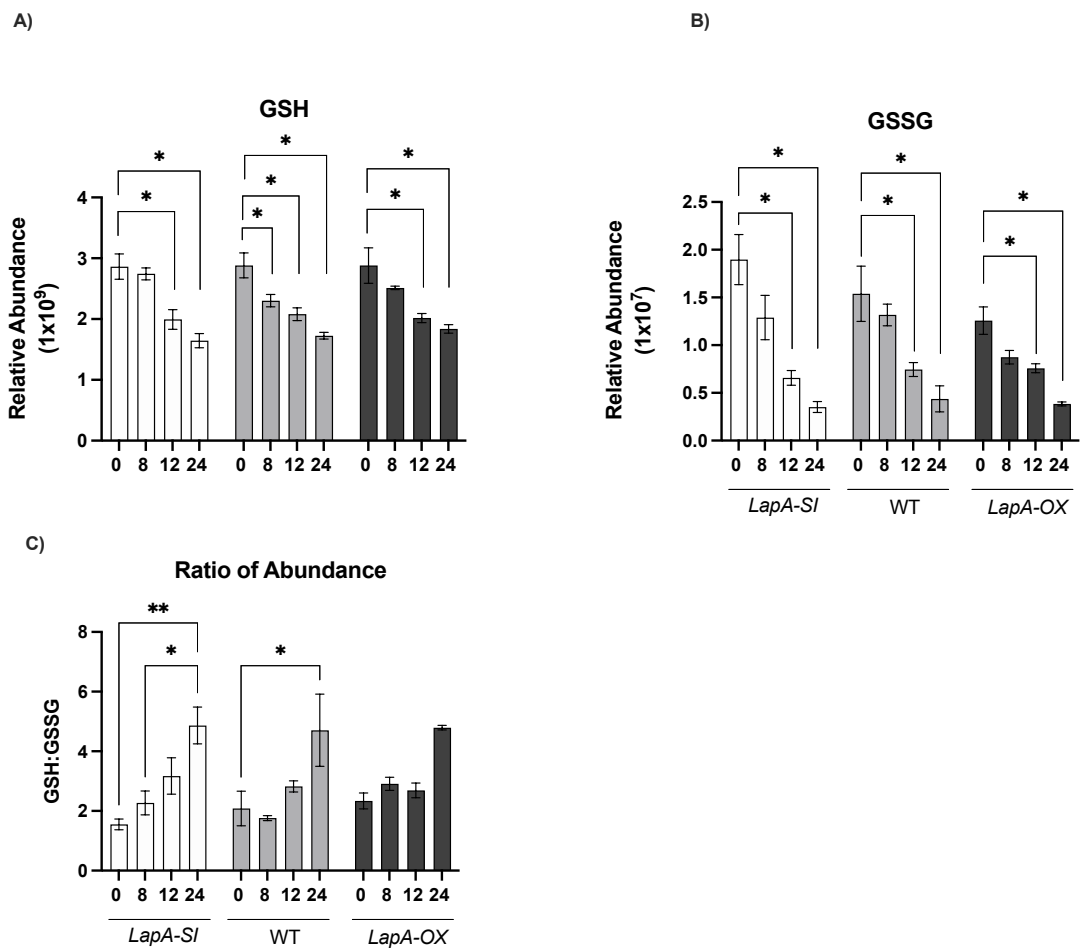
Figure 3.6 Glutathione relative abundance after MeJA treatments. A)Total GSH and B)Total GSSG was measured in WT, LapA-SI, and LapA-OX leaves at 0, 8, 12, and 24 h after MeJA treatment in untargeted metabolomics analyses using LC-MS (see Chapter 2 for primary data set and methods) Welch's t-test was used to determine statistical significance at adjusted P-values <0.05 (*). D) GSH:GSSG abundance for total GSH and total GSSG levels in Two-way ANOVA statistics was done. Asterisks represent statistically different values at adjusted P-values between <0.05 (*), <0.035 (**), <0.0025 (***) and <0.0001 (****) are shown.
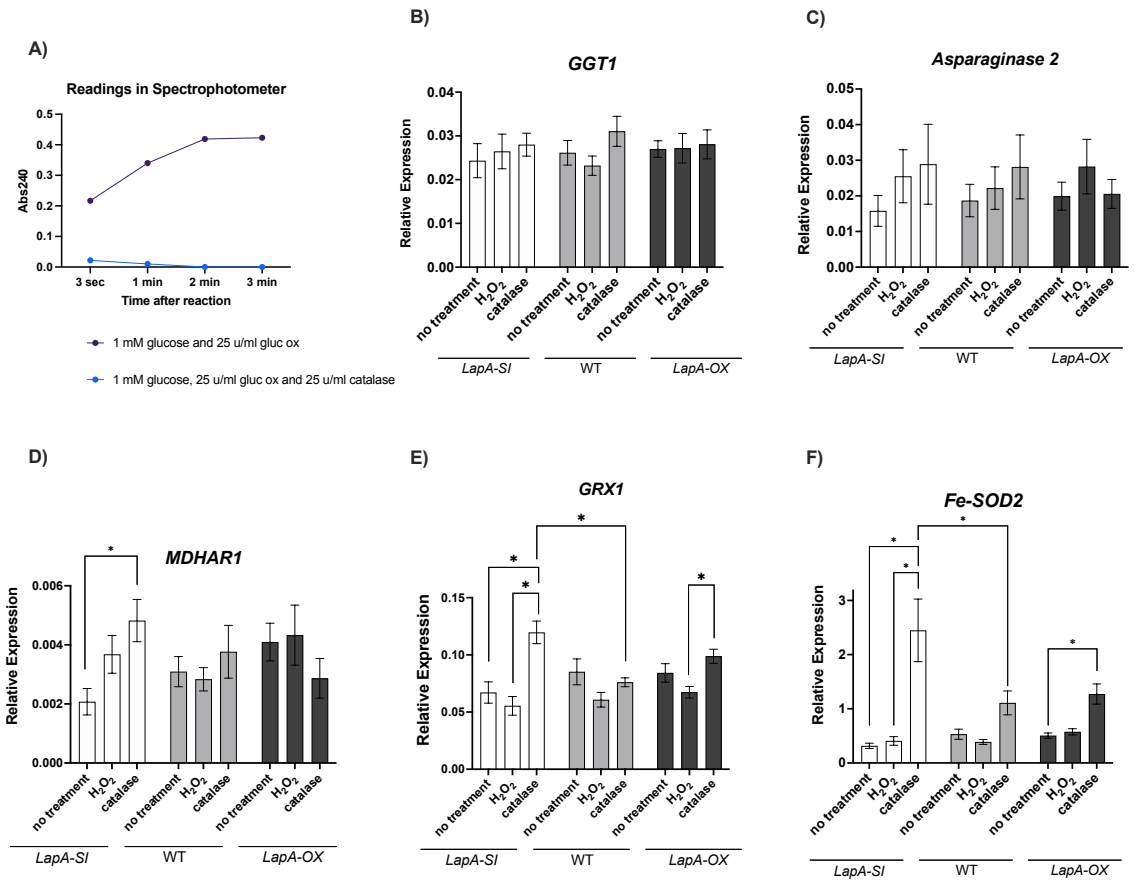
Figure 3.7 Transcript levels for selected ROS-response genes in WT, LapA-SI, and LapA-OX leaves after H_2O_2 and catalase treatments. A) Plants were treated with 1 mM glucose and 25 U/ml glucose oxidase (gluc ox) in phosphate buffer to demonstrate H2O2 evolution, which was measured as increases in absorbance at 240 nm. Readings were taken every 3 sec for a total of 3 min. Catalase control reactions with 1 mM glucose, 25 U/ml glucose oxidase (gluc ox), and 25 U/ml catalase in phosphate buffer (1 mL volume) demonstrated that catalase effectively catabolized H_2O_2 to O_2 and H_2O. B-F) WT, LapA-SI and LapA-OX shoots were excised and immediately immersed for 8 h in water (no treatment), in (glucose and glucose oxidase for the H_2O_2 treatment), or in (glucose, glucose oxidase, and catalase to catabolize H_2O_2 to O_2 and H_2O (control treatment)). RNAs were extracted and relative RNA levels were determined using RT-qPCR with Tip41 (TAP42 interacting protein of 41 kDA) and eIF1 (Elongation factor 1-alpha) as controls for normalization. B) GGT1 (Gamma-glutamyltransferase), C) Asparaginase 2 D) MDHAR1 (NADH-monodehydroascorbate reductase 1) E) SOD2 (Superoxide dismutase2) F) GRX (Glutaredoxin). Data was analyzed using a Welch's t-test and values that varied significantly (adjusted P-value < 0.05) after wounding or between genotypes are indicated (*).

268
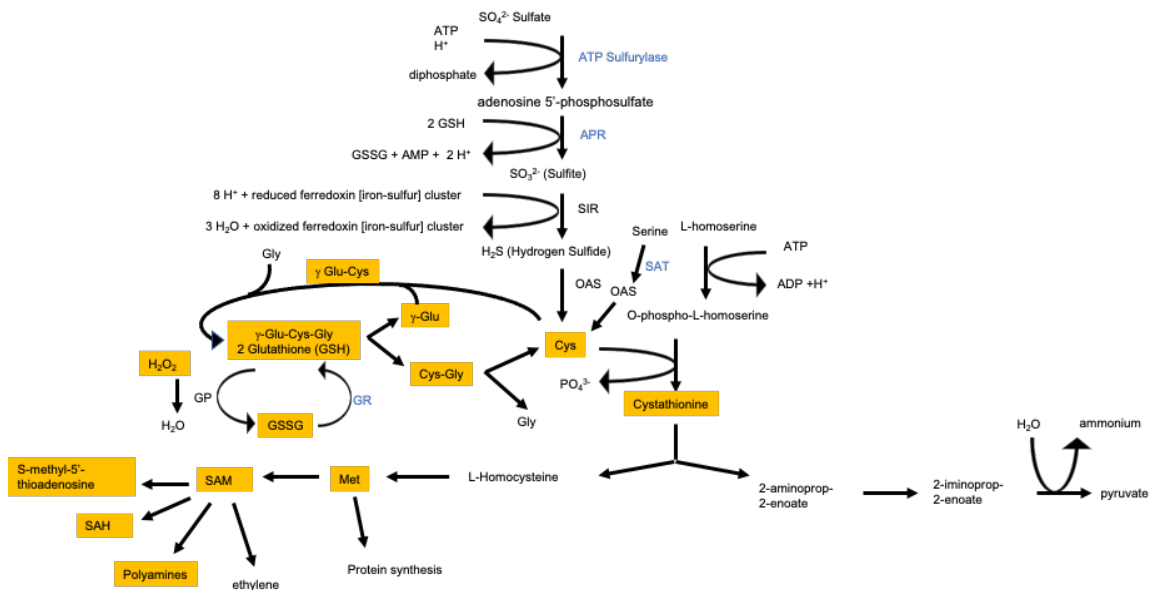
Figure 3.8 Sulfur metabolism. Sulfate undergoes several intermediate steps in plant cells before converted into a nutrient source for plants. Acronyms used are: APS (ATP sulfurylase/ Sulfate adenylyltransferase), APR (5'-adenylylsulfate reductase), SIR (sulfite reductase), oas (O-acetylserine sulfhydrylase), Cys (Cysteine), Glu (Glutamate), Gly (Glycine), Met (Methionine), SAM (S-adenosylmethionine), SAH (S-adenosylhomocysteine). Yellow boxes represent plant metabolites. PlantCyc was used as a source to inform the sulfur pathways. Metabolites highlighted in orange were detected in the targeted or untargeted metabolomics studies.
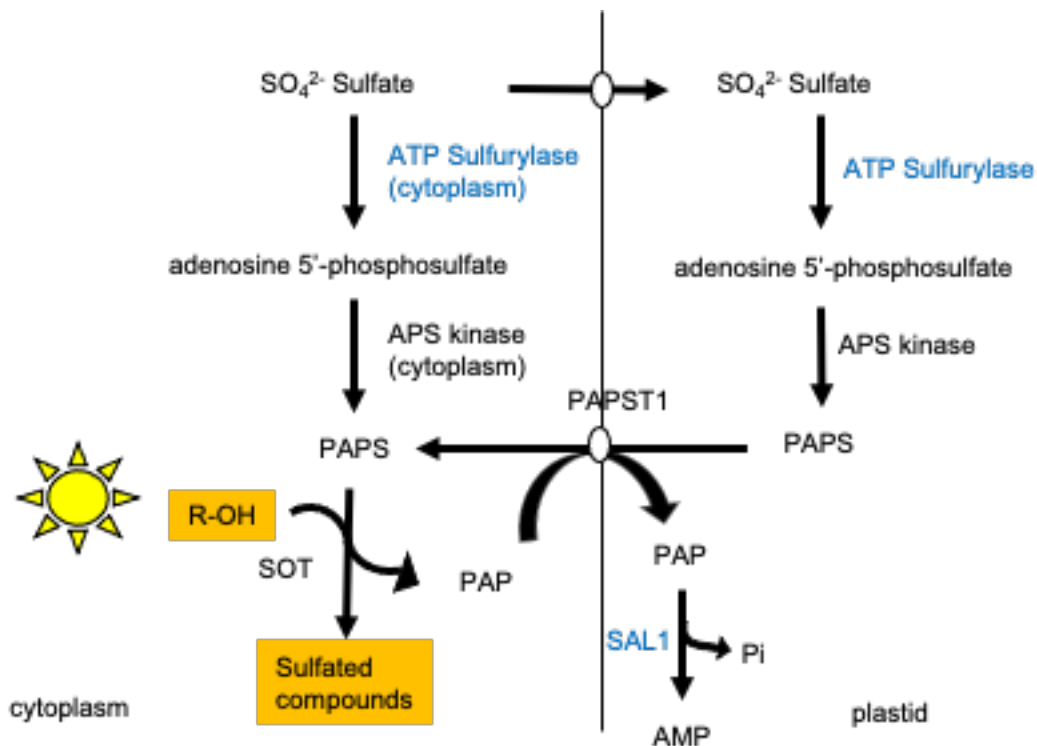
Figure 3.9 Sulfate is used in a secondary metabolic pathway to synthesize PAPS (3'-phosphoadenosine 5'phosphosulfate). In the secondary sulfur metabolic pathway, sulfate undergoes several biochemical steps in the cytoplasm and plastid before beginning converted into sulfated compounds associated with retrograde signaling. PAP (3'-phosphoadenosine 5'phosphate) is catalyzed by SAL1 (phosphoadenosine phosphatase) in the plastid. During stress due to high light (sun image) or drought, there is an accumulation of R-OH, which leads to inactivation of SAL1, which results in PAP accumulation. PAP activates stress responses such as transcription of stress-responsive genes. PlantCyc was used as a source to inform the secondary sulfur pathways. Metabolites highlighted in orange were detected in the targeted or untargeted metabolomics studies.

A)

SAT1

B) *APR3B (Solyc02g032860.2.1)*

C) *APR3A (Solyc02g080640.2.1)*

D) *APR2 (Solyc03g031620.2.1)*
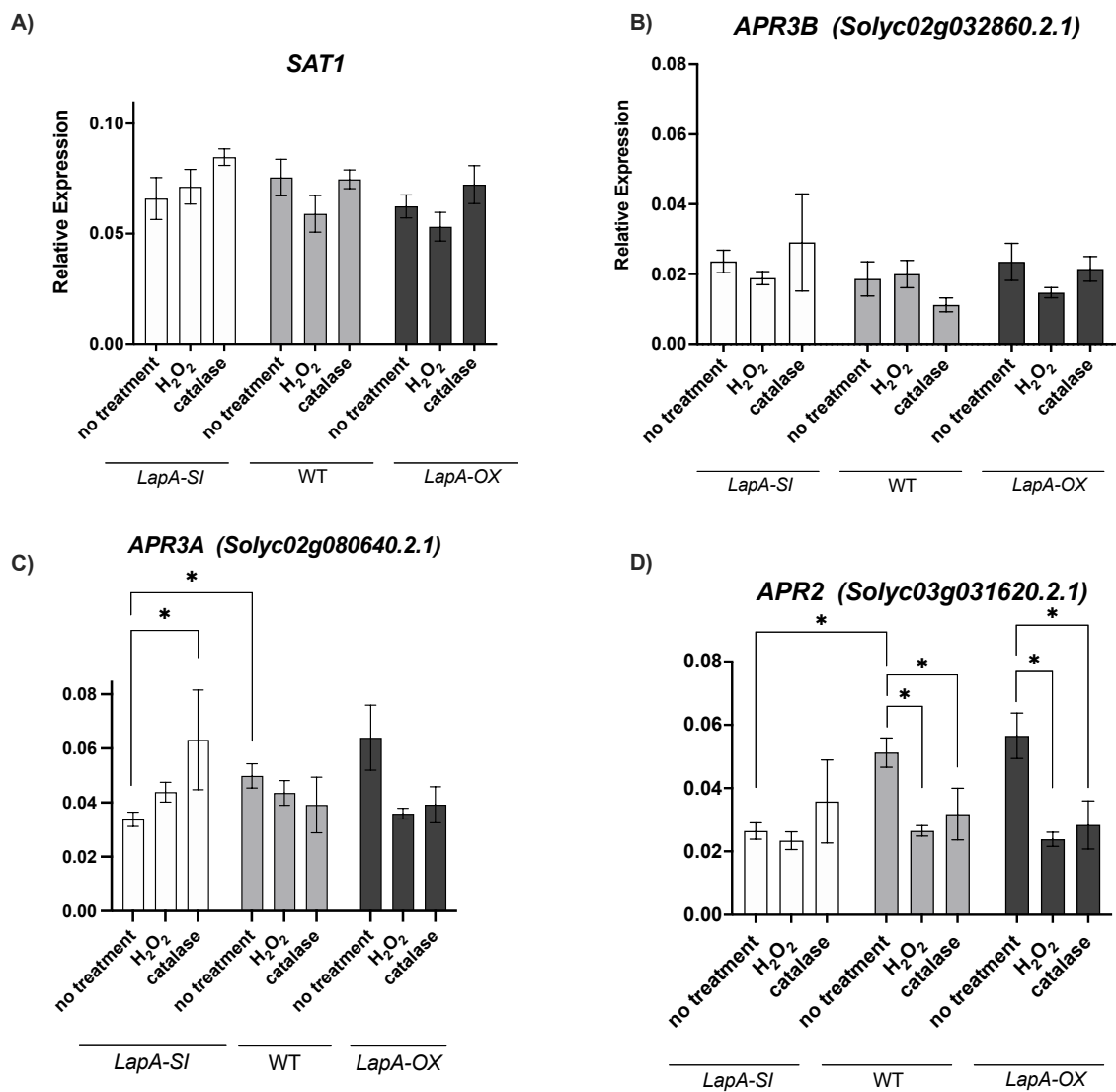
Figure 3.10 Transcript levels for APR and SAT1 in WT, LapA-SI, and LapA-OX leaves after H_2O_2 and catalase treatments. A) SAT1 (Serine acetyltransferase1), B) APR3B (Phosphoadenosine phosphosulfate reductase 3B), C) APR3A, D) APR2. Asterisks represent statistically different values at adjusted P-value ≤ 0.05 for Welch's t-test.
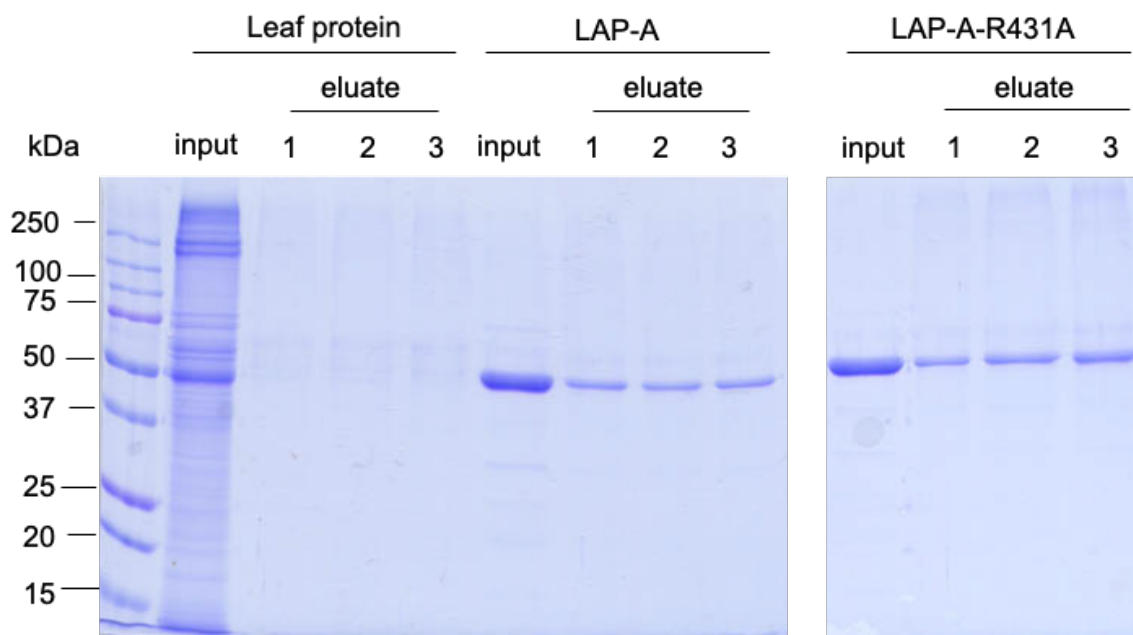
Figure 3.11 Putative LAP-A interactors identified by affinity chromatography. Total leaf protein (12 µg), His-tagged proteins and non-His-tagged proteins were loaded onto a column with nickel-affinity resin (n=3). Purified LAP-A (3 µg) was used as a LAP-A mass reference. Proteins were separated by SDS/PAGE and visualized by Coomassie blue staining. The masses of marker proteins are indicated (kDa).

LAP-A and *R431A* interactors classified by functions
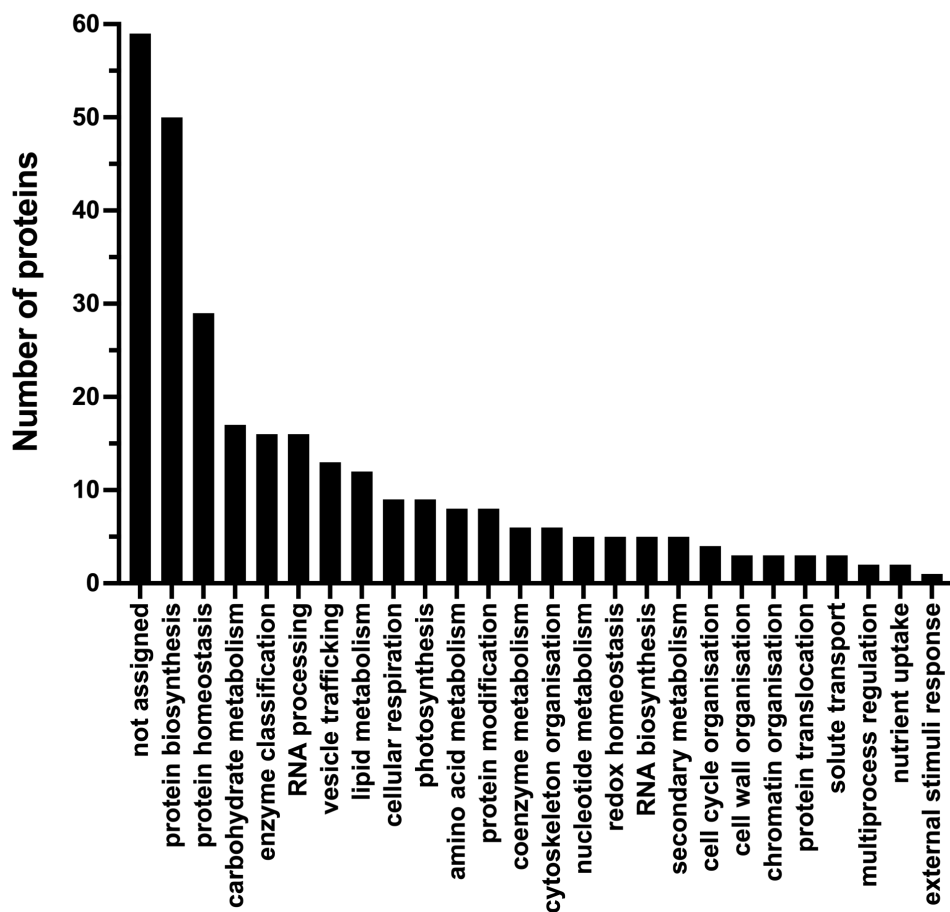
Figure 3.12 LAP-interactors classified by function. A total of 299 leaf proteins interacted with His-tagged LAP-A and His-tagged R431A.
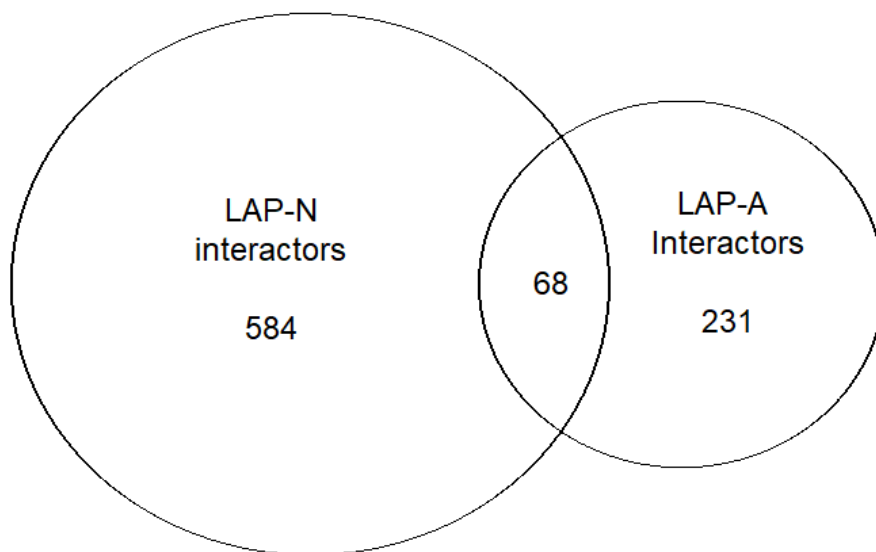
Figure 3.13 Venn Diagram shows overlap between LAP-A and LAP-N interactors. There are 68 shared proteins. There are 584 specific LAP-A and/ or LAP-A mutant R431A interactors. There are 231 specific LAP-N and/ or LAP-N K357E interactors.
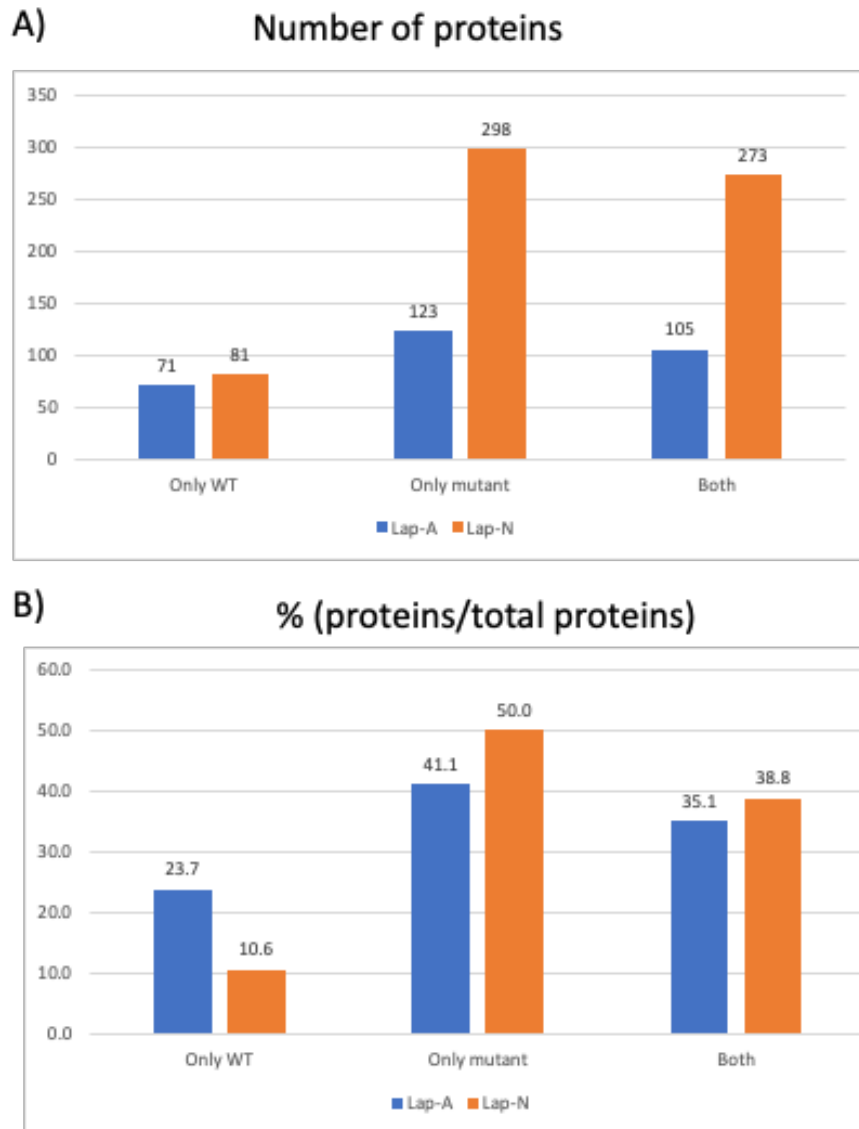
Figure 3.14 High affinity LAP-A and LAP-N interactors. A) Number of proteins that interact only with WT or mutant forms (R431A or K357E) of LAP-A or LAP-N or both WT and mutant proteins. B) Percentage of interacting proteins in each interaction category.
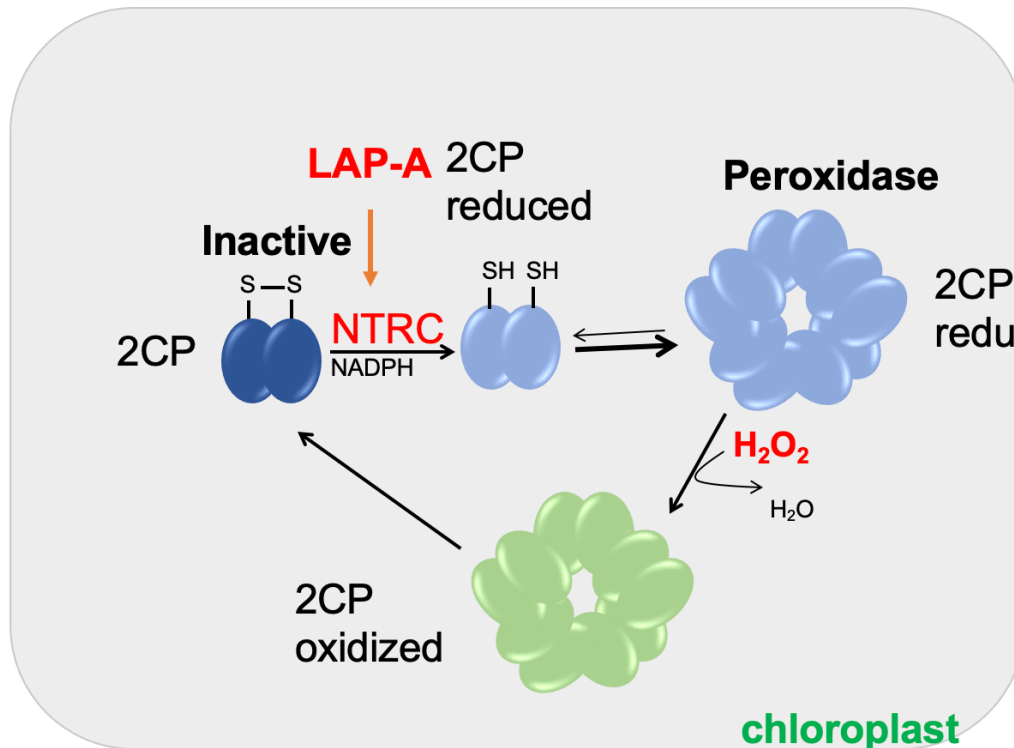
Figure 3.15 LAP-A-dependent redox model. LAP-A may directly interact with NADPH thioredoxin reductase-C (NTRC). By binding to or hydrolyzing NTRC, LAP-A enhanced the reductase activity of NTRC to reduce 2-Cys-Peroxiredoxin (2-CysPrx) and, thereby, enhances 2-CysPrx antioxidant activity to scavenge H_2O_2. 2-CysPrx is a redox sensor that changes its form (dimer, decamer, and high molecular weight (HMW) oligomers) and activity (peroxidase vs chaperone vs inactive aggregate) dependent on the redox status. This model also needs a way to restore redox homeostasis and H_2O_2 catabolism.

Conclusions

Our challenge is to identify the retrograde signal(s) that LAP-A generates to modulate nuclear genes (Fowler et al. 2009; Jung and Chory 2010; Jiang and Dehesh 2021; de Souza et al. 2017). Previous studies have shown that the chloroplast-localized LAP-A positively and negatively regulates nuclear genes encoding antiherbivory proteins (eg., *Pins* and *PPOs*) and stress-induced proteins (eg., *PR1c* and *dehydrins*), respectively (Fowler et al. 2009; Scranton et al. 2013). I initially proposed to *in silico* identify LAP-A substrates, which could lead me to a likely retrograde signaling mechanism. This was proposed because while the tomato LAP-A is well characterized biochemically, we only understood the nature of residues in the P1 and P2 positions that were preferred by LAP-A but we did not understand the influence on the P3-P6 residues in putative LAP-A substrates (Gu et al. 1999; Gu and Walling 2000; Walling 2013; Gu and Walling 2002; Duprez et al. 2014). For this reason, I constructed an *in silico* database that included proteins predicted to be in tomato chloroplast (the Atlas). I proposed to identify putative LAP-A substrates using the knowledge of the geometric constraints of the LAP-A substrate-binding pocket based on the emerging X-ray crystal structure. I proposed to use the residues at the +1 to +4 positions of chloroplast localized proteins to identify LAP-A substrates. The subsequent determination of the X-ray crystal structure (Duprez et al. 2014) showed the substrate-binding pocket of each LAP-A protomer was relatively large and predicting the residues at the +2, +3 and +4 positions was not possible.

Never-the-less, the Atlas has had a lot of utility. I used the Atlas to help define the tomato stromal proteome in a collaborative project with Ms. Oindrila Bhattacharya (UC Riverside PhD candidate). It was imperative to identify the chloroplast stromal proteome

using the Atlas because to date there are few chloroplast stromal proteome studies, and they have primarily emerged from studies in Arabidopsis (Olinares et al. 2010; Peltier et al. 2006; Lundquist et al. 2017). Therefore, tomato stromal proteome described in Chapter 1 is a significant contribution to the chloroplast proteome field and bioinformatics field for proteins' subcellular predictions. In addition, it is possible one of the proteins identified in the stromal proteome will be or will modulate the LAP-A-dependent retrograde signal. With the Walling lab's current multi-omics approaches to define LAP-A's regulatory roles, we anticipate in the near future that the LAP-A signal will be defined.

Comparisons of the characteristics of LAP-dependent signaling in tomato with several known retrograde operational signals, that are best characterized in Arabidopsis, has revealed both similarities and differences. The best known operational signals, MEcPP and PAP-SAL1 share similarities to LAP-A as they have a link to plant defense. High levels of MEcPP induce the expression of the SA biosynthetic enzyme gene *ISOCHORISMATE SYNTHASE 1* (*ICS1*) and, the *ceh1* mutant that causes MEcPP accumulation also induces high levels of SA leading to enhanced resistance to the biotrophic pathogen *Pseudomonas syringae* (Xiao et al. 2012). In addition, high levels of MEcPP causes elevation of JA-response gene transcripts, despite the presence of SA (Lemos et al. 2016). It seems unlikely that LAP-A mutants are associated with high levels of MEcPP. First, MEcPP was not detected in our metabolomics studies; although, this should be taken with a grain of salt since we did not detect any metabolites of the MEP pathway; even though the stroma proteome described in Chapter 1 identified all MEP pathway enzymes. Second, LAP-A does not modulate JA or SA levels (Scranton 2013), while *ceh1* causes increases in both phytohormones (Xiao et al. 2012). Third,

278

LAP-A is suppressed by SA (Chao et al. 1999) and it modulates a regulatory step downstream of JA biosynthesis and perception (Fowler et al. 2009). Fourth, LAP-A deficiency or overexpression does not impact *P. syringae* virulence on tomato plants (Pautot et al. 2001)(Medina-Yerena and Walling, unpublished results). Finally, similar to the *ceh1* mutant, LAP-A does influence herbivore success. *LapA-SI* plants are more susceptible to herbivores and *LapA-OX* plants are more resistant than wild-type plants.

PAP also has impacts on defense (Ishiga et al. 2017). High levels of PAP in Arabidopsis *sal1* mutants (*fry1-2* and *alx8*) are less resistant to the pathogens *Pseudomonas syringae* pv. *tomato* DC3000 (a hemibiotroph) and *Pectobacterium carotovorum* subsp. *carotovorum* EC1 (a nectrotroph) compared to wild-type Col-0 and *SAL1*-overexpression plants (Ishiga et al. 2017). There is a striking reciprocity of the MEcPP and SAL1 impacts on plant defense. Unlike *sal1* mutants, *P. syringae* replicates to equivalent levels in *LapA-SI* and *LapA-OX* plants (Pautot et al. 2001)(Medina-Yerena and Walling, unpublished results). LAP-A clearly regulates the wound signaling in tomato and the role of PAP in herbivory has not been investigated to date.

Despite these differences, it would be interesting to determine if MEcPP or PAP levels are significantly different in *LapA-SI* and *LapA-OX* plants in a targeted metabolomics assay. SAL1 was reliably detected in the tomato stromal proteome (Chapter 1) and was also identified as an upregulated protein in the MeJA proteome. the SAL1 protein was 2-fold more abundant in *LapA-OX* plants compared to wild-type (Bhattacharya, Ortiz and Walling, unpublished results). Finally, *SAL1* transcripts were not MeJA-regulated in wild-type plants (Roche and Walling, unpublished results).

In Chapters 2 and 3, there were several sets of data that suggested that sulfur metabolism was controlled by MeJA, and in part by LAP-A. While LAP-A did not control

the levels of glutathione (GSH) or its redox status, we discovered that GSH was differentially regulated by wounding and MeJA treatments. GSH levels were upregulated by wounding and downregulated by MeJA treatments (Figs. 3.4, 3.6). While MeJA is a proxy for wounding, our data indicate that it is clearly does not mimic all events of wounding. The differences in GSH levels could be due to the fact, unlike MeJA, wounding significantly damages cells and releases DAMPs (eg., eATP, DNA, etc) that can be perceive and trigger plant defenses (Hou et al. 2019). Alternatively, MeJA treatments are likely to provide levels of MeJA that are above physiologically relevant concentrations. The differences in GSH levels after MeJA and wounding is intriguing. It will be interesting to determine if wounding and MeJA treatments differentially impact the metabolites MEcPP, PAP and PAP's regulatory enzyme SAL1.

Solid genetic and metabolomics data in Chapter 2 indicated that MeJA and LAP-A regulated primary and secondary metabolism as 78 MeJA regulated and 57 MeJA and LAP-A modulated metabolites were identified. Of these metabolites several were associated with plant defense: 5-amino valeric acid, pipecolic acid and steroidal glycosides. Using untargeted metabolomics, 5-aminovaleric acid and pipecolic acid were detected, derived from Lysine and are involved in plant defense (Adam et al. 2018). This is the first report of the regulation of these metabolites and biosynthetic enzymes by MeJA. 5-aminovaleric acid is produced by two pathways. It is produced from 5-aminopentanal or 6-amino-2-oxohexanoate/ketocaproic acid (KAC) (Chapter 2, Fig 2.9A) (Shimizu et al. 2019). KAC reacts spontaneously with H_2O_2 to form 5-aminovaleric acid. Although the precursors for 5-aminovaleric acid were not identified in the untargeted metabolomics assay, there were higher levels of H_2O_2 in *LapA-SI* compared to wild-type plants, which was well correlated with increased levels of 5-aminovaleric acid in *LapA-SI*

lines compared to wild-type plants (Chapter 3, Fig 3.3). However, *LapA-OX* plants did not display a reciprocal phenotype. Instead, the *LapA-OX* plants had a phenotype similar to *LapA-SI* lines suggesting that the regulation is complex. In addition, LAP-A regulation was demonstrated for pipecolic acid, which is also derived from KAC, and serves as the precursor of N-hydroxy-pipecolic acid. N-hydroxy-pipecolic acid is an SA induced signal that is associated with SAR in Arabidopsis (Chen et al. 2018; Hartmann and Zeier 2018; Wang et al. 2018). We did not detect N-hydroxy-pipecolic acid in our metabolomics studies and this is likely to do the strong negative regulation of *FMO1* RNAs by MeJA. This is in alignment with the antagonism for many SA and JA-regulated responses during pathogen and pest attack. Finally, there are MeJA- and LAP-dependence of several steroidal glycoside alkaloids, which negatively impact bacteria, fungi and herbivorous insects. LAP-A induces tomatidine and enzymes for the synthesis of tomatidine and dehydrotomatine (Fig 2.13 and 2.14). LAP-A suppresses the metabolites dehydrotomatine (Fig 2.13). These data suggest that LAP-A may enhance production of the more toxic compound tomatidine compared to dehydrotomatine.

In Chapter 3, I demonstrated LAP-A negatively regulates H_2O_2 levels, which is a known positive regulator of the late branch of wound signaling (Orozco-Cárdenas et al. 2001) and a retrograde signal (Exposito-Rodriguez et al. 2017). As LAP-A did not regulate GSH levels or redox status, LAP-A must regulate another step within the chloroplast that produces or dissipates H_2O_2 levels. In Chapter 3, I discovered NADPH thioredoxin reductase-C (NTRC1) is a strong LAP-A interactor and therefore LAP-A may exert its effect on H_2O_2 via NTRC1 (Chapter 3). In Arabidopsis, NTRC controls the status of the major plastidial redox hub, as it reduces the antioxidant 2-CysPrxA and B (2-Cys peroxiredoxin) that scavenges H_2O_2 (Muthuramalingam et al. 2009). I proposed the LAP-

A dependent redox model (Fig 3.15) builds upon on the 2-Cys-Prx and NTRC pathway elucidated in Arabidopsis. As LAP-A-deficient *LapA-SI* plants accumulate more H_2O_2 than wild-type plants, LAP-A must enhance NTRC1's reduction of 2-CysPrx to control the H_2O_2 burst that occurs in response to wounding. I hypothesize that LAP-A indirectly enhances the amount of bioactive 2-CysPrx (reduced form) to: (1) control H_2O_2 levels (2) limit protein and lipid damage, (3) limit accumulation of insoluble protein aggregates that cause plant cell death, and (4) regulate key redox sensitive chloroplast enzymes (Table 3.3). As LAP-A is not an on-off switch, it must act as a modulator or rheostat that finely tunes H_2O_2 levels after wounding, MeJA treatments and herbivory. LAP-A allows sufficient H_2O_2 to accumulate to signal the presence of a stressor, but must maintain H_2O_2 at sufficiently low levels to prevent excessive cellular damage. In *LapA-SI* plants, the rheostat is lost and I propose excessive damage to cellular components may occur to prevent H_2O_2 signaling.

Interestingly, the preliminary data from a transcriptomics study that examined transcript abundance in wild-type, *LapA-SI* and *LapA-OX* plants after MeJA treatment showed that MeJA downregulated *NTRC1* transcript levels within 30 min after treatment (Paul Roche and Linda Walling, unpublished results). Furthermore, NTRC1 protein levels are downregulated by MeJA in *LapA-SI* plants compared to wild-type plants treated with MeJA (Bhattacharya, Ortiz and Walling. unpublished results). Therefore, LAP-A must be important in maintaining the activity of NTRC1 after rises in JA after pathogen or pest attack.

The impact of LAP-A on NTRC1 is a solid direction for future experiments. As LAP-A is both an aminopeptidase and chaperone, it may alter the N-terminal residues of NTRC1 and enhance its turnover. Alternatively, LAP-A may keep NTRC1 in an active

folded state to promote the 2-CysPrx-NTRC1 redox hub's ability to catabolize H_2O_2. It will be of interest to determine if LAP-A hydrolyzes the N-terminal residue(s) of the mature NTRC1 using a standard aminopeptidase assay. NanoLC-MS/MS can be used to detect the number of residues hydrolyzed in the N-termini of NTRC1. In addition, the peptide profiles of NTRC1 from the stromal proteome (Chapter 1) will be compared to NTRC1 peptides from *LapA-SI* and *LapA-OX* plants treated with MeJA to detect if there are changes in the N-terminal residues of NTRC1. Finally, our stromal proteomics studies may be able to determine if LAP-A, NTRC1 and or 2-CysPrx is oxidatively damaged after MeJA treatments and it the damage is correlated with LAP-A levels in wild-type, *LapA-SI* and *LapA-OX* plants.

In the future, it would be prudent to provide additional evidence to support my model that predicts LAP-A suppresses H_2O_2 *in planta* after wounding. I propose that LAP-A serves a modulator (or a rheostat) to produce sufficient H_2O_2 for signaling acute attack by herbivores but to keeps H_2O_2 at low levels to prevent excess damage to photosystem proteins, and other proteins and lipids within the chloroplast. If LAP-A is a rheostat to control H_2O_2, additional experiments that exogenously manipulate H_2O_2 levels might provide further support for this model. I should be able to follow these responses by monitoring transcript levels for several sentinel genes that are up or down-regulated by LAP-A (e.g., *Pins* and *PPO vs PR1c* and *Dehydrins,* respectively) (Fowler et al. 2009; Scranton et al. 2013)*.* This can be achieved by treating excised shoots of wild-type, *LapA-SI* and *LapA-OX* plants with: (1) a range of glucose/glucose oxidase concentrations to deliver different levels of H_2O_2, (2) glucose/glucose oxidase levels as described in Figure 3.7 and alter the amounts of catalase to control the levels of H_2O_2, or (3) with glucose/glucose oxidase as described in Figure 3.7 but varying the time of

treatment. Furthermore, we can generate and dissipate H_2O_2 using paraquat or vitamin B6 and concentration. The time dependence of H_2O_2 generation and sentinel gene expression can be monitored in wild-type, *LapA-SI* and *LapA-OX* plants. I could also monitor the levels of 5-aminovaleric acid (Chapter 2), which is produced spontaneously in the presence of H_2O_2 (Fig 2.9) and is LAP-A dependent.

I hypothesize that in our current experiments and in vivo, H_2O_2 is high enough to damage the residual LAP-A that exists in *LapA-SI* plants and this will prevent LAP-A from promoting NTRC1 activity. But at lower H_2O_2 treatment levels, the residual levels of *LapA-SI* may be able to promote NTRC1 activity and promote the H_2O_2 signal to activate the wound-response pathway. Whereas at higher H_2O_2 concentrations, *LapA-SI* plants will incur sufficient protein damage and wound signaling would be impaired. We expect similar responses in wild-type but we anticipate higher concentrations of H_2O_2 may be needed to impair wound signaling.

The large-scale studies performed in the Walling lab (transcriptomics, proteomics, interactome and metabolomics) has opened the door to infinite possibilities of LAP-A's role in plant defense, retrograde signaling and cell's redox status. My contributions were in the proteomics, interactome and metabolomics fields to demonstrate LAP-A's many roles.

References

Adam AL, Nagy ZA, Katay G, Mergenthaler E, Viczian O (2018) Signals of Systemic Immunity in Plants: Progress and Open Questions. Int J Mol Sci 19 (4). doi:10.3390/ijms19041146

Chao WS, Gu YQ, Pautot V, Bray EA, Walling LL (1999) Leucine aminopeptidase RNAs, proteins, and activities increase in response to water deficit, salinity, and the wound signals systemin, methyl jasmonate, and abscisic acid. Plant Physiology 120 (4):979-992. doi:10.1104/pp.120.4.979

Chen YC, Holmes EC, Rajniak J, Kim JG, Tang S, Fischer CR, Mudgett MB, Sattely ES (2018) N-hydroxy-pipecolic acid is a mobile metabolite that induces systemic disease resistance in Arabidopsis. Proc Natl Acad Sci U S A 115 (21):E4920-e4929. doi:10.1073/pnas.1805291115

de Souza A, Wang JZ, Dehesh K (2017) Retrograde Signals: Integrators of Interorganellar Communication and Orchestrators of Plant Development. Annu Rev Plant Biol 68:85-108. doi:10.1146/annurev-arplant-042916-041007

Duprez K, Scranton MA, Walling LL, Fan L (2014) Structure of tomato wound-induced leucine aminopeptidase sheds light on substrate specificity. Acta Crystallographica Section D-Biological Crystallography 70:1649-1658. doi:10.1107/s1399004714006245

Exposito-Rodriguez M, Laissue PP, Yvon-Durocher G, Smirnoff N, Mullineaux PM (2017) Photosynthesis-dependent H_2O_2 transfer from chloroplasts to nuclei provides a high-light signalling mechanism. Nature Communications 8 (1):49. doi:10.1038/s41467-017-00074-w

Fowler JH, Narvaez-Vasquez J, Aromdee DN, Pautot V, Holzer FM, Walling LL (2009) Leucine Aminopeptidase Regulates Defense and Wound Signaling in Tomato Downstream of Jasmonic Acid. Plant Cell 21 (4):1239-1251. doi:10.1105/tpc.108.065029

Gu YQ, Holzer FM, Walling LL (1999) Overexpression, purification and biochemical characterization of the wound-induced leucine aminopeptidase of tomato. European Journal of Biochemistry 263 (3):726-735. doi:10.1046/j.1432-1327.1999.00548.x

Gu YQ, Walling LL (2000) Specificity of the wound-induced leucine aminopeptidase (LAP-A) of tomato - Activity on dipeptide and tripeptide substrates. European Journal of Biochemistry 267 (4):1178-1187. doi:10.1046/j.1432-1327.2000.01116.x

Gu YQ, Walling LL (2002) Identification of residues critical for activity of the wound-induced leucine aminopeptidase (LAP-A) of tomato. European Journal of Biochemistry 269 (6):1630-1640. doi:10.1046/j.1432-1327.2002.02795.x

Hartmann M, Zeier J (2018) l-lysine metabolism to N-hydroxypipecolic acid: an integral immune-activating pathway in plants. Plant J 96 (1):5-21. doi:10.1111/tpj.14037

Hou S, Liu Z, Shen H, Wu D (2019) Damage-Associated Molecular Pattern-Triggered Immunity in Plants. Frontiers in plant science 10:646-646. doi:10.3389/fpls.2019.00646

Ishiga Y, Watanabe M, Ishiga T, Tohge T, Matsuura T, Ikeda Y, Hoefgen R, Fernie AR, Mysore KS (2017) The SAL-PAP Chloroplast Retrograde Pathway Contributes to Plant Immunity by Regulating Glucosinolate Pathway and Phytohormone Signaling. Mol Plant Microbe Interact 30 (10):829-841. doi:10.1094/mpmi-03-17-0055-r

Jiang J, Dehesh K (2021) Plastidial retrograde modulation of light and hormonal signaling: an odyssey. New Phytol 230 (3):931-937. doi:10.1111/nph.17192

Jung HS, Chory J (2010) Signaling between Chloroplasts and the Nucleus: Can a Systems Biology Approach Bring Clarity to a Complex and Highly Regulated Pathway? Plant Physiology 152 (2):453-459. doi:10.1104/pp.109.149070

Lemos M, Xiao Y, Bjornson M, Wang JZ, Hicks D, Souza A, Wang CQ, Yang P, Ma S, Dinesh-Kumar S, Dehesh K (2016) The plastidial retrograde signal methyl erythritol cyclopyrophosphate is a regulator of salicylic acid and jasmonic acid crosstalk. J Exp Bot 67 (5):1557-1566. doi:10.1093/jxb/erv550

Muthuramalingam M, Seidel T, Laxa M, de Miranda SMN, Gaertner F, Stroeher E, Kandlbinder A, Dietz K-J (2009) Multiple redox and non-redox interactions define 2-Cys Peroxiredoxin as a regulatory hub in the chloroplast. Molecular Plant 2 (6):1273-1288. doi:10.1093/mp/ssp089

Orozco-Cárdenas ML, Narváez-Vásquez J, Ryan CA (2001) Hydrogen Peroxide Acts as a Second Messenger for the Induction of Defense Genes in Tomato Plants in Response to Wounding, Systemin, and Methyl Jasmonate. The Plant Cell 13 (1):179-192

Pautot V, Holzer FM, Chaufaux J, Walling LL (2001) The induction of tomato leucine aminopeptidase genes (LapA) after Pseudomonas syringae pv. tomato infection is primarily a wound response triggered by coronatine. Molecular Plant-Microbe Interactions 14 (2):214-224. doi:10.1094/mpmi.2001.14.2.214

Scranton MA (2013) Elucidation of the Role of Leucine Aminopeptidase A in the Wound Response Pathway in Tomato. UC Riverside.

Scranton MA, Fowler JH, Girke T, Walling LL (2013) Microarray Analysis of Tomato's Early and Late Wound Response Reveals New Regulatory Targets for Leucine Aminopeptidase A. Plos One 8 (10). doi:10.1371/journal.pone.0077889

Shimizu Y, Rai A, Okawa Y, Tomatsu H, Sato M, Kera K, Suzuki H, Saito K, Yamazaki M (2019) Metabolic diversification of nitrogen-containing metabolites by the expression of a heterologous lysine decarboxylase gene in Arabidopsis. The Plant Journal 100 (3):505-521. doi:10.1111/tpj.14454

Walling LL (2013) Leucyl Aminopeptidase (Plant). Handbook of Proteolytic Enzymes, Vols 1 and 2, 3rd Edition. doi:10.1016/b978-0-12-382219-2.00331-8

Wang Y, Schuck S, Wu J, Yang P, Döring A-C, Zeier J, Tsuda K (2018) A MPK3/6-WRKY33-ALD1-Pipecolic Acid Regulatory Loop Contributes to Systemic Acquired Resistance. The Plant Cell 30 (10):2480-2494. doi:10.1105/tpc.18.00547